2016

Identifying Common Therapeutic Targets in Merlin-deficient Brain Tumours

Bassiri, Kayleigh

Identifying common therapeutic targets in Merlin-deficient brain tumours

By

Kayleigh Bassiri

A thesis submitted to Plymouth University in partial fulfilment for the degree of

DOCTOR OF PHILOSOPHY (PhD)

(Medical studies)

Institute of translational and stratified medicine

April 2016

Copyright statement

Thesis supervisors

Professor Clemens Oliver Hanemann MD, PhD

Institute of translational and stratified medicine

Plymouth University Peninsula Schools of Medicine and Dentistry

Plymouth, UK

Dr Edwin Lasonder, PhD

Centre for biomedical and healthcare sciences

Plymouth University

Plymouth, UK

Dr Sara Ferluga, PhD

Institute of translational and stratified medicine

Plymouth University Peninsula Schools of Medicine and Dentistry

Plymouth, UK

Acknowledgements

I would like to extend my thanks to Professor Oliver Hanemann for giving me this opportunity and for making my lifelong dream of doing a PhD possible. Your expertise and knowledge have been indispensable over the last 3.5 years, and your straight-talking approach always got the best out of me.

I would also like to thank Dr Sara Ferluga for making such a huge impact on my project, and joining the team at a time when I felt I had lost my way. Your enthusiasm for science and research really boosted my confidence and made me believe in myself again. Thank you so much for everything.

I would like to acknowledge Dr Edwin Lasonder for sharing his extensive knowledge of proteomics with me, and for never, ever being too busy to help. On that note, I would also like to thank Dr Vikram Sharma for putting what seems like endless samples of mine through the mass spectrometer, for answering every single question, and for always being cheery no matter what issues I caused!

My personal journey in the years leading up to this PhD was somewhat turbulent, and getting to this point today would not have been possible without a very special selection of people. First and foremost, my heartfelt thanks and admiration go to my sister Mina. You have always been such a wonderful role model, and someone I could only aspire to be like. You've been my mentor, my best friend and have always kept me on the straight and narrow. You'll never know how grateful I am to have you in my life.

To my oldest and dearest friend Amy T; the person that knows me better than I know myself. No matter what the situation, you always have the answers and you always keep it real. You are one of the most caring and loyal people I have ever known, and I count my blessings that I am able to call you my friend. To your wonderful family who gave me a place to call home, I love and appreciate you all more than I can say.

To my partner in crime, Jade whom has shared this PhD journey with me, with its many ups and downs. You painstakingly scrutinised my thesis sometimes to my dismay, but the time you put in to doing that for me is testament to the kind of person you are. I can't wait to see what our future holds; I guess this is just the beginning.

To my very special friends; Steph, how far we've come in the 14 years we've known each other; to you, Alice, Samantha and Sarah; your constant belief that I would succeed and your endless words of encouragement dragged me through the times when the end seemed so far away! Thank you from the bottom of my heart. I count myself lucky to have you all as my friends.

And finally, perhaps the biggest acknowledgement of all goes to my mum, Karen. I have always been so determined to achieve my goals and never to give up even if something seems impossible. I am the person I am today because of you. You were the most amazing, brave and strong woman I will ever know. Even though you've not been with us for almost 14 years, you still inspire me every, single day. If I become half the person you were, that will truly be my greatest achievement. Thank you, I dedicate this thesis to you.

AUTHORS DECLARATION

'Identifying common therapeutic targets in Merlin-deficient brain tumours' submitted by Kayleigh Bassiri of the Peninsula Schools of Medicine and Dentistry to Plymouth University as a thesis for the degree of Doctor of Philosophy in April 2016.

This thesis, printed or electronic format, is available for library use on the understanding that it is copyright material and that no quotation from the thesis may be published without proper acknowledgement.

I certify that all material in this thesis which is not my own work has been identified and that no unchanged or acknowledged material has previously been submitted and approved for the award of a degree by this or any other University.

At no time during the registration for the degree of Doctor of Philosophy has the author been registered for any other University award without prior agreement of the Graduate Committee.

This study was financed with the aid of a studentship from Plymouth University.

Word count of main body of thesis: 29,922

Signed:

Date:

Kayleigh Bassiri

Title: Identifying common therapeutic targets in Merlin-deficient brain tumours

Abstract

Neurofibromatosis type 2 (NF2) is an autosomal dominant inherited condition that predisposes individuals to develop multiple nervous system tumours, primarily schwannoma, meningioma and ependymoma. NF2 is characterised by loss of the tumour suppressor protein Merlin, caused by bi-allelic mutations of the encoding gene *NF2* or by loss of heterozygosity. These tumours can occur either sporadically or as part of the NF2 condition. The majority are slow growing and display benign features, but this benignancy renders them largely unresponsive to classic chemotherapeutic agents leaving surgery and radiosurgery as the only remaining treatment options. Depending on their location, NF2-related tumours can cause a number of side effects, including nausea, balance problems, and in some cases hearing and/or vision loss.

Phosphorylation is a key regulatory mechanism leading to changes in cell signalling. By identifying phosphoproteins that are significantly activated in tumour cells, novel therapies can be developed aiming to specifically target the phosphorylated status of these proteins thus 'switching off' the signalling cascade. The objective of this study is to identify and validate common targets in both Merlin-deficient meningioma and schwannoma to eventually exploit in novel therapeutic approaches.

Using phosphoprotein purification followed by mass spectrometry analysis, we identified Signal Transducer and Activator of Transcription 1 (STAT1), phosphorylated at Serine (S) 727 and Tyrosine (Y) 701, PDZ and LIM domain protein 2 (PDLIM2), Heat Shock 70kDa Protein 1A (HSPA1A) and Filamin B (FLNB) as potential common, novel therapeutic targets. We validated these candidates in human primary meningioma and schwannoma tumour cells using a variety of techniques. We also showed that specific

knockdown of STAT1 and PDLIM2 was related to a significant decrease in cellular proliferation.

Additionally, we performed co-immunoprecipitation using PDLIM2 as the bait protein and identified STAT1, HSPA1A and FLNB as binding partners, suggesting a novel interaction network involving all of the potential targets identified in this study. We also identified activation of several pathways and/ or biological processes in both tumour types that warrant further investigation i.e. endocytosis in schwannoma and the proteasome in meningioma.

In conclusion, with our approach we substantially increased the overall body of knowledge regarding the proteome and phosphoproteome of meningioma and schwannoma. We generated a comprehensive set of data that highlighted several potential therapeutic targets and dysregulated pathways which will be further investigated.

List of contents

List of Figures

List of tables

Abbreviations

AA	Amino Acid
ABC	Ammonium Bicarbonate
ACN	Acetonitrile
AJ	Adherens Junction
BP	Biological Process
BSA	Bovine Serum Albumin
CC	Cellular component
CER	Cytoplasmic Extraction Reagent
COL	Collagen
CTT	C-terminal tail
DAB	Diaminobenzidine
DAVID	Database for Annotation, Visualisation and Integrated Discovery
DHB	2,5-dihydroxybenzoic acid
DMEM	Dulbeccos Modified Eagle Medium
DPI	Dots Per Inch
DSS	Disuccinimidyl Suberate
ECL	Enhanced Chemiluminescence
ECM	Extracellular Matrix
EDTA	Ethylenediaminetetraacetic acid
EGFR	Epidermal Growth Factor Receptor
ErbB	Erb receptor tyrosine kinase
ERK	Extracellular Signal-Regulated Kinase
ERM	Ezrin Radixin Moesin
FAK	Focal Adhesion Kinase
FASP	Filter Aided Sample Preparation
FBS	Foetal Bovine Serum
FC	Fold change
FDR	False Discovery Rate
FERM	Band 4.1, Ezrin, Radixin, Moesin
FFPE	Formalin Fixed Paraffin Embedded
FLNA	Filamin A
FLNB	Filamin B
GAPDH	Glyceraldehyde-3-Phosphate Dehydrogenase
GBM	Glioblastoma Multiforme
GO	Gene Ontology
HDAC	Histone Deacetylase
HMC	Human Meningeal Cells
HSPA1A	Heat shock 70kDa protein 1A
HSPA2	Human Meningeal Cells
IgG	Immunoglobulin
IMAC	Immobilized Metal Affinity Chromatography
IP	Immunoprecipitation
KLF4	Kruppel-like Factor 4
LC	Liquid Chromatography
LFQ	Label Free Quantification
LIM	Lin11, Isl-1 & Mec-3

MAPK	Mitogen Activated Protein Kinase
MCT	Multiple Correction Testing
MF	Molecular Function
MnCl	Magnesuim Chloride
MNG	Meningioma
MOS	Schwann cell
MS	Mass Spectrometry
mTOR	Mammalian Target Of Rapamycin
NaOH	Sodium Hydroxide
NER	Nuclear Extraction Reagent
NF1	Neurofibromatosis type 1
NF2	Neurofibromatosis type 2
NFκB	Nuclear Factor Of Kappa Light Polypeptide Gene Enhancer In B-Cells
NGS	Next-Generation sequencing
PAK1	P21 Protein (Cdc42/Rac)-Activated Kinase 1
PAK2	P21 Protein (Cdc42/Rac)-Activated Kinase 2
PBS	Phosphate Buffered Saline
PDGFR	Platelet-derived Growth Factor Receptor
PDLIM2	PDZ and LIM domain protein 2
PDZ	PSD-95, Discs Large, and Zona Occludens 1 proteins.
PI3K	Phosphoinositide-3 Kinase
PTM	Post-Translational Modification
PVDF	Polyvinyl Difluoride
RAC	Ras-Related C3 Botulinum Toxin Substrate
RAF1	Raf-1 Proto-Oncogene, Serine/Threonine Kinase
RAS	Rat Sarcoma Viral Oncogene
RIPA	Radioimmunoprecipitation assay
RPPA	Reverse Phase Protein Array
RT	Room Temperature
RTK	Receptor Tyrosine Kinase
RT-PCR	Real-Time Polyermase Chain Reaction
SDS	Sodium Dodecyl Sulphate
SDS-PAGE	SDS-Polyacrylamide Gel Electrophoresis
SER	Serine
shRNA	Short Hairpin RNA
SILAC	Stable Isotopic Labelling with Amino Acids in cell Culture
SMAD2	Mothers Against Decapentaplegic 2
SMARCB1	SWI/SNF-related matrix-associated actin-dependent regulator of chromatin subfamily B member 1
SMO	Smoothened
STAT1	Signal Transducer and Activator of transcription 1
TBST	Tris-Buffered Saline and Tween
TFA	Trifluoroacetic Acid
TGLN	Transgelin
TGM2	Transglutaminase 2
THR	Threonine
THY1	Thy-1 cell surface antigen
TiO_2	Titanium dioxide

TRAF7	Tumor necrosis factor Receptor-Associated Factor 7
TSP	Tumour Suppressor Protein
TYR	Tyrosine
UPLC	Ultra-Performance Liquid Chromatography
VCL	Vinculin
VEGFR	Vascular Endothelial Growth Factor Receptor
VS	Vestibular Schwannoma

Chapter 1- Introduction

1.1 Background to this study

Meningiomas are usually low-grade tumours affecting the brain and spinal cord, while schwannomas are found in the peripheral nervous system (Ammoun and Hanemann 2011). There are currently no drugs clinically approved for the treatment of either meningioma or schwannoma. Individuals with the genetic condition neurofibromatosis type 2 (NF2) suffer with frequent recurrences of both tumour types, and must endure multiple surgeries and occasionally radiosurgery throughout life as their primary treatment option, which can have profound effects on patient's quality of life. The identification of novel therapeutic targets will help to inform the search for more efficient and less invasive ways of treating patients with NF2, and potentially many spontaneous meningiomas, schwannomas and other Merlin-deficient tumours (Ammoun and Hanemann 2011).

The importance of this thesis lies in the fact that most studies focus solely on one or the other tumour type and are frequently hypothesis driven, thus biased. In this project, both meningioma and schwannoma were extensively studied to identify common features that could be exploited in both tumours, so that they could be treated simultaneously with the same drug leading to the same therapeutic benefit, especially important in NF2 patients. The following introduction will discuss the current literature in more detail and summarize some of the technologies utilized in drug target discovery, including how they have been used specifically for identifying therapeutic targets.

1.2 Schwannoma and meningioma aetiology

1.2.1 The neurofibromatoses

There are three genetic conditions that fall under the general term of neurofibromatoses, these are; Neurofibromatosis type 1 (NF1), Neurofibromatosis type 2 (NF2), and schwannomatosis. Each of these conditions predisposes individuals to

various tumours. NF1 is the most common of the three and is characterised by the presence of neurofibromas and malignant peripheral nerve sheath tumours (MPNST). It has a prevalence of 1:2500-3000 (Jones, Tep *et al.* 2008, Rodriguez, Stratakis *et al.* 2012) and is caused by mutations in the gene encoding for the tumour suppressor protein neurofibromin. Neurofibromas can undergo malignant transformation, are difficult to resect without residual nerve damage and are usually histopathologically distinct from schwannomas. Schwannomas are only rarely associated with NF1 and meningiomas are not associated with loss or mutation of NF1 (Hilton and Hanemann 2014).

1.2.2 Schwannomatosis

Schwannomatosis was first alluded to in 1984 (Shishiba, Niimura *et al.* 1984) and is pathologically distinct from NF2 due to the absence of bilateral vestibular schwannomas (VS) associated with the condition and absence of ependymomas (Jacoby, Jones *et al.* 1997). There are few patients with schwannomatosis who have a demonstrated family history of the condition, therefore most cases are deemed sporadic (Hilton and Hanemann 2014). MacCollin *et al.* studied 14 patients presenting with multiple schwannomas and found that one patient had a positive family history (MacCollin, Woodfin *et al.* 1996). Schwannomatosis therefore, although bearing similarity to NF2, is a largely distinct condition.

In 2007, a study reporting a link between *SMARCB1* gene mutation and schwannomatosis was published, identifying it as an underlying genetic cause of the condition (Hulsebos, Plomp *et al.* 2007). More recently in 2014, Piotrowski and colleagues showed that loss of function mutations in the *LZTR1* gene also predispose individuals to the formation of multiple schwannomas and in some of those cases, SMARCB1 mutations were not observed (Piotrowski, Xie *et al.* 2014).

1.2.3 Neurofibromatosis type 2

Neurofibromatosis type 2 (NF2) is an autosomal dominant inherited condition that predisposes individuals to develop multiple nervous system tumours; primarily schwannomas, meningiomas and ependymomas. Prevalence is considered to be 1:33000-40000 (Rodriguez, Stratakis *et al.* 2012). NF2 is characterised by loss of the tumour suppressor protein Merlin, first identified as the product of the *NF2* gene in 1993 (Rouleau, Merel *et al.* 1993). A number of mutations have been described including nonsense mutations, frame-shift deletions and splice site mutations (Ruttledge, Andermann *et al.* 1996). Disease severity was shown to correlate with type of mutation, and those with only single amino acid mutations tended to have milder disease than those with mutations leading to protein truncation.

Individuals with NF2 are born with a germline mutation in one *NF2* allele leading to a genetic predisposition to develop multiple tumours early in life, frequently and often simultaneously (Bijlsma, Brouwer-Mladin *et al.* 1992, Rouleau, Merel *et al.* 1993). Most people with NF2 accumulate a somatic mutation in the wild-type allele and it is at this point that tumours start to develop; in accordance with the knudson 2-hit hypothesis where the second mutation is necessary for loss of tumour suppressor function (Knudson 2001).

1.2.4 Non-NF2 related schwannoma and meningioma

Sporadic schwannomas not associated with the aforementioned genetic conditions all harbour *NF2* mutations resulting in Merlin loss (Hanemann 2008). It has been estimated that overall one in 1000 people will be diagnosed with a vestibular schwannoma in their lifetime (Evans, Moran *et al.* 2005).

Meningiomas are one of the most common brain tumours representing 30% of all cases, second only to glioma (Laurendeau, Ferrer *et al.* 2010). Hereditary meningiomas arise as part of genetic predisposition syndromes, most commonly loss of the *NF2* gene resulting in neurofibromatosis type 2, or to a much lesser extent

familial multiple meningiomas; the latter less well defined in its aetiology. Mutations in the *SMARCB1* gene have been associated with some familial meningiomas. For instance, a study conducted on a family of patients with multiple meningiomas concluded that along with *NF2* gene mutation, mutation in exon 2 of *SMARCB1* was a relevant factor in these particular tumours (Christiaans, Kenter *et al.* 2011). A year later, another study on a Finnish family identified loss of function in the *SUFU* gene in seven meningiomas from the same family and not in healthy controls (Aavikko, Li *et al.* 2012). *SUFU* is linked to the Hedgehog signalling pathway, important in oncogenesis and previously implicated in *NF2* deficient malignant pleural mesothelioma (Felley-Bosco and Stahel 2014), meningioma (Mawrin and Perry 2010) and some schwannomas (Yoshizaki, Nakayama *et al.* 2006). Mutations in *SMARCE1*, *EPB41L3* and *SHH* have also been reported (Smith 2015).

Genomic screens are pivotal in identifying mutated genes that allow tumours/ patients to be placed in particular sub-groups that only contain those most likely to respond to a particular drug. Heterogeneity among tumours in different patient populations is perhaps the largest barrier in the way of successful drug therapy (Marte 2013). Most recently, there have been a number of mutations identified in large-scale studies of meningioma that have been hailed as the most significant in non-NF2 tumours and may pave the way for the development of personalized treatment regimens. These are *AKT1*, *SMO*, *TRAF7* and *KLF4* (Brastianos, Horowitz *et al.* 2013, Clark, Erson-Omay *et al.* 2013)

Brastianos and colleagues identified a subset of meningiomas with oncogenic mutations in *SMO* and *AKT1*. The authors defined significance of each mutation identified in the analysis relative to genome wide background rates. In doing this, they identified six genes with significant mutation rates in meningioma. These included *SMO* and *AKT1*, as well as *NF2*, *KDM5C*, *RGPD3* and *CD300C* (Brastianos, Horowitz *et al.* 2013). The *AKT1* mutation identified, E17K, has already been implicated as an oncogenic determinant in breast cancer and is able to activate downstream mTOR

signalling, known to be relevant in Merlin deficient tumours. Similarly, mutations in *SMO* contribute to activated hedgehog signalling in meningiomas and may act as a therapeutic target (Laurendeau, Ferrer *et al.* 2010).

Clark *et al* also identified *SMO* and *AKT1* mutations although they found *TRAF7* to be the most frequently mutated gene, in almost 35% of 300 meningiomas analysed (Clark, Erson-Omay *et al.* 2013). A conclusion drawn by the authors was that that these distinct subsets of meningiomas generally convey chromosomal stability, whereas meningiomas harbouring NF2 mutations tended to be more atypical in nature, with chromosomal instability, indicating that NF2 mutation is a potent stimulus for further mutations in downstream signalling pathways.

Studies like these represent a mainstay of translational cancer research and are becoming indispensable in the search for novel targets and more effective therapies.

1.3 Diagnosis and pathogenesis of NF2

NF2 is diagnosed clinically according to the Manchester criteria listed in meningiomas 1.1 (Evans 2009). The majority of NF2-related schwannomas occur around the vestibular branches of the eighth cranial nerve, responsible for transmitting sound and balance information from the inner ear to the brain. The presence of these schwannomas often leads to hearing loss, tinnitus and loss of balance (Evans, Huson *et al.* 1992, Sabha, Au *et al.* 2012).

Meningiomas originate from the arachnoidal cap cells of the meninges and can occur either in the brain or the spinal cord (James, Lelke *et al.* 2008). Their presence can impact on surrounding tissue and compress adjacent nerves and blood vessels resulting in focal deficits and seizures. Meningiomas also cause increased intracranial pressure that can lead to sickness and headaches.

Diagnostic 'Manchester criteria' for neurofibromatosis type 2 (NF2) (Hilton and Hanemann, 2014)	
1	Bilateral vestibular schwannoma (VS) *or* family history of NF2 *plus* unilateral VS *or* two of; meningioma, glioma, neurofibroma, schwannoma, posterior subcapsular lenticular opacities.
2	Unilateral VS *plus* two of meningioma, glioma, neurofibroma, schwannoma, posterior subcapsular lenticular opacities.
3	Two or more meningioma *plus* unilateral VS *or* two of; glioma, neurofibroma, schwannoma, cataracts.

Table 1.1: The Manchester criteria for NF2 diagnosis.

Schwannomas associated with NF2 are exclusively benign, as are around 80% of meningiomas. Around 15% are classified as 'atypical,' defined by higher recurrence rates and decreased survival compared to benign meningiomas. The remaining few are anaplastic meningiomas, and these are characterised by malignant brain invasion and poor prognosis (Commins, Atkinson *et al.* 2007). This benignancy renders them largely unresponsive to classic chemotherapeutic agents, leaving surgery and radiosurgery as the only remaining treatment options. Furthermore, NF2 patients not only have multiple tumours but often experience tumour regrowth following resection (Maillo, Orfao *et al.* 2007). As no drugs are currently approved for the treatment of NF2, an effective therapeutic is urgently required.

NF2 also predisposes to the development of ependymomas which belong to the glioma family and effect ependymal tissue within the central nervous system. Around 6% of NF2 patients will develop ependymomas (Hanemann 2008), making them the least common of the three tumours associated with the condition. Whilst they have not been studied in this project, the aetiology they share with meningiomas and schwannomas suggests that the findings presented here may also be relevant for their treatment.

1.4 Other Merlin-deficient tumours

In addition to tumours associated with NF2, Merlin loss is also implicated in a number of other cancers including Malignant Pleural Mesothelioma (MPM). This is an aggressive form of lung cancer caused by asbestos exposure (Bianchi, Mitsunaga *et al.* 1995). The association was first reported in 1995 and 40-50% of cases are thought to be linked to Merlin loss. More recently, a 2014 study showed that Merlin-deficient mesothelioma cells were sensitive to VS-4718 (Shapiro, Kolev *et al.* 2014) a drug targeting the Focal Adhesion Kinase (FAK) pathway, also commonly abrogated in schwannomas (Ammoun, Schmid *et al.* 2012). This suggests that any therapeutic targets identified in schwannomas may also be beneficial for a subset of MPM patients.

Merlin deficiency has also been linked to melanoma where Merlin knockdown in a melanoma cell line led to increased growth and proliferation. The mammalian ste20 kinases 1 and 2 (MST1/2) of the Hippo pathway were rendered inactive in this experiment and therefore were unable to phosphorylate Yes activated protein (YAP), leading to an increase in transcription and thus cell growth (Murray, Lau *et al.* 2012).

Merlin loss has further been linked to malignant breast cancer, where upon Akt-induced phosphorylation, it is degraded. Re-establishment of Merlin expression in breast cancer cell lines led to decreased invasion, migration and cell motility (Morrow, Das *et al.* 2011). Most recently, Merlin expression was assessed in colorectal cancer where a distinct pattern of Merlin phosphorylation was detected in tumour compared to normal tissue (Cacev, Aralica *et al.* 2014).

NF2 aberrations have also been reported in thyroid, endometrial and liver cancers, as well as glioblastoma (GBM) (Houshmandi, Emnett *et al.* 2009, Schroeder, Angelo *et al.* 2014, Garcia-Rendueles, Ricarte-Filho *et al.* 2015). Recently in 2015, a link between Merlin deficiency and pancreatic cancer was identified. The study showed that restored Merlin expression led to decreased growth and metastasis in pancreatic cancer cells (Quan, Cui *et al.* 2015).

Taken together, these studies indicate a wider role for Merlin loss in tumorigenesis outside of NF2 related nervous system tumours and thus make any findings from this project potentially valuable for a broad range of cancers.

1.5 Merlin

Merlin is an acronym derived from '**M**oesin, **E**zrin and **R**adixin **l**ike prote**in**,' named so because of its structural similarity to the ERM superfamily which includes the aforementioned proteins. Their function is to transmit signals from the cell membrane/ extracellular matrix (ECM) to downstream components inside the cell (Bretscher, Chambers *et al.* 2000, Li, Nance *et al.* 2007). ERM proteins are able to interact directly with actin and can play crucial roles in cell remodelling and the localization of receptor

tyrosine kinases (RTKs) to the cell membrane. A FERM domain is shared by all members of this family and its amino acid sequence is highly conserved. Found at the *N*-terminus, the FERM domain facilitates the interaction between ERM proteins and the cell membrane, and is the key functional feature of these 'membrane-cytoskeletal linker proteins' (Chishti, Kim *et al.* 1998).

Merlin is expressed as two isoforms; predominantly isoform 1, the structure of which can be viewed in Figure 1.1A**.** Isoform 1 is 595 amino acids (AA) in length, whereas isoform 2 is 590 AA. The two share identical sequence homology for 579 residues, but after this point isoform 2 lacks the necessary *C*-terminal motif required for intramolecular binding (Cooper and Giancotti 2014). Nonetheless, isoform 2 has been shown to possess tumour suppressive capabilities much in line with those reported for isoform 1 (Lallemand, Saint-Amaux *et al.* 2009, Sher, Hanemann *et al.* 2012).

1.5.1 Regulation of Merlin

Post-translational control of Merlin is crucial to its proper functioning. Like other ERM proteins, Merlins FERM domain is able to interact directly with its *C*-terminus tail (CTT) forming a closed loop structure (Gary and Bretscher 1995) (Figure 1.1B). In most ERM proteins, this association is regulated by phosphorylation of a conserved threonine (Thr) residue contained within the CTT. When this Thr is phosphorylated, the interaction is disrupted, leading to an open and activated state. Merlin on the other hand is phosphorylated at a unique Serine (Ser/ S) residue, S518. Rong *et al* observed that S518 phosphorylation, induced by PAK2, reduced the association between the two domains, leading to an open conformation of the protein. Interestingly, in contrast to other ERM proteins this renders Merlin inactive by negatively modulating its ligand binding capability (Rong, Surace *et al.* 2004).

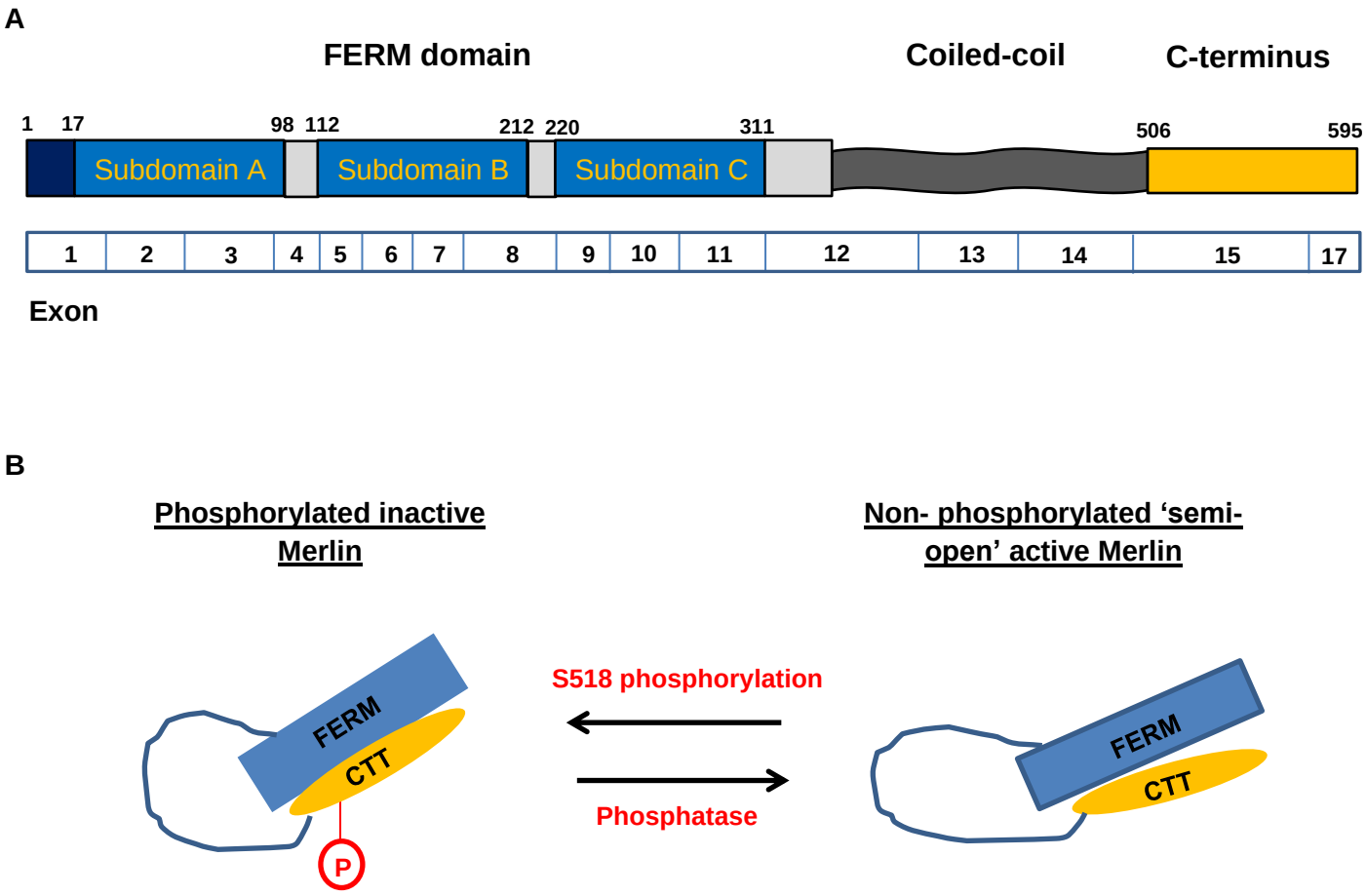

Figure 1.1: *A)* A schematic representation of the structure of Merlin (Adapted from Giancotti and cooper (Cooper and Giancotti 2014)) *B)* Regulation of Merlin by phosphorylation of S518 (Adapted from Li *et al* (Li, Zhou *et al.* 2015)). CTT: *C*-Terminal Tail.

Most recently, an idea has been proposed that Merlin is neither fully open nor fully closed and that this is dependent on its environment at any given time (Sher, Hanemann *et al.* 2012). This study concluded that S518 phosphorylation points Merlin towards a more, but not fully, closed conformation whereby its growth suppressive function is compromised, and that unphosphorylated Merlin is in a more, but not fully, open state. As such, there is a high degree of flexibility whilst Merlin remains in this conformation allowing subtle changes dependent on post-translational modifications.

1.6 Merlin as a tumour suppressor protein

The most significant characteristic that sets Merlin apart from other ERM proteins is its putative role as a tumour suppressor protein (TSP). There are a variety of mechanisms by which Merlin is able to perform its tumour suppressive duties, and these are summarised in Figure 1.2.

In contrast to other TSPs Merlin generally localizes to the interface between the cell membrane and the Extracellular Matrix (ECM). In 2003 it was reported that the major consequence of Merlin deficiency in primary cells is the inability to undergo contact-dependent growth arrest (Lallemand, Curto *et al.* 2003). In the normal confluent cell, Merlin translocates to adherens junctions (AJ) where it is able to orchestrate contact-inhibition signals and encourage growth arrest (Flaiz, Utermark *et al.* 2008). Adherens junctions are important for the stabilization of cell-cell adhesion and are central to contact inhibition of cell growth, and as such are important for tumour suppression (Hartsock and Nelson 2008). Merlin interacts specifically with β-catenin at adherens junctions, as identified by Lallemand *et al.* who were able to show that the two proteins co-immunoprecipitate.

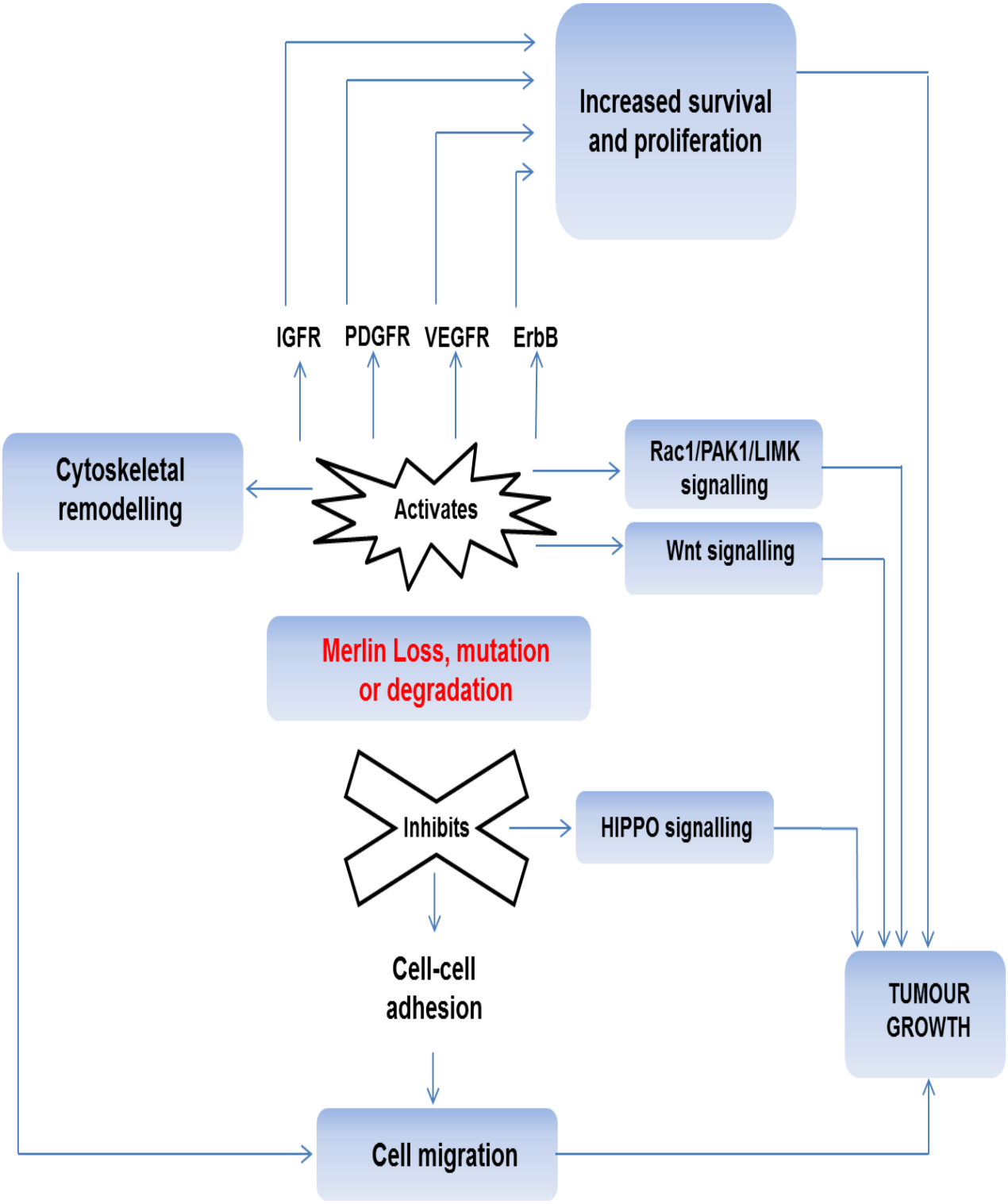

Figure 1.2: A flowchart highlighting the tumour suppressive activities of Merlin. Merlin loss leads to the activation of several Receptor Tyrosine Kinases (RTKs) in turn permitting tumour growth, survival and proliferation.

Later, Zhou *et al.* showed that Merlins interaction with β-catenin at the site of adherens junctions is inhibitory to cell growth and proliferation. In Merlin-deficient schwannoma cells an increase of β-catenin phosphorylation was observed at tyrosine (Tyr/ Y) Y654, mediated by Src/ PDGFR (Platelet Derived Growth Factor Receptor) which contributed to enhanced nuclear translocation of β-catenin and subsequent AJ destabilization (Zhou, Ercolano *et al.* 2011).

1.7 Receptor tyrosine kinase expression in meningioma and schwannoma

Merlin controls membrane receptor availability by regulating endocytic trafficking (Fraenzer, Pan *et al.* 2003, Maitra, Kulikauskas *et al.* 2006, Muranen, Gronholm *et al.* 2007). Muranen *et al.* proposed that Merlin deficiency leads to a decrease in microtubule polymerization and that resultant microtubule dysregulation then leads to slower receptor recycling. As a result, receptors are not internalized as efficiently or quickly ultimately leading to prolonged activation of downstream signalling pathways. This was supported by Hennigan *et al*. in 2013 who showed that Merlin loss led to decreased intracellular vesicular trafficking, in a Rac dependent manner (Hennigan, Moon *et al.* 2013). Maitra *et al.* suggested that Merlin plays a role in sorting of cargo between endosomes and lysosomes for degradation (Maitra, Kulikauskas *et al.* 2006). As such, the authors showed that in Merlin-deficient cells, there was an increased presence of receptors on the cell membrane. Further, Scoles *et al.* showed that Merlin co-localized to early endosomes with a Hepatocyte Growth Factor (HGF) receptor substrate (Scoles, Huynh *et al.* 2000). As early endosomes are important for determining membrane receptor fate, this study supports the notion that Merlin in part exhibits its tumour suppressive effects via early endosome regulation.

The PDGFR-BB is a cell surface tyrosine kinase receptor highly expressed in meningioma and schwannoma cells, as such it has been extensively studied in both cell types (Yang and Xu 2001, Fraenzer, Pan *et al.* 2003, Ammoun, Flaiz *et al.* 2008). In 2014, Agnihotri and colleagues performed gene expression profiling of 47 vestibular

schwannomas and identified PDGFRβ as upregulated with an overall fold change of 37.2 compared to seven normal control nerves (Agnihotri, Gugel *et al.* 2014). PDGFRβ activation was most recently confirmed in meningioma in 2015, with 83% of tumours staining positive for the receptor upon immunohistochemical analysis (Hilton, Shivane *et al.* 2015). A study by Fraenzer *et al*. found that overexpression of Merlin increased the rate of PDGFR degradation and decreased the proliferation rate of a human schwannoma cell line (Fraenzer, Pan *et al.* 2003). Mukherjee *et al.* also showed that Imatinib (Gleevec) treated schwannoma cells exhibited deceased viability and proliferation, as mediated by deactivation of PDGFRα and PDGFRβ (Mukherjee, Kamnasaran *et al.* 2009). Ammoun *et al.* also showed that Imatinib was able to decrease PDGFRβ mediated ERK1/2 and Akt phosphorylation in primary schwannoma cells (Ammoun, Schmid *et al.* 2011). Payre and colleagues demonstrated a correlation between Merlin loss and PDGFR expression in human meningioma samples, and showed that NF2-deficient mice overexpressing PDGF developed malignant meningiomas (Peyre, Salaud *et al.* 2015).

Merlin is also able to regulate ErbB family receptors and several studies have highlighted the Epidermal Growth Factor Receptor (EGFR) family as potential therapeutic targets for both meningioma and schwannoma. Merlin knockdown in primary human Schwann cells led to the upregulation of ErbB2/3 and consequent increased proliferation (Ahmad, Brown *et al.* 2010). Curto and colleagues showed that Merlin is able to regulate EGFR at the site of adherens junctions, by sequestering it in a membrane compartment where it is not able to signal (Curto, Cole *et al.* 2007). In Merlin-null mouse embryonic fibroblasts, osteoblasts and liver-derived epithelial cells, the EGFR was able to constitutively drive proliferation that could be abrogated by EGFR inhibitors. Similarly Ammoun and Cunliffe identified consistent overexpression and activation of ErbB receptors, and showed that their inhibition led to significant decreases in primary schwannoma cell proliferation (Ammoun, Cunliffe *et al.* 2010).

Baxter *et al.* found that over 80% of meningiomas stained positive for EGFR suggesting it as a possible therapeutic target (Baxter, Orrego *et al.* 2014). This was supported by Wernicke *et al.* who found that almost all of 85 meningioma samples analysed were EGFR positive. Furthermore, they found staining to be highest in benign tumours, suggesting it might be more relevant for these than those of higher grade (Wernicke, Dicker *et al.* 2010). In contrast to these findings, Hilton and colleagues performed immunohistochemical analysis in 30 meningioma samples of varying grade and sub-type, and were only able to identify EGFR activation in NF2 wild type tumours, concluding that it may not be a good target for Merlin-deficient meningiomas (Hilton, Shivane *et al.* 2015). Whilst there are several studies of EGFR expression in meningioma, there are no reported functional studies of the receptor in these tumours. There have however been a number of clinical trials assessing the effectiveness of various EGFR inhibitors, and these will be discussed in more detail later.

Another receptor known to be important in schwannomas is the Insulin-like growth factor receptor (IGFR). Ammoun *et al.* showed that the IGF-IR is strongly expressed and activated in primary human schwannoma cells (Ammoun, Schmid *et al.* 2012). This overexpression was linked to enhanced growth and survival via ERK1/2 and AKT, and inhibition of the receptor led to reductions in both. Lallemand and colleagues also found that the levels of IGF1R on the membrane of Merlin-null Schwann cells were elevated compared to control cells expressing Merlin (Lallemand, Manent *et al.* 2009). Dysregulation of IGFs has also been proposed as a marker of anaplasia in meningiomas, and a high ratio of IGF-II *vs*. IGFBP-2 stimulates proliferation (Nordqvist, Peyrard *et al.* 1997). Later studies were also able to identify various members of the IGF signalling family as upregulated in meningioma, with Wrobel *et al.* also suggesting this phenomenon as an indicator of meningioma progression (Watson, Gutmann *et al.* 2002, Wrobel, Roerig *et al.* 2005, Hilton, Shivane *et al.* 2015).

Another RTK that has been studied in both tumour types is the Vascular Endothelial Growth Factor Receptor (VEGFR) that is integral to angiogenesis in a wide variety of

tumours. The receptor has been reported as highly expressed in both meningioma and schwannoma (Uesaka, Shono *et al.* 2007, Baumgarten, Brokinkel *et al.* 2013, Hilton, Shivane *et al.* 2015), and as a direct contributor to vestibular schwannoma growth (Caye-Thomasen, Werther *et al.* 2005). Pfister *et al.* also observed that VEGF is able to signal through the PDGFR-β causing tyrosine activation and a proliferative response in meningiomas, comparable to that after stimulation with its own ligand (Pfister, Pfrommer *et al.* 2012). In 2010 Wong and colleagues implanted mice with Merlin-deficient cells that would mimic growth of central and peripheral schwannomas. They found that treatment with Bevacizumab and Vandetanib led to reductions in growth and increased apoptosis (Wong, Lahdenranta *et al.* 2010). Collectively these data support the VEGFR as a suitable therapeutic target; however the validity of VEGFR inhibitors in a clinical setting will be re-visited later on in the chapter.

Merlin-deficient cells exhibit increased mitogenic signalling in part due to integrin overexpression on the cell membrane. Utermark *et al.* identified integrins alpha6, beta1 and beta4 clustered on the schwannoma cell surface and showed that they were largely responsible for the enhanced ECM adhesion observed in schwannoma cells, compared to normal Schwann cells (Utermark, Kaempchen *et al.* 2003). Integrin overexpression was previously shown to activate mitogenic signalling inside the cell and an earlier study demonstrated that the coupling of integrin alpha6 and beta4 was able to stimulate both RAS and ERK activation (Mainiero, Murgia *et al.* 1997). This helps to explain the hyper-activation of these signalling cascades that contribute to schwannoma pathology, and highlight disruption of integrin mediated signalling as a promising avenue for therapeutic intervention.

Merlin also plays a role in FAK/Src signalling via a variety of mechanisms. FAK is important for transducing signals from integrins and RTKs at the membrane inside the cell and is overexpressed in schwannoma (Ammoun, Flaiz *et al.* 2008). Ammoun *et al*. demonstrated that FAK signalling can be regulated by Axl, an RTK that is upregulated in schwannoma and meningioma (Ammoun, Provenzano *et al.* 2014, Hilton, Shivane *et*

al. 2015) and is negatively regulated by Merlin. Increased Axl signalling increases FAK expression leading to pathological cell-matrix adhesion and enhanced survival.

1.8 Regulation of downstream signalling pathways by Merlin

Merlin can directly bind to tubulin increasing stability and reducing turnover (Smole, Thoma *et al.* 2014). The resulting disequilibrium between polymerization and depolymerisation that occurs when Merlin is lost contributes to enhanced cytoskeletal reorganization and tumorigenesis, and forms the basis of pathologies associated with Merlin deficiency.

Merlin is also a potent inhibitor of p21-Activated kinase 1 (PAK1). PAK1 and other members of this protein family are regulators of cell morphology, motility and apoptosis (Jaffer and Chernoff 2002). It has been shown that Merlin interacts with PAK1 thereby modulating its function (Kaempchen, Mielke *et al.* 2003, Kissil, Wilker *et al.* 2003, Hirokawa, Tikoo *et al.* 2004, Xiao, Gallagher *et al.* 2005). In normal cells, PAK1 is inhibited by Merlin leading to suppression of Rac signalling and ultimately growth arrest. Shaw *et al.* found that inhibition of Rac by Merlin in the mouse embryonic fibroblast cell line NIH3T3 led to decreased colony formation and reduced levels of downstream phosphorylated c-Jun N-terminal kinase (JNK). Merlin is also able to inhibit PAK1 induced cyclin D1 expression, causing a decrease in proliferation rate through G1 cell cycle arrest in mesothelioma cell lines (Xiao, Gallagher *et al.* 2005).

Merlin has also been linked to the Hippo pathway, which is important for organ size control and contributes to tumorigenesis when deregulated. In confluent cells, the Hippo pathway is activated resulting in phosphorylation of Yes Activated Protein (YAP) that leads to its retention in the cytoplasm; whereby it cannot translocate to the nucleus and act as a transcriptional activator (Zhao, Li *et al.* 2010). A 2010 study found that inactivation of Merlin led to liver cell hyperplasia and a decrease in YAP phosphorylation, supporting Merlins cytoplasmic role as a facilitator of growth suppressive Hippo signalling (Zhang, Bai *et al.* 2010). In addition, Merlin is also able to

act in the nucleus directly, by binding to and inhibiting the promitogenic E3 ubiquitin ligase and general transcription regulator, $CRL4^{DCAF1}$ (Li, Cooper *et al.* 2014). The authors found that Merlin re-expression induced similar effects to DCAF1 silencing in primary human schwannoma cells, indicating that $CRL4^{DCAF1}$ activation caused by loss of Merlin is significant in tumorigenesis.

Another pathway in which Merlin is centrally involved is the Mitogen Activated Protein Kinase (MAPK) pathway that is notably deregulated in schwannoma (Kaempchen, Mielke *et al.* 2003, Morrison, Sperka *et al.* 2007, Ammoun, Flaiz *et al.* 2008). Merlin deficient schwannoma cells displayed prolonged ERK1/2 activation in comparison to healthy Schwann cells in response to elevated PDGFB signalling. Yi *et al.* found that Merlins action on the MAPK pathway is related to another protein, angiomotin (Yi, Troutman *et al.* 2011). The two were found to co-localize in Schwann cells functioning antagonistically to regulate signalling. When Merlin is bound to angiomotin, an effector protein, rich1, is released and able to inactivate Rac1 leading to decreased proliferation.

Merlin is also implicated in PI3K/Akt/mTOR signalling. A 2004 study showed that Merlin disrupts the binding of PIKE-L to PI3K, inhibiting its kinase activity and attenuating the signalling cascade (Rong, Tang *et al.* 2004). PI3K signalling is linked to enhanced proliferation in a variety of tumours and is associated with both meningioma and schwannoma tumorigenesis.

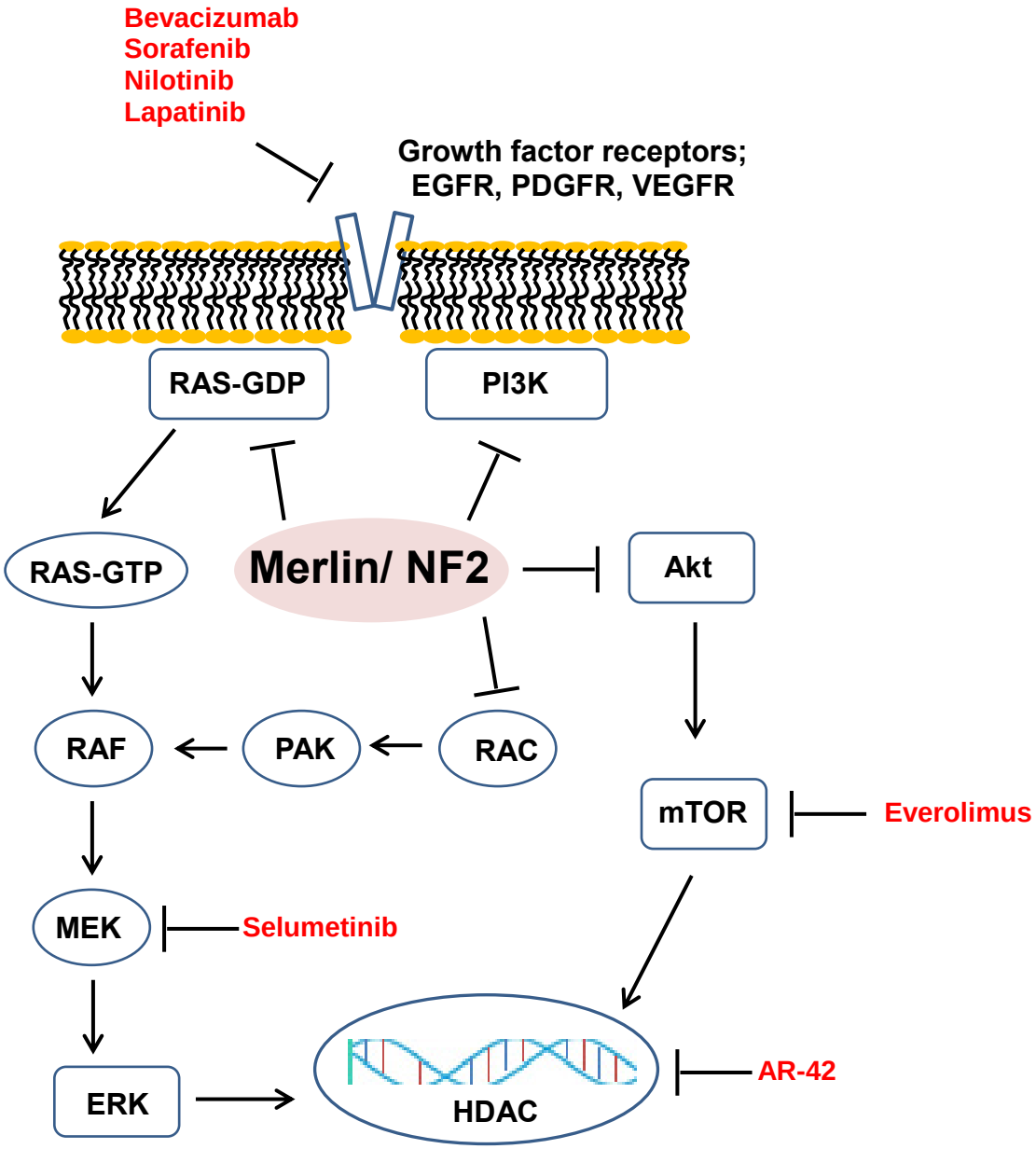

Figure 1.3: Drug targets and inhibitors reported to have beneficial effects on NF2 tumours. There are several proteins that have been identified as drug targets for NF2 tumours including growth factor receptors that are overexpressed in both schwannoma and meningioma (adapted from (Agarwal, Liebe *et al.* 2014)

Studies have shown via both immunohistochemistry and microarray that PI3/Akt components are upregulated and activated in schwannomas compared to normal nerve, thus representing potential therapeutic targets (Hanemann, Bartelt-Kirbach *et al.* 2006, Jacob, Lee *et al.* 2008, Hilton, Ristic *et al.* 2009). Similarly in meningiomas, 100% of tumours of all grades stained positively for pAkt (Hilton, Shivane *et al.* 2015). In 2014, Petrilli *et al.* identified an effective PI3K inhibitor (AS605420) via high-throughput compound screening and showed that it had potent pro-apoptotic effects on functionally Merlin-null Schwann cells inducing autophagy in those cells (Petrilli, Fuse *et al.* 2014). Altogether, the PI3K/ mTOR pathway represents a promising avenue for therapeutic intervention and inhibitors targeting this signalling cascade have been trialled in both meningioma and schwannoma. These results will be discussed in more detail later in the chapter.

1.9 Molecular targets and NF2 drug candidates

The mainstays of treatment for NF2, surgery and radiosurgery, have been associated with complications including vestibular dysfunction and the development of secondary malignancies (Evans, Birch *et al.* 2006). As no drugs have been approved for patients with NF2, translational research remains ongoing in efforts to identify new targets and/or therapies already approved for other tumour types that might be effective also for NF2 brain tumours. Figure 1.3 highlights the most relevant signalling pathways in NF2 and also shows some of the inhibitors known to have beneficial effects in NF2-related tumours models.

The most straightforward way to target cancer cells is to inhibit receptors at the cell membrane. Since the VEGFR is highly expressed in meningioma and schwannoma, targeting its ligand VEGF represents a promising treatment strategy for NF2. A phase II trial of PCT299, a VEGF inhibitor, began recruiting in 2009 but is yet to report any findings. Another VEGF inhibitor that has received considerable attention is Bevacizumab, that has been previously studied in glioblastoma (Uesaka, Shono *et al.*

2007, Chamberlain 2011). A 2012 retrospective review of 31 patients found that bevacizumab treatment led to tumour shrinkage in over 50% of NF2 patients with vestibular schwannomas, accompanied by hearing improvement (Plotkin, Merker *et al.* 2012). Another review of 12 NF2 patients showed that bevacizumab was effective in 50% of the cases. One patient however died from cerebral haemorrhage possibly in response to the therapy, highlighting the chance of fatal complications (Alanin, Klausen *et al.* 2014). Bevacizumab has also been linked to long-term toxicity relating to blood pressure and proteinuria in NF2 patients, emphasizing the need for rigorous dose control and monitoring by clinicians (Slusarz, Merker *et al.* 2014). This is because any therapy approved for NF2 treatment must confer long-term tolerability, given the benign nature of these tumours and the requirement for lifelong drug treatment. In meningioma, a response to bevacizumab was observed in only 14 out of 48 tumours indicating that it is not ideal as a general treatment for NF2 (Nunes, Merker *et al.* 2013).

A clinical trial for another VEGFR inhibitor, Axitinib, began recruiting in 2014 and aims to assess whether the drug is able to reduce schwannoma and possibly meningioma volume in NF2 patients. It has already been shown to have a favourable tolerability profile in renal cell carcinoma (Escudier and Gore 2011), and may therefore represent a good alternative to Bevacizumab.

As studies have identified the RTKs EGFR and ErbB2 as overexpressed/ activated in schwannoma (Curto, Cole *et al.* 2007, Ammoun, Cunliffe *et al.* 2010), the efficacy of the dual inhibitor Lapatinib was assessed in a phase II clinical trial for vestibular schwannoma (Karajannis, Legault *et al.* 2012). 17 out of 21 patients experienced a reduction in tumour volume of at least 15%, although usually a 20% reduction is considered to be a significant response. Several of those also experienced improvements in hearing. The authors concluded that, whilst objectively efficacious in some patients, Lapatinib might be more suitable as a combinatorial therapy alongside Bevacizumab. A phase II trial testing this combination found it effective in several patients with metastatic breast cancer (Rugo, Chien *et al.* 2012) . An inhibitor of ErbB2,

Trastuzumab, has also been assessed in a preliminary study looking at VS xenografts in mice. The inhibitor was able to induce a significant decrease in tumour growth, warranting further investigation (Clark, Provenzano *et al.* 2008).

Nilotinib, a small molecular inhibitor targeting both the PDGF receptor and the BCR-ABL oncoprotein has also been assessed *in vitro* for the treatment of schwannoma (Ammoun, Schmid *et al.* 2011, Sabha, Au *et al.* 2012). Both studies showed significant anti-tumour effects demonstrated by downregulation of PDGF mediated cell growth and proliferation. As Nilotinib has already been shown through trials to have generally high safety and tolerability, it therefore represents a good candidate for clinical trials in schwannoma. A phase II trial began in 2010 (NCT01201538) however no results have yet been reported.

Sorafenib, another small molecular inhibitor targeting the PDGFR and VEGFR is currently being assessed in a phase 0 trial for the treatment of schwannomas. This is based on *in vitro* results obtained by Ammoun *et al.* that showed Sorafenib treatment decreased ERK1/2 activity and decreased proliferation in human primary schwannoma cells (Ammoun, Flaiz *et al.* 2008).

The mTOR pathway is also an important mediator of growth and proliferation in Merlin null tumour cells (James, Han *et al.* 2009) thus warranting investigation as a potential target in NF2 treatment. The mTOR inhibitor Everolimus has been tested in clinical trials as a general therapy for NF2. The results of a phase II study assessing the effectiveness of Everolimus in NF2 patients were published early in 2015. The primary endpoint was a reduction of > 20% in tumour volume from baseline, which 0/10 patients were able to achieve (Goutagny, Raymond *et al.* 2015). Goutagny *et al.* found that although Everolimus was unable to induce VS shrinkage, it was able to increase stabilization and cause growth delay (Goutagny, Raymond *et al.* 2015). Everolimus was also able to decrease cell survival and growth in both malignant and benign meningioma cell lines (Pachow, Andrae *et al.* 2013). Whilst Everolimus was unable to

reduce tumour size in schwannoma, its ability to cause growth delay means that it might still represent a potential drug therapy for NF2.

The MEK inhibitor Selumetinib (AZD6244) has also been tested pre-clinically in primary schwannoma cells and was shown to completely abolish PDGF mediated cell proliferation (Ammoun, Ristic *et al.* 2010). As this pathway is the most prominent in schwannoma pathogenesis, these results highlight MEK as a promising therapeutic target that may also be useful for meningioma treatment.

Another inhibitor that has proven efficacy in both meningioma and schwannoma is AR-42, targeting Histone deacetylases (HDAC). Burns and colleagues showed that AR-42 induced the pro-apoptotic protein Bim and decreased the potential for tumour re-growth after treatment in meningioma cells (Burns, Akhmametyeva *et al.* 2013). Further, Jacob *et al.* also showed that AR-42 was able to suppress growth and induce apoptosis in murine schwannoma xenografts (Jacob, Oblinger *et al.* 2012). Both studies also concluded that AR-42 is well tolerated. Subsequently, a phase 0 trial began recruiting in 2014 (NCT02282917) assessing AR-42 in both schwannomas and meningiomas and is still actively recruiting.

1.10 Omics approaches to identify novel targets in NF2

“Omics” is a term used to describe holistic approaches to the study of expression and/or regulation in any given organism. As such, omics techniques may be used to study genomes, proteomes, transcriptomes and metabolomes, among others (Chambliss and Chan 2016). Commonly used methods include Next Generation Genome Sequencing (NGS) which is a collection of techniques useful for identifying DNA mutations or epigenetic regulatory mechanisms that can be exploited in disease therapy, particularly in cancer (Chambliss and Chan 2016). Mass spectrometry is used to study protein expression, and also post-translational modifications (PTMs) such as phosphorylation and acetylation. The main advantage of omics technologies is their provision of large, complex, unbiased data sets otherwise difficult to obtain. Most omics

techniques are intended to identify biomarkers for more efficient diagnostics, and new targets for disease treatment. There have been a wealth of studies conducted utilizing genomics technologies in the search for NF2 biomarkers, drug targets and markers of progression (Buckley, Mantripragada *et al.* 2005, Lusis, Chicoine *et al.* 2005, Wrobel, Roerig *et al.* 2005, Hanemann, Bartelt-Kirbach *et al.* 2006, Aarhus, Bruland *et al.* 2010, Caye-Thomasen, Borup *et al.* 2010, Chang, Shi *et al.* 2013, Agnihotri, Gugel *et al.* 2014) and also for predicting disease recurrence (Bie, Zhao *et al.* 2011).

Hanemann *et al.* identified 41 genes by cDNA microarray and validated 36 of those by Real-Time Polymerase Chain Reaction (RT-PCR), finding seven to be significantly upregulated in schwannoma compared to Schwann cell cultures including VEGF and IGFBP-1 (Hanemann, Bartelt-Kirbach *et al.* 2006). A 2014 study of 49 schwannomas *vs.* 7 vestibular nerve tissues, the largest to date, identified over 4000 differentially expressed genes by Affymetrix gene expression profiling. They concluded that the PI3K/Akt/mTOR pathway is the most relevant therapeutic target for schwannoma patients (Agnihotri, Gugel *et al.* 2014). Caye-Thomasen *et al.* performed microarray analysis of 16 schwannomas compared to vestibular nerves and found proteins linked to the extracellular matrix and cell adhesion to be the most relevant (Caye-Thomasen, Borup *et al.* 2010). Finally Torres-Martin and colleagues performed a genomic analysis of 31 vestibular schwannomas and identified dysregulation among 1,516 genes compared to normal control nerves, concluding that there is considerable upregulation of several miRNAs that may represent therapeutic targets (Torres-Martin, Lassaletta *et al.* 2013).

Several studies looking at gene expression in meningioma have focussed on obtaining specific genomic signatures relating to WHO grade I, II or III (Wrobel, Roerig *et al.* 2005, Carvalho, Smirnov *et al.* 2007, Fevre-Montange, Champier *et al.* 2009). Carvalho *et al.* failed to find any significant difference in expression between benign, atypical and anaplastic meningioma (Carvalho, Smirnov *et al.* 2007), but found that tumours across all three grades can be defined collectively as either ‘low proliferative,’

or ‘high proliferative.’ The latter were generally classified based on the reduced expression of genes corresponding to Transforming Growth Factor-beta (TGF-β) signalling. These data indicate that perhaps targets should be identified that are overexpressed in all tumour grades compared to control, allowing us to treat all grades with the same therapeutic agents. In contrast, a 2012 study looking at differences between benign meningioma and brain arachnoid tissue by cDNA microarray found that ECM interaction and focal adhesion pathways were more highly activated in grade II meningioma compared to grade I. EGFL6, a member of the EGF family of proteins, was upregulated in benign tumours compared to healthy arachnoidal tissue and, similar to Agnihotris study in schwannomas, several components of the PI3K/Akt pathway were upregulated in meningioma tumour tissue (Wang, Gong *et al.* 2012). This reflects what was already known in the field and highlights it as a promising area for further study.

A recent genomic analysis between meningioma and schwannoma identified Platelet-Derived Growth Factor Alpha (PDGFA), Slit Guidance Ligand 2 (SLIT2), Cadherin-1 (CDH1) and tyrosine-kinase protein met (MET) as mutually upregulated compared to their respective controls. Functional annotation identified both the inflammatory response and cell migration as biological processes concomitantly upregulated in both tumour types (Torres-Martin, Lassaletta *et al.* 2014). The authors concluded that pathways relating to PDGF, c-MET and SLIT2 were the most promising targets for therapeutic intervention.

1.11 The proteomic approach

Proteomic methods are generally more time consuming and require more biological material than genomic techniques. For this reason, more studies have been published that look at gene expression, which does not always correspond to what is happening at the protein level. And since it is proteins that are more commonly exploited as drug

targets, analysing the proteome is a more relevant method to identify potential novel therapeutic candidates and/ or biomarkers.

Most proteomics studies utilize mass spectrometry (MS), which allows the identification of thousands of proteins in individual experiments. As it is quite a specialised and expensive technique, the number of studies published in this field is relatively few. The first example of a proteomic comparison between meningioma grades was published in 2006 (Okamoto, Li *et al.* 2006). Using 2D gel electrophoresis coupled with MS, the investigators identified nine proteins significantly overexpressed in atypical compared to benign meningiomas, and six that were downregulated. A later study compared grade I meningioma with arachnoid tissue and found 281 proteins to be differentially expressed, including several proteins of the minichromosome maintenance (MCM) family, many of which were exclusively expressed in tumours and might therefore represent reliable meningioma biomarkers (Saydam, Senol *et al.* 2010). In 2015, Sharma *et al.* identified 290 upregulated proteins across 14 grade I meningiomas compared to healthy brain tissue. These represented several biological pathways including integrin signalling and, as in the genomic studies discussed previously, mTOR signalling (Sharma, Ray *et al.* 2015).

There is one study published that utilized MS to analyse VS, which only compared two schwannomas against two healthy nerve specimens. The authors identified 29 differentially expressed proteins, and concluded that seven are involved in apoptosis. (Seo, Park *et al.* 2015). An earlier study was able to identify the most frequently activated RTKs in 68 schwannomas, using RTK arrays to confirm the activation of PDGFR and ErbB2. The study also used reverse-phase protein array (RPPA) to measure the activity of known components of mitogenic signalling pathways, and identified a YAP-driven network linked to proliferation (Boin, Couvelard *et al.* 2014). This is in keeping with Merlins known regulatory role within the Hippo pathway (Zhao, Li *et al.* 2010).

1.12 Studying the phosphoproteome

Phosphorylation is a post-translational modification and a key mechanism of protein regulation. Abnormalities in protein phosphorylation give rise to various disease states, including cancer (Blume-Jensen and Hunter 2001, Zhou, Di Palma *et al.* 2013). Approximately 30% of the whole eukaryotic proteome is transiently phosphorylated at any one time (Cohen 2000, Ruprecht, Koch *et al.* 2015). As phosphorylated proteins represent a relatively small fraction of the total proteome, enrichment is necessary to minimize background noise from more abundant non-phosphorylated proteins. The study of phosphorylation has seen the most advances over the course of the last 20 years, and there are now several methods that have been developed to enable the most comprehensive coverage of the phosphoproteome than ever before.

Phosphoprotein isolation (Figure 1.4, left) separates phosphorylated proteins from their unphosphorylated counterparts prior to in-gel digestion. Phosphoproteins bind by affinity chromatography to a column and non-phosphorylated proteins flow through. Phosphoproteins are then eluted, separated on an acrylamide gel, digested and measured by MS.

Phosphopeptide enrichment begins when whole cell lysates are first subjected to in-gel tryptic digestion, and resulting peptides are subsequently enriched. At this point, the majority of unphosphorylated peptides are washed away leaving only phosphorylated peptides for MS analysis (Figure 1.4, right).

1.12.1 Phosphopeptide enrichment

The primary enrichment techniques are Immobilized Metal Affinity Chromatography (IMAC) and the more recently developed Titanium dioxide (TiO_2). The latter has been used for phosphopeptide enrichment since 2004/5 when the first studies were published (Kuroda, Shintani *et al.* 2004, Pinkse, Uitto *et al.* 2004, Larsen, Thingholm *et al.* 2005) providing proof of concept that TiO_2 was a suitable material for this purpose. Larsen's study included 2, 5-dihydroxy- benzoic acid (DHB) in the loading buffer in an

attempt to decrease non-specific binding and found that this increased the selectivity to above that of previous reports for IMAC (Larsen, Thingholm *et al.* 2005). The authors tested both methods with a variety of different detergents/ buffers and found TiO_2 to retain some binding efficacy, even in the presence of strong detergents such as Sodium Dodecyl Sulphate (SDS). Whilst IMAC is still widely used and somewhat effective, TiO_2 may be considered superior simply because it is compatible with a wider spectrum of reagents. For this reason, TiO_2 was selected for use in this project.

1.12.2 Phosphoprotein purification

Phosphoprotein purification can be used to separate phosphorylated proteins from their non-phosphorylated counterparts prior to digestion. Whilst this method is effective, unlike phosphopeptide enrichment it is more difficult to derive phospho site-specific information. This is because there is generally a higher ratio of non-phosphorylated peptides in the final sample, which can affect the overall identification of phosphopeptides. However, advantageously the technique requires less material and is technically less challenging than the phosphopeptide enrichment procedure.

There are several examples in the literature detailing the successful application of this method, including studies in mammalian cells, yeast and plants (Metodiev, Timanova *et al.* 2004, Makrantoni, Antrobus *et al.* 2005, Meimoun, Ambard-Bretteville *et al.* 2007, Santamaria, Sanchez-Quiles *et al.* 2012). All of them concluded that the Qiagen™ affinity column is efficient and effective for the selective purification of phosphorylated proteins that can then be analysed by MS.

Metodiev and colleagues were able to demonstrate the striking capability of these columns to retain phosphorylated proteins whilst their non-phosphorylated counterparts flow through. Using a phospho-tyrosine specific antibody, the authors showed that the flow-through fraction did not contain any tyrosine-phosphorylated proteins whilst many were seen in the retained fraction. Similarly, Meimoun *et al.* used ^{32}p-phosphate labelled proteins to analyse the phosphoproteome of Sorghum plants, concluding that

the affinity column is able to capture at least 80% of phosphorylated proteins (Meimoun, Ambard-Bretteville *et al.* 2007).

Based on the positive results reported in these studies, this method was utilized extensively for the global phosphoproteomic analysis of meningioma and schwannoma cells compared to their respective controls.

1.13 Aim

The aim of this study is to identify and validate novel therapeutic targets to enable treatment of Merlin-deficient meningiomas and schwannomas especially when they arise as part of the genetic condition NF2. This study presents a novel, comparative exploration of commonly aberrantly phosphorylated proteins in both cell types, as a step towards an effective treatment for NF2 patients. Using a combination of phosphoprotein purification, MS and complex data analysis, we aim to identify phosphoproteins that have the potential to be further analysed and eventually harnessed in a clinical setting.

The datasets obtained for both tumour types will first be analysed independently to identify changes specific to either schwannoma or meningioma. Following that, the data will be analysed comparatively to identify common potential therapeutic targets that will be validated and functionally assessed in both cell types.

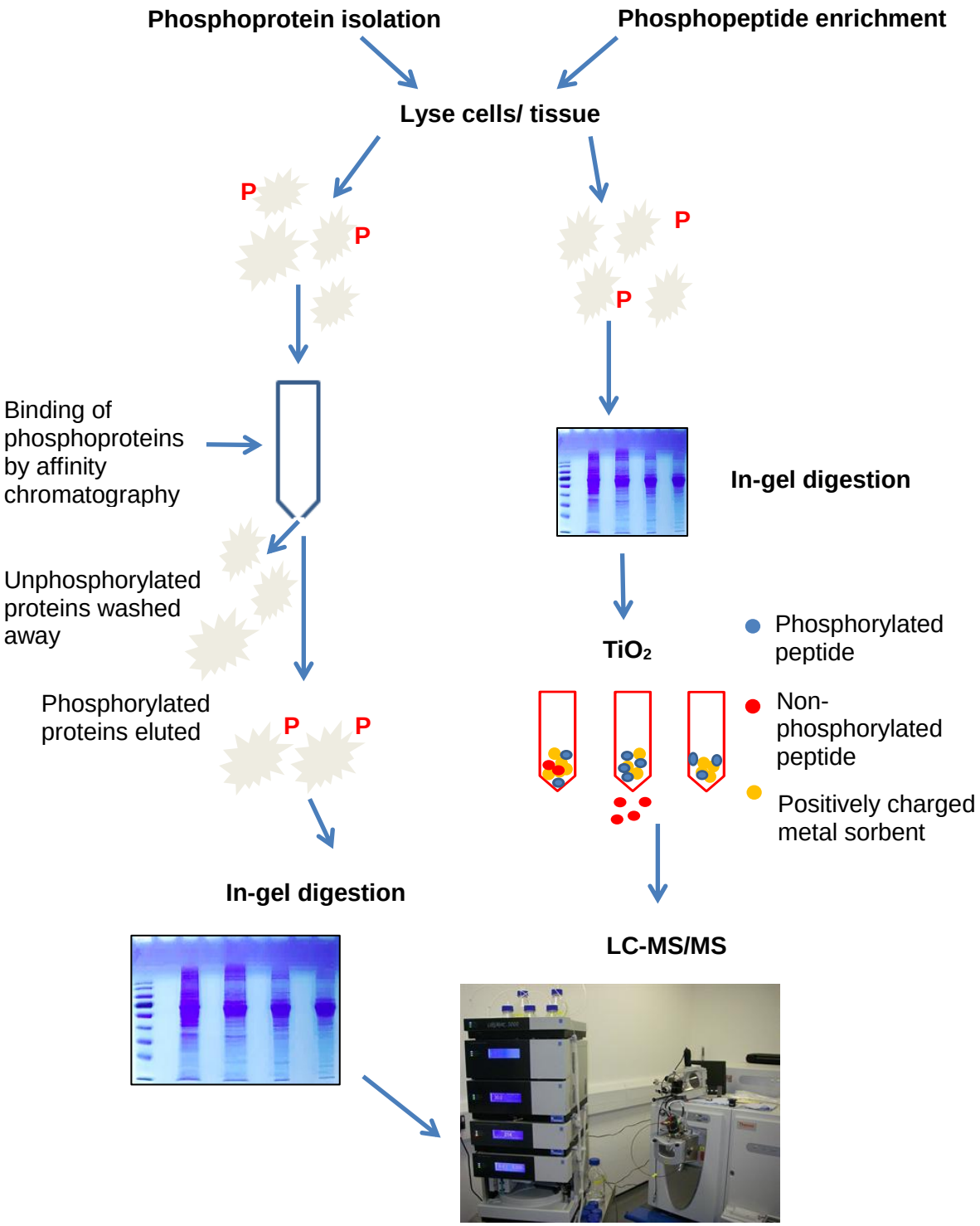

Figure 1.4: A schematic representation of the phosphoproteomic workflow. Phosphoprotein isolation separates phosphorylated whole proteins from non-phosphorylated whole proteins. Phosphopeptide enrichment is performed on digested peptides. In both cases, proteins/ peptides that are not phosphorylated do not bind to the column and are washed away.

.

Chapter 2- Materials and methods

Antibodies

Table 2.1: Antibodies used in this study				
Antibody	**Type**	**Clone**	**Company**	**Dilution**
Merlin/ NF2	Rabbit polyclonal	D1D8	Cell signalling	1:1000
GAPDH	Mouse monoclonal	6C5	Millipore	1:50000
STAT1_Y701(Western blot)	Rabbit polyclonal		R and D systems	1:1000
STAT1_Y701 (Immunoprecipitation)	Rabbit monoclonal	D4A7	Cell signalling	1:40
STAT1_S727	Rabbit polyclonal		Cell signalling	1:1000
STAT1	Rabbit polyclonal		Santa Cruz biotechnology	1:1000
pERK	Rabbit polyclonal		BD biosciences	1:1000
Total ERK	Rabbit monoclonal	137F5	Cell signalling	1:2000
PDLIM2 (western blot)	Rabbit polyclonal		Cell signalling	1:500
PDLIM2 (Immunocytochemistry and immunoprecipitation)	Rabbit polyclonal	H-71	Santa Cruz biotechnology	1:200
HSPA1A	Mouse monoclonal	C92F3A-5	Novus biologicals	1:1000
HSPA1A_Y525 (Immunohistochemistry)	Rabbit polyclonal		Biorbyt	1:200

HSPA1A_Y41	Rabbit polyclonal		Pierce	1:200
FLNB	Mouse monoclonal		Santa Cruz biotechnology	1:1000
KI-67	Rabbit polyclonal		Abcam	1:1000
pFLNA/FLNB	Rabbit polyclonal		Abcam	1:1000
IgG control	Rabbit polyclonal	D145	Santa Cruz Biotechnology	1µg/mg
EGFR_T693	Rabbit polyclonal	EP2256Y	Cell signalling	1:1000
SMAD2_T8	Rabbit polyclonal		Abcam	1:500

2.1 Cell culture

2.1.1 Sample collection and culture conditions

All primary tumour and normal tissue specimens used throughout this project were obtained either as part of the 'Investigation into the expression of signalling molecules in human brain tumour samples (REC number 6/Q2103/123)' or the 'Identifying and validating molecular targets in low grade brain tumours (REC number 14/SW/0119) study'. Fresh tumours were made in to cell cultures by tumour digestion with collagenase upon arrival at the laboratory.

Human Schwann cells were obtained from post mortem tissue of consented individuals with no medical history of peripheral neuropathy. Donated tissue was transported from the hospital to the laboratory in DMEM (Gibco, Life technologies) supplemented with 10% FBS, 500 U/ml Penicillin/ Streptomycin (Gibco) and 2.5 µg/ml Amphotericin B (Simga- Aldrich). Tumours were obtained after surgery and upon arrival were incubated for 24 hours in petri dishes containing DMEM supplemented with 10% FBS, 500 U/ml Penicillin/ Streptomycin (penstrep), 2 µM forskolin (Sigma-Aldrich) and 2.5 µg/ml Amphotericin B at 37^{o}C and 10% CO_2. Primary meningiomas were transported in media containing 10% FBS/500 U/ml penstrep and incubated for 24 hours at 37^{o}C/ 5% CO_2.

Tumour/ nerve samples were mechanically digested with glass pipettes of decreasing diameter and thereon cultured in respective media; for Schwann/ schwannoma cells: DMEM, 10% FBS, 100 U/ml Penicillin/ Streptomycin, 0.5 µM forskolin, 2.5 µg/ml amphotericin, 2.5 µg/ml insulin and 10nM β-heregulin, at 37^{o}C and 10% CO_2. Schwann and schwannoma cells were cultured on plates coated with poly-L-lysine (PLL) (30 minutes at room temperature) followed by laminin (overnight at 4^{o}C). Meningioma cells were cultured in HAMS F-12 media (Gibco) containing 10% FBS, 1% Penicillin/ streptomycin and 12.5 ng/ ml insulin.

2.1.2 Cell lines

A meningioma cell line, Ben-Men-1, was used throughout this project. This is an immortalized cell line derived from a benign meningioma originally developed by Puttmann *et al.* (Puttmann, Senner *et al.* 2005). Cells were grown in DMEM, 10% FBS and 100 U/ml Penicillin/Streptomycin and kept at 5% CO_2/ 37ºC. Human meningeal cells (HMC) were obtained from Sciencell™ and maintained in the manufacturers recommended media and grown under the same conditions.

2.1.3 Passaging of cells

Primary cells were cultured until confluent or required cell density. For passaging, cells were washed once with phosphate buffered saline (PBS, Gibco®) and incubated with trypsin/EDTA (Gibco®) at 37ºC for approximately 2 minutes until all cells were detached. Trypsin was neutralised with normal medium and solutions were resuspended in an appropriate volume of culture medium before seeding in fresh flasks (Greiner®).

2.2 Western blotting

2.2.1 SDS-PAGE

Cells were lysed in RIPA buffer consisting of 150mM NaCl, 5mM of 0.5 M EDTA, pH 8.0, 1M Tris, pH 8.0, 1% NP-40, 0.5% of 10% sodium deoxycholate, 10% SDS, 84% H_2O. Protein concentration was determined using a colorimetric BCA protein assay (Pierce®) by measuring absorbance at 562 nm. A reference curve was generated based on protein standards of decreasing concentration from a stock solution of 2 mg/ml Bovine Serum Albumin (BSA). Comparison of sample absorbencies to the standard curve provided a relative analysis of protein concentration. Equal sample amounts were mixed with 4x reducing buffer (250 mM Tris-HCL [pH6.8], 8% SDS, 40% glycerol, 200 mM DTT and 0.4% bromophenol blue) and boiled for 5 minutes at 90ºC.

Table 2.2: Gel recipes				
Component	**Percentage acrylamide (resolving gel)**			**Stacking gel**
	6%	**8%**	**10%**	**4%**
40% acrylamide	1.2ml	1.6ml	2ml	0.75ml
1.5M Tris HCl, pH 8.8	2ml	2ml	2ml	X
1M Tris HCl, pH 6.8	X	X	X	1.25ml
10% SDS	80µl	80µl	80µl	50µl
10% ammonium persulfate	80µl	80µl	80µl	50µl
TEMED	8µl	8µl	8µl	5µl
Distilled H_2O	4.6ml	4.2ml	3.8ml	2.9ml

Proteins were then separated via SDS-PAGE electrophoresis. 6-10% resolving gel/ stacking gel recipes are shown in table 2.2. Gels were run at constant amperage of 30 mA for 60 minutes at Room Temperature (RT). Samples intended for MS measurement were separated using 4-15% gradient pre-cast gels (Biorad).

2.2.2 Transfer and immunoblotting

Proteins were transferred to PVDF membranes (Biorad) at 400 mA constant for 70 minutes at RT, via wet blotting in transfer buffer (25 mM Tris, 19.2 mM glycine and 15% methanol). Membranes were blocked for 1 hour at RT in blocking milk (5% dried skimmed milk and 0.1% Tween in PBS) before being probed with primary antibody, shaking overnight at 4^{o}C. Membranes were then washed in PBS-tween and incubated with appropriate HRP-conjugated secondary antibodies (Biorad) diluted 1:5000 in blocking milk for 1 hour at room temperature. After three washes in PBS-tween, ECL was used for detection (Pierce®) and light sensitive films (hyperfilm ECL, Amersham) were used for exposure. GAPDH was used as a loading control in all cases.

2.2.3 Protein quantification and statistical analysis

Films were scanned in greyscale at a resolution of 600 dpi. Image J was used for relative quantification of Western blots, where amounts of protein are recorded as ratios - protein band: loading control band in the same lane. Prior to density measurement, all blots were inverted so bands appeared white on a black background. The rectangle tool was selected and used to draw a box around the largest band and was subsequently used to measure the density of all other bands. The same box was used to take a background measurement containing no protein bands which would later be subtracted from each individual band measurement. The same was done for loading control bands corresponding to each protein band. Finally, protein band densities were normalized to corresponding loading control values.

Average values were calculated across control samples and across tumour samples. The average for tumour samples was then divided by the average for the control. The control value was divided by itself, giving a reference value of 1, against which the average tumour value would be plotted graphically. T-tests were then performed on normalized density values to determine whether the difference between control and tumour values were significant.

2.3 Proteomics

2.3.1 In-Gel Digestion

In-gel digestion was performed based on a previously published protocol (Shevchenko, Wilm *et al.* 1996). Protein gels were stained with colloidal coomassie blue stain (life technologies) for 3 hours at RT. De-staining was achieved by incubation with mass spectrometry grade water (Fisher) overnight at RT. Gels were fractionated by cutting in to small 1 mm x 1 mm pieces before the in-gel digestion protocol proceeded as follows. Per slice, equilibration in 200 µl of 50 mM Ammonium Bicarbonate (ABC) for 5 minutes at 37^{o}C, de-staining in 200 µl of 50% acetonitrile (ACN)/ 50% H_2O for 5 minutes at 37^{o}C then 200 µl of 100% ACN for 5 minutes at 37^{o}C. These steps are repeated 3

times. 200 µl of reduction buffer (10 mM dithiothreitol in ABC) was added to the gel slices and incubated for 20 minutes at 56°C. Slices were then shrunk using 100% ACN for 5 minutes at RT and alkylated using 200 µl of alkylation buffer (23.35 mg 2-choloroacetamide, 5ml of 50 mM ABC) for 20 minutes at RT in the dark. The gel pieces were incubated with digestion buffer (12.5 ng/µl trypsin in ABC) overnight at 37 °C. Digested peptides were extracted by the addition of 2% Trifluoroacetic Acid (TFA) to the digestion buffer incubated for 20 minutes on a shaker at 37ºC. Peptide solutions were then transferred to fresh tubes, and 100 µl of buffer B **(**80% ACN, 0.5% acetic acid, 1% TFA) was added to the gel pieces and incubated for a further 20 minutes on a shaker at 37ºC. The buffer B solution was then combined with the respective solution from the first peptide extraction, and samples were concentrated in a DNA centrifuge (Labconco centrivap®) until less than 40 µl of sample was left.

2.3.2 Stage Tips

Stage-tipping was performed as previously described (Rappsilber, Ishihama *et al.* 2003). Stage tips were assembled by placing high performance extraction disk (C18) into a pipette tip using a picking tool. 50 µl of methanol was added to the prepared stage tips and centrifuged until the whole volume has passed through in order to hydrate the matrix. This is repeated with buffer B (80% acetonitrile, 0.5% acetic acid) and then twice with buffer A (0.5% acetic acid) for equilibration. Samples are centrifuged (1 minute; 10,000 g; room temperature) and added to stage tips and centrifuged again till the sample has passed through. 50 µl of buffer A was added and centrifuged until all the volume has passed through. Peptides are then eluted by addition of 20 µl of buffer B and centrifugation. The samples are then concentrated using a concentrator and buffer A is added to give a final volume of 25 µl.

2.3.3 Titanium dioxide (TiO_2) phosphopeptide enrichment

Titanium dioxide (TiO_2) was performed based on a report published in 2013 (Fukuda, Hirabayashi-Ishioka *et al.* 2013). Peptide concentration per sample was determined before being mixed with TiO_2 beads in a 2:1, peptide: bead ratio. First, the beads were equilibrated with 200 µl of buffer A (5% TFA, 5% glycerol, 60% ACN, 30% H_2O), shaking for 5 minutes at RT. 200 µl of buffer B (5% TFA, 5% glycerol, 60% ACN, 30% H_2O) was then added to the beads and mixed for 5 minutes on a shaker. During this time, samples were sonicated to sheer DNA and dissolve peptides. Samples were then mixed with beads and incubated for 1 hour at RT on a shaker. During incubation, individual columns were constructed by inserting small silica frits in to pipette tips. After incubation, samples were added to the pipette tips and centrifuged (7000 g, 3 minutes) to pack the beads and allow unbound phosphopeptides to flow through. The beads were then washed three times with buffer A, and then three times with buffer A for 1 min at 300 g each time. Bound phosphopeptides were then eluted with two subsequent 100 µl volumes of NaOH, before neutralization with an equal volume of 10% TFA ready for stage tipping.

2.3.4 Phosphoprotein purification

Phosphoprotein purification kits were purchased from Qiagen® and incorporate affinity chromatography for the selective isolation of phosphorylated proteins. The procedure was performed on cultured cells using lysis buffer containing 0.25% CHAPS, benzonase and protease inhibitors supplied by the company. For each sample, a T75 flask (Greiner) of cells was lysed and incubated for 30 minutes at on ice with vortexing every 10 minutes before centrifugation at 10000 g for 30 minutes at 4^{o}C. During centrifugation columns were equilibrated with 4ml lysis buffer that was allowed to flow through. Supernatant was harvested from centrifuged samples and protein concentration was adjusted to 0.1 mg/ml to ensure accessibility and maximal binding of phosphoproteins. Half of the lysate was added to the column and allowed to flow

through, followed by the second half. When all the lysate passed through, 6 ml of lysis buffer was applied to wash the column. After, 3 ml of elution buffer (supplied with the kit) was added to the column to elute the phosphoproteins. SDS-PAGE and in-gel digestion were subsequently performed prior to MS.

2.4 Mass spectrometry

2.4.1 Liquid Chromatography Tandem Mass Spectrometry

MS was carried out using an ultimate 3000 UPLC system (Thermo Fisher, Germany) connected to an Orbitrap Velos Pro mass spectrometer (Thermo Fisher, Bremen, Germany). The prepared peptides were loaded on to a 2 cm Acclaim™ PepMap™100 Nano-Trap Column (Thermo Fisher, Germany) and separated by a 25cm Acclaim™ PepMap™100 Nano LC column (Thermo Fisher, Germany) that is packed with C18 beads of 3 µm and running a 120 min gradient of 95 % buffer A /5% buffer B (buffer A contains 0.5% acetic acid and buffer B contains 0.5% acetic acid in 100% acetonitrile) to 65% buffer A /35 % buffer B and a flow rate of 300 nl/min. Eluted peptides were electrosprayed into the mass spectrometer at a spray voltage of 2.5 kV. The Orbitrap instrument performs data acquisition in a data dependent mode to switch between MS and MS2. The Orbitrap cell with a resolution of 60,000 acquires a full-scan MS spectra of intact peptides (m/z 350–1500) with an automated gain control accumulation target value of 10,000,000 ions. In the linear ion trap the ten most abundant ions are isolated and fragmented by applying collision induced dissociation using an accumulation target value of 10,000, a capillary temperature of 275°C, and normalized collision energy of 30%. A dynamic exclusion of ions previously sequenced within 45 s was applied. Any singly charged ions and unassigned charged states were excluded form sequencing and also a minimum of 10000 counts was required for MS2 selection.

2.4.2 Peptide identification and Quantification

The Andromeda search engine (Cox, Neuhauser *et al.* 2011) integrated in Maxquant version 1.5.3.8 (Cox and Mann 2008) was used to identify the proteins. Protein sequences were downloaded from UNIPROT. A mass tolerance of six ppm for the parental peptide, 0.8 Da for fragmentation spectra and a trypsin specificity allowing up to 2 mis-cleaved sites were set as Andromeda search parameters. Fixed modification of carboxyamidomethylation of cysteines and variable modification of deamidation of glutamine, and a minimal peptide length of six amino acids were set. Maxquant performed an internal mass calibration of measured ions and peptide validation by the target decoy approach as described (Elias and Gygi 2010). Proteins and peptides with better than 1% false discovery rate (FDR) were accepted. Proteins were quantified by normalised summed peptide intensities computed as label free quantification (LFQ) values in Maxquant (Cox, Hein *et al.* 2014).

2.4.3 Raw data processing

Data generated by Maxquant were processed using Microsoft Excel and specially developed proteomics software, Perseus®. LFQ values were Log2 transformed and fold change was calculated based on the equation: Average Log2 LFQ tumour – Average Log2 LFQ control. A 2 sample t-test with equal variance was performed generating p-values for each identified protein/ phosphoprotein. The proteins with a p-value < 0.05 were considered for further analysis. Benjamani-Hochberg False Discovery Rate (FDR) was explored using Perseus but was not used for the final selection of candidates. Significantly changed phosphoproteins were then compared against respective total protein changes to identify those with ‘true’ activation i.e. a significant change in phosphorylation and little/no change or a decrease in total protein abundance.

2.5 Immunostaining

2.5.1 Immunocytochemistry

Cells were cultured to desired confluency in labtek™ 8-well chambers. Fixation was carried out using ice-cold methanol for five minutes. Cells were blocked in 10% BSA/1% PBS for one hour at RT and washed three times for five minutes in PBS. Primary antibodies were diluted in 1% BSA and applied overnight at 4°C. Slides were then washed twice for five minutes in PBS before the addition of appropriate fluorescent secondary antibodies (Alexa, Life technologies) for one hour in the dark at RT. After one five minute wash with PBS, DAPI nuclear stain (1:500 from a stock solution of 1 mg/ml) was added for 10 minutes at RT in the dark. Slides were washed three times in PBS for five minutes each before the addition of vectashield® mounting medium and cover slips. Slides were then stored at 4°C in the dark until imaging.

To determine the localization of proteins, imaging was performed using a Leica TCS SP8 confocal microscope and images were taken using the associated LAS X software. All images were captured at 40x magnification.

2.5.2 Immunohistochemistry

Formalin fixed Paraffin Embedded Tissue (FFPE) tissue sections were cut at 20 µm. Paraffin was removed from the sections by incubation at 60°C for 20 minutes. This was performed at the histopathology lab at Derriford hospital, Plymouth. Preliminary experiments were performed by Leanne Kirk to determine the optimal pre-treatment and antibody dilution conditions.

For phospho-Heat Shock 70kDa Protein 1A (pHSPA1A) staining: Sections were washed twice in xylene for five minutes followed by a five minute wash in 100% ethanol. Sections were then washed for five minutes in running water before blocking with 3% H_2O_2 in methanol for 60 minutes. Sections were then washed in running water for ten minutes, and boiled for 30 minutes in citrate buffer as a pre-treatment (2.1 g of citric

acid in 2L of deionised water, pH 6.0) for the purpose of antigen retrieval to allow the antibody to bind. Slides were subsequently washed for ten minutes in running water before immersion for five minutes in TBST for equilibration. After, sections were blocked for 30 minutes in 5% normal horse serum in TBST. Primary antibody was then applied at 1:200 overnight at 4^{o}C.

Slides were washed twice in TBST for five minutes each before secondary antibody was applied for 30 minutes at RT. After, slides were washed twice in TBST for five minutes each and tertiary antibody was applied for 30 minutes at RT which is designed to bind to the secondary antibody. The tertiary antibody is conjugated to horse radish peroxidase that yields a coloured product upon reaction with the substrate, that is detectable using a light microscope. Slides were washed again in TBST for five minutes before DAB (3,3'-diaminobenzidine) solution was applied for five minutes to produce brown staining. After a ten minute wash in running water, slides were immersed in copper sulphate DAB enhancer for five minutes. Slides were washed again in running water for five minutes, before haematoxylin counterstain was applied for a further two minutes. Slides were finally washed twice for five minutes in 100% ethanol for complete dehydration, followed by two washes in xylene. DPX mounting media was applied to coverslips, and slides were applied face down.

Images were acquired using a Leica DMRB and the intensity of staining was assessed semi-quantitatively with the help of consultant neuropathologist, Dr David Hilton (Derriford hospital, Plymouth).

2.6 shRNA mediated gene silencing

Cultured cells were seeded at 80% confluency before transfection with lentiviral particles directed towards either STAT1 (Santa Cruz) or PDLIM2 (Sigma) in the presence of 5 µg/ml polybrene (Santa Cruz biotechnology), using a multiplicity of infection (MOI) of 5 in each case. Lentivirus was applied for 24 hours, at which point media was removed and replaced with normal media for a further 24 hours. Puromycin

was then applied to cells at a concentration of 5 µg/ml to facilitate selection of those expressing the Puromycin resistance gene. Selection took place over 4-5 days, at which point cells were lysed for Western blot analysis, fixed and stained for Ki-67 expression.

2.7 Antibody crosslinking

Prior to MS analysis, antibodies were cross-linked to agarose beads to inhibit co-elution of IgG fragments with the bait protein and to stabilize the transient interactions between binding partners, replacing weak interactions with covalent bonds. These large proteins make it difficult for the instrument to identify signals from less abundant proteins that have also co-eluted. Antibody crosslinking was performed using a commercial kit from Pierce ® and all centrifugation steps were performed at 1000g for one minute unless stated otherwise.

For each antibody, 20 µl of protein A/G plus agarose slurry was pipetted into a Pierce spin column and centrifuged. The resin was then washed twice with 1x coupling buffer (0.01 M sodium phosphate, 0.15 M NaCl; pH 7.2) and centrifuged each time. 10 µg of antibody, 20x coupling buffer and water were mixed together to a final volume of 100 µl. This mixture was then applied to the column and incubated on a mixer at RT for 60 minutes. After this time, the column was centrifuged and the resin was washed three times with 1x coupling buffer.

Cross-linking of the bound antibody was achieved using disuccinimidyl suberate (DSS). 2.5 µl of coupling buffer, 9 µl of 2.5 M DSS and 38.5 µl of ultrapure water were added to the column containing the antibody resin. The column was the incubated on a mixer for one hour at RT. The column was then centrifuged and the flow-through discarded. 50 µl of elution buffer (containing primary amine, pH 2.8) was added to the column and centrifuged. The column was then washed twice with elution buffer to quench the reaction and remove any non-crosslinked antibody. After two wash steps with 200 µl cold IP/ lysis buffer (0.025 M Tris, 0.15M NaCl, 0.001M EDTA, 1% NP-40, 5%

glycerol; pH 7.4),the column was either stored in PBS containing 0.02% sodium azide or utilized for the co-immunoprecipitation (co-ip) protocol.

2.8 Co-immunoprecipitation

Cultured Ben-Men-1 cells were washed once in PBS before IP/ lysis buffer was added to the flask and incubated on ice for five minutes. The lysate was then transferred to a micro centrifuge tube and centrifuged at 13000g for 10 minutes. The supernatant was transferred to a new tube, before determination of the protein concentration using the BCA protein assay (as described previously).

Lysates were pre-cleared to reduce non-specific binding prior to each co-ip experiment. For 1 mg of lysate, 80 µl of control agarose slurry was added to a spin column and centrifuged to remove storage buffer. 100 µl of coupling buffer was added and centrifuged. 1 mg of lysate was added to the column and incubated for one hour with gentle end-over-end mixing at 4^{o}C and then centrifuged. The pre-cleared lysate was added to the column containing the antibody cross-linked resin and incubated overnight with end-over-end mixing at 4^{o}C.

After overnight incubation, the column was centrifuged and washed twice with 200 µl of IP/ lysis buffer. A final wash with 100 µl of 1x conditioning buffer (neutral pH) preceded elution. First, 10 µl of elution buffer was added to the column and centrifuged. A further 30 µl of elution buffer was then added to the column and incubated at RT for five minutes. The column was then centrifuged and the eluate retained for subsequent analysis. 5x reducing buffer was added to each eluted sample before and boiled at 90^{o}C for five minutes prior to SDS-PAGE followed by either Western blotting or MS analysis.

2.9 Ki-67 immunofluorescent proliferation assay

The KI-67 proliferation assay was employed after shRNA protein knockdown in order to assess the subsequent effects on cellular proliferation. Cells were first washed in PBS

before fixation in ice-cold methanol for 5 minutes. The cells were then blocked in 0.1% PBS-tween containing 10% normal goat serum and 0.3 M glycine for one hour at RT. The cells were then incubated with anti-ki67 antibody at 1:1000 overnight at 4^{o}C. Alexa fluor 488 anti-rabbit secondary antibody was then applied for 1 hour at RT, followed by DAPI nuclear stain for 10 minutes at 4 µg/ml. Cover slips were applied to slides using vectashield and stored at 4^{o}C until imaging.

Stained slides were visualised under a Nikon Eclipse 80i Fluorescence microscope (Nikon, Kingston upon Thames, Surrey). Photos were taken using an intensilight C-HGF1E lightbox (Nikon) and the NIS Elements software package. Photos were taken under the 40x objective lens.

2.10 Cytoplasmic and nuclear extraction

In order to ascertain the cellular location of PDLIM2, a cytoplasmic and nuclear extraction assay (Thermo scientific) was performed. Primary adherent meningioma cells were harvested with trypsin and centrifuged at 500 g for 5 minutes. The cell pellet was then washed once in PBS, transferred to a micro centrifuge tube and centrifuged for 3 minutes at 500 g. Ice cold CER I reagent (Cytoplasmic Extraction Reagent, provided with the kit) was added to the pellet, vortexed vigorously for 15 seconds and incubated on ice for 10 minutes. Ice cold CER II was then added to the tube and vortexed for 5 seconds on the highest setting before incubation on ice for 1 minute. The tube was then centrifuged for 5 minutes at 16000 g and the supernatant immediately transferred to a pre-chilled tube (the cytoplasmic fraction). Ice cold NER (Nuclear Extraction Reagent, provided with kit) was added to the remaining pellet and vortexed for 15 seconds. After incubation on ice for 40 minutes with rigorous vortexing every 10 minutes, the tube was centrifuged at maximum speed for 10 minutes. The supernatant (nuclear fraction) was transferred to a clean tube and both extracts were stored at -80^{o}C until analysis by Western blot.

2.11 Lambda phosphatase assay

In the absence of phospho-specific antibodies to PDLIM2, it was necessary to perform a lambda phosphatase assay that would theoretically lead to a change in protein mobility, detected via a band shift upon Western blot analysis. After lysis in RIPA buffer containing protease inhibitors, 20ug of protein was mixed with 4 µl of lambda phosphatase, 2.5 µl MnCl, 2.5 µl 10x buffer (New England Biolabs) and H_2O to a final reaction volume of 25 µl. The reaction was allowed to proceed for 2 hours on a mixer at 30^{o}C. This lysate was then analysed in parallel with non-phosphatase treated lysate.

Chapter 3- Total and phosphoproteomic analysis of primary human schwannoma *vs.* Schwann cells.

3.1 Introduction

Individuals with the genetic condition NF2 experience multiple tumour growths throughout life, including both schwannoma and meningioma. No drugs are currently approved for the treatment of NF2 reflecting the urgent need for an effective therapeutic (Evans 2009). Proteomic techniques afford the possibility of high-throughput, unbiased screens between normal and tumour tissue to identify the most promising candidates that might represent attractive novel therapeutic targets.

This chapter presents the data obtained from global analyses of both total and phosphoprotein expression in human Schwann and schwannoma cells. Previous studies of the proteome in meningioma and schwannoma have provided some data from which potential therapeutic targets have been identified (Boin, Couvelard *et al.* 2014, Sharma, Ray *et al.* 2015). These studies looked at the genome or at the proteome, and Boin's study in particular was a biased approach centred on targets already known in schwannoma. The research presented here aims to take target identification a step further - by analysing the phosphoproteome to identify aberrantly activated proteins and dysregulated signalling networks. Targeting the phosphoproteome has the potential to inhibit entire signalling cascades, in turn providing a powerful tool to interrupt tumorigensis, cellular growth and proliferation. We analysed both total and phosphoprotein expression in order to identify overexpressed protein aberrantly phosphorylated compared to normal Schwann cells.

Presented here will be a list of potential therapeutic targets, both phosphorylated and not, that warrant further investigation.

3.2 Phosphoprotein purification and data processing

At the outset of this project, three primary Merlin-deficient schwannoma-derived cell populations were analysed *vs.* one sample of human primary Schwann cells (three technical repeats). Their Merlin status was confirmed by Western blot prior to MS (Figure 3.1). As expected, the analysis confirmed the Merlin-deficient status of all schwannomas. We wanted to ensure that the schwannomas were Merlin-deficient so that any targets identified would potentially be translated across all Merlin-deficient tumours associated with NF2.

Over 2000 phosphoproteins were identified in primary schwannoma and Schwann cells, as represented in the scatter plot (Figure 3.2, the full list of significantly changed phosphoproteins is provided in supplementary table S1). All the dots above the blue line represent phosphoproteins that are significantly changed between the two cell types ($P < 0.05$, $-\log_2 P > 4.32$). A total of 101 phosphoproteins were significantly downregulated with a log2 fold change of at least -1, and 122 were significantly upregulated with a log2 fold change of at least 1. This corresponds to fold changes of at > 2 and < 0.5, and only these were considered for further analysis.

To maximise the number of proteins for the eventual comparative analysis with meningioma cells, Multiple Correction Testing (MCT) was avoided and unadjusted p-values were used for defining statistical significance. The reason for this is because MCT can substantially reduce the number of proteins identified as statistically significant (Gyorffy *et al.* 2005). Our approach was to maximise the number of proteins that could be taken forward for common target selection, and the candidate proteins that were selected would be validated by Western blot later on in chapter 5.

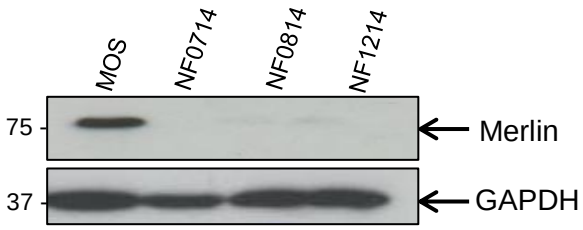

Figure 3.1: The Merlin status of all Schwann and schwannoma samples. Western blot analysis of all schwannoma and Schwann cells further analysed by MS. MOS= normal human Schwann cells, NF= human schwannoma cells.

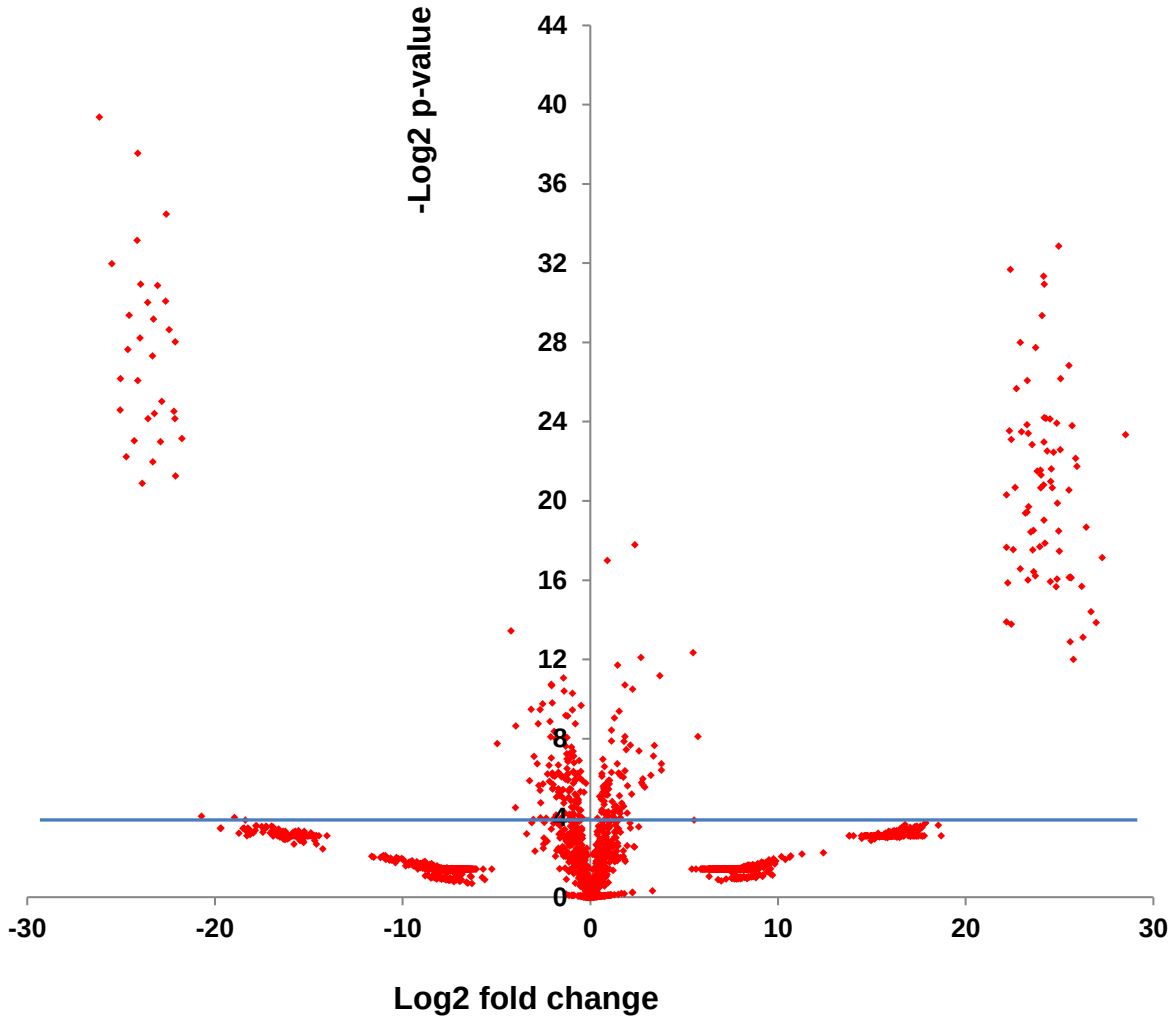

Figure 3.2: Scatter graph representation of Schwannoma phosphoprotein dataset. 2628 phosphoproteins identified in a comparison between Schwann and schwannoma cells are represented by each point in the scatter graph. Dots below the blue line represent those that failed to reach the significance threshold of $P < 0.05$ ($-\log_2 P > 4.32$).

3.3 Schwannoma phosphoprotein data

3.3.1 Functional enrichment analysis of schwannoma phosphoprotein data

In order to identify individual proteins that may be of interest, it is useful to first analyse the dataset with respect to whole pathways and/ or biological processes that are significantly represented. Using DAVID (Database for Annotation, Visualization and Integrated Discovery (Huang da, Sherman *et al.* 2009), the upregulated phosphoproteins were mapped to several pathways (Figure 3.3A). DAVID compares uploaded datasets against a defined background proteome. In this case, the dataset submitted was compared to the background 'Homo sapiens' to identify pathways and/ or processes that are 'functionally enriched' within the submitted dataset. Functional enrichment is calculated based on the proportion of a particular class of proteins in the users dataset (i.e. kinase) compared to the proportion in the background overall. For instance, if 10% of submitted proteins are kinases *vs.* 1% of the background, kinases would be statistically over-represented in the data set by 10-fold, and would therefore be assumed to play an important role within the experimental cell type.

Among the statistically enriched pathways (Benjamini-Hochberg Adjusted $P < 0.05$) are focal adhesion, regulation of the actin cytoskeleton and the MAPK pathway. These are well characterised in relation to schwannoma pathology, and Merlin is known to play a key role in each. As such, we would expect to identify them in a global phosphoproteomic analysis. As we have done so, it can be inferred that the experiment worked well and that the dataset as a whole is reliable. Among the proteins are MEK1 and NFκB, both already identified as upregulated in schwannoma and integral to mitogenic signalling.

Glycolysis and gluconeogenesis were also identified as significant (Figure 3.3A), suggesting increased metabolism and/or glucose production to aid the growth and survival of schwannoma cells. Among those proteins involved in glycolysis is enolase 1 alpha (ENO1, Log2 FC 2.9) which has been reported to promote proliferation and

migration in cancer cells, and has been shown to interact with tubulin (Diaz-Ramos, Roig-Borrellas *et al.* 2012).

Phosphofructokinase (PFKL), a component of the pentose phosphate pathway (PPP) and a key glycolysis enzyme, was also found to be upregulated with a log2 FC of 24.9. Targeting PPP components has shown promise in leukaemia (Chen, Xu *et al.* 2015) and may also represent a potential therapeutic approach for schwannomas.

Functional enrichment analysis was also performed to identify the most significantly enriched Gene Ontology (GO) terms within this same dataset. Gene ontology is a system of classification that allows genes/ proteins identified by omics experiments to be grouped together within distinct 'annotation terms,' depending on their function and or/ location within the cell. These include; Biological Processes (BP), Cellular Components (CC) and Molecular Functions (MF).

Unsurprisingly, given its known contribution to schwannoma pathology, RAS protein signal transduction is the most enriched biological process with a fold enrichment value of 8.75 (Figure 3.3B), further demonstrating the reliability of the dataset. The most enriched GO term overall is 'AP-2 adaptor complex,' linked to a process known as clathrin-mediated endocytosis. The second and third most enriched GO terms are also related to this process i.e. 'clathrin coated endocytic vesicle membrane,' and 'clathrin coat of endocytic vesicle.'

Clathrin mediated endocytosis is important for intracellular transport, and can mediate several processes including membrane protein turnover and nutrient uptake (Robinson 2015). The implications of increased endocytosis in schwannoma cells are or in some cases e.g. that of the EGF receptor can actually facilitate constitutive signalling by constant receptor recycling.

A

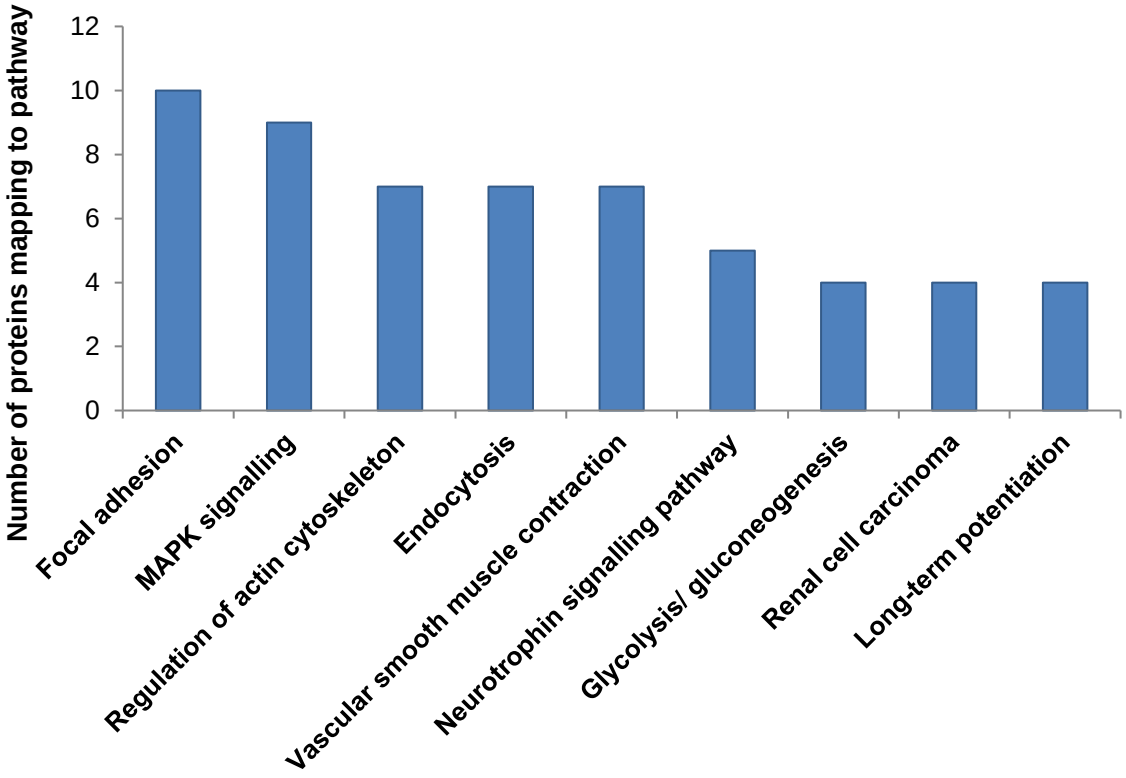
Number of proteins mapping to pathway
12
10
8
6
4
2
0
Focal adhesion
MAPK signalling
Regulation of actin cytoskeleton
Endocytosis
Vascular smooth muscle contraction
Neurotrophin signalling pathway
Glycolysis/ gluconeogenesis
Renal cell carcinoma
Long-term potentiation

B

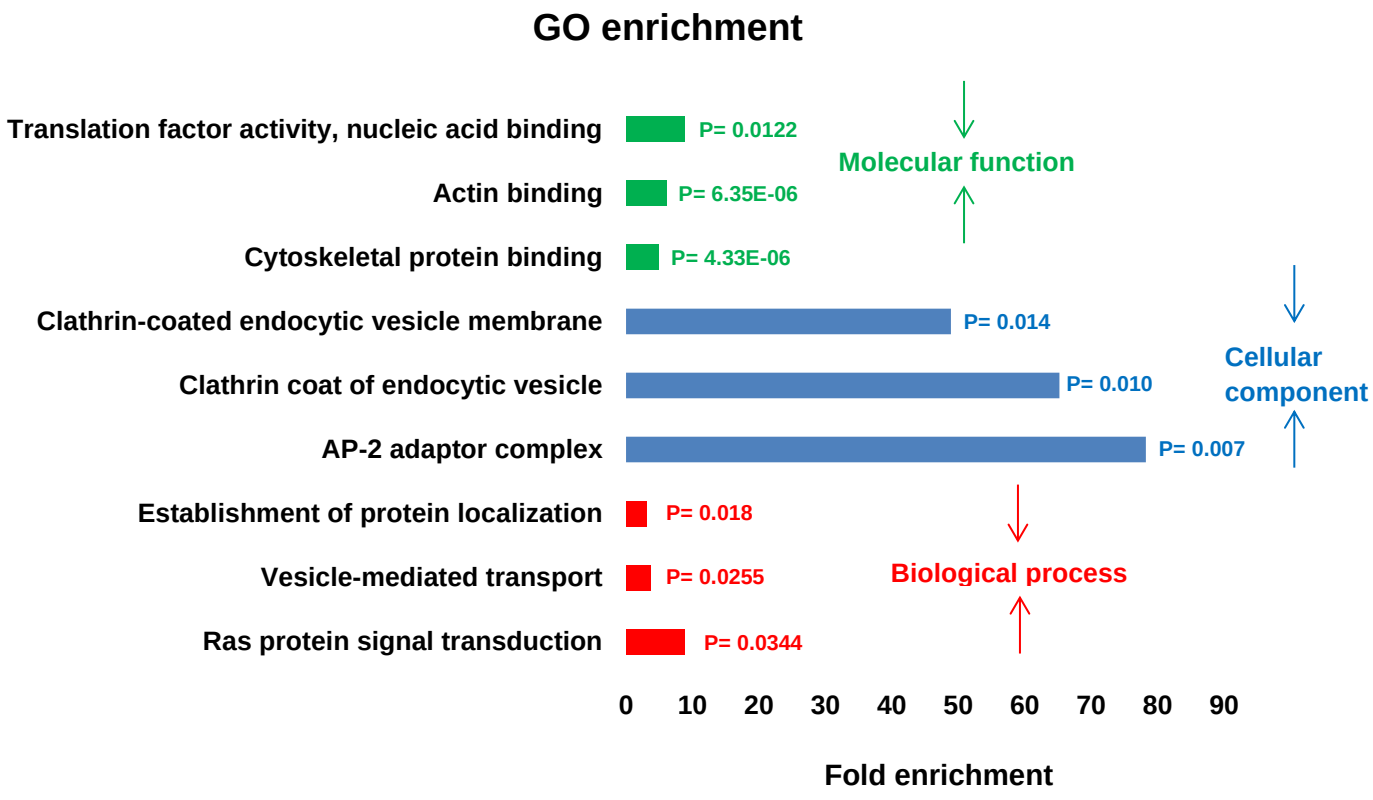
GO enrichment
Translation factor activity, nucleic acid binding
P= 0.0122
Molecular function
Actin binding
P= 6.35E-06
Cytoskeletal protein binding
P= 4.33E-06
Clathrin-coated endocytic vesicle membrane
P= 0.014
Cellular component
Clathrin coat of endocytic vesicle
P= 0.010
AP-2 adaptor complex
P= 0.007
Establishment of protein localization
P= 0.018
Biological process
Vesicle-mediated transport
P= 0.0255
Ras protein signal transduction
P= 0.0344
0 10 20 30 40 50 60 70 80 90
Fold enrichment

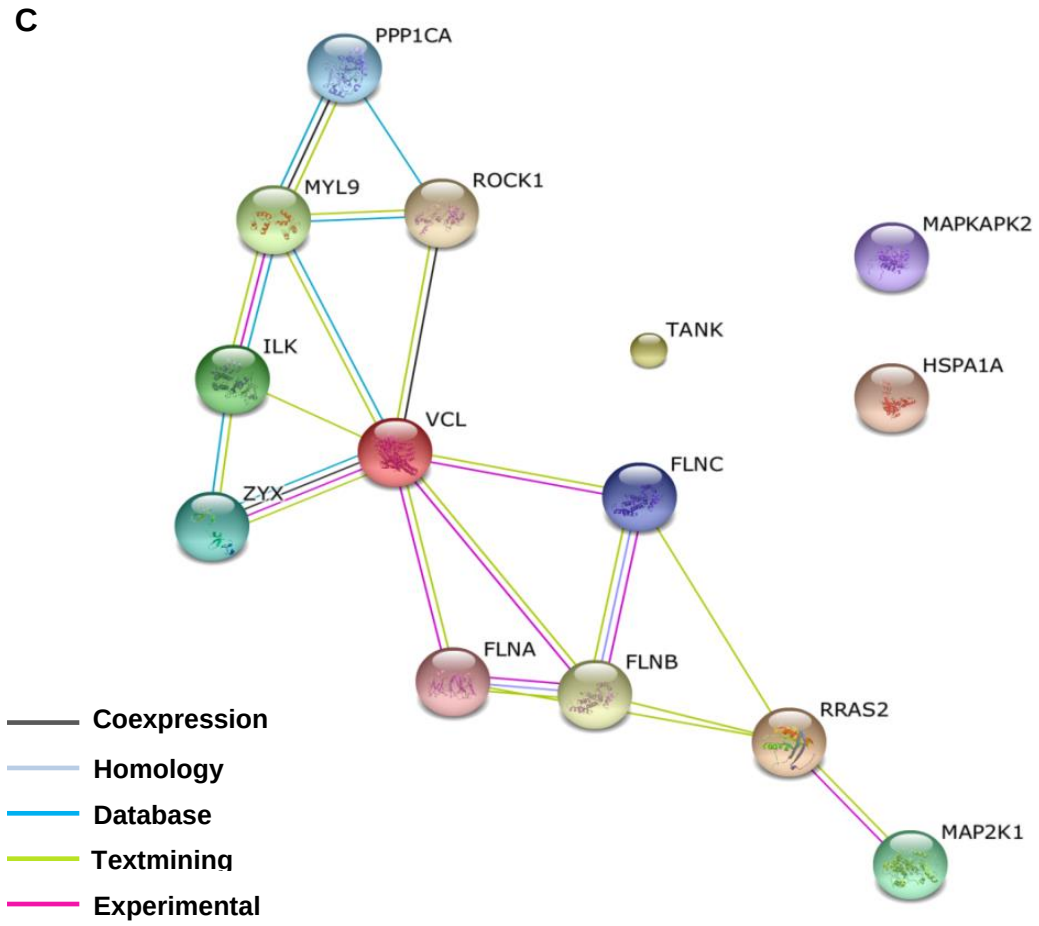

Figure 3.3: Functional enrichment analysis and associations between upregulated phosphoproteins in schwannoma cells. **A.** The pathways represented by the largest number of proteins are focal adhesion and the MAPK pathway. **B.** The most enriched processes, cellular components and molecular functions represented by upregulated phosphoproteins in schwannoma. GO= Gene Ontology (Benjamani-Hochberg adjusted $P < 0.05$). **C.** The upregulated phosphoproteins that interact with either the MAPK or focal adhesion pathways, and their associations with each other as identified by string.db.

Further, these findings are in concordance with the reported consequences of Merlin deficiency i.e. deregulation of endocytic vesicle sorting (Hennigan, Moon *et al.* 2013) and may help us to understand more about the regulation of the proteins involved in these processes. The data may indicate increased endocytosis in an attempt to remove signalling molecules from the cell membrane to downregulate mitogenesis, however in the absence of Merlin the number of those targeted for degradation may be fewer. Determining site-specific phosphorylation information would be useful in determining the consequences of AP-2 component overexpression in schwannoma compared to normal cells.

Figure 3.3C shows a STRING (Search Tool for the Retrieval of Interacting Genes (Franceschini, Szklarczyk *et al.* 2013) generated predicted protein-protein interaction map highlighting the proteins from the data set involved specifically in the MAPK and focal adhesion pathways that have been linked to each other previously. String identifies associations between proteins based on direct experimental evidence, computational prediction methods and also co-occurrence in published literature. Identifying specific interactions using string can help to identify proteins that, if targeted therapeutically, could affect multiple other proteins within the cell.

These pathways were investigated in more detail because of their relation to schwannoma pathology. Filamin A (FLNA), Filamin B (FLNB) and Filamin C (FLNC) appear as central nodes in Figure 3.3C suggesting that they may be important effectors of MAPK/ focal adhesion signalling in schwannoma. The filamins are important for anchoring transmembrane proteins to cytoskeleton and have been shown to interact directly with integrins, which are known to play a role in schwannoma growth and proliferation (van der Flier and Sonnenberg 2001). They have not been previously linked to schwannoma however their roles in the above pathways highlight them as potential therapeutic targets.

3.3.2 Gene functional classification of schwannoma phosphoprotein data

DAVID also provides another feature termed ‘Gene functional classification.’ This is designed to identify functionally related clusters of genes based on their co-occurrence within different annotation terms e.g. cytoskeletal binding. The difference between this and functional enrichment analysis is that functional classification does not compare proteins to any background, but rather simply categorizes them into groups based on their structure/ function. This allows large numbers of proteins to be condensed into biologically related and therefore meaningful clusters, from which useful information can be extracted.

Using this tool we were able to identify a cluster of proteins with several unifying features, the identities of which can be viewed in Table 3.1. The overriding feature of these proteins is their cytoskeletal binding capability. Given Merlin’s role as a master regulator of the cytoskeleton, the activation of these proteins might be a consequence of Merlin deficiency in schwannoma cells. Secondly, all six proteins contain a LIM domain, and several contain a PDZ domain.

LIM domains orchestrate protein-protein interactions and play roles in a number of signalling pathways. PDZ domains are also important for the organization of macromolecular signalling complexes, particularly for linking membrane proteins to the cytoskeleton (Krcmery *et al.* 2010). We also performed Maxquant analysis setting ‘phosphorylation,’ as a variable modification allowing us to identify specific phosphorylation sites. In doing so, we identified phosphorylation sites for two of these PDZ/ LIM domain proteins; LASP1_S146 and MICAL1_S613. These may be important when assessing their suitability as therapeutic targets.

Table 3.1		
Gene symbol	**Protein name**	**Function**
PDLIM2	PDZ and LIM domain containing protein 2	Cytoskeletal binding protein that promotes migration and adhesion.
PDLIM5	PDZ and LIM domain containing protein 5	Cytoskeletal binding. Functions as a scaffold protein in cardiac cells.
PDLIM7	PDZ and LIM domain containing protein 7	Cytoskeletal binding. Involved in actin-filament complex formation.
ZYX	Zyxin	Actin binding, important for the formation of focal adhesions.
LASP1	LIM and SH3 domain protein 1	Regulation of actin based cytoskeletal activity.
MICAL1	Protein-methionine sulfoxide oxidase MICAL1	Promotes depolymerisation of F-actin.

Table 3.1: Functional cluster of phosphoproteins that are upregulated in schwannoma compared to Schwann cells.

3.3.3 Downregulated phosphoprotein analysis

Among the downregulated phosphoproteins, there is significant enrichment of lysosomal proteins (Figure 3.4). These are ARSA, AGA, CTSD, GUSB, PSAP and SMPD1. CTSD, or Cathepsin D, in particular is associated with caspase-3 induction of cell death and its downregulation may be related to schwannoma cell survival. Downregulation of lysosomal proteins coupled with the upregulation of AP-2 complex proteins discussed earlier may indicate increased receptor internalization counteracted by decreased degradation.

DAVID analysis also highlighted a functional cluster of proteins that are linked to the spliceosome, with an enrichment p-value of 2.4E-7, suggesting significant downregulation of phosphoproteins relating to mRNA processing. The proteins within the cluster are RALY, U2AF2, HNRNPC and SNRPD2. Spliceosome activity gives rise to alternative splicing and thus different protein isoforms. Deregulation may lead to the expression of inactivated tumour suppressors, or certain protein isoforms that can influence tumour progression (Ghigna, Valacca *et al.* 2008). As such, spliceosome deregulation may represent a therapeutic target for schwannoma.

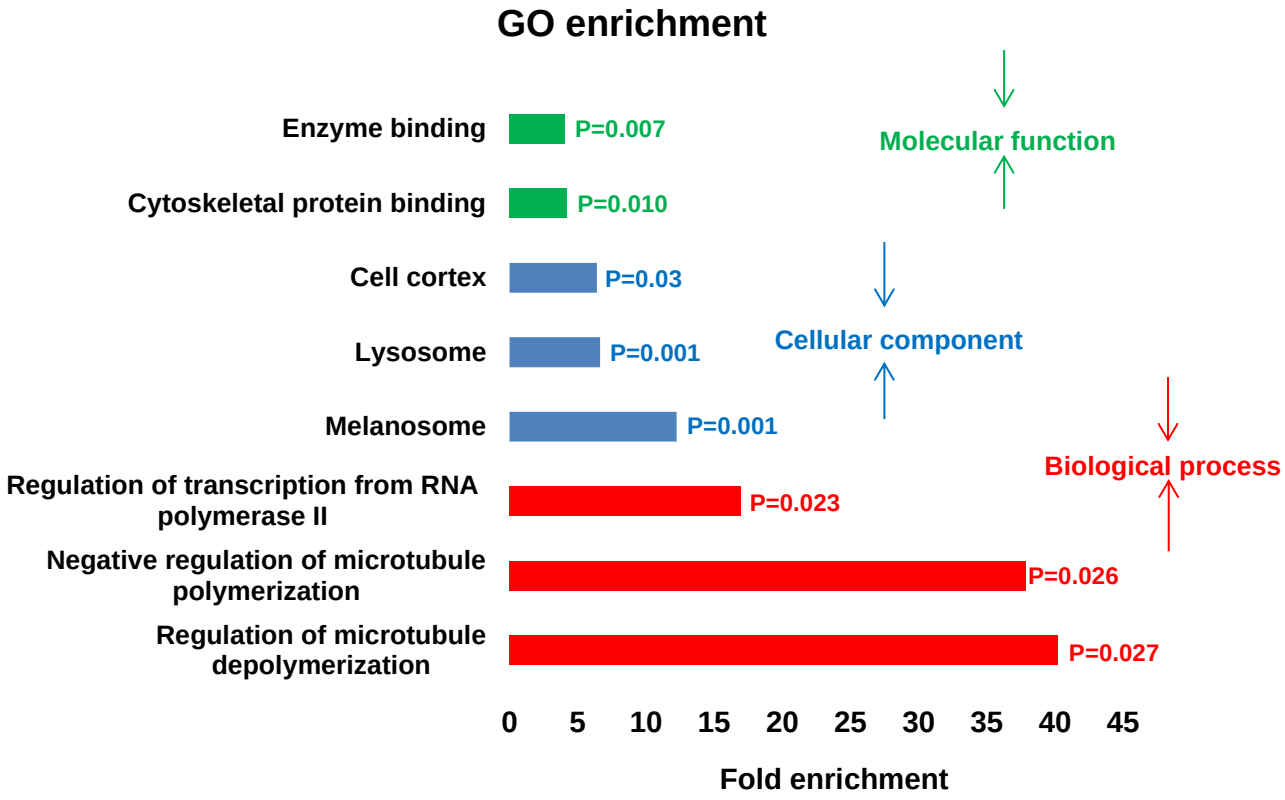

Figure 3.4: GO enrichment analysis of downregulated phosphoproteins identified in schwannoma *vs.* Schwann cells.

3.4 Primary schwannoma total protein data analysis

Total protein was measured in parallel with phosphoprotein to allow an indirect comparison between total and phosphoprotein abundance, and also to identify potential non-phosphorylated protein targets. The comparison was indirect because although the total protein sample was taken from the lysate just before it was subject to phosphoprotein purification, the samples were measured independently of one another resulting in two distinct data sets that were then compared with each other. A scatter plot representing the total protein data is shown in Figure 3.5. 16 proteins were found to be upregulated with a log2 fold change of > 1, and 93 proteins were significantly downregulated with a log2 fold change of < -1 (the full list of significantly changed proteins can be seen in supplementary Table S2).

All upregulated proteins were grouped based on protein class and are represented by a pie chart (Figure 3.6A). The largest proportion of upregulated proteins are cytoskeletal. Interestingly, 11 of the 16 upregulated proteins interact with one another, as identified by string.db (Figure 3.6B). ALDOC and ALDOA are both enzymes involved in gluconeogenesis, echoing the results obtained in the phosphoproteomic analysis and further suggesting that this pathway may be a potential therapeutic target for schwannoma. ALDOA in particular has been identified as an important enzyme promoting the survival of glioblastoma xenografts and may represent a way of targeting this potentially key metabolic pathway in schwannoma (Sanzey, Abdul Rahim *et al.* 2015).

We also identified two proteasomal subunits as upregulated, PSMB5 and PSMA1. Since the proteasome is important for the degradation of proteins which promote proliferation and cell survival, targeting it represents a useful therapeutic strategy. Bortezomib, an inhibitor targeting PSMB5, has already been shown to have efficacy in multiple myeloma (Hideshima, Chauhan *et al.* 2005) and may also warrant investigation in schwannomas.

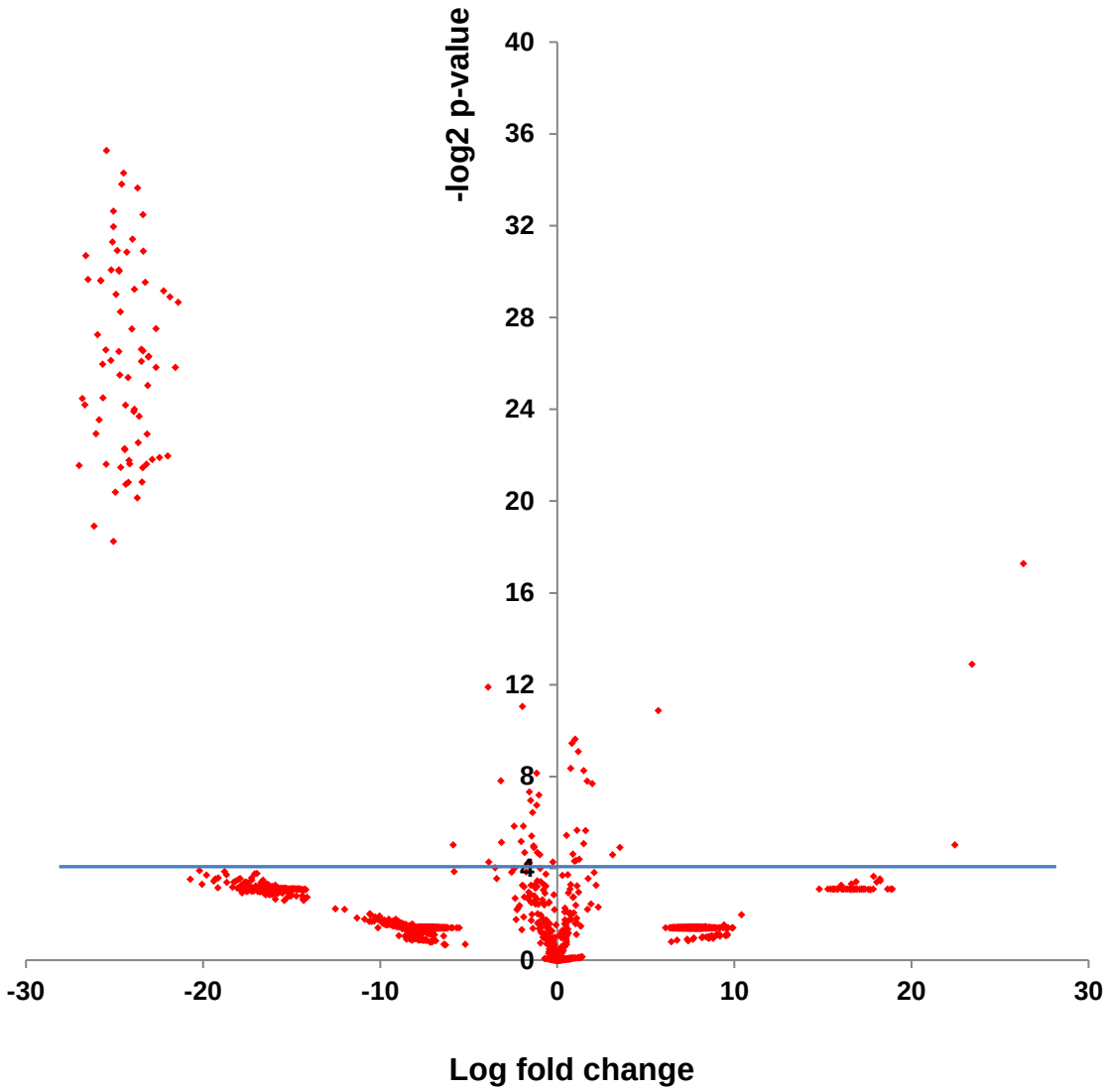

Figure 3.5: Scatter graph representation of schwannoma total protein dataset. 1659 proteins identified in a comparison between Schwann and schwannoma cells are represented by each point in the scatter graph. Points below the blue line represent those that failed to reach the significance threshold of $P < 0.05$ ($-\log_2 P > 4.32$).

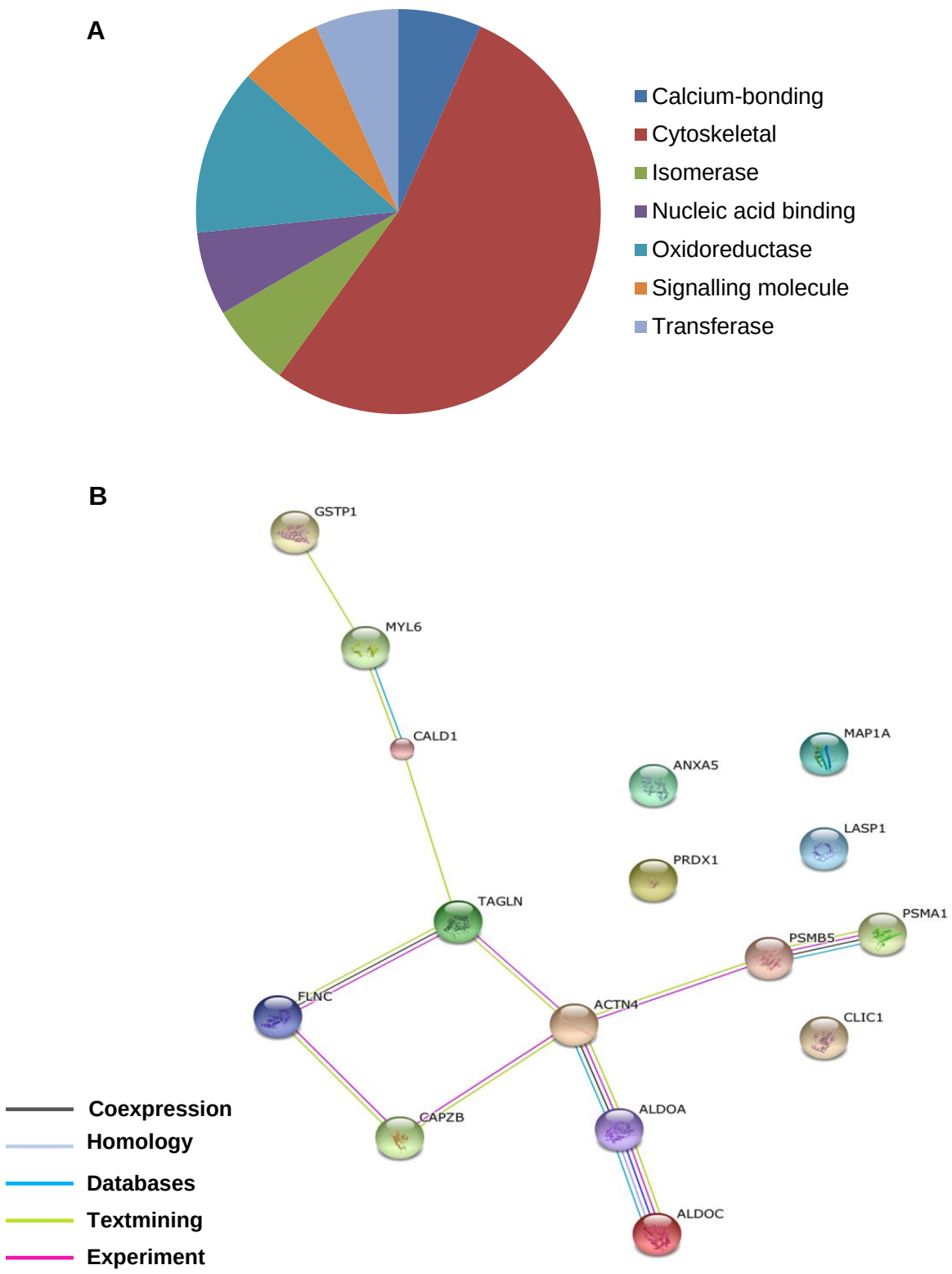

Figure 3.6: Schwannoma total protein data analysis. **A.** Classification based on protein class shows that half of the upregulated proteins are related to the cytoskeleton. **B.** 11 are known to be associated with each other, as identified by string.db. Several of those are cytoskeletal binding proteins.

DAVID analysis of the downregulated total protein dataset identified significant enrichment of ribosomal proteins. Whilst ribosomal proteins are generally regarded as housekeeping genes, their significant representation among the downregulated protein data set for schwannoma cells may cause decreased global protein synthesis. Additionally, downregulation of ribosomal proteins might also affect apoptosis and DNA damage responses, and many of them may act as tumour suppressors including L13, L36 and S15 (Amsterdam, Sadler *et al.* 2004), all identified as significantly downregulated in the present study.

3.5 Phosphoproteins *vs.* total proteins

The primary aim of this study was to identify phosphorylated protein targets, as they present the opportunity to 'switch off' tumorigenic signalling. Therefore, it was necessary to identify proteins that displayed a small change in total abundance relative to phosphoprotein changes or a decrease in overall total protein. This would be the most appropriate method to identify proteins that are 'truly' activated.

In the absence of a quantifiable labelling technique e.g. Stable Isotopic Labelling with Amino acids in Cell culture (SILAC), that allows phosphorylated peptides to be measured simultaneously and normalized to their non-phosphorylated counterparts during the same MS run, it is not possible to directly compare separate, label-free experiments. Therefore, a method of comparing two distinct datasets was necessary. The simplest way of doing this was to plot both datasets against each other, in a graph (Figure 3.7), allowing for fast visual identification of the best targets. Significantly changed phosphoproteins with a p-value of < 0.05 are plotted on the x axis, against their respective total protein amounts (irrespective of p-value).

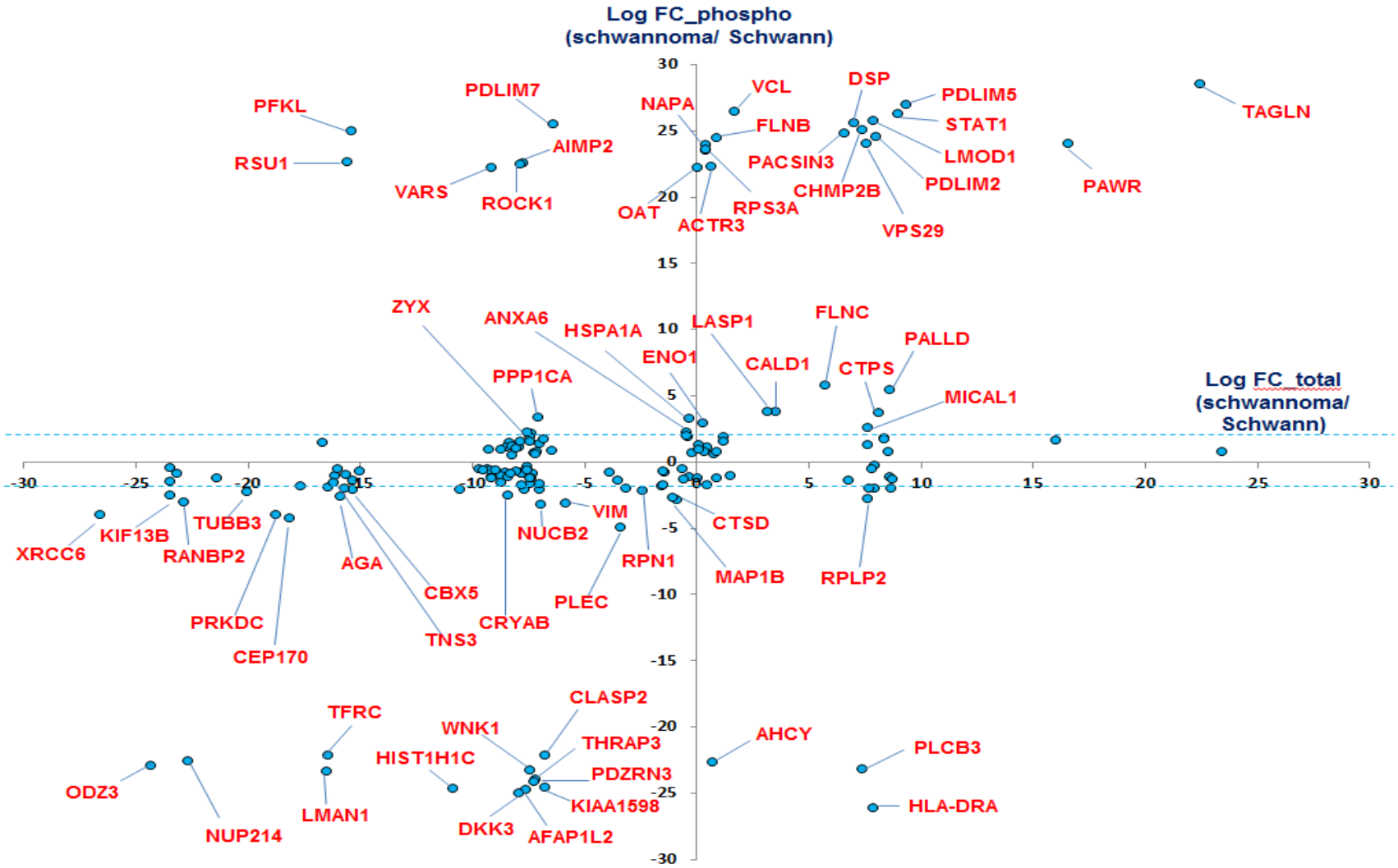

Figure 3.7: A graphical aid to represent the relationships between significantly changed phosphoproteins and total protein abundance in schwannoma cells. Phosphoproteins significantly up or downregulated ($P < 0.05$) in primary schwannoma cells compared to Schwann cells plotted against their respective total protein amounts.

LASP1 for instance represents a good therapeutic target when considering phosphoprotein data alone. It is significantly increased in schwannoma cells compared to Schwann cells and is also a member of the functionally enriched cluster of proteins discussed earlier in the chapter. However, as it also increases to a similar degree in total protein abundance, it becomes a less attractive candidate in this particular study.

3.6 Potential therapeutic targets

Only upregulated candidates were selected for further analysis. A selection of ideal schwannoma phosphoprotein candidates based on the criteria outlined above is displayed in Table 3.2. The final selection will come in chapter 5, after acquisition of meningioma data, in order to identify common targets.

Table 3.2			
Gene symbol	**Protein name**	**Gene symbol**	**Protein name**
PFKL	Phosphofructokinase, liver	RPS3A	Ribosomal protein S3A
RSU1	Ras suppressor protein 1	ACTR3	Actin related protein 3 homolog
VARS	Valyl-TRNA synthetase	CHMP2B	Charged multivascular body protein 2B
ROCK1	Rho-associated protein kinase 1	VPS29	Vacuolar protein sorting-associated protein 29
PDLIM7	PDZ and LIM domain 7	PDLIM2	PDZ and LIM domain protein 2
AIMP2	ARS-Interacting Multi-Functional Protein 2	LMOD1	Leiomodin-1
OAT	Omithine aminotransferase	PDLIM5	PDZ and LIM domain protein 5
NAPA	N-Ethylmaleimide-Sensitive Factor Attachment Protein Alpha	STAT1	Signal transducer and activator of transcription-1
VCL	Vinculin	DSP	Desmoplakin
FLNB	Filamin-B	PACSIN3	Protein Kinase C and casein kinase substrate in neurons protein 3

Table 3.2: 21 phosphoproteins that represent ideal schwannoma therapeutic targets, displaying little or no change in total protein abundance.

3.7 Discussion

This chapter has explored (phospho) proteomics as a tool to identify potential therapeutic targets for the treatment of schwannoma. We were able to implement phosphoprotein purification followed by MS analysis, successfully leading to the identification of over 2000 proteins. We also analysed total protein abundance in parallel, culminating in an indirect comparison between total and phosphoprotein abundancies in order to select the most promising, activated potential targets.

As identified earlier in the chapter, there are three significantly changed phosphoproteins belonging to the PDZ and LIM domain family of proteins; PDLIM2, PDLIM5 and PDLIM7. These each show a decrease in total protein or a relatively small increase when compared to their phosphorylated equivalents. There are no reports in the literature referring to the role of these particular proteins in schwannoma. There are a large and diverse range of functions reported for this family of proteins and it would be interesting to learn more about their roles in schwannoma pathology.

Vinculin (VCL) may also be an interesting target for further investigation, given its role in cell-cell/ cell-matrix adhesion in similar fashion to Merlin. It has been shown to stabilize focal adhesions and promote tumour progression in breast cancer and could represent a useful way to target pathological focal adhesion in schwannomas (Rubashkin, Cassereau *et al.* 2014). Desmoplakin (DSP) also signifies an interesting target for further validation. The human protein atlas (www.proteinatlas.org) shows that it is largely absent in most cancers, therefore it has been proposed as a tumour suppressor whose downregulation is a tumour promoting factor.

The total protein analysis also identified proteins that warrant further investigation, not least Transgelin (TAGLN), a protein involved in actin cross-linking. It was recently identified as an important driver of progression in Malignant Peripheral Nerve Sheath Tumours (MPNST) associated with the genetic condition neurofibromatosis type 1

(NF1) (Park, Lee *et al.* 2014). As NF1 and NF2 share commonality in their activated signalling networks, TAGLN may be a candidate target for both conditions. In this experiment, it showed a Log2 FC of 22 in total protein abundance, and a Log2 FC of 28 in phosphoprotein amount. As such, TAGLN is most likely a relevant therapeutic target for schwannoma treatment.

In summary, this global total and phosphoproteomic analysis of schwannoma has highlighted several areas, not previously reported, that warrant further investigation including; the AP-2 adaptor complex and lysosomal degradation, the specific roles of endocytosis in schwannoma pathogenesis and the PDZ and LIM domain containing family of proteins as potential therapeutic targets.

Chapter 4 - Total and phosphoproteome analysis of meningioma cells compared to normal meningeal cells.

4.1 Introduction

Meningiomas represent the second most common intracranial brain tumours, accounting for almost 35% of all cases (Wiemels, Wrensch *et al.* 2010). Around half of those are attributable to loss of the Merlin protein, commonly as part of the genetic condition neurofibromatosis type 2 (NF2). There are currently no drugs approved for NF2 and the need to identify novel therapeutic targets remains urgent. This chapter explores phosphopeptide enrichment and phosphoprotein purification to identify potential therapeutic targets for meningiomas, and the results of each of these analyses will be presented throughout this chapter.

Three primary human meningioma-derived cell populations and a meningioma cell line (Ben-Men-1) were analysed against a common normal control cell line, Human Meningeal Cells (HMC). All samples were analysed for Merlin expression by Western blot prior MS (Figure 4.1).

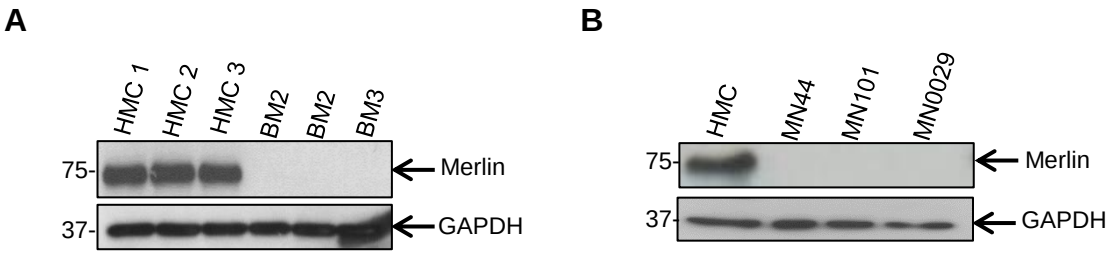

Figure 4.1: The Merlin status of all meningioma samples submitted for MS analysis. **A.** As expected three HMC cell populations that were separately cultured and processed from one another were confirmed as Merlin-positive by Western blot, and three independently cultured populations of Ben-Men-1 cells were confirmed as Merlin-negative. **B.** Three primary meningioma cell populations (MN) were confirmed as Merlin-negative.

As with schwannoma, samples were passed through a commercial affinity column to achieve phosphoprotein purification. A total protein aliquot was removed prior to this for parallel measurement of total protein abundance. After mass spectrometry, data were processed as described in the previous chapter. Fold changes and p-values were calculated for each quantified protein.

4.2 Analysis of primary meningioma

4.2.1 Phosphoprotein analysis of primary meningiomas

In a comparative analysis between HMC and three primary meningioma-derived cell populations, we identified a total of 3464 proteins and quantified 2647. Of those, 500 were significantly changed between the two cell types. 35 proteins were significantly upregulated and 443 were significantly downregulated (Log2 FC > 1, < -1). Table 4.1 shows all the upregulated proteins (the complete list of significantly downregulated proteins is presented in supplementary Table S3).

There was a lot of missing data across the primary meningioma phosphoprotein dataset that meant LFQ values were not assigned for each protein across each of the three repeats. As such, statistical analyses revealed considerably more significantly downregulated proteins than upregulated proteins compared to HMC. Enrichment analysis of the upregulated phosphoproteins identified one significantly enriched pathway, the proteasome. There were four proteasome subunits included in the list; PSMC2, PSME1, PSMB3 and PSMB2. This indicates that proteasome inhibition may be a therapeutic strategy in meningioma.

The phosphoprotein with the largest fold change was TGM2, or transglutaminase 2. The expression of this protein has been previously studied in meningioma and was found to be highly upregulated and a proposed therapeutic target (Huang, Wei *et al.* 2014) . The authors also showed that loss of the *NF2* gene was associated with high expression of TGM2.

Table 4.1		
Gene symbol	**Protein name**	**Log2 FC**
TGM2	Protein-glutamine gamma-glutamyltransferase 2	25.03
CNPY2	Protein canopy homolog 2	24.75
CTSD	Cathepsin D	24.61
CARHSP1	Calcium-regulated heat stable protein 1	24.47
TXNL1	Thioredoxin-like protein 1	24.34
PDCD5	Programmed cell death protein 5	24.25
TUBA4A	Tubulin alpha-4A chain	24.22
SMAD2	Isoform Short of Mothers against decapentaplegic homolog 2	23.72
KPNA3	Importin subunit alpha-4	23.48
CCDC6	Coiled-coil domain-containing protein 6	22.64
NUCB2	Nefastin-1	22.64
KPNA1	Importin subunit alpha-5	22.60
NUCB1	Nucleobindin-1	22.19
TXNDC5	Isoform 2 of Thioredoxin domain-containing protein 5	22.06
IFIT2	Interferon-induced protein with tetratricopeptide repeats 2	21.30
DNAJA1	DnaJ homolog subfamily A member 1	21.15
TSSC1	Protein TSSC1	20.64
C1QBP	Complement component 1 Q subcomponent-binding protein	3.74
TUFM	Elongation factor Tu, mitochondrial	2.39
FASN	Fatty acid synthase	2.28
PSMB2	Proteasome subunit beta type-2	2.06
COPB2	Coatomer protein complex, subunit beta 2 (Beta prime)	1.82
CALU	Calumenin	1.74
MAGOHB	Protein mago nashi homolog 2	1.71
PSMB3	Proteasome subunit beta type-3	1.69
PSME1	Proteasome activator complex subunit 1	1.63
PPME1	Protein phosphatase methylesterase 1	1.61
NT5C2	Cytosolic purine 5-nucleotidase	1.54
PDIA6	Protein disulfide-isomerase A6	1.52
TUBB4B	Tubulin beta-4B chain	1.40
HSPH1	Isoform Beta of Heat shock protein 105 kDa	1.39
MYO1C	Unconventional myosin-Ic	1.23
CHMP3	Charged multivesicular body protein 3	1.10
PSMC2	26S protease regulatory subunit 7	1.10
ATP5A1	ATP synthase subunit alpha, mitochondrial	1.06

Table 4.1: 35 phosphoproteins were significantly upregulated in primary meningioma cells compared to HMC ($P < 0.05$, Log2 FC > 1).

Phosphorylated SMAD2 was also found to be highly upregulated in meningioma cells. SMAD2 is a major component of TGF-beta signalling, which itself can have either pro or anti-proliferative consequences for cancer cells (Massague 2008). We were able to identify a specific phosphorylation site for SMAD2 by setting phosphorylation as a variable modification in Maxquant.

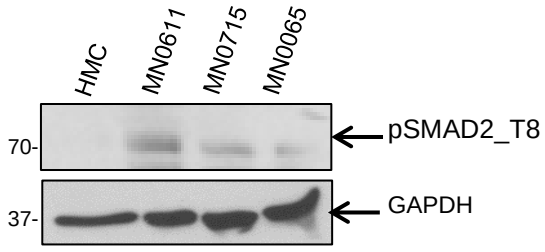

Figure 4.2: Analysis of SMAD2_T8 expression in primary meningioma cells. HMC cells do not express SMAD2_T8, whilst all primary meningioma samples do.

We found that that SMAD2 is phosphorylated at Thr8 (T8) and confirmed this finding in three primary meningioma samples (Figure 4.2). Phospho-SMAD_T8 is expressed in meningioma and is not present in HMC cells. Total SMAD2 expression was previously identified as upregulated in meningioma by Wang *et al.* along with several other members of the TGF-beta signalling family (Wang, Gong *et al.* 2012).

Fatty Acid Synthase (FAS) was also identified as upregulated, with a log2 FC of 2.28. This has already been identified as overexpressed in several cancers and its inhibition may represent a plausible therapeutic strategy (Mullen and Yet 2015). Unpublished data from our group has already shown FAS to be upregulated in Merlin-deficient cells and could represent a good target for Merlin-deficient tumours. The data obtained here confirms that, and suggests that FAS phosphorylation may also be important for the pathogenic consequences of its overexpression compared to normal cells. Phospho-cathepsin D is also upregulated in primary meningioma however as it was significantly downregulated in schwannoma cells; it is not an ideal common target.

4.2.2 Downregulated phosphoproteins in primary meningioma

As there was a large amount of missing data for the primary meningioma samples, functional analysis of the downregulated data may have been misleading. For a large number of the downregulated proteins, mass spectrometry failed to identify any peptides in many proteins across the three meningioma repeats. These particular proteins were assigned a 0 value in meningioma, and when fold changes were calculated between normal and tumour cells, large fold change values were assigned, even though in reality the protein was never actually identified in the sample. This makes it difficult to make a proper conclusion regarding the quantitative difference between the two cell types, as the question must be raised; is the protein truly absent or was it simply not identified or quantified for any number of different reasons. This is something that should be considered in all proteomic analyses, but that becomes much more pertinent in datasets that contain lots of missing values (Karpievitch, Dabney *et al.* 2012).

As such, functional enrichment analysis of the downregulated dataset included only entries that had at least one quantitative value in meningioma. Significantly enriched pathways represented by these phosphoproteins were monosaccharide metabolism and ribose phosphate metabolism; two pathways employed by cells in order to generate energy.

4.2.3 Primary meningioma total protein data

There were more total proteins identified and significantly changed than in the phosphoprotein experiment. A total of 2886 quantified proteins are represented in a scatter plot (Figure 4.3). 540 were significantly downregulated and 197 were significantly upregulated (the full list can be viewed in supplementary Table S4).

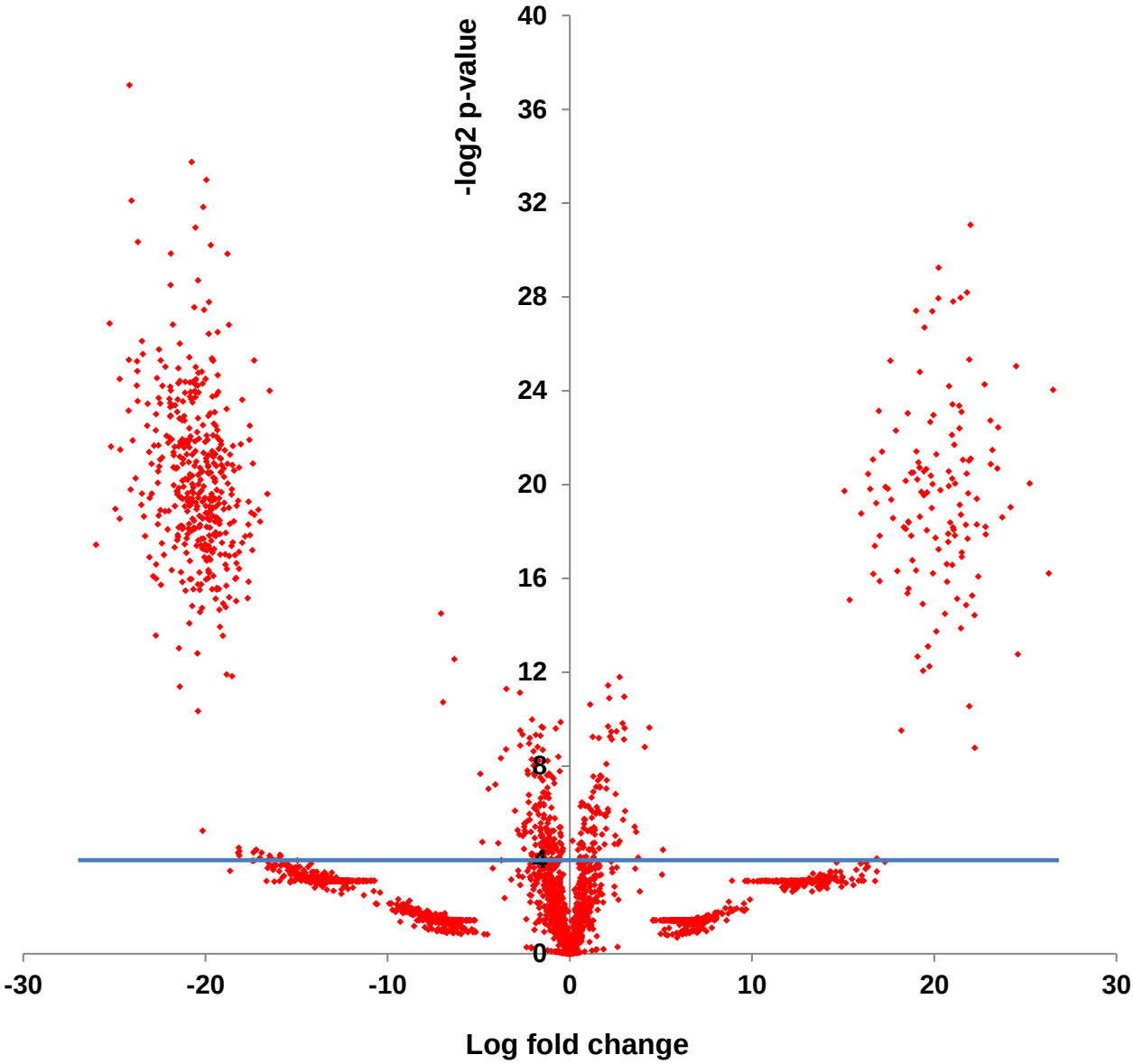

Figure 4.3: Scatter graph representation of primary meningioma total protein data set. A total of 2886 proteins were identified in a comparison between primary meningioma cells and HMC. 197 proteins were significantly upregulated and 540 were significantly downregulated.

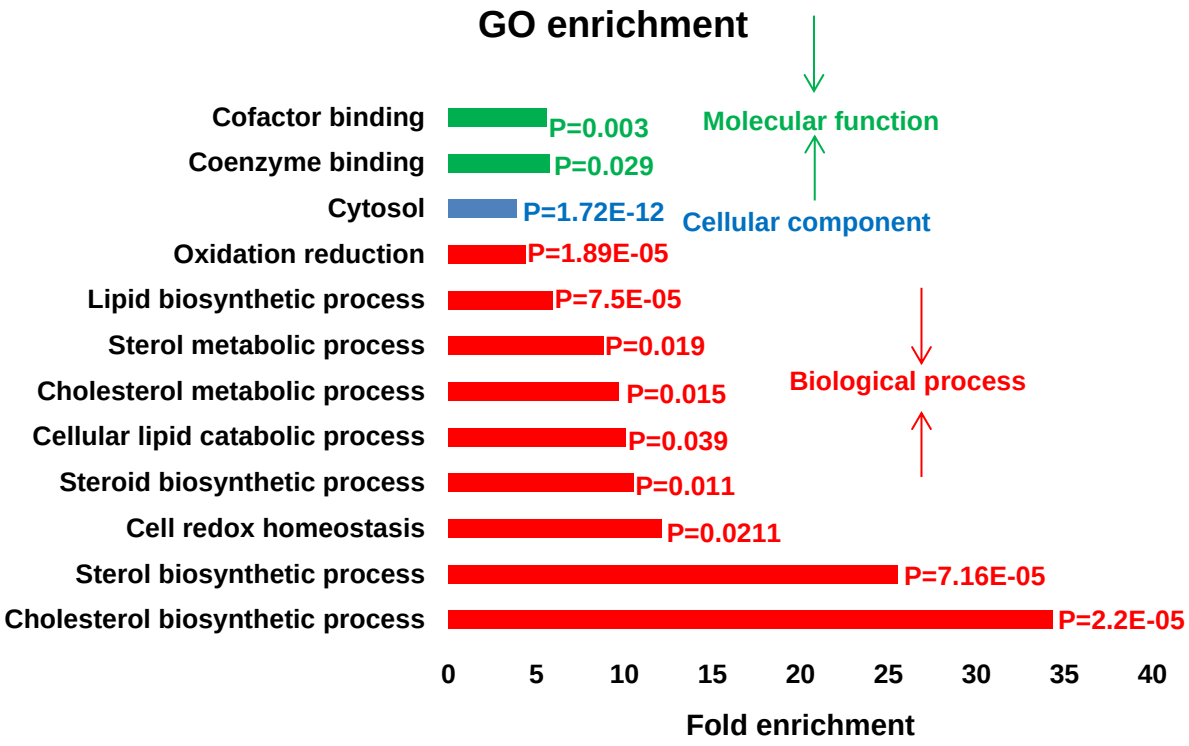

Figure 4.4: GO enrichment analysis of proteins significantly upregulated in primary meningioma cells compared to Human Meningeal Cells (HMC). A majority of the identified terms relate to cellular metabolic processes (Benjamini-Hochberg adjusted $P < 0.05$).

GO enrichment analysis of the upregulated proteins identified 12 significantly enriched (Benjamani-Hochberg adjusted $P < 0.05$) GO terms overall (Figure 4.4). Many of them are related to processes involving cholesterol, lipids and steroids, suggesting that these processes are perhaps growth permissive for meningioma and are therefore potential targets for therapeutic intervention.

4.2.4 Phosphoprotein *vs.* total protein expression in primary meningioma

A graph plotting significantly changed phosphoproteins against their respective non-phosphorylated counterparts can be viewed in Figure 4.5. At first glance, there are a number of proteins that might represent potential therapeutic targets, owing to their large change in phosphorylation compared to total protein abundance. These include Nucleobindin 1 (NUCB1), Interferon-Induced Protein With Tetratricopeptide Repeats 2 (IFIT2), Transglutaminase 2 (TGM2), Thioredoxin-like protein (TXNL), Thioredoxin domain-containing protein 5 (TXNDC5), heat shock protein J2 (DNAJA1), Nucleobindin 2 (NUCB2), cathepsin D (CTSD) and karyopherin α (KPNA).

There were several proteins identified that do not change in total protein amount but display large decreases in phosphoprotein abundance. These correspond to the cluster at the bottom of the Y-axis in Figure 4.5 that were difficult to label on the graph. Of those, MAP1S in particular is regarded as a tumour suppressor protein via its ability to induce autophagy in tumour cells (Xie, Nguyen *et al.* 2011). The amount of total protein hardly changed between the two cell types however the phosphorylated protein is downregulated with a log2 fold change of 24.18. This suggests that phosphorylation of MAP1S is important for its activity, and that its downregulation in meningioma cells is beneficial. As such it would be interesting to investigate it further.

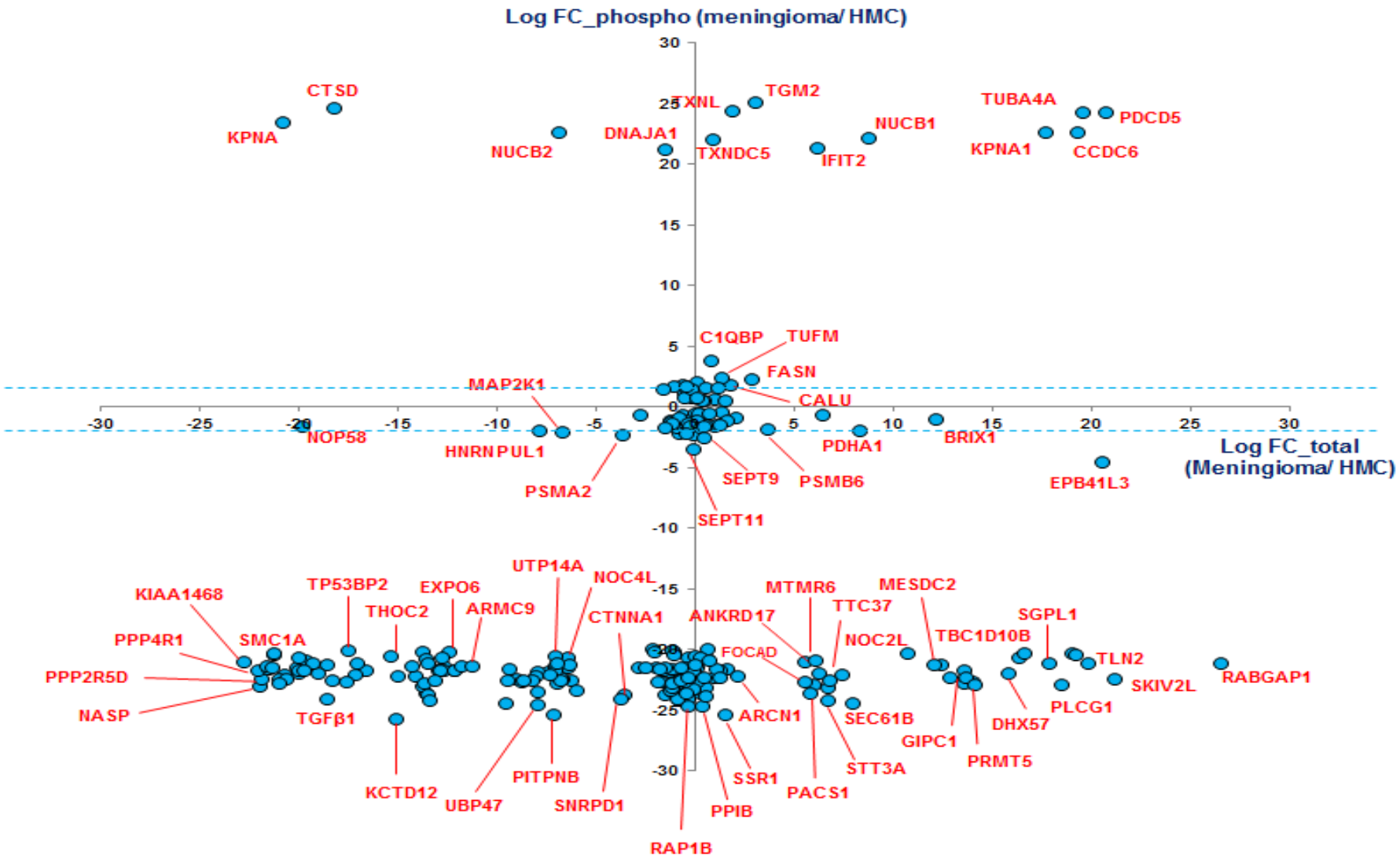

Figure 4.5: A graphical aid to show the relationship between significantly changed phosphoproteins and respective total protein abundance in primary meningioma compared to Human Meningeal Cells (HMC). Significantly changed phosphoproteins (P < 0.05) plotted against total protein change (irrespective of significance).

4.3 Analysis of Ben-Men-1 cells

4.3.1 Ben-Men-1 phosphoprotein data

A comparison between normal HMC and the benign meningioma cell line Ben-Men-1 was the next experiment performed. All phosphoproteins identified are represented in a scatter plot (Figure 4.6). A total of 243 phosphoproteins were significantly upregulated, whilst 196 were significantly downregulated ($P < 0.05$, Log2 FC > 1/ < -1, all significantly changed phosphoproteins can be viewed in supplementary Table S5). The upregulated phosphoproteins were submitted for functional enrichment analysis using DAVID. The top enriched pathways are the ribosome and spliceosome (Figure 4.7A). The spliceosome has been proposed to represent an attractive therapeutic target in tumour cells and may warrant investigation in meningiomas (Bonnal, Vigevani *et al.* 2012).

There is also significant representation of phosphoproteins involved in non-homologous end joining and nucleotide excision repair. The data therefore also indicates there may be alterations in DNA repair mechanisms. We identified functional enrichment of the cell-cycle among the upregulated phosphoproteins including Cyclin-dependent kinases 1 and 2 (CDK1/ CDK2). Both proteins are known to drive cell-cycle progression and proliferation, particularly in cancer. CDK inhibition is a valuable strategy in cancer treatment, and targeting CDKs 4 and 6 is emerging as the most effective option (Asghar, Witkiewicz *et al.* 2015). We identified CDK4 with a log2 fold-change of 2.9 in Ben-Men-1 cells that fell just below the significance threshold with a p-value of 0.07.

Gene Ontology (GO) enrichment analysis identified significant enrichment of proteasome activation with almost 80-fold enrichment (Figure 4.7B) echoing what was observed in primary meningioma cells. This may indicate an increase in the degradation of proteins that would otherwise be detrimental to tumour growth and

proliferation and also further adds to the body of evidence highlighting the proteasome as a therapeutic target.

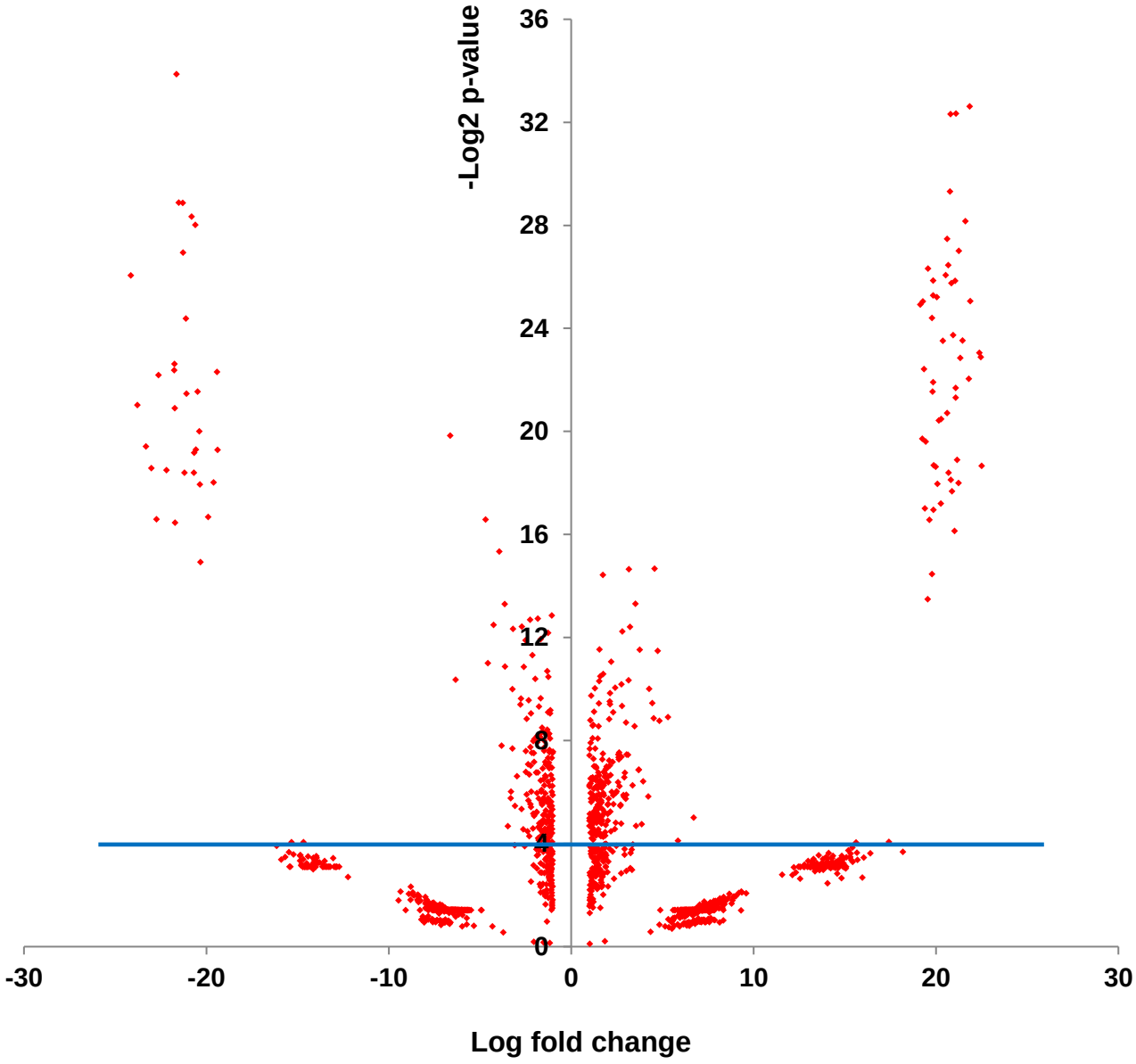

Figure 4.6: 2827 phosphoproteins identified in a comparison between Human Meningeal Cells (HMC) and Ben-Men-1 cells. The points above the blue line represent phosphoproteins that are significantly (-log2 P = > 4.32) up (243) or downregulated (196) in Ben-Men-1 cells.

A

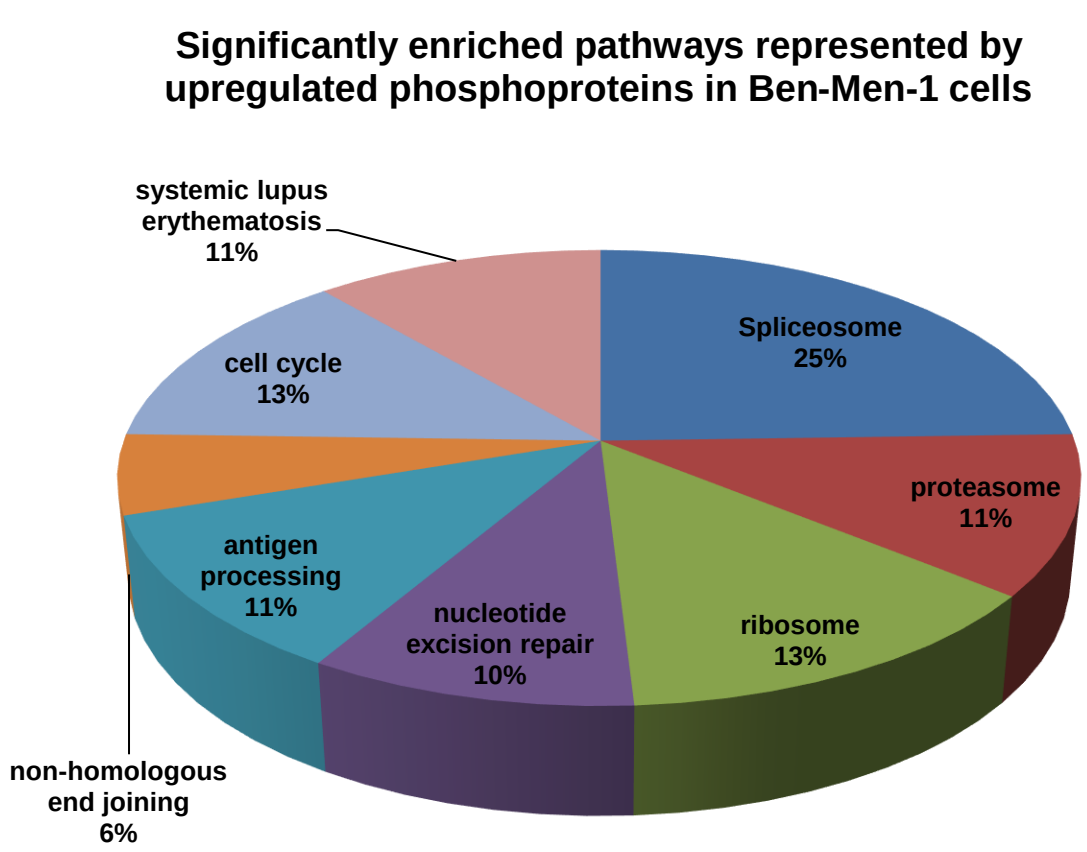
Significantly enriched pathways represented by upregulated phosphoproteins in Ben-Men-1 cells
systemic lupus erythematosis 11%
Spliceosome 25%
cell cycle 13%
proteasome 11%
antigen processing 11%
nucleotide excision repair 10%
ribosome 13%
non-homologous end joining 6%

B

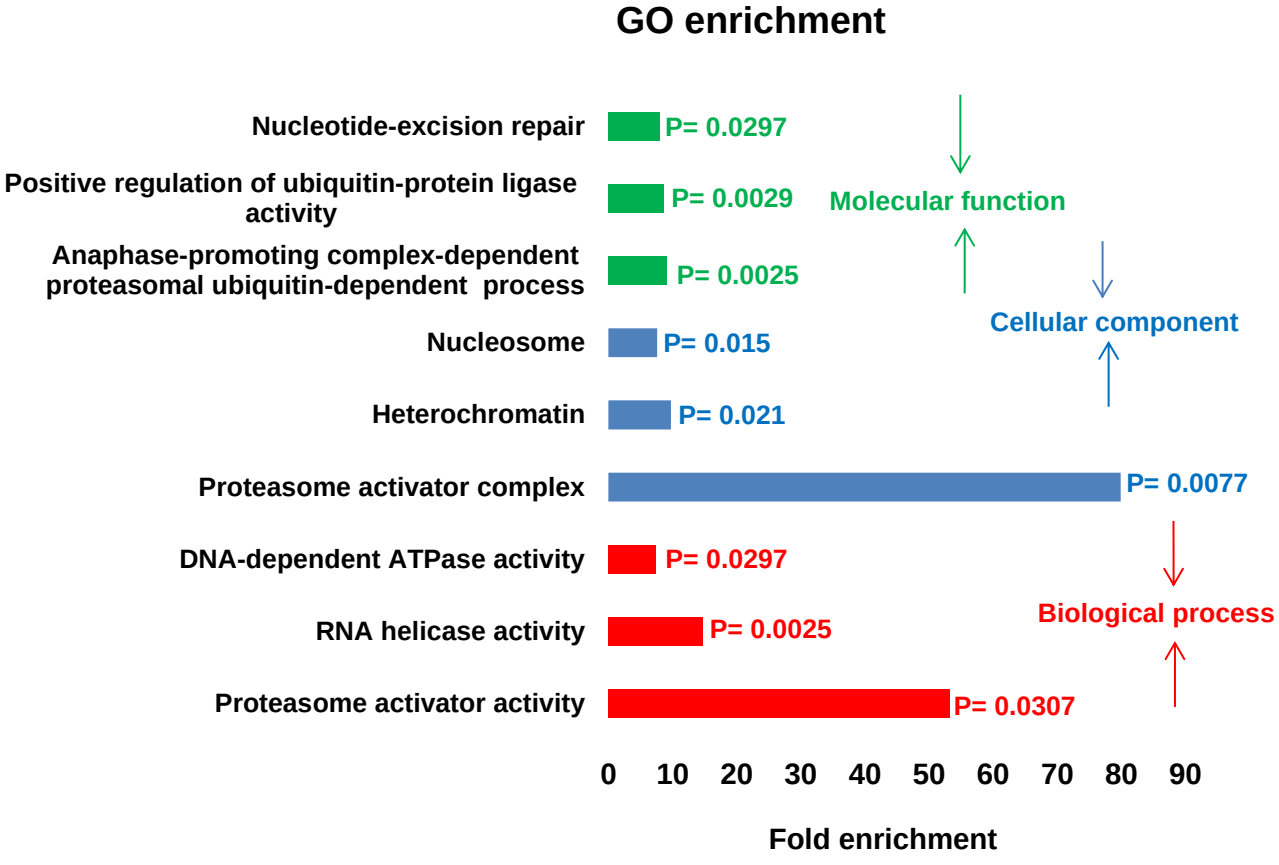
GO enrichment
Nucleotide-excision repair
P= 0.0297
Positive regulation of ubiquitin-protein ligase activity
P= 0.0029
Molecular function
Anaphase-promoting complex-dependent proteasomal ubiquitin-dependent process
P= 0.0025
Cellular component
Nucleosome
P= 0.015
Heterochromatin
P= 0.021
Proteasome activator complex
P= 0.0077
DNA-dependent ATPase activity
P= 0.0297
Biological process
RNA helicase activity
P= 0.0025
Proteasome activator activity
P= 0.0307
0 10 20 30 40 50 60 70 80 90
Fold enrichment

C

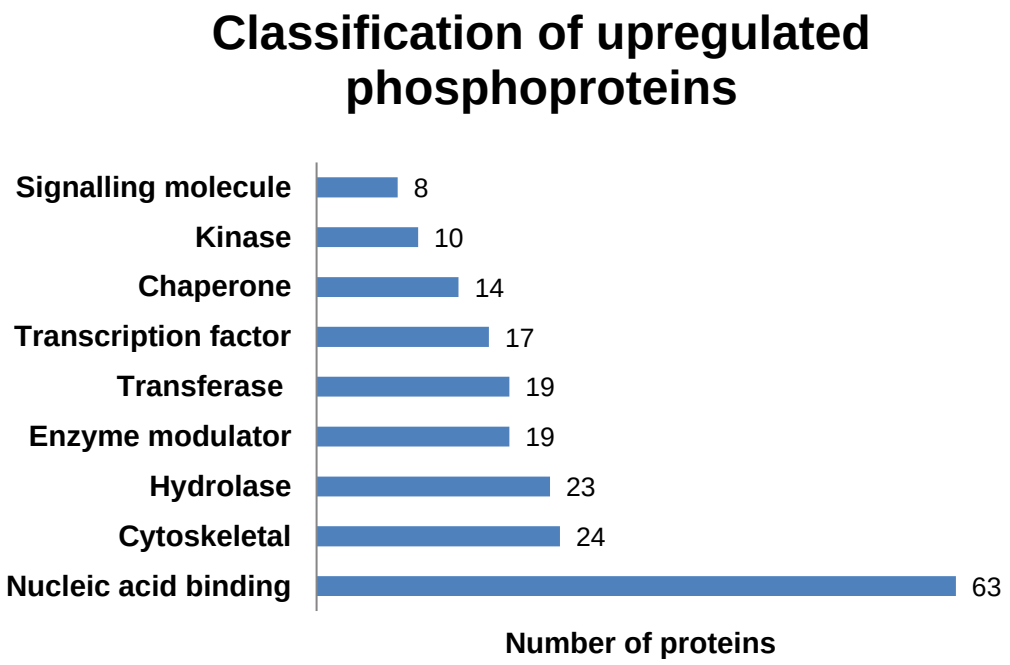

Figure 4.7: **Functional enrichment analysis of phosphoproteins upregulated in Ben-Men-1 cells A.** Pathways significantly enriched in Ben-Men-1 cells (Benjamani-Hochberg adjusted P < 0.05). **B.** Gene Ontology (GO) enrichment analysis highlighting a number of enriched GO terms (Benjamini-Hochberg adjusted P < 0.05). **C.** Classification of upregulated phosphoproteins based in protein class shows that the majority are nucleic acid binding proteins.

Classification of the upregulated phosphoproteins based on protein class shows that 63 are nucleic acid binding proteins, including several DEAD-box helicase (DDX) proteins and ribosomal proteins (Figure 4.7C). DDX5 in particular, which we identified with a log2 FC of 2.05, has been implicated in breast, colon, ovarian and prostate cancer, as a key contributor to tumour growth and proliferation (Janknecht 2010). As such, it might represent a potential therapeutic target for meningioma.

The next largest group is represented by 24 cytoskeletal proteins. Included in that list was PDLIM2, already identified as a potential target in primary schwannoma cells.

4.3.2 Downregulated phosphoproteins

There were several proteins identified as downregulated that are related to organization of the cytoskeleton (Figure 4.8), including Merlin. Unlike in schwannoma cells, PDLIM5 was identified as downregulated ruling it out of common target selection. Another cytoskeletal protein, Junction Plakoglobin (JUP) was also found to be downregulated with a fold change of -20.663. The total protein abundance was almost completely unchanged indicating that decreased phosphorylation of JUP in tumour cells is perhaps growth permissive. JUP, also known as γ-catenin is structurally and functionally related to β-catenin. Phosphorylated β-catenin was also found to be downregulated in Ben-Men-1 cells. The specific site of phosphorylation would first need to be elucidated before the effects of this downregulation can be fully appreciated.

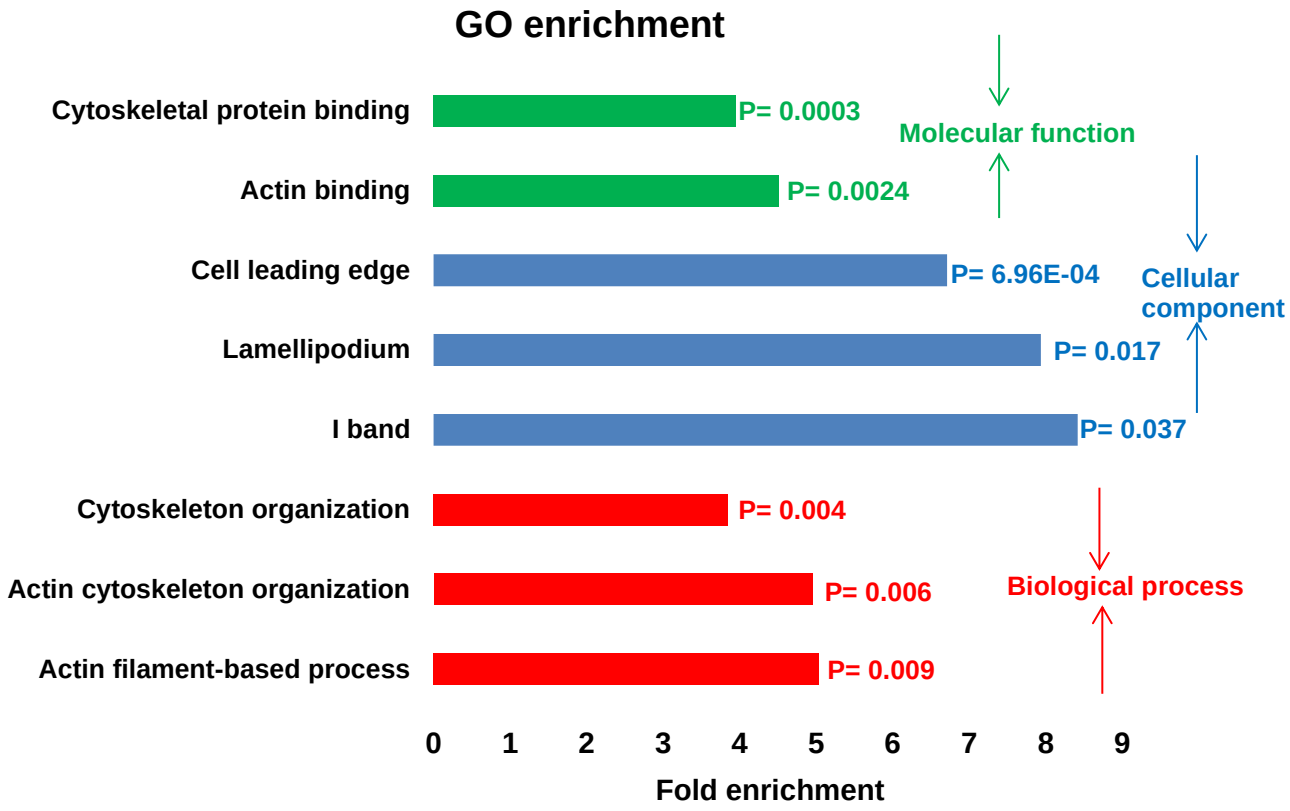

Figure 4.8: Gene Ontology (GO) enrichment of significantly downregulated phosphoproteins in Ben-Men-1 cells. The majority of enriched GO terms correspond to cytoskeletal regulation (Benjamini-Hochberg adjusted $P < 0.05$).

A number of downregulated phosphoproteins also mapped to the GO term 'lamellipodium' (Figure 4.8), which are actin projections on the leading edge of the cell and are important in cell migration and invasion (Kiosses, Shattil *et al.* 2001). The proteins involved include β-catenin and paxillin. Like β-catenin, the amount of total paxillin protein did not significantly change between normal and tumour cells. The activity of paxillin can change depending on exactly where it is phosphorylated therefore site-specific information would need to be obtained to understand the consequences of phospho-paxillin downregulation.

4.3.3 Ben-Men-1 total protein data

There were 3176 proteins originally identified and quantified, represented by a scatter plot (Figure 4.9). 177 were significantly upregulated, and 233 were significantly downregulated (the full list is presented in supplementary Table S6).

Among the pathways significantly enriched in Ben-Men-1 cells were focal adhesion and ECM-receptor interaction, largely characterised by the upregulation of several integrins (Figure 4.10A). Expression has been studied previously in meningioma and all three WHO grades have been shown to express a variety of integrins including beta 3 and alpha 5, as identified by Bello and colleagues (Bello, Zhang *et al.* 2000).

Significant enrichment of spliceosomal proteins was also observed. Among them was HSPA2 which has been identified as overexpressed in a large number of cancers and therefore represents a potential novel target in meningioma (Scieglinska, Gogler-Piglowska *et al.* 2014).

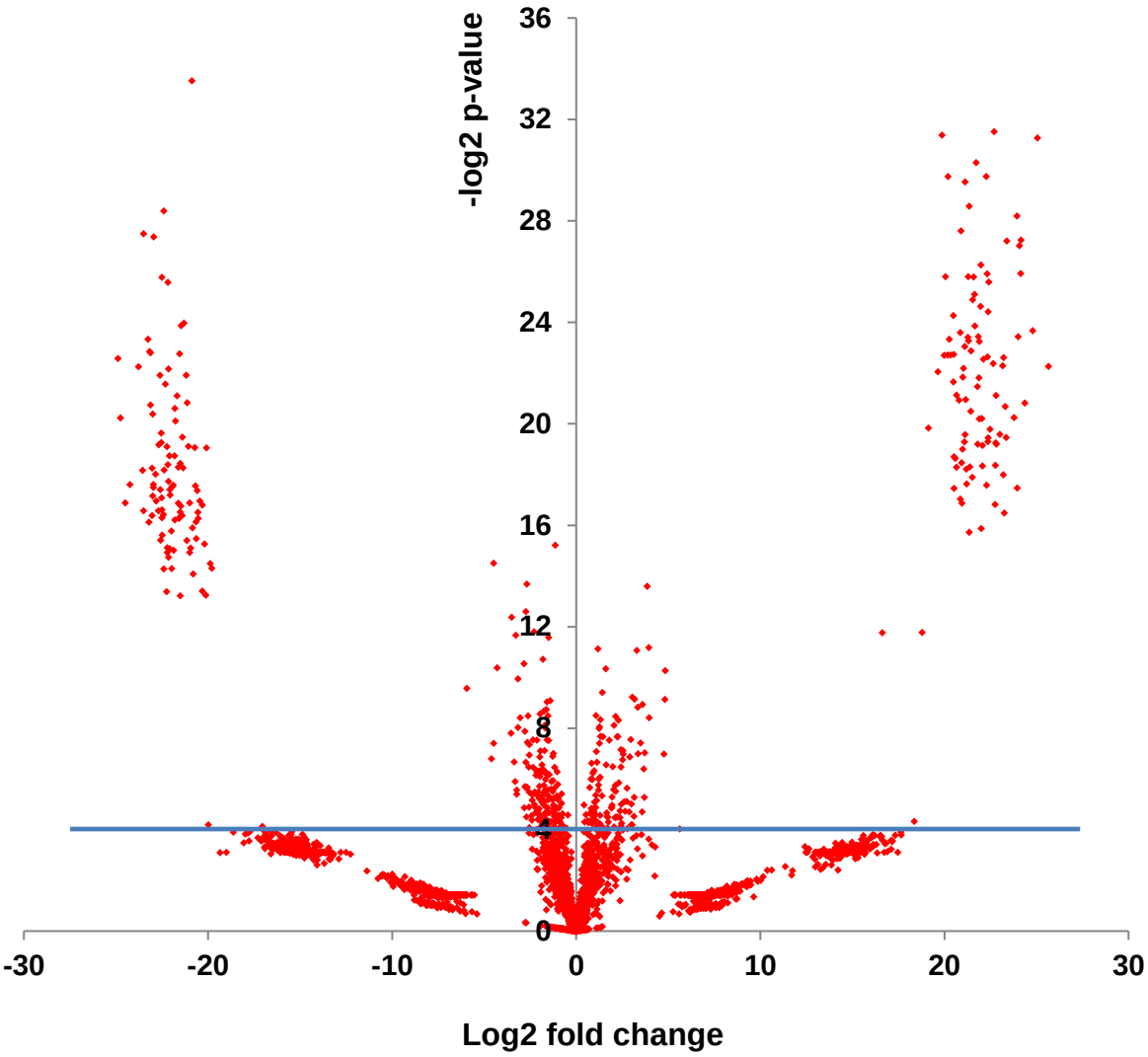

Figure 4.9: Scatter graph representation of meningioma total protein data set. A total of 3176 proteins identified in a comparison between Ben-Men-1 and HMC cells. The points above the blue line represent proteins that are significantly up (177) or downregulated (233) in Ben-Men-1 cells compare to HMC.

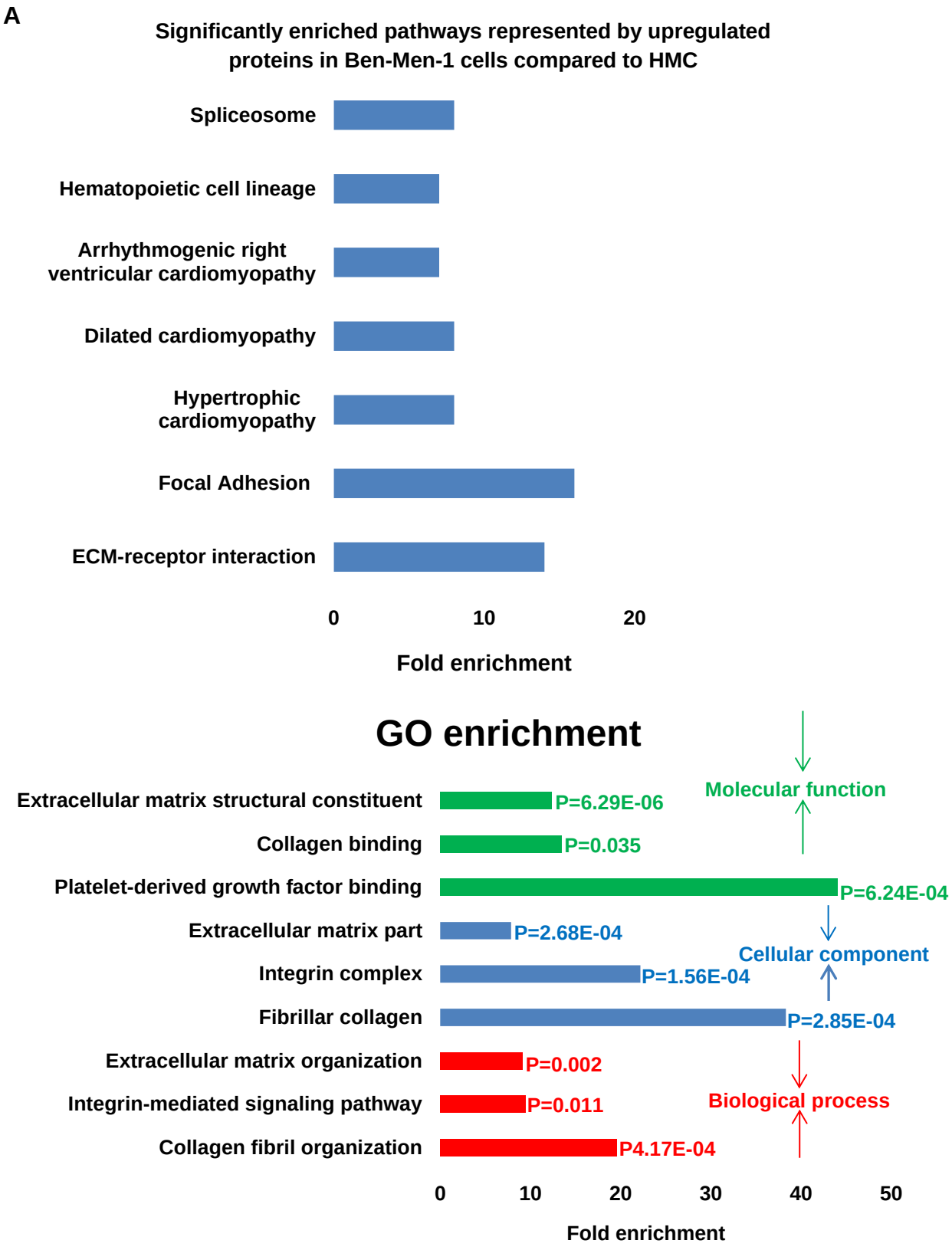

Figure 4.10: Functional enrichment analysis of proteins upregulated in Ben-Men-1 cells compared to Human Meningeal Cells (HMC) **A.** ECM-receptor interaction and focal adhesions are among the functionally enriched pathways (Benjamini-Hochberg adjusted P < 0.05) **B.** GO enrichment analysis identified collagen binding and ECM organization as significantly enriched (Benjamini-Hochberg adjusted P < 0.05).

GO enrichment analysis of upregulated proteins identified terms relating largely to ECM interaction, collagen and integrin mediated signalling (Figure 4.10B). We also found the PDGFRβ receptor as upregulated with a log2 FC of 1.6. Previous work within the group has shown that the overexpression of PDGFRβ is closely linked to integrin signalling. Collagen can also have major implications on tumour growth and progression, and can dictate to which degree a tumour is vascularized or how strongly it associates with its matrix (Fang, Yuan *et al.* 2014). There are in total seven collagens upregulated in Ben-Men-1 cells (COLL11A1, COL18A1, COL1A1, COL1A2, COL4A1, COL5A1, COL6A2), each with varying functions.

4.3.4 Downregulated total protein data

The most downregulated protein identified was THY1, or CD90. The significant decrease observed in Ben-Men-1 cells would suggest an important role for this protein in inhibiting tumorigenesis. Many of the downregulated proteins are involved in cellular metabolism including purine metabolism, starch and sucrose metabolism and like in schwannoma several are also related to lysosomes. There is downregulation of cathepsins C, D and Z indicating defects in lysosomal protein degradation.

4.3.5 Phosphoprotein *vs.* total protein in Ben-Men-1

Significantly changed phosphoproteins were plotted in a graph against their respective non-phosphorylated counterparts (Figure 4.11). There are several proteins that warrant further investigation as potential phosphorylated targets in meningiomas. They display large changes in phosphoprotein abundance and either no change or a decrease in total protein. Several of the most promising phosphorylated targets are shown in Table 4.2, chosen because they have all been previously linked with cancer and are among the most highly upregulated in Ben-Men-1 cells. Whilst these proteins and many others represent potential therapeutic targets, it would be necessary to confirm their expression by Western blot in subsequent analyses.

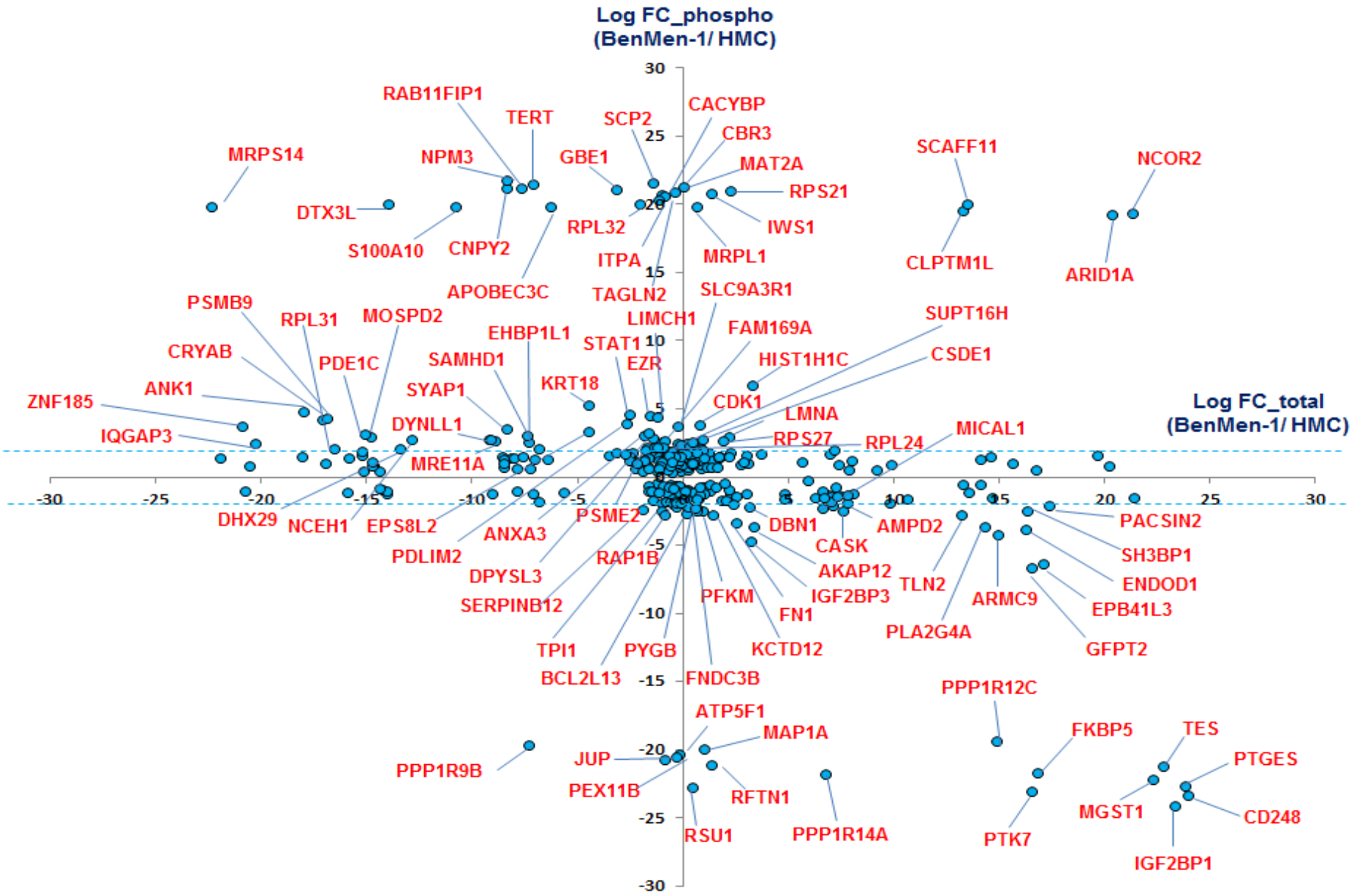

Figure 4.11: A graphical aid to represent the relationships between total and phosphoprotein levels in Ben-Men-1 cells.

Phosphoproteins significantly up or downregulated ($P < 0.05$) in Ben-Men-1 cells plotted against their respective total protein amounts.

Table 4.2		
Gene symbol	**Protein name**	**Function**
CACYBP	Calcyclin binding protein	Drives glioma proliferation
DTX3L	Deltex-3-like E3 ubiquitin ligase	DNA damage response modulation
RAB11FIP1	Rab11 family interacting protein 1	Promotes breast cancer growth, activates RAS and ERK
TAGLN2	Transgelin 2	Stabilizes actin filaments

Table 4.2: Potential therapeutic targets identified from a comparative analysis between a benign meningioma cell line, Ben-Men-1 and the normal meningeal cells HMC.

TAGLN2 is a protein similar in its function to TAGLN, which was identified as a possible therapeutic target in schwannoma. The transgelins are a family of proteins able to influence a diverse range of cellular processes, including proliferation, migration and apoptosis (Dvorakova, Nenutil *et al.* 2014). Non-phosphorylated TAGLN has been identified as a tumour suppressor in several cancers, but there has been limited research in to the phosphorylated form of either TAGLN or TAGLN2. Site-specific phosphorylation modulation may have different effects on TAGLN2, depending on the region of modification. It might be that phosphorylation is in fact an inhibitory mechanism interfering with tumour suppressive activity. Overall, the transgelins represent potential common NF2 targets, although this would require further investigation, particularly elucidation of specific phosphorylation sites.

CACYBP (Calcyclin binding protein) is a protein reported to have a number of functions in the cell, and can act as either an oncogene or a tumour suppressor, depending on the type of cancer (Topolska-Wos, Chazin *et al.* 2016). It can function as a component of E3 ubiquitin ligase complexes, is able to bind to the actin cytoskeleton

and may play a role in cell cycle regulation. CACYBP therefore represents an interesting target for further investigation in meningioma.

RAB11FIP1 is able to regulate Integrin alpha 5 trafficking which leads to the formation of membrane ruffles and increased cell invasiveness (Paul, Allen *et al.* 2015). Given the role of integrins in meningioma pathology, targeting RAB11FIP1 might be a valuable therapeutic strategy.

DTX3L is an E3 ubiquitin ligase able to modulate DNA damage responses rendering cancer cells resistant to certain chemotherapy drugs, and also promotes invasion in melanoma cells (Thang, Yajima *et al.* 2015). As we were also able to identify the DNA damage response as dysregulated in Ben-Men-1 cells, DTX3L could be an important protein through which this pathway can be targeted.

4.4 Phosphopeptide enrichment

In addition to phosphoprotein purification, phosphopeptide enrichment was utilized in an attempt to identify site-specific information that may have been of use in functional analysis. Firstly, Filter Aided Sample Preparation (FASP) was trialled in conjunction with SDS lysis buffer. This was to achieve buffer exchange and eliminate any detergent incompatible with subsequent phosphopeptide enrichment. The advantage of FASP is that it facilitates the use of SDS, which is considered the strongest and most effective lysis buffer particularly for permitting comprehensive membrane proteome coverage (Wisniewski, Nagaraj *et al.* 2010). Identifying active, targetable receptors on the cell membrane would be of particular importance in the search for possible therapeutic targets. However, detergents like SDS are incompatible with downstream enrichment techniques, hence the requirement for FASP. Urea buffer was also tested and is routinely used in phosphopeptide enrichment experiments. RadioImmunoprecipitation (RIPA) buffer was tested in parallel, as a gentler alternative to SDS. Neither of these requires FASP. In this comparative experiment, lysis with SDS followed by buffer exchange led to the lowest protein concentration overall. RIPA buffer and urea buffer yielded concentrations within 1ug/ml of each other (Table 4.3). Based on these results, RIPA buffer was chosen for the enrichment experiment.

Table 4.3

Lysis buffer	Protein concentration (ug/ml)	No. cells
RIPA	331	10^6
SDS	258	10^6
Urea	330	10^6

Table 4.3: Analysis of different lysis buffers prior to phosphopeptide enrichment. Three lysis buffers were tested and the resulting total protein yield was measured. RIPA buffer was identified as the buffer yielding the highest amount of protein.

4.4.1 Phosphopeptide data analysis

Titanium dioxide (TiO_2) enrichment was performed as described in chapter 2. 1 mg of Ben-Men-1 cell lysate was first digested with trypsin overnight, before three sequential incubations with TiO_2 beads and subsequent MS analysis of the pooled eluates. Figure 4.12 presents the data obtained. Identified peptides were filtered to contain only those with a localization probability of > 0.75 and only phosphopeptides with a peptide score of > 50 were allowed through the second filter. These are criteria set by Olsen et al in 2006 based on specially developed algorithms to ensure data quality and maximise correct phospho-site assignment. Further, the authors also state that the majority of identified peptides should be Serine (S) phosphorylated, followed by Threonine (T) with Tyrosine (Y) phosphorylated peptides representing the smallest group (Figure 4.12A) (Olsen, Blagoev *et al.* 2006). There were 216 phosphopeptides identified that fit the specified criteria, corresponding to 144 proteins. The full list can be viewed in supplementary Table S7. Functional enrichment using DAVID identified five significant pathways (Figure 4.12B). The majority of these have been previously linked to Merlin deficient tumours.

Figure 4.12C shows specific phospho-site information for proteins related to focal adhesion, regulation of the actin cytoskeleton and adherens junctions, chosen because they are the most pertinent and well characterized in Merlin-deficient tumours.

A

Amino acid	Number of peptides
Serine (S)	155 (71.8%)
Threonine (T)	46 (21.3%)
Tyrosine (Y)	15 (6.9%)

B

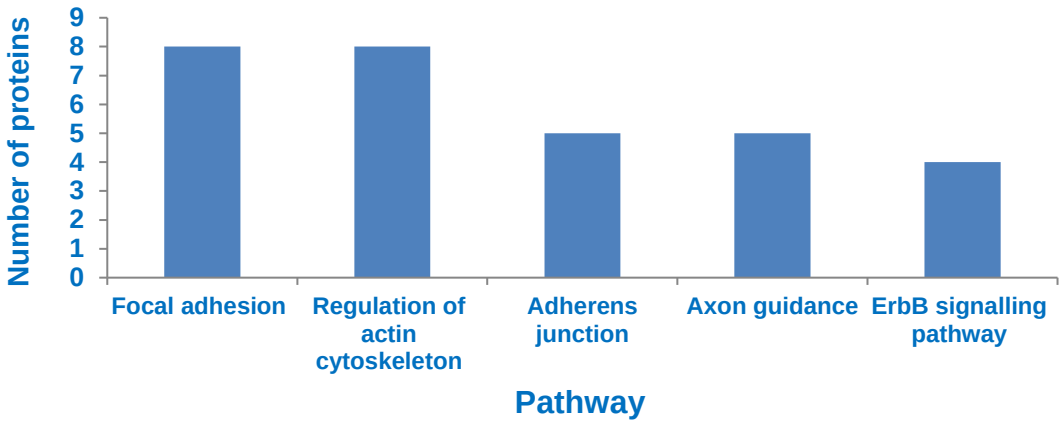

C

Gene symbol	Modified sequence	Phospho site
PAK2	_YIS(ph)FTPPEK_	S141
EGFR	PIT(ph)PSGEA	T693
FLNB	S(ph)PGSANET	S2478
LAMA5	IAIS(ph)AS(ph)IGR	S2715
PDPK1	ANS(ph)FVGT	S241
PPP1CA	MSDS(ph)EKIN	S4
PPP1R12A	GS(ph)YGAIAE	S445
CFL1	AS(ph)GVAVSD	S3
CFL2	S(ph)GVTVND	S3
BAIAP2	FNPS(ph)IRN	S27
LMO7	S(ph)PTSPFS/ S(ph)IDNID	S991/ S1510
CTNNA1	DDS(ph)DFETE	S641
MAPK37	S(ph)IQDITVTG	S439
SLIT3	Y(ph)VEIASA	Y1168
EIF4EBP1	TT(ph)PGGTIFS	T46

Figure 4.12: Ben-Men-1 phosphopeptide data analysis. **A.** The proportion of Serine (S), Threonine (T) and Tyrosine (Y) phosphorylated peptides identified in Ben-Men-1 cells via TiO_2 enrichment. **B.** Functional enrichment analysis identified five significantly enriched pathways represented by the dataset (Benjamini-Hochberg adjusted $P < 0.05$) **C.** Specific phospho-sites that correspond to proteins mapping to cytoskeletal, focal adhesion and adherens junction pathways.

The acquisition of site specific information can assist greatly in the identification of suitable drugs and in the drug design process. It gives us a greater chance of identifying specific kinases that can also be exploited as a therapeutic strategy. The PAKs in particular are known to be implicated in schwannoma pathogenesis via their involvement in RAC signalling (Flaiz, Chernoff *et al.* 2009). PAK2_S141 has not been previously reported in schwannoma or meningioma and may represent a novel target.

We were also able to identify two cofilins, CFL1 and CFL2, phosphorylated at S3 by LIM-domain kinases, which have been previously linked to schwannoma (Petrilli, Copik *et al.* 2014). A study published in 2014 identified an inhibitor, T56-LIMKi, which was able to decrease the level of S3 phosphorylation of cofilin in a schwannoma cell line, thus leading to decreased growth. It may therefore represent a valuable therapeutic option for Merlin-deficient tumours (Rak, Haklai *et al.* 2014).

We also identified the EGF receptor, phosphorylated at T693. The EGFR has been previously identified as constitutively active at this site in lung cancer (Assiddiq, Tan *et al.* 2012) and the receptor is known to be linked to several pathways including the MAPK and PI3K/Akt, known to be important in meningioma pathology. As such, we validated the expression of pEGFR_T693 by western blot in Ben-Men-1 cells compared to HMC, detecting it in Ben-Men-1 cells but not in the control (Figure 4.13A). Figure 4.13B shows that pEGFR_T693 was also activated in primary meningioma cells, further pEGFR_T693 activation was detected in grade I meningioma tumours, but not in normal meningeal tissue lysate (Figure 4.13C). The data also highlights the fact that EGFR_T693 activation appears to be independent of Merlin status.

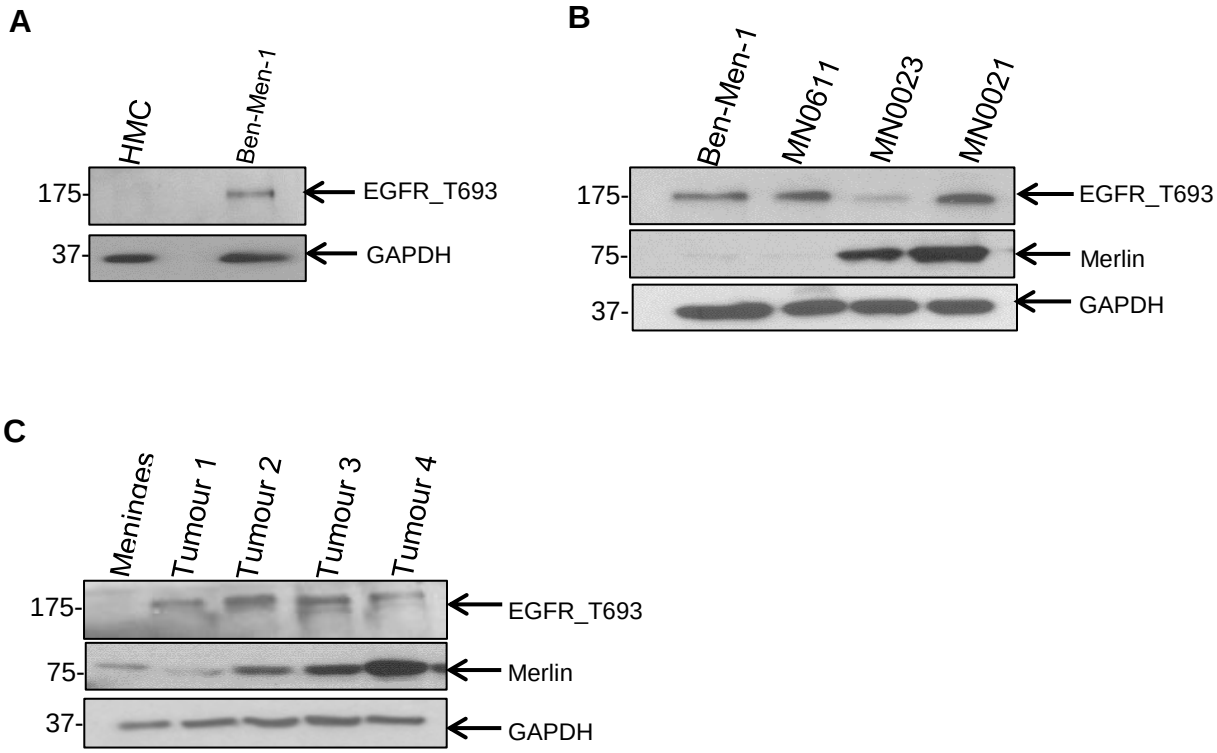

Figure 4.13: Phosphopeptide data validation for pEGFR_T693 expression in meningioma cells. **A.** Western blot showing that EGFR_T693 is detected in Ben-Men-1 cells but not in HMC **B.** EGFR_T693 is activated in primary meningioma cells. **C.** Western blot analysis of pEGFR_T693 detected in grade I meningioma tumours, but not in normal meningeal tissue.

4.5 Discussion

We have been able to identify several potential therapeutic targets for the treatment of meningioma. One of the important points learned from the analysis presented here is that MS results need to be interpreted carefully. Raw data must be scrutinized to make clear distinctions between proteins that are genuinely differentially expressed, and those that appear to be so. It must be stressed that any information identified by MS should be properly validated by other means before firm conclusions are drawn.

As part of the analysis to identify targets in meningioma, we analysed both a meningioma cell line, Ben-Men-1 and three primary meningioma cell populations, both against a common control, normal Human Meningeal Cells (HMC). We were able to identify many more proteins in the cell lines than we were in primary cells, the possible reasons for which will be discussed in more detail throughout the final discussion. In the two sets of significantly changed phosphoproteins, there were 80 that were common to both Ben-Men-1 and primary meningioma cells (Supplementary Table S8). One of these was CTSD (Cathepsin D). This upregulation can lead to a number of cellular responses including increased angiogenesis, and enhanced invasion (Pranjol, Gutowski *et al.* 2015). Further characterization would be required to determine the suitability of CTSD as a meningioma target. Of note, phospho-CTSD was downregulated in schwannoma cells, which rules it out as a common NF2 drug target.

The data presented here provides further rationale for targeting the proteasome in meningioma treatment, as it was among the most significantly enriched pathways represented by upregulated phosphoproteins in Ben-Men-1 cells and primary meningioma cells. There is also scope for investigating DNA repair mechanisms and the spliceosome as potential therapeutic targets. The phosphorylated proteins fatty acid synthase (FAS), transglutaminase 2 (TGM2) and Mothers against decapentaplegic 2 (SMAD2), identified as upregulated in primary meningioma are also candidates for further analysis as potential meningioma targets.

We have also identified a number of phosphorylation sites corresponding to several proteins. Although this was not a comparative analysis of phosphopeptides between tumour and normal cells, it does provide an indication of which proteins are activated in Ben-Men-1 cells that might act as therapeutic targets. We confirmed the expression of EGFR_T693 in primary meningioma cells and tumour samples, and it would be interesting to further analyse this phosphoprotein in relation to meningioma pathogenesis.

Chapter 5- Selection, validation and functional assessment of candidate therapeutic targets

5.1 Introduction

The aim of this thesis has been to identify targets common to both meningioma and schwannoma in an innovative step toward the simultaneous treatment of NF2-related tumours. We demonstrated in the previous chapters that the use of MS in conjunction with phosphoproteomics is a valuable tool for identifying upregulated and aberrantly activated proteins in both primary meningioma and schwannoma cells that might represent novel therapeutic targets.

This chapter will describe the process of candidate target selection for further analysis, and present validation data of a number of potential, common targets. Whilst until now the datasets obtained from each individual experiment were treated independently of one another, this chapter focusses on the data overall. Particular proteins that were identified as potential therapeutic targets in the previous chapters may not appear on the final list chosen for further analysis, simply because in looking for commonality between distinct datasets, the pool was somewhat reduced. It must therefore be stressed at this point that a number of potential targets have not been taken forward as part of this project, but hold promise for future analyses.

5.2 Common targets in primary meningioma and schwannoma

We compared primary meningioma with primary schwannoma to identify potential targets for future analyses. There were 42 phosphoproteins that were commonly and significantly changed in both primary meningioma and primary schwannoma cells, compared to their respective controls. Of these, the majority showed opposite differential expression in either cell type i.e. if a protein was upregulated in schwannoma, it was downregulated in meningioma and vice versa. There were 10 that were commonly up or downregulated, and these are listed in Table 5.1.

Table 5.1			
Gene symbol	**Protein name**	**Log2 FC meningioma**	**Log2 FC schwannoma**
SPAG9	C-Jun-amino-terminal kinase-interacting protein 4	-2.05	-1.99
TRIO	Triple functional domain protein	-23.52	-1.16
TALDO1	Transaldolase	-1.13	-1.25
TUFM	Elongation factor Tu, mitochondrial	2.39	1.56
NT5C2	Cytosolic purine 5-nucleotidase	1.54	1.25
CLASP1	CLIP-associating protein 1	-22.00	-1.69
PPIL4	Peptidyl-prolyl cis-trans isomerase-like 4	-21.31	-1.02
PSMB7	Proteasome subunit beta type-7	-1.72	-1.32
YTHDC2	Probable ATP-dependent RNA helicase YTHDC2	-22.33	-2.13
KIF13B	Kinesin-like protein KIF13B	-21.47	-2.51

Table 5.1: Phosphoproteins commonly and significantly up or downregulated in primary meningioma and primary schwannoma cells ($P < 0.05$).

Of the 10, there were two phosphoproteins that were commonly upregulated in both cell types; TUFM and NT5C2. Mitochondrial Tu translation elongation factor (TUFM) is involved in mitochondrial protein translation and has been linked to several cancers. NT5C2, or 5'-Nucleotidase, Cytosolic II is an enzyme involved in purine metabolism and mutations of this protein have been heavily linked with leukaemia. Both therefore warrant further investigation as common NF2 targets.

5.3 Common targets in Ben-Men-1 and primary schwannoma

When significantly changed phosphoproteins in Ben-Men-1 cells were compared with those in primary schwannoma cells, the majority again showed opposite expression in both cell types and of those, 15 were commonly up or downregulated (Table 5.2). There was however considerably more overlap between these two datasets than between primary meningioma and schwannoma, and so the final selection of candidate targets was based on this comparison.

To select candidates for further analysis we applied the following criteria; firstly, it was decided that only upregulated proteins would be considered as it is not feasible to target downregulated proteins. This reduced the pool to 11 proteins.

Availability of phospho-specific antibodies was also a consideration and of the 11 remaining proteins, there were commercially available antibodies only for STAT1 and HSPA1A. We had previously identified two STAT1 phospho-sites, S727/ Y701, by selecting phosphorylation as a variable modification using maxquant and these were confirmed by Western blot. We did not obtain site-specific information for HSPA1A therefore two sites were analysed using two available antibodies; Y525 and Y41.

Finally, because we had previously identified FLNB and PDLIM2 by phosphopeptide enrichment in Ben-Men-1 cells, these were also selected for further analysis; however no phospho-specific antibodies are currently available. For validation experiments, we were able to obtain an antibody dually targeting pFLNA /pFLNB. Table 5.3 summarizes the candidate targets selected and briefly describes their known functions.

Table 5.2			
Gene symbol	**Protein name**	**Log2 FC Ben-men-1**	**Log2 FC schwannoma**
CORO1C	Coronin-1C	2.60	1.45
CTPS	CTP synthase 1	1.23	3.70
CUTA	Protein CutA	1.44	1.50
EPS8L2	Epidermal growth factor receptor kinase substrate 8-like protein 2	3.36	24.27
FLNB	Filamin-B	1.22	24.49
HSPA1A	Heat shock 70 kDa protein 1A/1B	1.21	3.23
PDE1C	Calcium/calmodulin-dependent 3,5-cyclic nucleotide phosphodiesterase 1C	3.16	1.36
PDLIM2	PDZ and LIM domain protein 2	3.94	24.53
PSMB8	Proteasome subunit beta type-8	1.40	1.29
STAT1	Signal transducer and activator of transcription 1-alpha/beta	4.57	26.24
TCEB2	Transcription elongation factor B polypeptide 2	1.01	1.02
MAP1A	Microtubule-associated protein 1A;MAP1 light chain LC2	-19.89	-1.00
PACSIN2	Protein kinase C and casein kinase substrate in neurons protein 2	-2.11	-1.19
PSMB7	Proteasome subunit beta type-7	-1.17	-1.32
UFL1	E3 UFM1-protein ligase 1	-1.14	-1.43

Table 5.2: Phosphoproteins commonly and significantly up or downregulated in Ben-Men-1 and primary schwannoma cells ($P < 0.05$).

Table 5.3		
Protein name	**Gene symbol**	**Function**
Filamin B	FLNB	Actin cross-linking, providing a communicative link between the cell membrane and the cytoskeleton.
Heat shock protein family A member 1A	HSPA1A	Facilitates correct protein folding, transport and degradation.
PDZ and LIM domain containing protein 2	PDLIM2	Promotes cell migration and adhesion, and has E3 ubiquitin ligase activity.
Signal Transducer and Activator of Transcription 1	STAT1	Activated in response to Interferons and various RTKs, involved in inflammation.

Table 5.3: The candidate therapeutic targets selected for further analysis based on commonality between overexpression in Ben-Men-1 cells compared to control, and primary schwannoma cells compared to control.

5.4 Candidate target validation

The next stage of the project involved validation of chosen targets in several primary tumour samples, as overexpressed compared to their respective controls. Following that, the most promising candidate therapeutic targets were functionally assessed *in vitro* forming the initial stages of valuation of their suitability as novel drug targets for the treatment of NF2.

These targets represent those that are truly activated, and not just increased because of changes in total protein amount, potentially making them important targets for the 'switching off' of tumorigenic signalling.

5.4.1 Total and phospho STAT1 expression in meningioma and schwannoma

Total STAT1, pSTAT1_S727 and pSTAT1_Y701 expression were analysed in primary meningioma cells and tissue. Western blot analysis showed a significant increase of total STAT1 in Ben-Men-1 cells and primary meningioma cells, compared to HMC (Figure 5.1A and B). Analysis of phospho-STAT1 confirmed expression of both phospho-STATs in Ben-Men-1 and primary meningioma cells, and also showed that HMC cells do not express either pSTAT1_Y701 or S727.

We were also able to confirm the expression of both STAT1 phosphorylation sites by immunohistochemistry (IHC) in primary meningioma tissue sections (Figure 5.2A and B). Positive staining for both Y701 and S727 was seen in all cases - a total of 30 sections. STAT1_Y701 stained strongly in the cytoplasm (Figure 5.2A) and conversely 727 stained exclusively in the nucleus (5.2B). We additionally confirmed localization of Y701 and S727 in primary meningioma cells by immunocytochemistry (ICC) (Figure 5.2C and D). Again, pSTAT1_Y701 was expressed strongly in the cytoplasm but not in the nucleus (Figure 5.2C), and pSTAT1_S727 was seen exclusively within the nucleus, and not at all in the cytoplasm (Figure 5.2D).

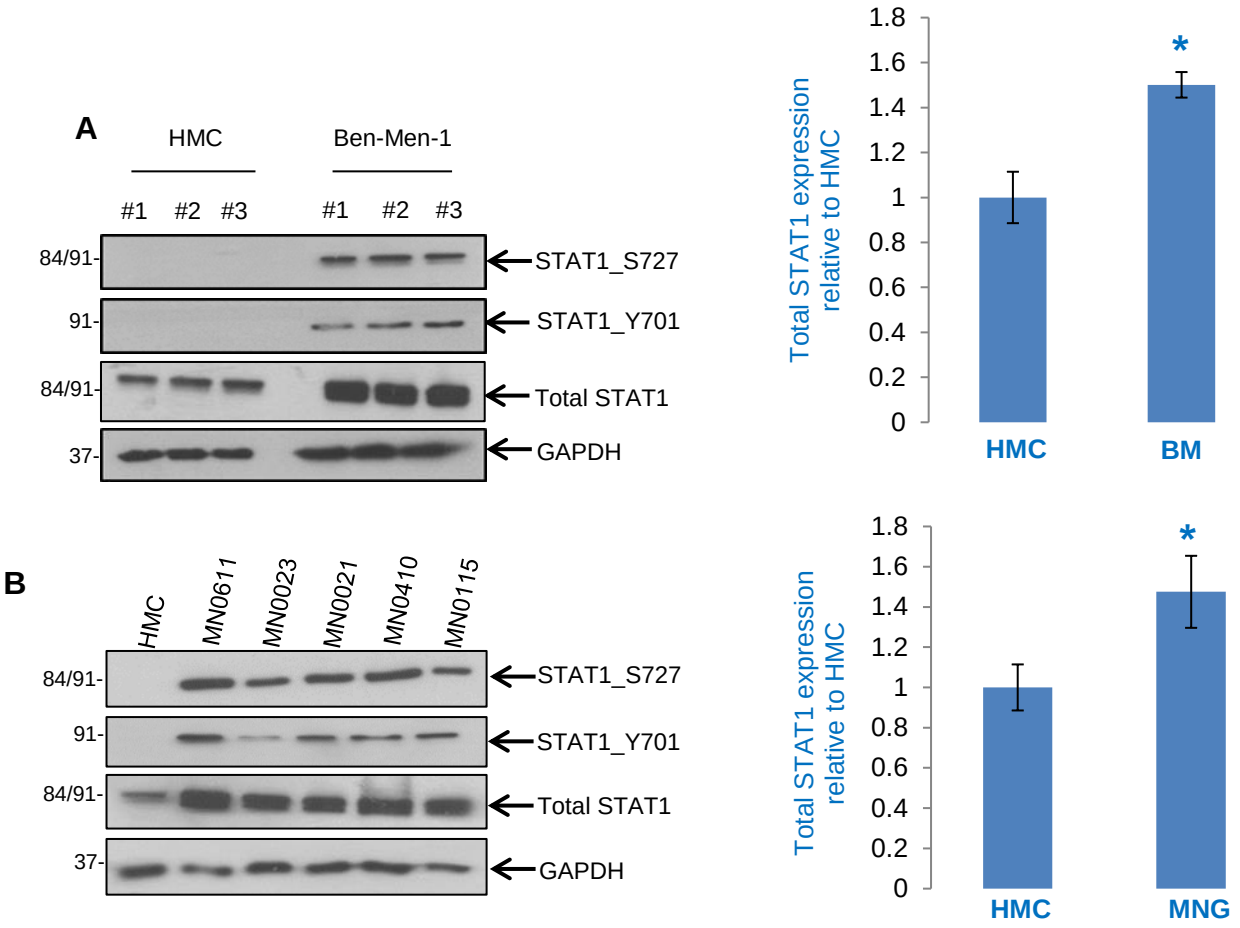

Figure 5.1: Total and phospho STAT1 expression in primary meningioma cells. **A.** Total and phospho-STAT1 expression were analysed by Western blot in Human Meningeal Cells (HMC) and Ben-Men-1 cells (BM) in triplicate. Total STAT1 was significantly increased in BM cells, and both pSTAT1_Y701 and pSTAT1_S727 were expressed in BM but not in HMC. **B.** Total STAT1 and phospho-STAT1 expression in primary meningioma cells (MN) was analysed by Western blot. Total STAT1 expression was significantly increased in primary meningioma cells compared to HMC.

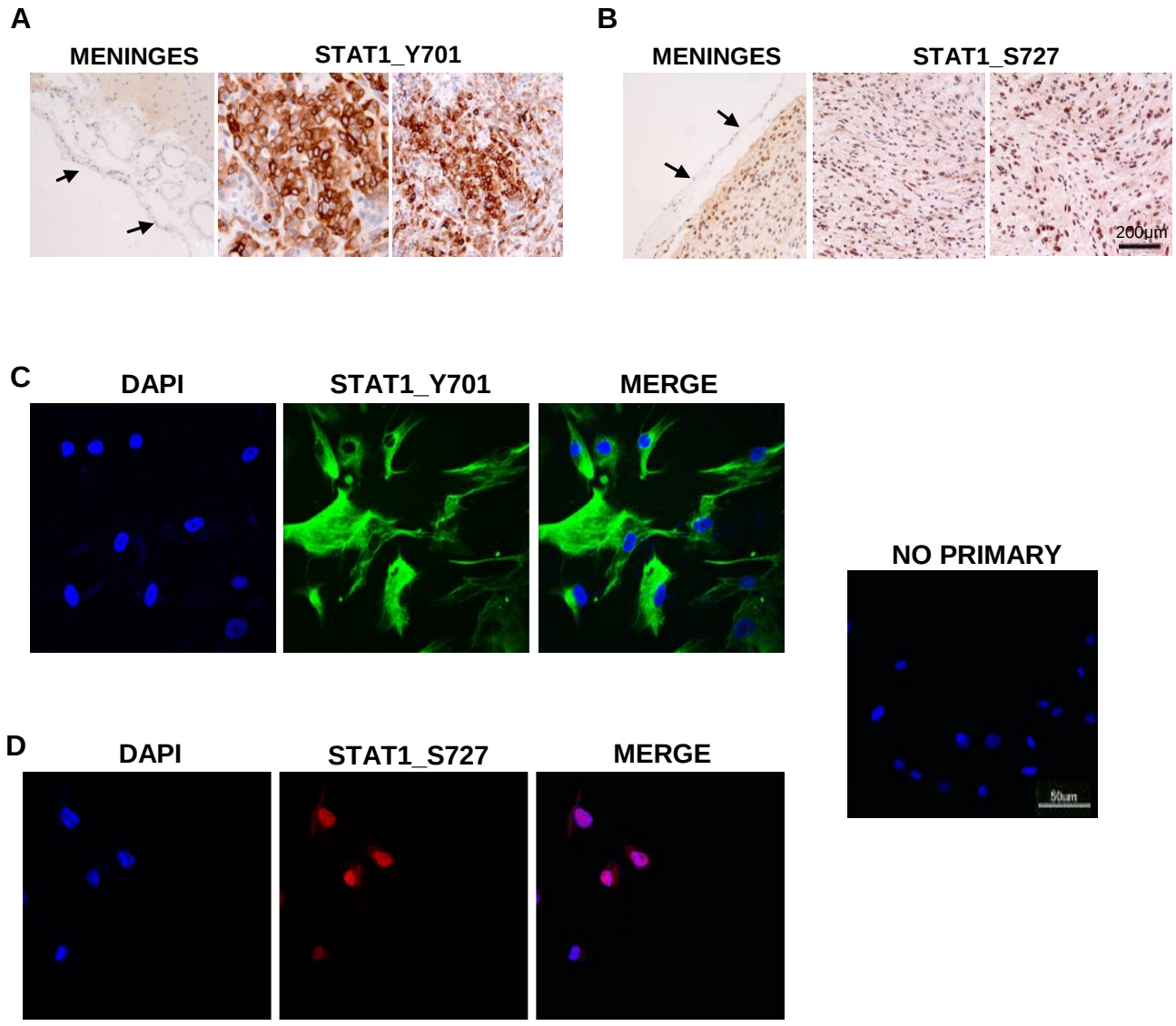

***Figure 5.2: Phospho-STAT1 in primary meningioma cells and tissue.* A/ B.** pSTAT1_Y701 and S727 were analysed by IHC in frozen grade I meningioma tissue. Neither Y701 nor S727 were observed in normal meningeal tissue. Phospho-STAT1_Y701 was exclusively cytoplasmic and pSTAT1_S727 was almost entirely nuclear. **C/ D.** pSTAT1_Y701 and pSTAT1_S727 were analysed by ICC in primary meningioma cells. Again pSTAT1_Y701 stained exclusively in the cytoplasm and S727 was observed in the nucleus. All ICC images were taken at 40x magnification and all IHC images at x200. No primary= no primary antibody control. The same antibody was used for control and tumour samples.

5.4.2 Confirming total and phospho STAT1 expression in primary schwannoma cells

Western blot analysis of seven primary schwannoma *vs.* three primary Schwann cell samples showed an overall non-significant (NS) increase in total STAT1 expression (Figure 5.3A) in tumours compared to controls. Expression of pSTAT1_701 and S727 varies among the seven tumours analysed, with four out of seven expressing both phospho-STATs and three of seven not expressing them at all. None of the controls were found to express either phospho-STAT1. As was observed in primary meningiomas, in the four schwannomas that do express phosphoprotein, both sites were simultaneously activated.

Immunofluorescent staining showed that pSTAT1_Y701 was cytoplasmic, and that STAT1_S727 was nuclear (Figure 5.3B and C).

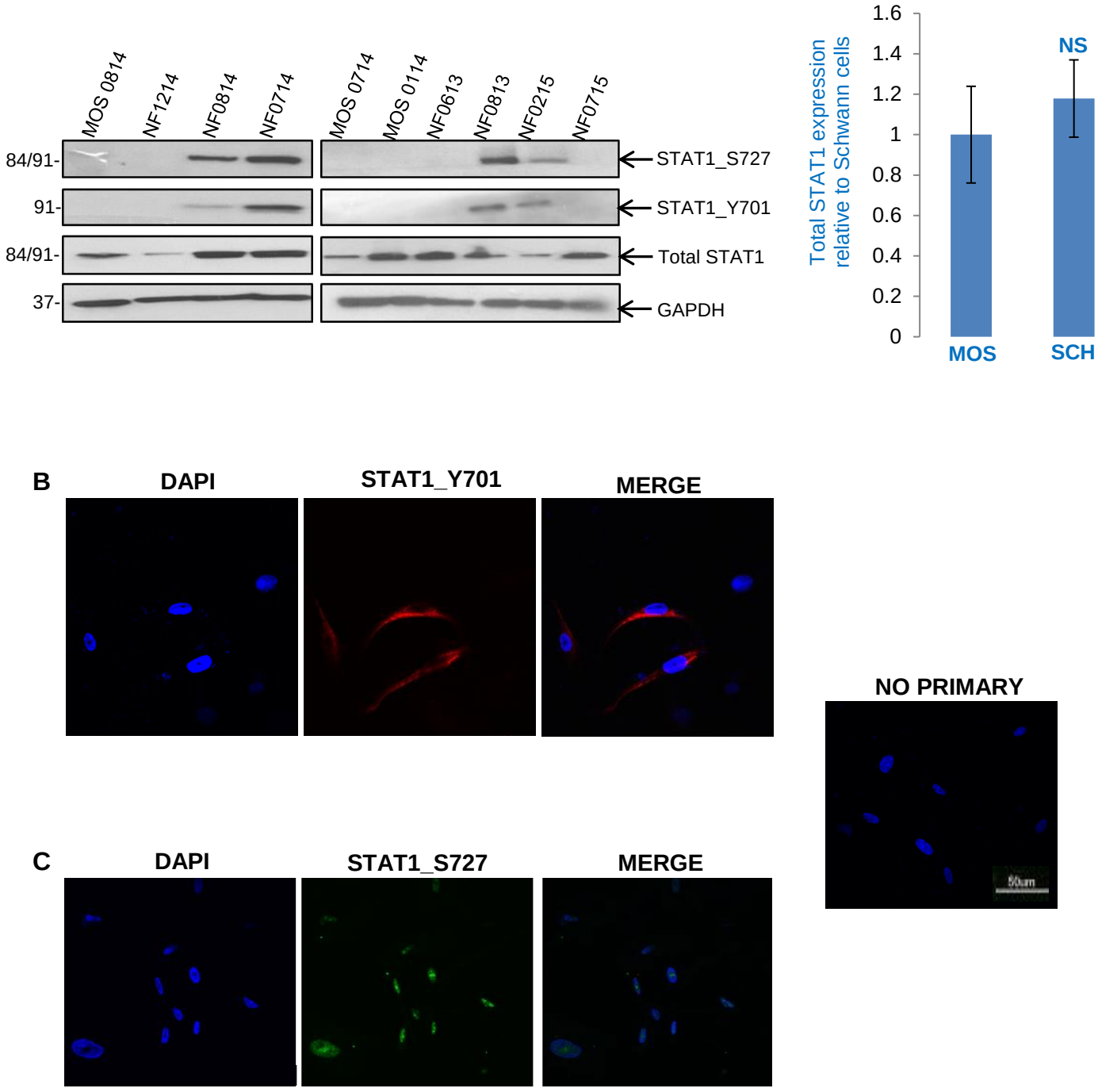

Figure 5.3: Total and phospho-STAT1 expression in primary schwannoma cells. **A.** Western blot analysis of total and phospho- STAT1 in primary Schwann (MOS) and schwannoma (NF) cells. Total STAT1 expression was non-significantly increased in primary NF and both pSTAT1_Y701 and S727 were co-expressed in four out of seven NF samples, and not at all in MOS. **B*/* C**. pSTAT1 expression was analysed by ICC in NF cells. Phospo-STAT1_Y701 was localized to the cytoplasm (B) while pSTAT1_S727 was completely nuclear (C). All Images were taken at 40x magnification. NS= non-significant, no primary= no primary control.

5.4.3 PDLIM2 protein expression in primary meningioma and schwannoma

We next sought to validate PDLIM2 expression in primary meningioma cells. We were unable to find any phospho-specific antibodies, including for PDLIM2_S137 that was identified by phosphopeptide enrichment (Table S7). Reports in the literature have shown this phosphorylated form of PDLIM2 is able to act specifically on STAT1, targeting it for degradation via its E3 ubiquitin ligase activity (Guo, Mi *et al.* 2010). Without a specific antibody, unfortunately it would be difficult to test this mechanism in our cells.

Total PDLIM2 expression was analysed in five primary meningioma samples as well as Ben-Men-1 and HMC cells. PDLIM2 was not detected in HMC but was expressed to varying degrees in all Ben-Men-1 and primary meningioma samples (Figure 5.4A and B). Analysis of grade I primary meningioma tissue samples further confirmed that PDLIM2 was not expressed in primary meningeal tissue, and was expressed in all meningioma tissue samples (Figure 5.4C).

Western blot analysis also showed that PDLIM2 was not detected in two out of three Schwann cells tested, but was very weakly expressed in MOS0114. PDLIM2 expression was observed in five out of seven primary schwannoma samples (Figure 5.4D).

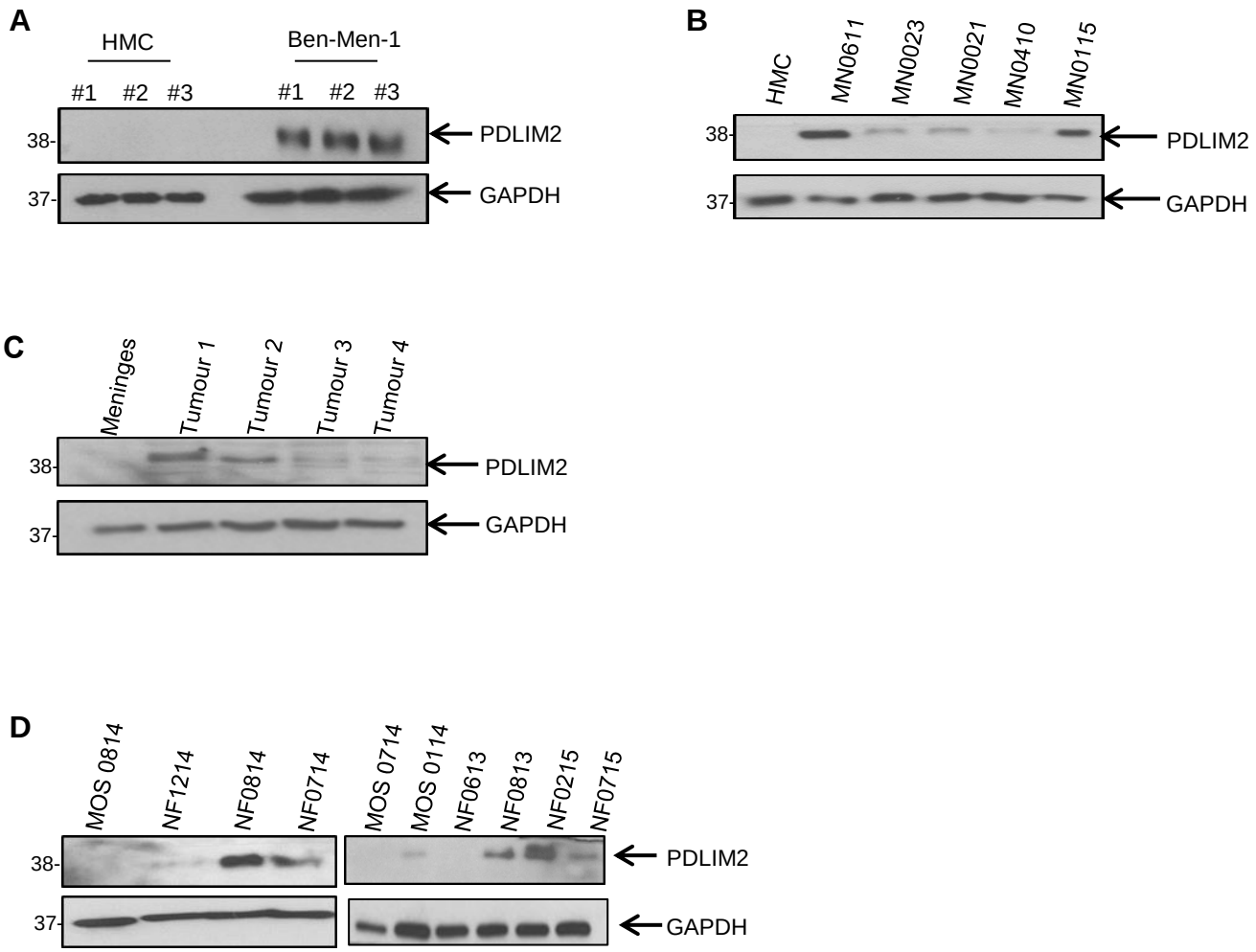

Figure 5.4: PDLIM2 expression in primary meningioma cells and tissue, and in primary Schwann and schwannoma cells. **A.** Western blot analysis of PDLIM2 expression in triplicate in Ben-Men-1. **B.** PDLIM2 immunoreactivity was detected in five primary meningioma cell samples *vs.* HMC. **C.** PDLIM2 was expressed in four primary meningioma tissue samples *vs.* normal meningeal tissue. **D.** Western blot analysis of PDLIM2 expression shown in five of seven NF samples and weakly in one out of three MOS samples.

5.4.4 PDLIM2 phosphorylation and localization in primary meningioma cells.

Given that PDLIM2 phosphorylation at S137 was identified by phosphopeptide enrichment in Ben-Men-1 cells, an *in vitro* dephosphorylation assay was performed using lambda phosphatase. This experiment would confirm whether the phosphorylated form of PDLIM2 is expressed in Ben-Men-1 cells. In the absence of a phospho-specific antibody, this is an alternative method of assessing the phosphorylation status of proteins. A shift in band mobility is detected via Western blot, where phosphorylated proteins migrate slower than their non-phosphorylated counterparts, leading to the detection of a higher molecular weight band after probing with a total protein antibody.

We were able to detect a lower molecular weight band by Western blot analysis after phosphatase treatment of Ben-Men-1 cell lysate, indicating that PDLIM2 is indeed phosphorylated in these cells (Figure 5.5A).

Nuclear and cytoplasmic extraction was also performed to determine the cellular localization of PDLIM2 in Ben-Men-1 cells and three primary meningiomas. This is because the cellular location of PDLIM2 may be important for its function. PDLIM2 was found to be almost entirely nuclear, with no bands present in the cytoplasmic fraction upon Western blot analysis apart from a very faint band in MN0065 cells (Figure 5.5B). HDAC was used as a nuclear control, and GAPDH was used as a cytoplasmic control to ensure successful fractionation.

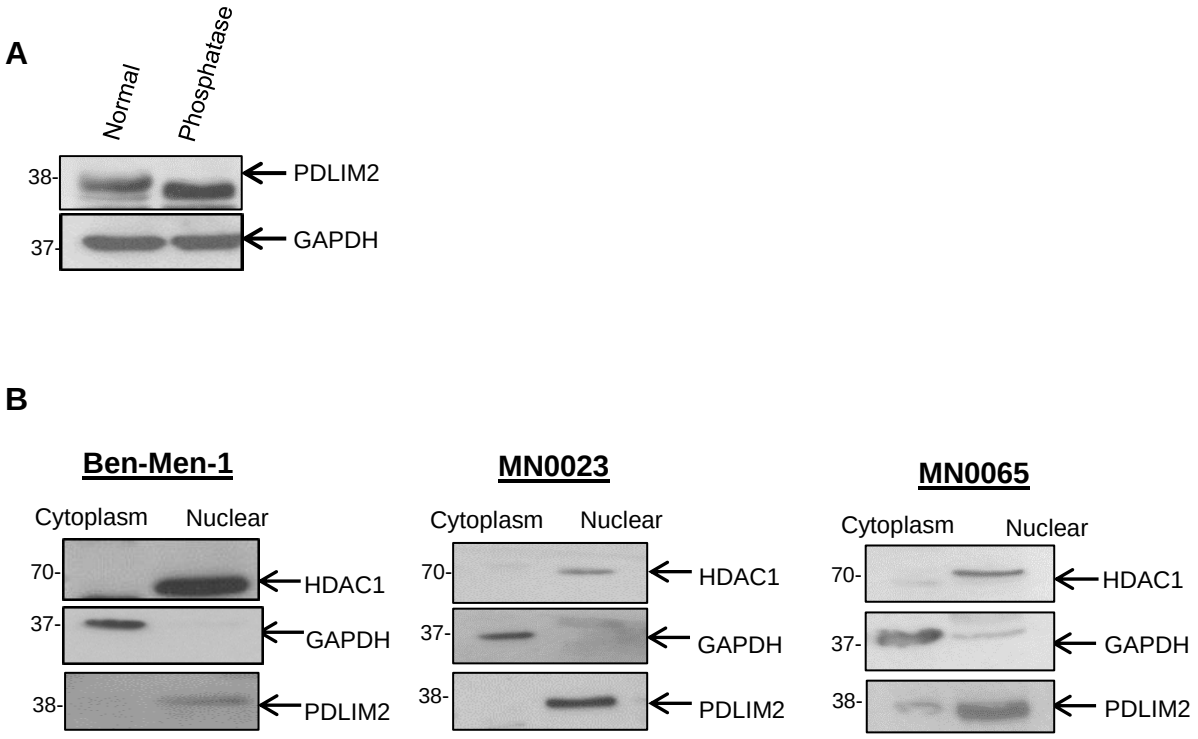

Figure 5.5: PDLIM2 phosphorylation and localization in Ben-Men-1 and primary meningioma cells. **A.** Ben-Men-1 cell lysate was treated with lambda phosphatase and analysed for the expression of PDLIM2. After phosphatase treatment, the band for PDLIM2 was of lower molecular weight. **B.** Nuclear and cytoplasmic extraction was performed using Ben-Men-1 and two MN cell populations to determine the localization of PDLIM2. In all cases, PDLIM2 was found to be almost entirely nuclear.

5.4.5 FLNB expression in primary meningioma cells and tissue

Due to unavailability of a phospho-FLNB, we tested total FLNB, and also an antibody dually targeting phospho-filamin A (FLNA) and phospho-FLNB_S2107.

There was overall a non-significant decrease observed in total FLNB expression between HMC and Ben-Men-1 cells repeated in triplicate (Figure 5.6A). FLNB expression in primary meningioma cells showed a non-significant increase compared to HMC (Figure 5.6B).

Again, a non-significant increase of pFLNA/pFLNB expression was observed in primary meningioma cells compared to HMC (Figure 5.6C). However, we identified pFLNA/pFLNB expression in four primary meningioma tumour tissue samples, but not in normal meningeal control tissue (Figure 5.6D).

5.4.6 FLNB expression in primary Schwann and schwannoma cells

We analysed total and phospho-FLNB expression by Western blot in primary Schwann and schwannoma cells. We identified a significant increase in total FLNB expression in schwannoma cells (Figure 5.7A), and an overall non-significant decrease in pFLNA/pFLNB expression (Figure 5.7B).

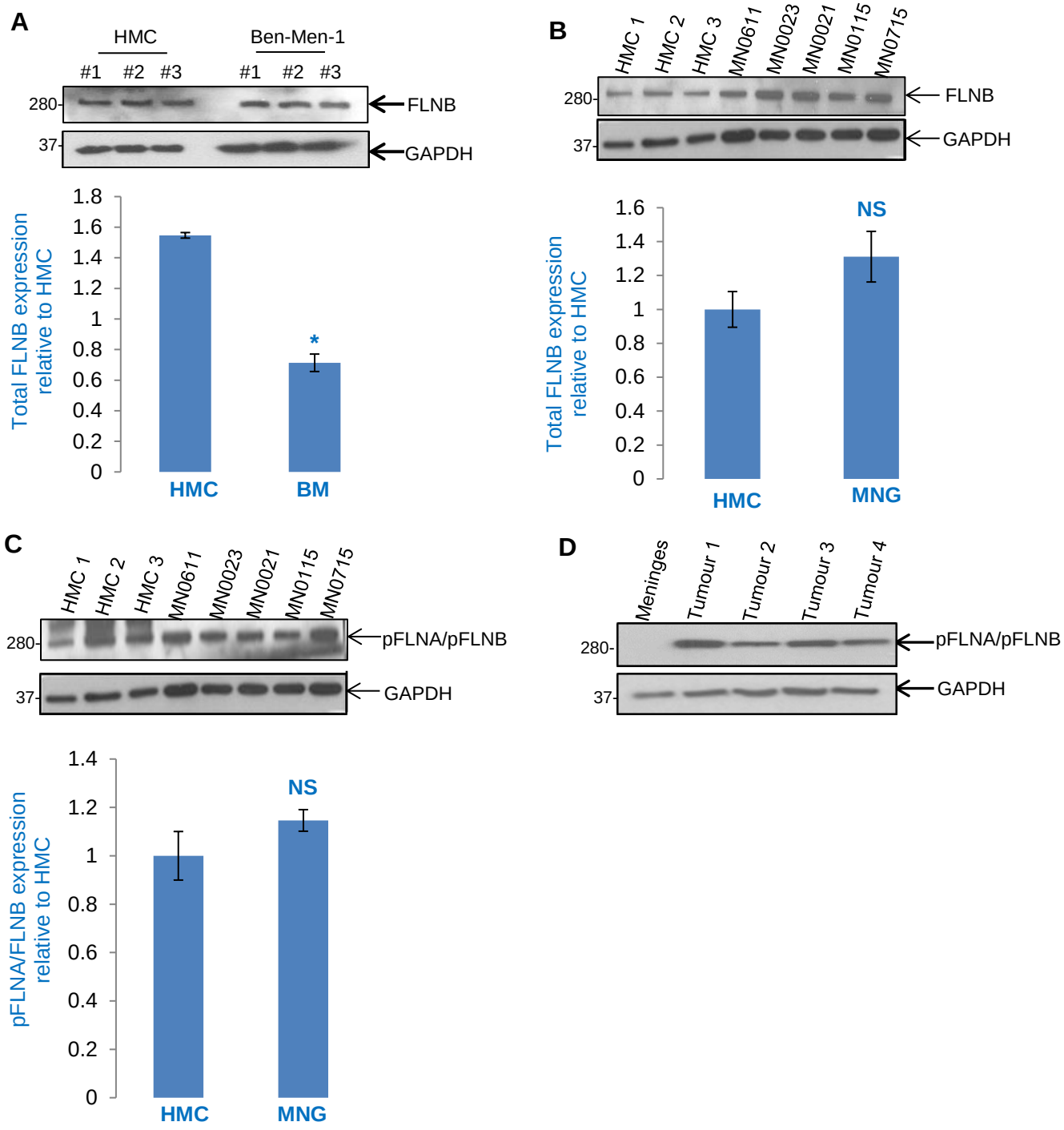

Figure 5.6: Total and phospho- FLNB expression in primary meningioma cells and tissue. **A.** Total FLNB was non-significantly decreased in Ben-Men-1 cells compared to HMC. **B.** Total FLNB expression was non-significantly increased in primary meningioma cells compared to HMC. **C.** pFLNA/pFLNB expression was non-significantly increased in MN cells compared to HMC. **D.** pFLNA/pFLNB was identified in four primary meningioma tumour samples, but not in normal meninges.

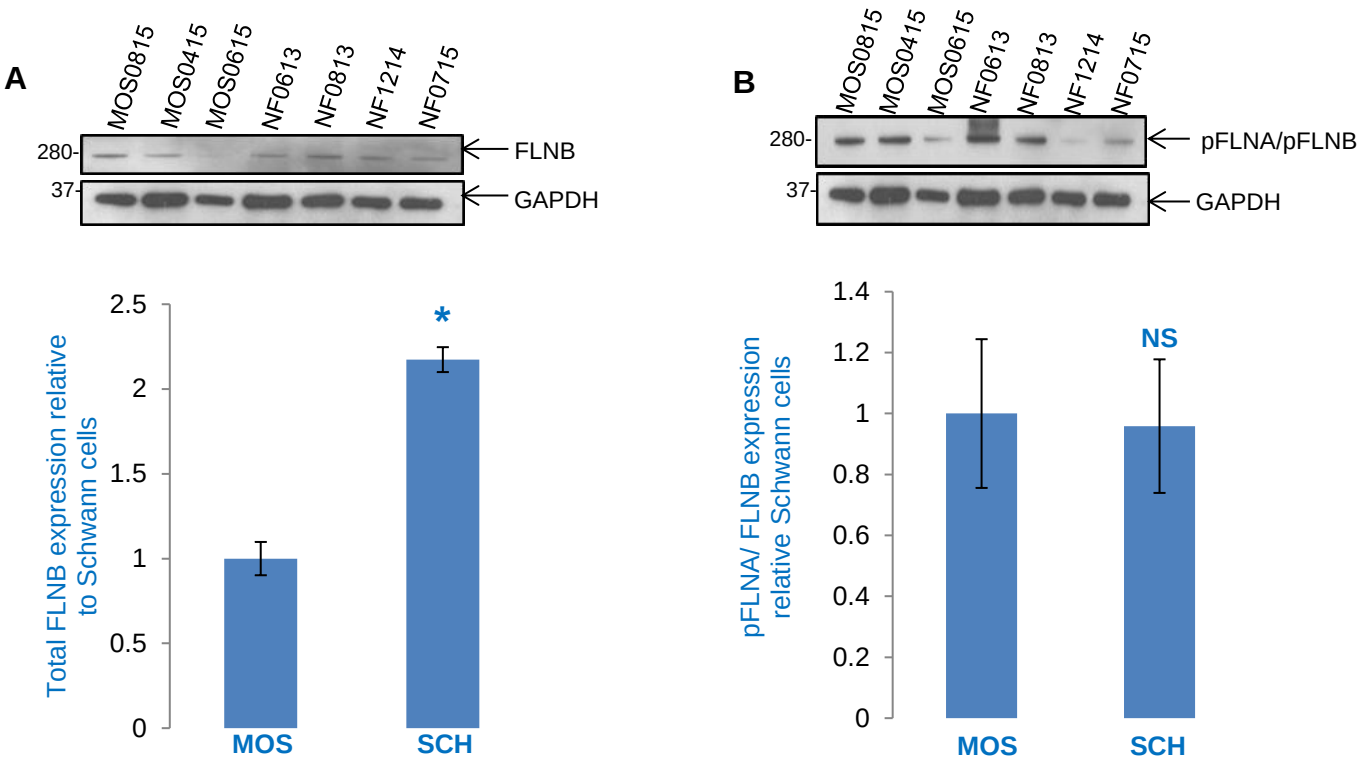

Figure 5.7: Total and phospho- FLNB expression in primary schwannoma. **A.** Western blot analysis showing FLNB expression in three MOS samples and five NF samples revealing a non-significant increase in schwannoma cells. **B.** pFLNA/pFLNB expression was found to be non-significantly decreased in primary schwannoma compared to Schwann cells.

5.4.7 Total and phospho-HSPA1A expression in primary meningioma cells and tissue

Total HSPA1A was significantly decreased in Ben-Men-1 cells compared to HMC (Figure 5.8A), as analysed by Western blot. However, a significant increase was observed in primary meningioma cells, compared to HMC, mainly due to clear increased expression in samples MN0611 and MN0715 (Figure 5.8B).

As we did not identify any specific phosphorylation sites on HSPA1A, we tested two different antibodies, one targeting pHSPA1A_Y41, and one targeting pHSPA1A_Y525. We analysed pHSPA1A_Y41 expression by Western blot and identified a non-significant increase in primary meningioma cells compared to HMC (Figure 5.8C). However, Western blot analysis of pHSPA1A_Y41 expression in primary meningioma tissue lysate revealed expression in four tumour samples and very little expression in normal meningeal tissue (Figure 5.8D).

We used anti-HSPA1A_Y525 to assess expression on frozen grade I meningioma tumour sections as anti-pHSPA1A_Y41 was not suitable for IHC. Weak or moderate staining was observed in all cases (10 in total). We also looked for HSPA1A_Y525 expression in five normal meningeal controls, and in all cases staining was either negative or weak (Figure 5.8E).

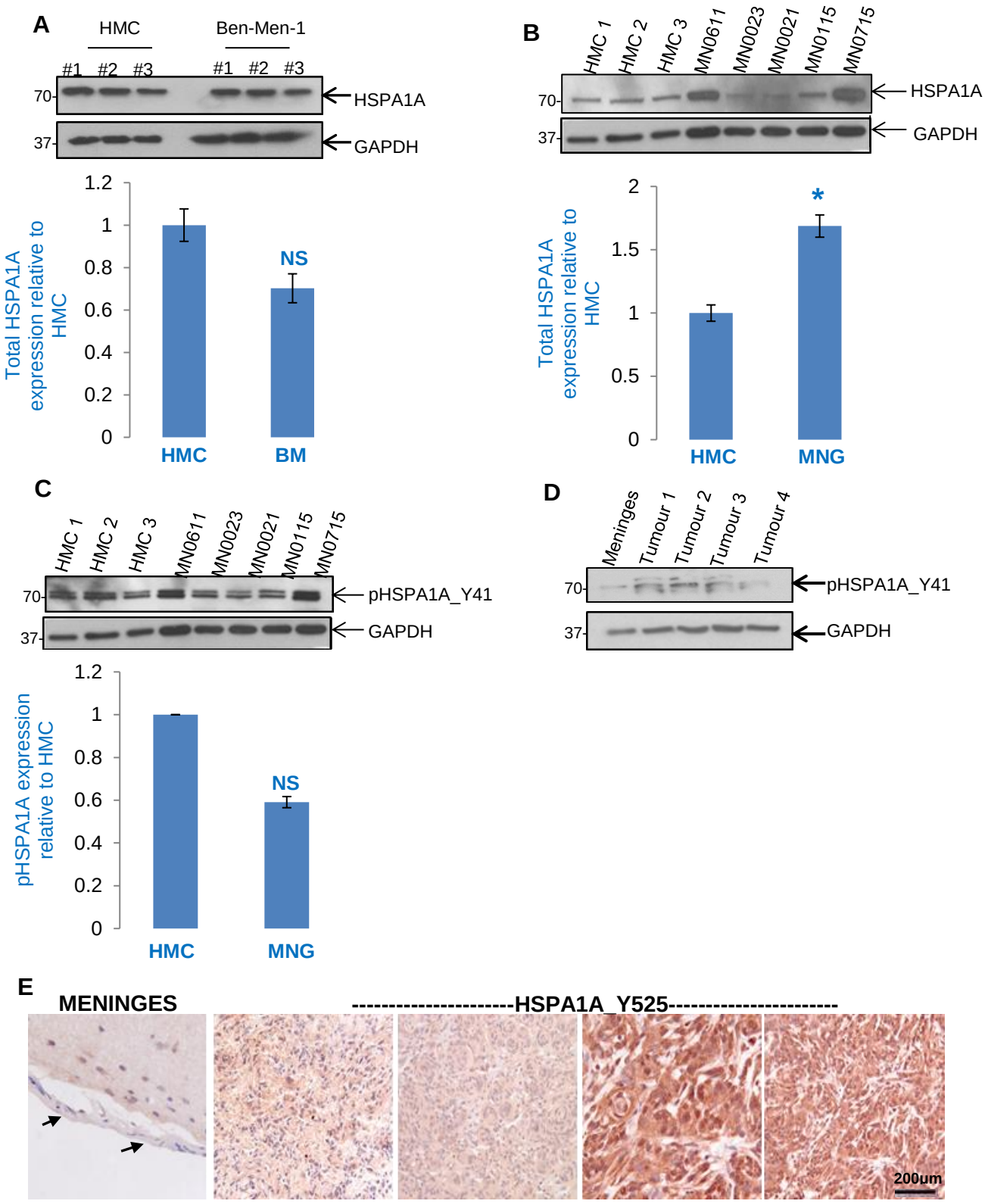

Figure 5.8: Total and phospho-HSPA1A expression in primary meningioma cells and tissue. **A.** Western blot analysis of total HSPA1A expression in Ben-Men-1 cells *vs.* HMC performed in triplicate. **B.** HSPA1A expression in primary meningioma's (MN) *vs.* HMC**. C.** Western blot analysis of pHSPA1A_Y41 in MN compared to HMC. **D.** pHSPA1A_Y41 was highly expressed in primary meningioma tumour tissue compared to normal meninges. **E.** Immunohistochemical analysis of grade I meningioma tissues showing weak to moderate HSPA1A_Y525 expression compared to no expression in normal meningeal tissue. The same antibody was used for control and tumour samples.

5.4.8 Total and phospho-HSPA1A expression in primary schwannoma cells and tissue

Western blot analysis showed Total HSPA1A expression was non-significantly increased in primary schwannoma compared to primary Schwann cells (Figure 5.9A). PHSPA1A_Y41 was also identified as non-significantly increased overall in primary schwannoma cells (Figure 5.9B). Immunohistochemical analysis of HSPA1A_Y525 expression in schwannoma revealed moderate or strong staining across 10 sections from different tumours (Figure 5.9C). We also analysed five normal nerve specimens that were all negative or weakly positive for HSPA1A_Y525.

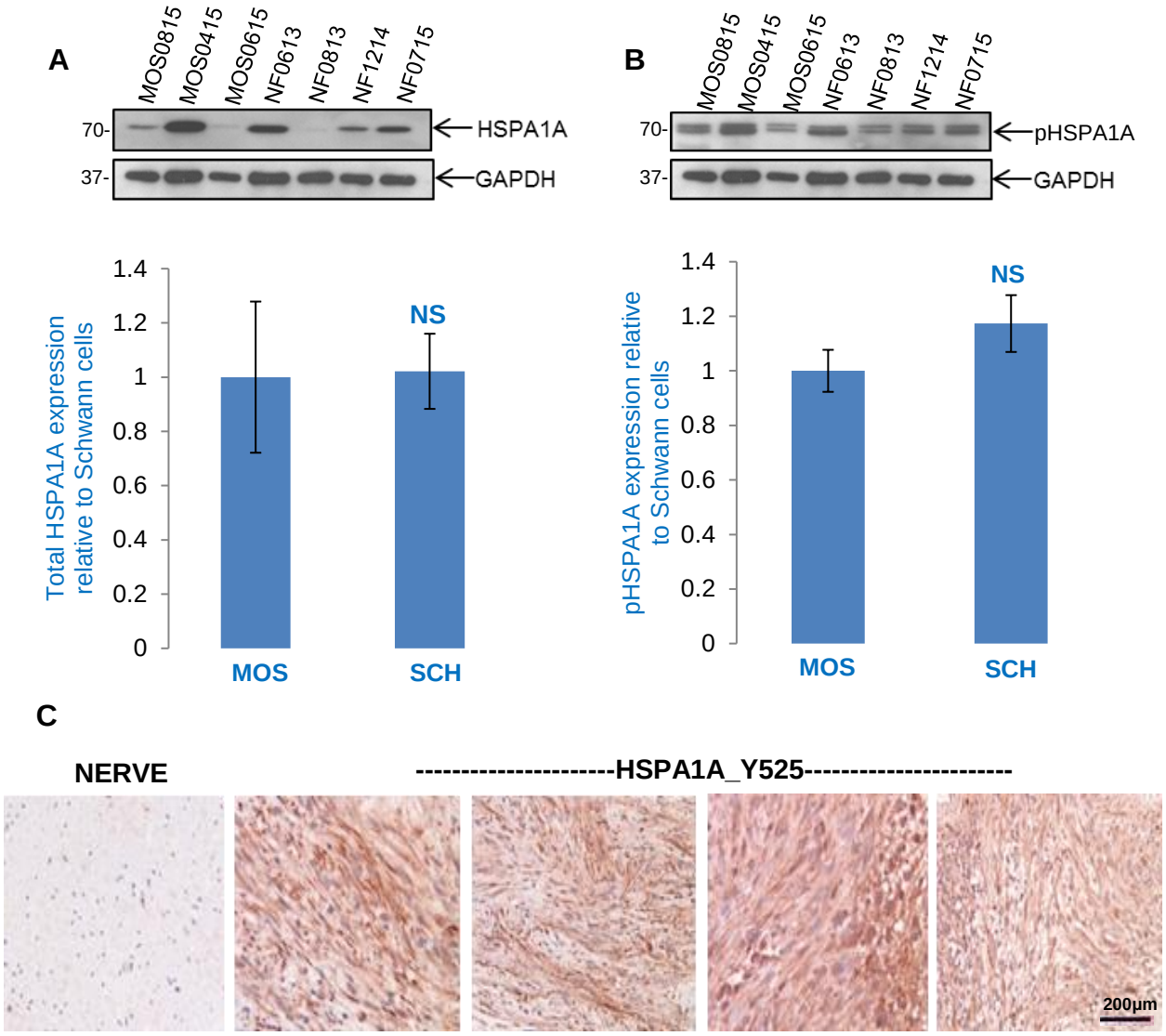

Figure 5.9: Total and phospho-HSPA1A expression in primary schwannoma cells. **A.** Western blot showing a non-significant increase of total HSPA1A expression in NF compared to MOS cells. **B.** pHSPA1A_Y41 expression was identified by Western blot as non-significantly higher in NF than Schwann cells. **C.** Immunohistochemical analysis of pHSPA1A_Y525 expression in schwannoma tissue showing moderate to strong expression compared to normal nerve tissue. All IHC images were recorded at x200 magnification. The same antibody was used for control and tumour samples.

5.5 PDLIM2 co-immunoprecipitation

At this point the most promising candidates among the four validated so far were STAT1 and PDLIM2. This is because these two proteins were not expressed in control cells or tissue, whereas FLNB and HSPA1A showed inconsistencies in expression between normal and tumour cells. Nonetheless, there is evidence to suggest overexpression of the latter two proteins in primary tumour tissue.

To understand how PDLIM2 might be involved in tumour pathogenesis, we performed an experimental co-immunoprecipitation (co-ip) of PDLIM2 in Ben-Men-1 cells that was then submitted for MS to identify binding partners and the wider interaction network. Approximately 1mg of total lysate was incubated with agarose beads that had been previously cross-linked to the PDLIM2 antibody. This step was performed to limit interference from co-eluted IgG peptides upon MS measurement that might otherwise limit the detection of less abundant, more important peptides. Prior to MS, we verified the success of the co-ip by Western blot analysis (Figure 5.10A). After MS, we were able to identify 243 proteins overall in both the PDLIM2 pull-down and the IgG control experiment (supplementary Table S9). 156 of those were unique to the PDLIM2 condition, and are listed in Table 19. Strikingly all of the potential targets identified previously co-eluted with PDLIM2 suggesting a novel signalling network involving STAT1, HSPA1A, FLNB and PDLIM2 that has not previously been reported in meningioma. Figure 5.10B shows a Western blot confirming that STAT1 does indeed co-elute with PDLIM2.

DAVID analysis reveals significant enrichment of ribosomal proteins compared to the human proteome background, with 22 ribosomal proteins eluting with PDLIM2. In addition, there were also several translation elongation factors identified. GO enrichment analysis of the dataset identified glycolysis, translation and ribosomal processes as functionally enriched (Figure 5.10C), indicating varied roles for PDLIM2 in Ben-Men-1 cells.

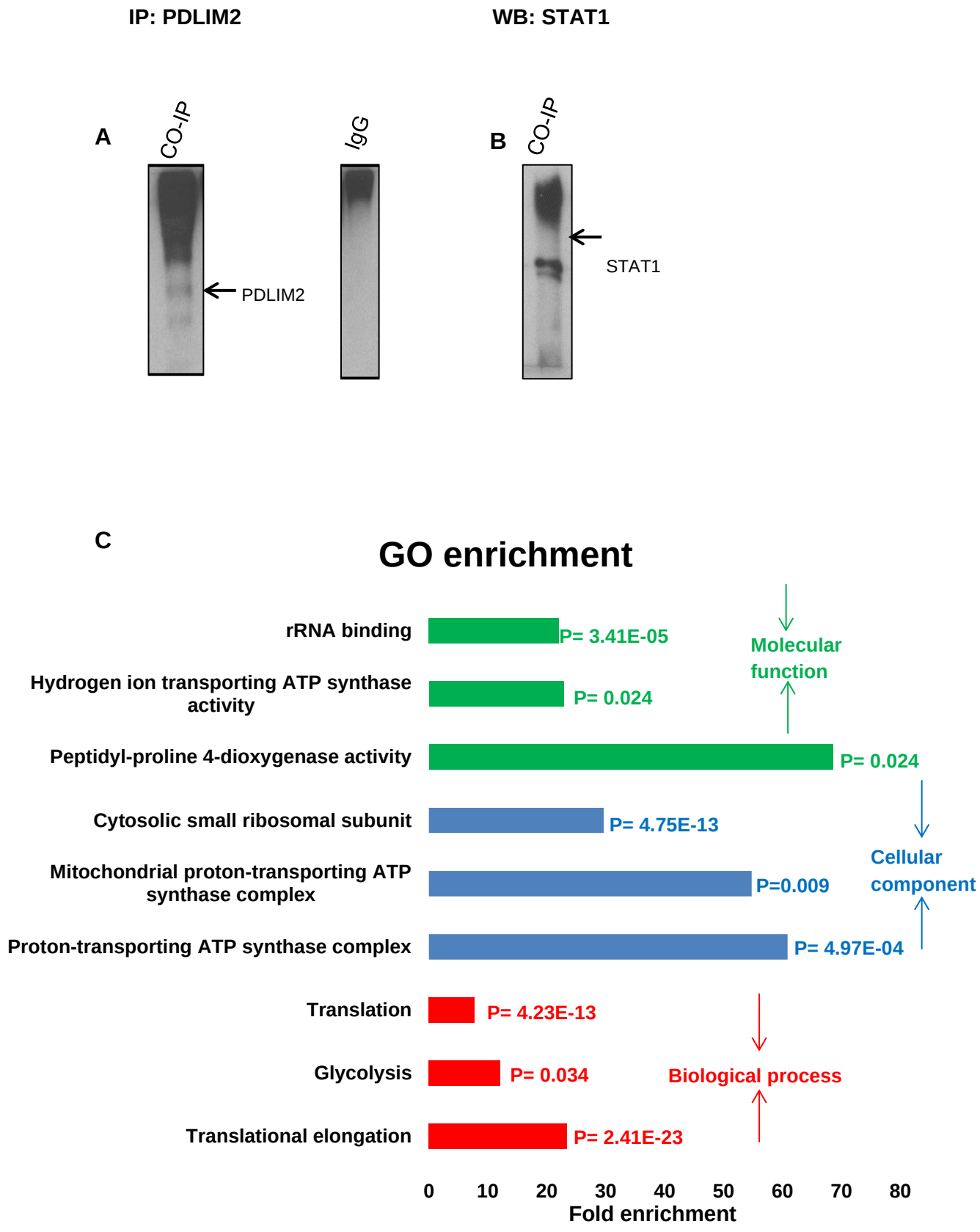

Figure 5.10: PDLIM2 co-immunoprecipitation data. **A.** Western blot analysis confirming that the co-ip experiment was successful. Co-ip with IgG antibody was performed as a control. **B**. STAT1 co-elutes with PDLIM2, as analysed by Western blot. **C.** Gene Ontology (GO) enrichment analysis corresponding to proteins that eluted with PDLIM2.

5.6 Phospho-STAT1_Y701 co-immunoprecipitation

As STAT1 was the other most promising candidate and had co-eluted with PDLIM2, we also performed a co-ip with pSTAT1_Y701.

PSTAT1_Y701 was chosen over 727 because Y701 is the primary phosphorylation site activated in response to Interferon-γ (IFNγ) stimulation in the classical signalling cascade. The cytoplasmic localization of pSTAT1_Y701 in our cells contrasts with several reports in the literature that show STAT1 translocates to the nucleus rapidly upon phosphorylation of the Y701 site. The failure of this to occur in this case suggested there may be other regulatory signals involved.

Using the cross-linking co-ip protocol as before, we identified 48 proteins that co-elute with pSTAT1_Y701 and not with the IgG control antibody (supplementary Table S10). Figure 5.11 shows a Western blot confirming the pull-down. There were several cytoskeletal proteins that co-eluted with pSTAT1_Y701 and JUP and DSG1 were also on the list. These are found at sites of cell-cell adhesion, suggesting that pSTAT1_Y701 may have a role in this process.

WB/IP: STAT1

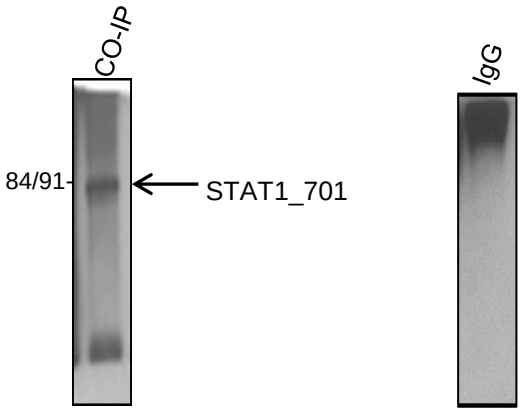

Figure 5.11: **Phospho-STAT1_Y701 co-immunoprecipitation.** PSTAT1_Y701 antibody was crosslinked to agarose beads prior to incubation with Ben-Men-1 cell lysate. Western blot analysis confirms a successful co-ip (left). Co-ip with IgG control antibody did not pull down pSTAT1_Y701 (right).

After confirming the overexpression of PDLIM2 and STAT1 highlighting them as potential therapeutic targets for both meningioma and schwannoma, it was necessary to understand whether the two proteins actually contribute to tumour proliferation. To do this, we used lentivirus mediated protein knockdown in primary meningioma and primary schwannoma cultured cells. In the absence of specific phosphorylation inhibitors, total protein knockdown was the best method to assess the suitability of both proteins as therapeutic targets. To analyse the effects of the knockdown on cellular proliferation, ki-67 staining was performed.

5.7 STAT1 protein knockdown

Using a multi-clone commercial mix of lentiviral particles, STAT1 was knocked down in three primary meningiomas and three primary schwannomas. STAT1 was successfully and significantly knocked down in three primary schwannoma cell cultures compared to cells infected with control shRNA particles (Figure 5.12A).

A ki-67 proliferation assay highlighted significantly decreased proliferation in response to STAT1 knockdown (Figure 5.12B). Of note, there are also a lot fewer cells after STAT1 knockdown, indicating some form of cell death. We performed a western blot assessing cleaved-caspase 3 induction but were unable to detect it upon Western blot analysis. These results overall indicate that STAT1 is a contributing factor in schwannoma proliferation, and therefore warrants further investigation as a novel schwannoma drug target.

We also attempted STAT1 knockdown in primary meningioma cells, but unfortunately were unable to achieve a significant level of knockdown across three cell populations (Figure 5.13).

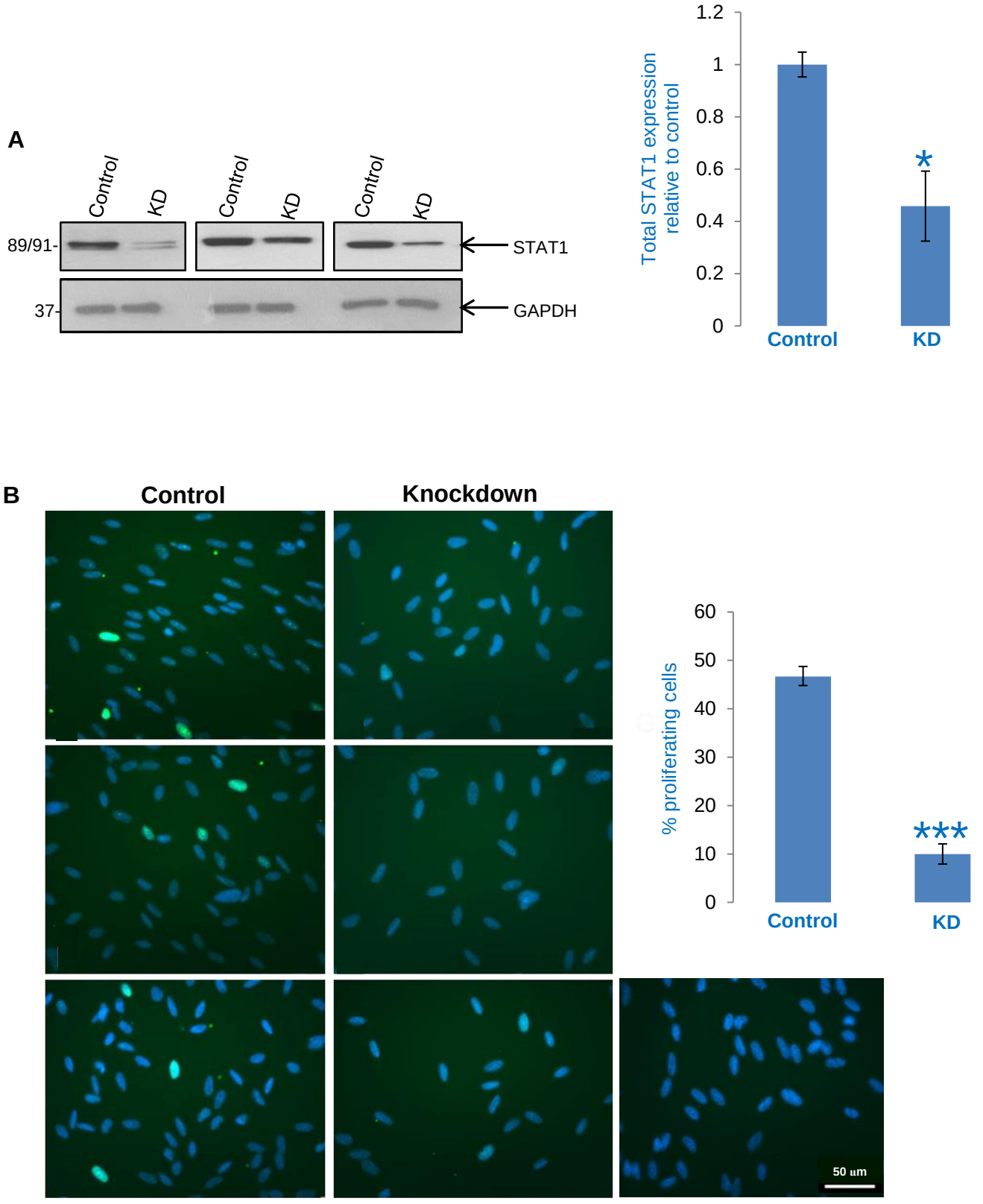

Figure 5.12: **STAT1 knockdown in primary schwannoma cells. A.** Western blot analysis confirmed that STAT1 was significantly knocked down in three primary schwannoma cell populations. **B.** The number of ki-67 (green) positive cells is significantly reduced ($P < 0.001$) in STAT1 knockdown cells compared to cells infected with control shRNA. The panels on the left represent three repeat control samples and the panels on the right represent their respective repeat knockdowns. DAPI (blue) was used as a nuclear stain. All images were taken at 40x magnification.

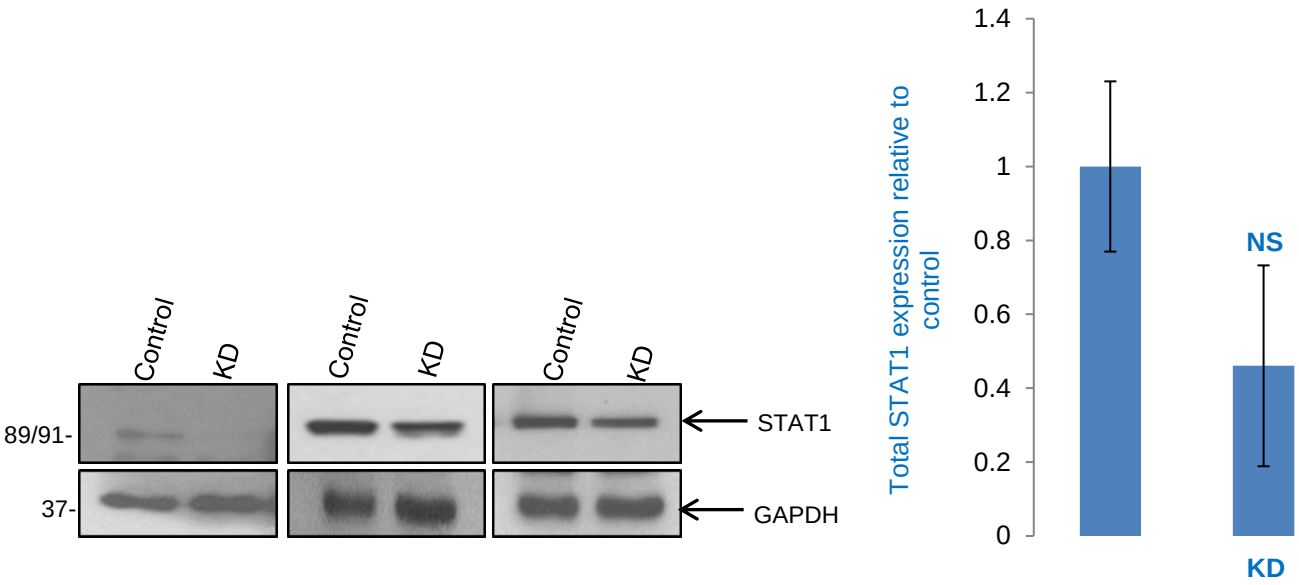

Figure 5.13: **STAT1 was not knocked down in these primary meningioma cells.** STAT1 was not significantly knocked down in three primary meningioma cell populations.

5.8 PDLIM2 protein knockdown

We used lentiviral particles to successfully knockdown PDLIM2 in three primary schwannomas (Figure 5.14A) and three primary meningiomas (Figure 5.14A). PDLIM2 was significantly knocked down in schwannomas, and this led to a significant reduction in ki-67 positive cells ($P < 0.001$), reflecting a substantial reduction in proliferation in response to the knockdown (Figure 5.14B).

A significant reduction was also observed in meningioma cells, again leading to a significant reduction in proliferation as measured by a ki-67 proliferation assay (Figure 5.15B). These data suggest that PDLIM2 is a novel drug target for schwannoma and meningioma treatment.

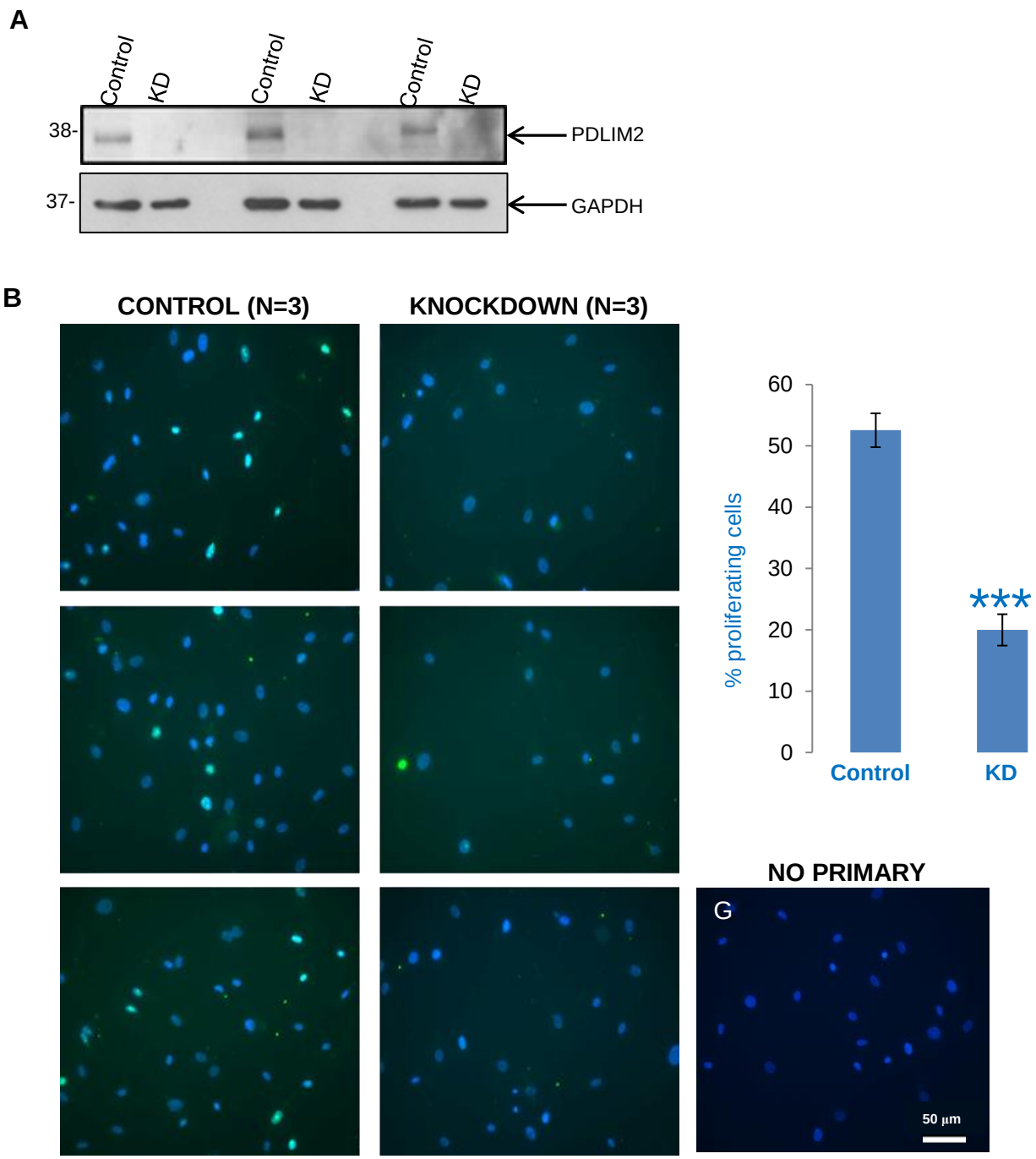

Figure 5.14: PDLIM2 knockdown in primary schwannoma cells (N=3) **A.** Western blot analysis confirmed significant PDLIM2 knockdown in three primary schwannoma cell populations. **B.** PDLIM2 knockdown led to a significant reduction ($P < 0.001$) in cell proliferation, as measured by the number of ki-67 (green) positive cells. The panels on the left represent three repeat control samples and the panels on the right represent their respective repeat knockdowns DAPI (blue) was used as a nuclear marker. All images were taken at x20 magnification.

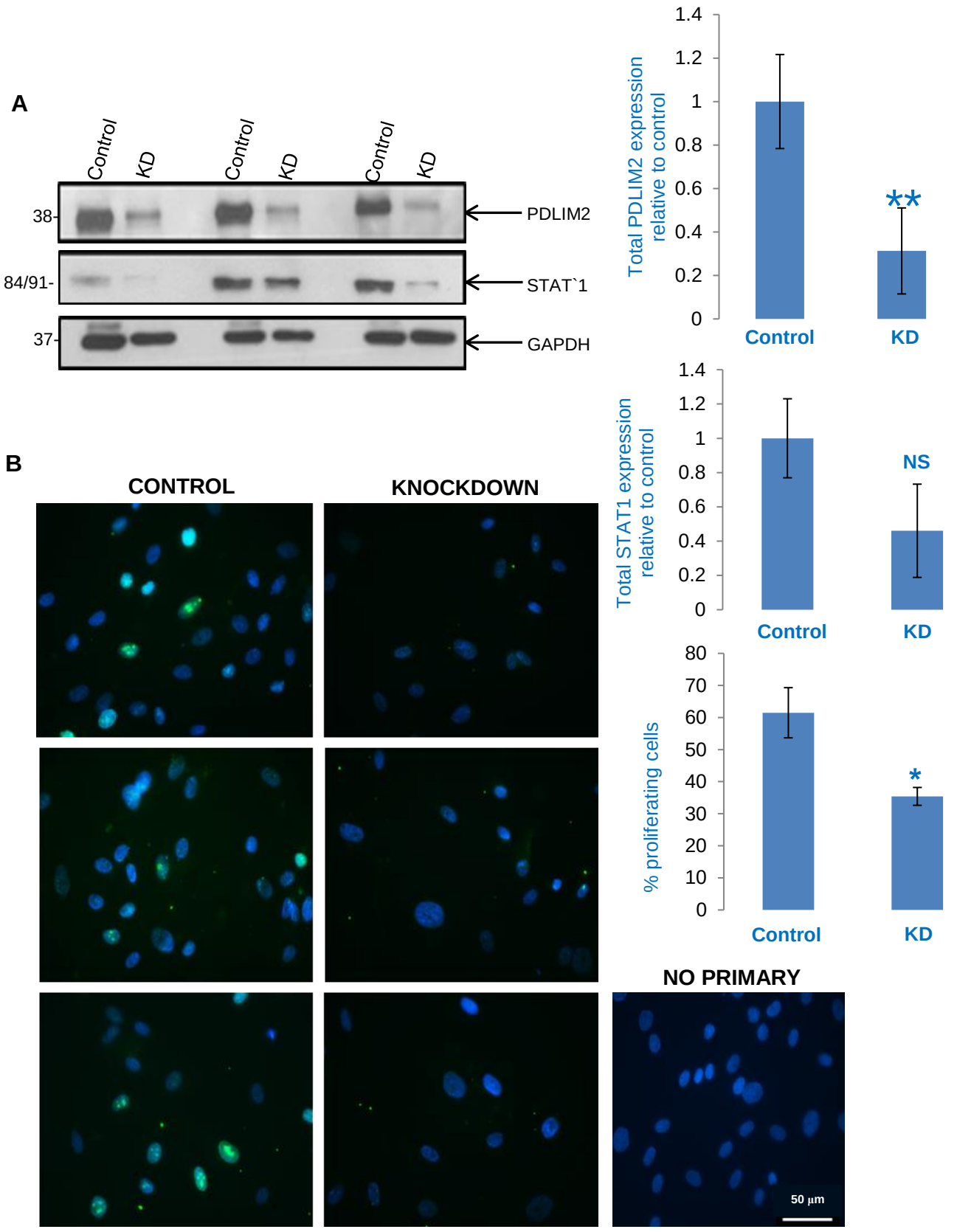

Figure 5.15: PDLIM2 knockdown in primary meningioma cells. **A.** Western blot analysis confirmed significant lentiviral mediated knockdown of PDLIM2 in three primary meningioma cell populations. STAT1 was also reduced in response to PDLIM2 knockdown, although this was not significant. **B**. Ki-67 (green) is significantly reduced in PDLIM2 knockdown cells, compared to cells infected with control shRNA. The panels on the left represent three repeat control samples and the panels on the right represent their respective repeat knockdowns. DAPI (blue) was used as a nuclear stain. All images were recorded at x40 magnification.

5.9 Discussion

We have been able to validate the expression of four candidate novel, therapeutic targets in primary meningioma and schwannoma cells. The data so far has suggested that the most promising candidates are PDLIM2 and STAT1 as these were not expressed at all in normal cells. Furthermore, Merlin has already been shown to inhibit the phosphorylation thus activation of STAT3 and STAT5 in schwannoma cells (Scoles, Huynh *et al.* 2000).

FLNB and HSPA1A showed inconsistencies in their expression between normal and tumour cells, and as such would not be ideal candidates for the treatment of patients. We were however able to demonstrate the expression of pHSPA1A_Y525 in both primary meningioma and schwannoma via IHC, and it was not strongly expressed in normal tissue. Therefore, this phosphorylated form of HSPA1A might still represent a therapeutic target.

We have uncovered interaction networks for both PDLIM2 and STAT1 via co-immunoprecipitation in Ben-Men-1 cells that suggest possible roles for both proteins. PDLIM2 is most likely related to ribosome biogenesis and/ or protein synthesis, whereas pSTAT1_Y701 may be linked to cellular adhesion. Furthermore, all of the candidates identified in our proteomic screen co-eluted with PDLIM2, suggesting a novel interaction network involving all candidate therapeutic targets. We confirmed the co-elution of STAT1 by Western blot, and future studies would focus on confirming the interaction between PDLIM2, STAT1 and HSPA1A/ FLNB, before concluding whether these interactions are important for meningioma/ schwannoma pathology.

STAT1 knockdown in primary schwannoma cells led to a marked decrease in proliferation and a dramatic decrease in cell number in schwannoma cell populations. This could however also be related to decreased cell density in comparison to control cells after the addition of lentiviral particles, which may also have contributed to decreased proliferation. While we also saw reduced proliferation in primary

meningioma, the knockdown would first need to be improved to ensure significant reduction of STAT1. Taken together, these data indicate that STAT1 is a promising therapeutic target for the treatment of schwannoma, and possibly also for the treatment of meningioma.

We later used lentiviral shRNA to significantly knockdown PDLIM2 in primary meningioma cells and primary schwannoma cells. In both cases, a significant reduction in proliferation was observed highlighting the potential of PDLIM2 as a therapeutic target. It would be important in future studies to further confirm the overexpression of PDLIM2 in several primary meningiomas and schwannomas, and potentially other Merlin-deficient tumours, to properly conclude that it represents an attractive target.

As there are currently no drugs available that target PDLIM2, it is difficult to test the therapeutic benefit of PDLIM2 in primary cell models, or patients. As such, specific inhibitors would need to be developed in order to fully characterise PDLIM2 as a common NF2 drug target.

Chapter 6 - Discussion

6.1 Introduction

The aim of this project was to utilize mass spectrometry to analyse the proteome and phosphoproteome of Merlin-deficient tumour cells. In doing so, common targets have been identified that have the potential to be exploited by existing and/or novel drugs for the treatment of NF2-related tumours. At present, there remain no FDA/EMEA approved drugs for meningioma or schwannoma and surgery/ radiosurgery remain the only treatment options, highlighting the urgent need for an effective drug therapy. Prior to this study, there was only one comparative analysis between meningioma and schwannoma reported in the literature, and this was only on the genomic level (Torres-Martin, Lassaletta *et al.* 2014). The novelty of the research presented in this thesis, is that it represents the first and only comparison between meningioma and schwannoma to identify novel phosphoprotein drug targets and potential biomarkers.

Past studies have identified biomarkers and therapeutic targets for a range of neoplasms, including meningioma and schwannoma (Seo, Park *et al.* 2015, Sharma, Ray *et al.* 2015). Omics technologies in general have become a mainstay in translational research and are indispensable in the era of personalized medicine, allowing patients to be placed in to separate groups and have treatments and/ or drugs tailored to them. The findings outlined in this thesis provide the foundations and rationale for further investigation in to pSTAT1 and PDLIM2 as novel common therapeutic targets for both meningioma and schwannoma, and potentially other Merlin-deficient tumours. There is also scope for further investigation of FLNB and HSPA1A as therapeutic targets, plus a myriad of proteins that may represent potential targets in meningioma or schwannoma. The following paragraphs will discuss the results obtained in more detail, their congruence with the literature and suggest future research directions.

6.2 Proteomics

6.2.1 Sample losses in proteomic sample preparation

There have been several phosphoproteomic studies reported in recent years that have identified thousands of phosphopeptides, using phosphopeptide enrichment (Wisniewski, Nagaraj *et al.* 2010, Zhou, Di Palma *et al.* 2013, Sharma, D'Souza *et al.* 2014). Since it has been proposed that over 500000 phosphorylation sites are likely to exist in a cellular proteome (Lemeer and Heck 2009), there is a wealth of information still to discover. The identification of specific phospho-sites requires meticulous sample preparation and a number of steps to maximise potential identifications (IDs). The enrichment experiment performed as part of this project used 1mg of starting material. Tryptic digestion was followed by TiO_2 enrichment, stage tipping and subsequent MS analysis. In contrast to previous studies, the number of IDs was quite low. A number of reasons may account for this including not least; low amounts of starting material and sample losses incurred during the workflow. As others have pointed out peptides can be lost during wash steps, elution steps and when samples are dried in a speed vac during sample preparation (Stewart, Thomson *et al.* 2001, Feist and Hummon 2015). Importantly, the percentage of sample loss seems to be largest when the amount of starting material is lowest. As such, future experiments utilizing this technique should incorporate more concentrated starting materials to maximise potential IDs. For example, using 100 mg of mouse brain tissue Wisniewski identified over 12000 phospho-sites (Wisniewski, Nagaraj *et al.* 2010), highlighting the enormous potential of these techniques when starting material is high. Also of note, Finehout was able to show that tryptic digestion at 48^{o}C, 11 degrees above the standard procedure, improved digestion efficiency and may be something to consider in future experiments (Finehout, Cantor *et al.* 2005).

6.2.2 Multiple correction testing

False Discovery Rate (FDR) correction was initially applied to both the schwannoma phosphoprotein and total protein datasets. This is designed to control the expected proportion of rejected null hypotheses or 'false positives' i.e. cases where a statistically significant difference has been identified when there is not one. In doing so, the significantly changed phosphoproteins decreased by almost 50%. 91 were upregulated (log2 FC > 1) and 53 were downregulated (log2 FC < -1). Generally, the proteins with the largest fold changes in schwannoma were still able to pass the FDR threshold. One of the proteins involved in MAPK signalling, MAP2K1 (MEK1), known to be central to schwannoma proliferation (Ammoun and Provenzano 2014), was unable to pass the threshold. Its relatively small fold change in this experiment (log2 FC 2.8) may be the main reason for this. However, as it is widely known as a therapeutic target in schwannoma, its failure to appear significant after FDR shows it is likely a false negative in this case, which is consistent with the drawbacks of multiple correction testing.

MCT also limited the potential for functional annotation of proteomic data. DAVID analysis of the upregulated phosphoproteins in schwannoma after FDR was applied led to only one significantly enriched pathway identification, endocytosis. Both the MAPK and focal adhesion pathways were no longer identified regardless of their well-known contribution to schwannoma pathogenesis (Ammoun and Hanemann 2011). For the total protein dataset, application of MCT reduced the number of statistically significant upregulated proteins by half, to 8. The downregulated proteins reduced to 77, again making it more difficult to identify potential targets.

As the goal of this project was to perform a global analysis to identify common therapeutic targets, it was our aim to have as many proteins as possible on which to perform the final comparative analysis. Therefore, a standard raw p-value of 0.05 was the only statistical criteria applied. The compromise is that of several targets selected

for further analysis in the absence of any form of MCT, there is a higher chance that some of those would turn out to be false positives.

6.3 Schwannoma proteomic data

We quantified 2628 phosphoproteins in primary schwannoma cells compared to Schwann cells and the data obtained largely correlates with what is known in the field. Thus we were able to identify both NFκB and MEK as upregulated in schwannoma, echoing previous work (Ammoun, Provenzano *et al.* 2014). We also identified pYAP as upregulated in schwannoma cells, and further, were able to identify three sites of phosphorylation (S127, S128 and S131). Merlin has been shown previously to induce phosphorylation of YAP_S127, and its absence is associated with dephosphorylation, translocation to the nucleus and transcription of pro-proliferative, anti-apoptotic genes (Zhao, Li *et al.* 2010, Li, Cooper *et al.* 2014). As the three schwannoma samples analysed were all Merlin-negative, one possible explanation could be that other members of the ERM family can phosphorylate YAP in the absence of Merlin. It would therefore be necessary to confirm phospho-YAP_S127 expression in several Schwann and schwannoma samples by Western blot, to fully understand the phosphorylation status and overall expression profile of this protein.

TGFβ1 was also identified as upregulated in line with recent reports that found it was upregulated at the genome level and was present in 95% of vestibular schwannomas upon immunohistochemical examination (Lottrich, Mawrin *et al.* 2007, Torres-Martin, Lassaletta *et al.* 2013). We also found significant enrichment of the focal adhesion and MAPK pathways, both known to be implicated in schwannoma tumorigensis.

Boin *et al.* published the results of a study in 2014 that used a reverse phase protein array to quantify the expression of certain proteins in schwannoma tumour samples. The authors found that the most frequently activated RTKs were Her2, Axl and RON (Boin, Couvelard *et al.* 2014). We were unable to identify these receptors in our screen however we did identify PDGFRβ as 7-fold upregulated in schwannoma, in accordance

with the literature (Ammoun, Flaiz *et al.* 2008). Boin *et al.* also identified YAP as a transcriptional activator of several RTKs, including the PDGFRβ and Axl. They also concluded that overexpression of YAP, regardless of its phosphorylation status, is a positive regulator or proliferation. As such, our identification of overexpressed YAP in schwannoma provides further rationale for therapies targeting the Hippo pathway as valuable options for schwannoma treatment.

Boin's study, whilst lacking global phosphoproteome analytical capability, did have the advantage of identifying activated receptors on the schwannoma membrane. Our approach is not specifically designed for membrane proteome coverage, and important receptors may be overlooked through the inability of the lysis buffer to efficiently disrupt the membrane. This is why FASP was developed, to allow comprehensive membrane coverage with the use of strong detergents (Wisniewski, Nagaraj *et al.* 2010). Unfortunately, such a technique can be associated with considerable sample loss, as was encountered when we attempted to use it in conjunction with phosphopeptide enrichment in chapter 4.

Nonetheless, we did identify some receptors that were significantly upregulated in schwannoma cells, including the transferrin receptor (TFRC). This has been proposed recently as a valuable target for treatment as it is upregulated in several cancers. It has been utilized with success pre-clinically in glioma treatment, allowing targeted therapy of cytotoxic drugs (Daniels, Bernabeu *et al.* 2012). Validation of TFRC upregulation compared to Schwann cells followed by functional analysis may therefore represent a therapeutic strategy for schwannoma.

Seo *et al.* also performed a proteomic analysis comparing vestibular schwannoma against normal nerve tissue (Seo, Park *et al.* 2015). They found 29 proteins to be upregulated, including two of which we identified to be upregulated in this experiment; Annexin A5 (ANXA5) and tropomyosin 4 (TPM4). However, we also found conflicting data between our datasets i.e. calreticulin and aldehyde dehydrogenase were

downregulated in our study but identified as upregulated by Seo *et al.* This could be attributed to the use of different types of mass spectrometry, or variances between primary tumour specimens. This again highlights the fact that any proposed therapeutic targets would have to be validated across many tumour samples and verified with Western blotting.

The most upregulated phosphoprotein identified, TAGLN, may also represent a therapeutic target as it has already been proposed to have therapeutic value in Malignant Peripheral Nerve Sheath Tumours (Park, Lee *et al.* 2014). Knocking it down was able to attenuate MAPK signalling leading to a decrease in proliferation. Targeting proteins with regulatory influence over the MAPK pathway is of value in schwannoma treatment, therefore inhibiting TAGLN in schwannoma cells represents a potentially very valuable therapeutic strategy.

6.3.1 Functional analysis of schwannoma proteomic data

Our analysis of the phosphoproteome highlighted a functional cluster of proteins upregulated in schwannoma cells, found to contain either a PDZ or LIM domain, or both. This family of proteins perform a diverse array of functions in the cell and can have profound effects on cell signalling (Krcmery *et al.* 2010).

We were able to highlight a potential role for clathrin-mediated endocytosis in schwannoma pathology, as Gene Ontology (GO) analysis revealed significant enrichment of a number of terms related to this process. The purpose of endocytosis is in part to facilitate degradation of membrane components (Robinson 2015). However, we were also able to identify downregulation of lysosomal proteins in schwannoma cells, suggesting decreased protein degradation. In other cases, ligand bound receptors can be endocytosed through clathrin-coated pits in to endosomes, and subsequently recycled back to the membrane to maintain constitutive signalling. Further, endocytosis of some receptors can lead to activation of signal transduction e.g.

in the case of EGFR which is able to continue signalling from within the endosome (Burke, Schooler *et al.* 2001).

Signalling through endosomes has also been linked to MAPK signalling. A protein, p14, was found to associate with the cytoplasmic face of endosomes and through its association with the MAPK scaffold protein MP1, was able to orchestrate intracellular ERK signalling in response to EGF stimulation (Teis, Wunderlich *et al.* 2002). As the MAPK pathway plays such a pivotal role in schwannoma, interruption of this process may be a valuable therapeutic strategy. Agnihotri and colleagues were also able to identify upregulation of endocytosis in their microarray analysis of 49 schwannomas (Agnihotri, Gugel *et al.* 2014), further highlighting it as a potential therapeutic target.

Glycolysis was also highlighted as a potential target pathway. Two upregulated proteins; ALDOA and ALDOC, are both aldolases involved in glycolysis and may represent therapeutic targets. An Increase in the rate of glycolysis is a hallmark of cancer and inhibition of this process holds potential as a cancer therapy (Hanahan and Weinberg 2011). ALDOA was knocked down in rat glioblastoma cells leading to an almost 90% reduction in cell proliferation (Ritterson Lew and Tolan 2012). Interestingly, the study also found that the reduction in proliferation was not due to the subsequent defects in glycolysis, indicating other roles for ALDOA in tumorigenesis. Further, ALDOC was identified as a positive regulator of Wnt signalling in colorectal cancer cells (Caspi, Perry *et al.* 2014). Our identification of both enzymes as upregulated in schwannoma therefore warrants further investigation.

6.4 Meningioma proteomic data

6.4.1 Meningioma cell culture

Although meningioma samples were prepared and measured in the same way as schwannoma, the final dataset contained many missing values (LFQ = 0), leading to a reliance on the comparison between HMC and Ben-Men-1 for the final selection of common candidate targets. Whilst this was a relevant comparison, the aim of the study

was to base candidate target selection on primary tumour samples. The following section will discuss the potential reasons that may explain the lack of good quality primary meningioma data.

Firstly, as the system in use for primary schwannoma cell culture is well established and optimized, schwannoma cell growth and protein production can be assumed as optimal. The culture media used for the primary meningioma cells in this study contained insulin, as was used in the media described by James *et al.*, who were able to maintain primary meningioma cells in culture for up to 10 passages (James, Lelke *et al.* 2008). We also attempted proteomics with meningioma samples that had been cultured in the same media as HMC cells that contains a number of growth factors, and ensured that no samples were analysed beyond passage 5. This did lead to a decrease in the number of missing values however could still be improved. Many studies looking at meningioma use a very basic medium without any added growth factors. Future proteomic studies involving primary meningioma might consider the addition of further growth factors to the media, to stimulate growth and protein production which must be maximal to ensure the best results.

James *et al.* noted that senescence is more rapidly induced in primary meningioma cells in culture than normal arachnoid cells. Senescence is characterised by reduced proliferative potential and, presumably, reduced global protein synthesis. Although the primary meningioma cells used in our study appeared to grow well, protein production may have been decreased overall due to some cells undergoing senescence.

6.4.2 Primary meningioma and Ben-Men-1 proteomic data

The most upregulated phosphoprotein identified in primary meningioma cells, TGM2 (Transglutaminase 2), was also recently identified by Huang *et al.* as a potential therapeutic target in primary meningioma cell cultures (Huang, Wei *et al.* 2014). Although the number of missing values affected the quality of the data obtained, this observation helps to demonstrate the validity of the dataset overall. Furthermore TGM2

has also been shown to activate both NFκB and FAK (Siegel and Khosla 2007) which are relevant to schwannoma growth and proliferation, adding to the rationale of targeting TGM2 as a therapeutic strategy. It would be interesting to validate TGM2 in more primary samples, to determine its significance in Merlin-deficient tumours and its suitability as an NF2 drug target.

We also validated SMAD2_T8 expression in three primary meningioma samples. T8 phosphorylation has been attributed to both CDK2 (Baughn, Di Liberto *et al.* 2009) and ERK (Funaba, Zimmerman *et al.* 2002), the first inhibiting SMAD2 and the latter positively regulating it. We did not detect SMAD2_T8 expression in control HMC cells, suggesting that it may be expressed in meningioma as a way of combating growth inhibitory TGFβ signalling, and thus is a consequence of CDK2 phosphorylation in this instance. We also observed downregulation of TGFβ1 in meningioma, further suggesting dysregulation of this signalling pathway and highlighting it as a potential target. Contrastingly, Wang *et al.* identified TGFβ as upregulated in meningioma however this was at the genome level and this does not always correlate with protein abundance (Wang, Gong *et al.* 2012).

Fatty Acid Synthase (FAS) was also identified as upregulated in meningioma cells at both the total and phosphoprotein levels (Log2 FC = 2.89, 2.28, respectively). It has been previously identified as a marker of meningioma progression and as a potential therapeutic target (Haase, Schmidl *et al.* 2010, Makino, Nakamura *et al.* 2012). Sharma *et al.* also identified FAS signalling as a potential target in their proteomic analysis of meningioma (Sharma, Ray *et al.* 2014).

We were able to identify significant enrichment of several pathways/ processes across our analysis of Ben-Men-1 and primary meningioma cells. We found proteasome activation to be a recurring theme throughout, highlighting it as an important target in meningioma, in concordance with other reports. A 2014 study looking at the proteasome inhibitor bortezomib showed that it was effective in

sensitizing meningioma cells to TRAIL-induced apoptosis (Koschny, Boehm *et al.* 2014). Further, the proteasome inhibitor MG132 was also found to increase levels of N-cadherin in schwannoma cells, which in turn decreased proliferation (Zhou, Ercolano *et al.* 2011). Our data and previous reports highlight proteasome inhibition as a valuable NF2 therapy, either alone or in combination with drugs targeting other relevant pathways.

Our analysis of Ben-Men-1 cells identified a large number of integrins and collagens as upregulated compared to normal HMC cells. This is in line with a number of previous reports (Bello, Zhang *et al.* 2000, Wang, Gong *et al.* 2012, Sharma, Ray *et al.* 2014) that identify upregulation of integrins in meningioma. Integrin signalling is related to a number of cellular processes including tumour proliferation and survival. Wilisch-Neumann *et al.* showed that an integrin inhibitor, cilengitide, was able to supress meningioma cell motility and suggest that it may be useful in a combined therapy approach (Wilisch-Neumann, Kliese *et al.* 2013). Cilengitide is also in clinical trials for glioblastoma, further highlighting its potential (Desgrosellier and Cheresh 2010). Torres-Martin *et al.* also identified clear upregulation of integrin alpha-4 in their genomic analysis of schwannoma. We identified a log2 FC for this protein of 23.01 in Ben-Men-1 cells compared to HMC, indicating that it might be a potential common target for NF2 tumours.

We also identified significant upregulation of phosphorylated cathepsin D (CTSD) in both primary meningioma and Ben-Men-1 cells, indicating that it may act as a therapeutic target. In both cases, the total amount of the protein was actually downregulated, suggesting that its phosphorylation is relevant to meningioma pathogenesis. As very little is known regarding the effects of phosphorylation on Cathepsin D function, further investigation would be required before concluding that phospho-CTSD is in fact a potential meningioma target. Total CTSD secreted by ovarian cancer cells has however been linked to a myriad of processes including tumour cell migration and proliferation (Pranjol, Gutowski *et al.* 2015).

6.5 Phosphopeptide data

We were able to identify 216 phosphopeptides in Ben-Men-1 cells corresponding to 144 proteins, many of which are involved in focal adhesion and regulation of the cytoskeleton. The data obtained also fit the criteria set by Olsen *et al.* (Olsen, Blagoev *et al.* 2006) regarding the expected proportions of serine, threonine and tyrosine phosphorylated peptides.

We identified PAK2_S141, which was previously shown to be activated in response to EGF and that this contributes to cellular transformation and proliferation via c-Jun. (Li, Zhang *et al.* 2011). As PAK2 is able to phosphorylate Merlin at position S518 (Rong, Surace *et al.* 2004), whereby inactivating it, and the EGFR is known to be upregulated in schwannoma and meningioma (Ammoun, Cunliffe *et al.* 2010, Wernicke, Dicker *et al.* 2010), this phosphorylated form of PAK2 might represent a novel therapeutic target for NF2. Similarly, we identified Cofilins 1 and 2 phosphorylated at S3 which is a known LIMK (LIM domain kinase) phosphorylation site. Petrilli and colleagues have already shown the potential of LIMK inhibitors for the treatment of NF2 tumours. They showed that LIMK inhibition decreased the viability of mouse Merlin-deficient Schwann cells (Petrilli, Copik *et al.* 2014). Our data provides further rationale for LIMK inhibition as a therapeutic strategy. Furthermore, Rak *et al.* demonstrated the effectiveness of a LIMK2 inhibitor, T56-LIMKi, in reducing proliferation of a schwannoma cell line mediated by inhibition of cofilin S3 phosphorylation (Rak, Haklai *et al.* 2014). As both studies are based in cell models of NF2, it would be interesting to conduct similar experiments using our primary cell culture system, to better understand the potential of T56-LIMKi and other inhibitors as therapeutic options for NF2 patients.

We were also able to validate EGFR_T693 in both primary meningioma cell cultures and primary tumour samples, irrespective of Merlin status, whilst seeing no expression in HMC or normal meningeal tissue. Maxquant identified T693, however in the cleaved, active form of the EGFR this changes to T669. It sits in the juxtamembrane region

spanning residues 664-682 which is crucial for activation of the receptor (Jura, Endres *et al.* 2009), and an earlier report showed that T669 is a MAPK phosphorylation site (Takishima, Griswold-Prenner *et al.* 1991). Li *et al.* found a mutant form of the EGFR that could not be phosphorylated at T669 was downregulated more slowly compared to the wild-type receptor upon EGF-induced stimulation (Li, Huang *et al.* 2008). This indicates that T669 phosphorylation is a negative regulator of the EGFR. Kluba *et al.* also show that T669 inhibits EGFR dimerization which is required for its activation (Kluba, Engelborghs *et al.* 2015). The fact that we detected this phosphorylation site in meningioma cells and not in normal controls would suggest that it might be beneficial to tumour growth. An experiment looking at the effects of EGFR_T693 inhibition in meningioma cells would be useful to better understand the specific function of the modified form of EGFR, given that the EGFR has already been identified as overexpressed and a potential target in both meningioma and schwannoma (Curto, Cole *et al.* 2007, Baxter, Orrego *et al.* 2014).

6.6 FLNB as a target in NF2-related meningioma and schwannoma

Western blot analysis showed the expression of total FLNB in primary meningioma cells was non-significantly increased compared to HMC cells. Overall, a significant increase in FLNB expression was observed in primary schwannoma compared to Schwann cells, although the intensity of the bands on the Western blot appear to be very similar across all samples (Figure 5.7A). The significant increase therefore is likely because one of the Schwann cell samples did not express FLNB at all.

The data obtained so far suggests that FLNB does not represent a good target, as it is expressed in normal as well as tumour cells. Interestingly though, a 2013 study looking at phosphorylation associated SNVs (Single Nucleotide Variants) identified pFLNB as a cancer driver gene frequently mutated at sites of phosphorylation leading to constitutive activation and enhanced oncogenic activity (Reimand and Bader 2013). We identified S2478 phosphorylation of FLNB in Ben-Men-1 cells via phosphopeptide

enrichment, but were unable to find a specific antibody to confirm this. There are also no reports in the literature regarding this specific phospho-site. Given FLNBs identified role as a driver of oncogenesis it would be interesting to investigate this phosphorylated form of FLNB in meningioma and schwannoma. The first stage would involve obtaining a specific antibody targeting S2478 to confirm its expression in primary tumour cells, before functional analysis experiments commence.

We also analysed pFLNA/ pFLNB expression in primary meningioma and schwannoma cells, as it was the only antibody available targeting any phosphorylated variant of FLNB. We found no significant difference between normal and cultured tumour cells but when we looked at its expression in meningioma tumours compared to meningeal tissue, we found it was not detected in the control but strongly in the tumours (Figure 5.6D). The reason for this could be that HMC are cultured in a system containing specific growth factors which are added to optimise and maximise growth in culture. The fact that we do not see activation in normal meningeal tissue implies that *in vivo,* external signals might instruct cells to 'switch off' pFLNA/ pFLNB. If this is the case, pFLNA/ pFLNB represents a valuable therapeutic target that may contribute to tumorigenesis, otherwise we would expect it to be expressed in normal tissue. What can be appreciated from this is that a cell culture system can provide a guide of *in vivo* signalling, but candidate therapeutic targets should also be properly validated in primary tissue samples.

6.7 HSPA1A as a target in NF2-related meningioma and schwannoma

When total HSPA1A was analysed in primary meningioma, we identified a significant increase compared to normal cells. It was however also expressed in HMC. In primary schwannoma cells, total HSPA1A expression was found to vary across tumours, and was also expressed in three primary Schwann cell samples. Overall these data indicate that total HSPA1A is not an ideal therapeutic target for meningioma or schwannoma. The expression of pHSPA1A_Y41 was similar to that of total HSPA1A. No significant

difference was observed overall in either primary meningioma or schwannoma compared to their respective controls.

IHC analysis of pHSPA1A_Y525 showed that it is expressed in both meningioma and schwannoma. It is generally cytoplasmic across all tumours with a small amount of nuclear staining observed, mostly in meningioma. It is generally expressed more strongly overall in schwannoma. The heat shock proteins in general promote cell survival and are cytoprotective in response to stress (Schmitt, Gehrmann *et al.* 2007). One group found that Y525 phosphorylation led to nuclear accumulation of HSPA1A in response to cell stress and that this enhanced its activity (Knowlton, Grenier *et al.* 2000). As we do not really see nuclear staining in this case, it is unlikely to function in the same way. The linear pattern of staining observed in schwannoma is particularly interesting and provides an indication that pHSPA1A_Y525 is associated with the cytoskeleton, at least in a subset of schwannomas. This could influence cytoskeletal dynamics and affect intracellular transport. To confirm the association, dual staining for common cytoskeletal proteins could be performed to identify co-localization. Following that, mutagenesis studies followed by proliferation and survival assays would help to determine whether pHSPA1A_Y525 represents a worthwhile therapeutic target.

Wu *et al.* showed that HSPA1A released extracellularly was able to promote tumour cell growth via activation of NFκB (Wu, Yuan *et al.* 2012). In clear contrast, Tanaka and colleagues showed that HSPA1A was actually a chaperone required for PDLIM2 mediated degradation of NFκB (Tanaka, Shibazaki *et al.* 2014). As we were able to identify HSPA1A in our PDLIM2 co-immunoprecipitation, this would suggest the latter. It would be beneficial to perform a co-ip with both HSPA1A and pHSPA1A_Y525 to see if PDLIM2 co-elutes, and also to identify other interactors that may provide more clues as to the specific function of this protein in meningioma cells. Leu and colleagues identified a HSPA1A inhibitor, termed PES (Leu, Pimkina *et al.* 2009), that has shown anti-tumour activity by promoting cell death and may represent a potential drug for

meningioma and schwannoma, should further experiments prove that pHSPA1A is a good target.

6.8 STAT1 as a target in NF2-related meningioma and schwannoma

We identified a significant increase in total STAT1 expression in primary meningioma cells compared to HMC. This is in concurrence with an earlier report, which also identified significant overexpression of STAT1 in 17 meningioma samples, compared to normal dura (Magrassi, De-Fraja *et al.* 1999). Overall, there was no significant difference observed between primary Schwann and schwannoma cells, and there have been no previous studies assessing STAT1 expression in schwannoma.

We were able to detect pSTAT1_Y701 and pSTAT1_S727 expression in several meningiomas and schwannomas, but not in respective controls. It has been reported that maximal transcriptional activity is only achieved when both sites are phosphorylated (Wen, Zhong *et al.* 1995), and transcriptionally active STAT1 must be located in the nucleus. However, we observed differences between the cellular localization of the two phosphorylated variants of STAT1; S727 was nuclear and Y701 was located in the cytoplasm, indicating that the two may function independently of one another in these cells. The function of these phosphorylated forms of STAT1 is unclear as no prior work has functionally assessed either protein in meningioma or schwannoma.

Shuai *et al.* showed that upon Y701 phosphorylation, STAT1 translocates in to the nucleus within minutes (Shuai, Ziemiecki *et al.* 1993). A report in 2000 showed however that nuclear localization requires another signal beyond that of Y701 phosphorylation, and that is inhibition of its nuclear export (Mowen and David 2000). The authors identified a NES (Nuclear Export Signal) region spanning amino acids 197-205 of STAT1 that is regulated by Janus Kinase 1 (JAK1). In the absence of active JAK1, pSTAT1_Y701 is not retained in the nucleus. They also showed that tyrosine phosphorylation at 701 can be achieved by other kinases (TYK2 and JAK2), but that for

nuclear accumulation, JAK1 is completely indispensable. Other members of our group have shown that JAK1 is not activated in meningioma cells, suggesting this might be the reason for the cytoplasmic localization of STAT1.

Phospho-STAT1_S727 has been identified as an MAPK regulated phosphorylation event (Zhang, Cho *et al.* 2004). Although most reports conclude that S727 phosphorylation is a secondary, less significant event to Y701 phosphorylation, Putz *et al.* showed that activating S727 phosphorylation can be observed independently of Y701 in natural killer cells, suggesting that STAT1 phosphorylated at either site can be functionally active, and that the two phospho variants can play different roles, as is probably the case in meningioma and schwannoma as they were not identified in the same location.

As such, future experiments functionally assessing phospho-STAT1 in NF2 tumours would need to focus on each variant individually. What we have achieved so far is the knockdown of total STAT1 which has provided an indication of its suitability as a drug target. Although we did not achieve significant knockdown in all three primary meningioma cell populations, we did observe a good level of knockdown in one out of three. There was a decrease in proliferation of those cells compared to the control however this needs to be repeated.

We achieved significant knockdown across three Merlin-deficient primary schwannomas. This led to a marked reduction in proliferation and a considerable reduction in cell number, compared to cells treated with control shRNA. We analysed cleaved caspase-3 as a measure of apoptosis but were not able to detect it in control or KD cells. This suggests another method of cell death causing the decrease in cell number, or perhaps that STAT1 KD has an effect on cell adhesion causing cells to become detached from culture vessels. A report by Xie *et al.* however found that depletion of STAT1 actually led to an increase in cell-matrix adhesion (Xie, Zhao *et al.*

2001). To understand if adhesion if affected by STAT1 KD, we would need to perform an adhesion assay in cells with and without knockdown.

Our co-immunoprecipitation experiment looking at the interaction network of pSTAT1_Y701 identified a number of proteins. We were able to identify HSP90 that has been previously linked to STAT1 signalling (Bocchini, Kasembeli *et al.* 2014). We also identified JUP (Junction Plakoglobin) that was identified as downregulated in Ben-Men-1 cells. JUP has a wide range of roles therefore it is difficult to infer the implications of its association with pSTAT1_Y701. As JUP is commonly found at the site of adherens junctions (Aktary and Pasdar 2012) it is plausible that JUP and pSTAT1_Y701 work together to regulate adhesion. This also supports what we found when STAT1 was knocked down in schwannoma cells i.e. a possible reduction in adhesion. Furthermore, another adhesion protein, DSG1 (Desmoglein) was also identified. This provides further evidence that STAT1 is involved in adhesion in NF2 tumour cells, and that this association is potentially tumorigenic.

Overall, our results suggest that STAT1 is a pro-tumorigenic factor in schwannoma. This is supported by recent studies in both malignant mesothelioma and endometrial cancer that also found it contributed to tumour progression (Arzt, Kothmaier *et al.* 2014, Kharma, Baba *et al.* 2014). Future work would focus on validating the interactions between STAT1 and the adhesion proteins mentioned, followed by further characterization of the importance of STAT1 in adhesion. It would also be important to understand whether STAT1 KD causes cell death by means other than apoptosis, e.g. autophagy or necroptosis. This could be achieved via knocking down STAT1 and analysing the expression of markers specific to these processes.

6.9 PDLIM2 as a target in NF2-related meningioma and schwannoma

We were able to confirm PDLIM2 expression in meningioma and schwannoma samples and also show that it is not expressed in HMC or normal meningeal tissue. We identified a very faint band for PDLIM2 in one of three Schwann cell samples. It would

be useful to analyse more Schwann cell control samples in future experiments to confirm that it is largely expressed only in tumour cells.

PDLIM2 was first described in 2004 as an adaptor protein linking other proteins to the cytoskeleton (Torrado, Senatorov *et al.* 2004). Since, it has been found to have a number of different roles, and has been particularly well studied in breast cancer (Loughran, Healy *et al.* 2005, Deevi, Cox *et al.* 2014) where it has been identified as a driver of tumour progression and invasion. It has not been linked previously with either meningioma or schwannoma.

Cytoplasmic and nuclear extraction showed that PDLIM2 is localized to the nucleus in Ben-Men-1, and primary meningioma cells. This could potentially have important implications on its role within these cells. It was previously reported that PDLIM2 acts as an E3 ubiquitin ligase within the nucleus, targeting NFκB for degradation (Tanaka, Grusby *et al.* 2007). The findings of Healy and O'Connor further corroborate this, as they found that cytoplasmic sequestration of PDLIM2 led to accumulation of NFκB (Healy and O'Connor 2009). Furthermore, we identified S137 phosphorylation of PDLIM2 in Ben-Men-1 cells which was shown by Guo *et al.* to be necessary for ubiquitination and subsequent degradation of STAT1 (Guo, Mi *et al.* 2010), although we were unable to validate this in the absence of a specific antibody. The fact that we identified PDLIM2 in the nucleus shows that it is in the correct location in order to perform its ubiquitin ligase activity. This suggests either that PDLIM2_S137 may have an entirely different function in these tumours, or that STAT1 degradation is being inhibited by another mechanism. Future studies might focus on site-specific mutagenesis of PDLIM2 to better understand the role of pPDLIM2_S137 in meningioma and schwannoma.

After performing a co-immunoprecipitation, we were able to identify the other candidate proteins HSPA1A, STAT1 and FLNB as interactors of PDLIM2. Associations between PDLIM2 and STAT1 (Tanaka, Soriano *et al.* 2005) and PDLIM2/ HSPA1A

(Tanaka, Shibazaki *et al.* 2014) have been described previously however there are no reported links between PDLIM2 and FLNB.

We performed GO enrichment analysis of the co-ip data and found significant enrichment of ribosomal proteins and protein translation. This implies a link between PDLIM2 and protein synthesis however we found PDLIM2 to be localized to the nucleus, where this process does not take place. This might indicate that PDLIM2 is associated with the process of ribosome biogenesis, which does occur in the nucleus. It has been proposed that cancer cells are able to sustain higher rates of proliferation by increasing their translational capacity compared to their normal counterparts (van Sluis and McStay 2014). If so, PDLIM2 may be a central mediator of tumour cell proliferation and as such represents a valuable therapeutic target.

Integrin beta 1 (ITGB1) also eluted with PDLIM2 suggesting a link between the two proteins. Association between integrins and PDLIM2 has been reported before (Geiger and Zaidel-Bar 2012) and places both proteins within the 'adhesome,' a large network of proteins with diverse and substantial influence over cell signalling. As ITGB1 is a membrane component and in the cells analysed here PDLIM2 is nuclear, the association between them is unlikely to be direct. ITGB1 has been shown previously as an important effector of Merlin deficiency and schwannoma pathology (Utermark, Kaempchen *et al.* 2003), suggesting that PDLIM2 is also implicated in the pathological adhesion associated with NF2 tumour cells.

We significantly knocked down PDLIM2 in three primary meningioma and three primary schwannoma cell populations. This led to significant reductions in cell proliferation in both cell types, suggesting that PDLIM2 is potentially a valuable therapeutic target. These results are in line with a previous study that found PDLIM2 suppression led to decreased proliferation in prostate cancer (Kang, Lee *et al.* 2016). Bowe *et al.* also showed that PDLIM2 was a significant contributor to malignant cancer cell invasion (Bowe, Cox *et al.* 2014). On the other hand, other studies have identified

PDLIM2 as an important tumour suppressor (Zhao L 2016, Sun F 2015). Our early studies indicate that PDLIM2 acts as a tumour promoting factor in both meningioma and schwannoma cells.

6.10 Conclusion

The aim of this project was to identify and validate novel therapeutic targets to enable simultaneous treatment of Merlin-deficient meningiomas and schwannomas that arise as part of the genetic condition Neurofibromatosis type 2 (NF2). Our global exploration of the phosphoproteome of primary meningioma and schwannoma cells led to the identification of many potential therapeutic targets and there is scope for validating a huge number of those in future studies. We have shown throughout this project that phosphoproteome profiling is an invaluable tool for elucidating new areas for therapeutic intervention. To name some; endocytosis may be an important target for schwannoma. Likewise, the proteome represents a promising area for further investigation in meningioma. STAT1, FLNB, PDLIM2 and HSPA1A were not previously linked to NF2 pathogenesis, and STAT1 and PDLIM2 in particular represent important targets for further characterization as much needed NF2 drug targets.

As surgery is at present the only available treatment option for NF2 patients, the work presented here provides a wealth of information upon which to build upon in future studies. Candidate targets identified as part of this project may eventually be translated in to the clinic, and thus may facilitate pioneering therapies for the combined treatment of all NF2 tumours; among the first therapies of their kind.

Supplementary Table S1: Phosphoproteins significantly up/ downregulated in primary schwannoma compared to Schwann cells

Gene symbol	Protein name	Log2 FC
HLA-DRA	HLA class II histocompatibility antigen, DR alpha chain	-26.15
GUSB	Beta-glucuronidase	-25.49
SCAF8	Protein SCAF8;Splicing factor, arginine/serine-rich 15	-25.04
DKK3	Dickkopf-related protein 3	-25.02
AFAP1L2	Actin filament-associated protein 1-like 2	-24.72
HIST1H1C	Histone H1.2	-24.63
KIAA1598	Shootin-1	-24.57
FAM192A	Protein FAM192A	-24.30
NDE1	Nuclear distribution protein nudE homolog 1	-24.14
THRAP3	Thyroid hormone receptor-associated protein 3	-24.11
RUNX1	Runt-related transcription factor 1	-24.11
EXOSC7	Exosome complex component RRP42	-23.98
PDZRN3	E3 ubiquitin-protein ligase PDZRN3	-23.95
PDCL	Phosducin-like protein	-23.87
WHSC2	Negative elongation factor A	-23.58
HDAC2	Histone deacetylase 2;Histone deacetylase	-23.57
LMAN1	Protein ERGIC-53	-23.32
WNK1	Serine/threonine-protein kinase WNK1	-23.31
CD74	HLA class II histocompatibility antigen gamma chain	-23.27
PLCB3	1-phosphatidylinositol 4,5-bisphosphate phosphodiesterase beta-3	-23.22
XRCC1	DNA repair protein XRCC1	-23.05
ODZ3	Teneurin-3	-22.90
VAV2	Guanine nucleotide exchange factor VAV2	-22.83
AHCY	Adenosylhomocysteinase	-22.62
NUP214	Nuclear pore complex protein Nup214	-22.58
MEF2A	Myocyte-specific enhancer factor 2C	-22.44
PWP1	Periodic tryptophan protein 1 homolog	-22.18
TFRC	Transferrin receptor protein 1	-22.13
CLASP2	CLIP-associating protein 2	-22.11

RBM15	Putative RNA-binding protein 15	-22.09
TCHH	Trichohyalin	-21.75
PLEC	Plectin	-4.95
CEP170	Centrosomal protein of 170 kDa	-4.22
XRCC6	X-ray repair cross-complementing protein 6	-3.99
PRKDC	DNA-dependent protein kinase catalytic subunit	-3.96
NUCB2	Nucleobindin-2	-3.23
VIM	Vimentin	-3.15
RANBP2	E3 SUMO-protein ligase RanBP2	-3.00
CTSD	Cathepsin D;Cathepsin D light chain	-2.83
ARSA	Arylsulfatase A;Arylsulfatase A component B	-2.78
RPLP2	60S acidic ribosomal protein P2	-2.74
MAP1B	Microtubule-associated protein 1B;MAP1 light chain LC1	-2.68
HMGB1	High mobility group protein B1	-2.67
AGA	N(4)-(beta-N-acetylglucosaminyl)-L-asparaginase	-2.64
CRYAB	Alpha-crystallin B chain	-2.53
KIF13B	Kinesin-like protein KIF13B	-2.52
TUBB3	Tubulin beta-3 chain	-2.28
HDAC1	Histone deacetylase 1	-2.19
RPN1	Dolichyl-diphosphooligosaccharide--protein glycosyltransferase subunit 1	-2.18
YTHDC2	Probable ATP-dependent RNA helicase YTHDC2	-2.14
NPC2	Epididymal secretory protein E1	-2.11
EZR	Ezrin	-2.08
HMGA1	High mobility group protein HMG-I/HMG-Y	-2.07
MYO9B	Unconventional myosin-IXb	-2.06
TMPO	Lamina-associated polypeptide 2, isoforms beta/gamma	-2.02
RALY	RNA-binding protein Raly	-2.01
SNRPN	Small nuclear ribonucleoprotein-associated protein	-2.00
SPAG9	C-Jun-amino-terminal kinase-interacting protein 4	-1.99
PSAP	Proactivator polypeptide	-1.99
SAFB	Scaffold attachment factor B1	-1.97

PCYT1A	Choline-phosphate cytidylyltransferase A	-1.92
P4HA2	Prolyl 4-hydroxylase subunit alpha-2	-1.89
HMGB2	High mobility group protein B2	-1.83
CAP1	Adenylyl cyclase-associated protein 1	-1.80
SAMHD1	SAM domain and HD domain-containing protein 1	-1.71
HNRNPC	Heterogeneous Nuclear Ribonucleoprotein C (C1/C2)	-1.70
LSM14A	Protein LSM14 homolog A	-1.70
CLASP1	CLIP-associating protein 1	-1.69
UBXN1	UBX domain-containing protein 1	-1.64
SNRPD2	Small nuclear ribonucleoprotein Sm D2	-1.56
RCC2	Protein RCC2	-1.55
TNS3	Tensin-3	-1.53
KLC1	Kinesin Light Chain 1	-1.47
SMAP	Small acidic protein	-1.44
UFL1	E3 UFM1-protein ligase 1	-1.43
CBX5	Chromobox protein homolog 5	-1.42
SGTA	Small glutamine-rich tetratricopeptide repeat-containing protein alpha	-1.41
PDIA4	Protein disulfide-isomerase A4	-1.39
U2AF2	Splicing factor U2AF 65 kDa subunit	-1.38
PSMB7	Proteasome subunit beta type-7	-1.33
TMED10	Transmembrane emp24 domain-containing protein 10	-1.31
ATG7	Ubiquitin-like modifier-activating enzyme ATG7	-1.30
TALDO1	Transaldolase	-1.26
SET	Protein SET	-1.25
GSK3B	Glycogen synthase kinase-3 beta	-1.24
ESYT1	Extended synaptotagmin-1	-1.24
KIAA1033	WASH complex subunit 7	-1.23
SMPD1	Sphingomyelin phosphodiesterase	-1.21
PACSIN2	Protein kinase C and casein kinase substrate in neurons protein 2	-1.20
RBM14	RNA-binding protein 14	-1.18
TRIO	Triple functional domain protein	-1.17

MYH10	Myosin-10	-1.16
PAPOLA	Poly(A) polymerase alpha	-1.15
EXOSC6	Exosome complex component MTR3	-1.13
HLA-B	HLA class I histocompatibility antigen, B-44 alpha chain	-1.11
PSMA7	Proteasome subunit alpha type-7	-1.10
DYNC1LI2	Cytoplasmic dynein 1 light intermediate chain 2	-1.09
PPIL4	Peptidyl-prolyl cis-trans isomerase-like 4	-1.03
ANP32B	Acidic leucine-rich nuclear phosphoprotein 32 family member B	-1.02
NAP1L1	Nucleosome assembly protein 1-like 1	-1.01
MAP1A	Microtubule-associated protein 1A;MAP1 light chain LC2	-1.00
ST13	Hsc70-interacting protein; Putative protein FAM10A5	-0.95
ADD1	Alpha-adducin	-0.95
MTDH	Protein LYRIC	-0.92
TEX264	Testis-expressed sequence 264 protein	-0.90
BABAM1	BRISC and BRCA1-A complex member 1	-0.90
RPL10	60S ribosomal protein L10	-0.89
CBX1	Chromobox protein homolog 1	-0.88
PTMA	Prothymosin alpha;Thymosin alpha-1	-0.87
ATXN2L	Ataxin-2-like protein	-0.86
NXF1	Nuclear RNA export factor 1	-0.86
HNRNPAB	Heterogeneous nuclear ribonucleoprotein A/B	-0.81
DYNC1I2	Cytoplasmic dynein 1 intermediate chain 2	-0.81
CYFIP1	Cytoplasmic FMR1-interacting protein 1	-0.80
HIST1H4A	Histone H4	-0.80
HNRNPK	Heterogeneous nuclear ribonucleoprotein K	-0.80
USP8	Ubiquitin carboxyl-terminal hydrolase 8;Ubiquitin carboxyl-terminal hydrolase	-0.73
PSMA6	Proteasome subunit alpha type-6;Proteasome subunit alpha type	-0.72
HSP90AA1	Heat shock protein HSP 90-alpha	-0.70
RPL27A	60S ribosomal protein L27a	-0.65
NAP1L4	Nucleosome assembly protein 1-like 4	-0.65
PLEKHF2	Pleckstrin homology domain-containing family F member 2	-0.64

PSMD1	26S proteasome non-ATPase regulatory subunit 1	-0.63
TRIM28	Transcription intermediary factor 1-beta	-0.58
TMX1	Thioredoxin-related transmembrane protein 1	-0.54
HNRNPH1	Heterogeneous nuclear ribonucleoprotein H	-0.53
ILF3	Interleukin enhancer-binding factor 3	-0.51
CALR	Calreticulin	-0.51
PSMA2	Proteasome subunit alpha type-2	-0.49
SVIL	Supervillin	-0.40
HNRNPUL1	Heterogeneous nuclear ribonucleoprotein U-like protein 1	-0.34
C1QBP	Complement component 1 Q subcomponent-binding protein, mitochondrial	-0.23
CTTN	Src substrate cortactin	0.50
CDC37	Hsp90 co-chaperone Cdc37	0.59
CHMP3	Charged multivesicular body protein 3	0.60
ARF3	ADP-ribosylation factor 3	0.61
ZC3HAV1	Zinc finger CCCH-type antiviral protein 1	0.62
SETD7	Histone-lysine N-methyltransferase SETD7	0.62
GSPT1	Eukaryotic peptide chain release factor GTP-binding subunit ERF3A	0.67
BRCC3	Lys-63-specific deubiquitinase BRCC36	0.67
RPL11	60S ribosomal protein L11	0.69
FLII	Protein flightless-1 homolog	0.72
PTGES3	Prostaglandin E synthase 3	0.75
RIC8A	Synembryn-A	0.75
SNX6	Sorting nexin-6	0.77
PGRMC2	Membrane-associated progesterone receptor component 2	0.80
RAB3GAP2	Rab3 GTPase-activating protein non-catalytic subunit	0.81
PSMB5	Proteasome subunit beta type-5	0.81
Uncharacterised	Uncharacterized protein FLJ45252	0.81
SKIV2L	Helicase SKI2W	0.84
CAND1	Cullin-associated NEDD8-dissociated protein 1	0.90
PSMD9	26S proteasome non-ATPase regulatory subunit 9	0.92
USO1	General vesicular transport factor p115	0.97

RAP1B	Ras-related protein Rap-1b;Ras-related protein Rap-1b-like protein	0.98
TCEB2	Transcription elongation factor B polypeptide 2	1.02
ACLY	ATP-citrate synthase	1.03
LRRC59	Leucine-rich repeat-containing protein 59	1.13
CORO1B	Coronin-1B	1.14
EIF2S1	Eukaryotic translation initiation factor 2 subunit 1	1.14
SSR3	Translocon-associated protein subunit gamma	1.16
NT5C2	Cytosolic purine 5-nucleotidase	1.25
EIF4A1	Eukaryotic initiation factor 4A-I	1.28
PSMB8	Proteasome subunit beta type-8	1.29
PDE1C	Calcium/calmodulin-dependent 3,5-cyclic nucleotide phosphodiesterase 1C	1.36
UBAP2L	Ubiquitin-associated protein 2-like	1.44
CORO1C	Coronin-1C	1.45
USP7	Ubiquitin carboxyl-terminal hydrolase 7;Ubiquitin carboxyl-terminal hydrolase	1.51
CUTA	Protein CutA	1.51
SCYL1	N-terminal kinase-like protein	1.54
SMTN	Smoothelin	1.56
TUFM	Elongation factor Tu, mitochondrial	1.56
MAP2K2	Dual specificity mitogen-activated protein kinase 2	1.58
UBE2H	Ubiquitin-conjugating enzyme E2 H	1.58
IPO5	Importin-5	1.61
CAMK2D	Calcium/calmodulin-dependent protein kinase type II subunit delta	1.68
TPD52L2	Tumour protein D54	1.76
ILK	Integrin-linked protein kinase	1.78
AP2B1	AP-2 complex subunit beta	1.80
RCN2	Reticulocalbin-2	1.85
AP2A1	AP-2 complex subunit alpha-1	1.85
ANXA5	Annexin A5;Annexin	1.85
FLNA	Filamin-A	1.92
TPI1	Triosephosphate isomerase	1.99
RAB18	Ras-related protein Rab-18	2.14

ZYX	Zyxin	2.20
ANXA6	Annexin A6;Annexin	2.26
EIF2S3	Eukaryotic translation initiation factor 2 subunit 3	2.38
MICAL1	Protein-methionine sulfoxide oxidase MICAL1	2.61
MVD	Diphosphomevalonate decarboxylase	2.71
RND3	Rho-related GTP-binding protein RhoE	2.73
BAG3	BAG family molecular chaperone regulator 3	2.80
MAP2K1	Dual specificity mitogen-activated protein kinase 1	2.81
ENO1	Alpha-enolase	2.90
HSPA1A	Heat shock 70 kDa protein 1A/1B	3.24
PPP1CA	Serine/threonine-protein phosphatase PP1-alpha catalytic subunit	3.37
EPS8	Epidermal growth factor receptor kinase substrate 8	3.42
CTPS	CTP synthase 1	3.71
LASP1	LIM and SH3 domain protein 1	3.79
CALD1	Caldesmon	3.80
PALLD	Palladin	5.48
FLNC	Filamin-C	5.74
HN1	Hematological and neurological expressed 1 protein	22.17
OAT	Ornithine aminotransferase, mitochondrial	22.17
VARS	Valine--tRNA ligase	22.18
VPS18	Vacuolar protein sorting-associated protein 18 homolog	22.24
ACTR3	Actin-related protein 3	22.34
MINK1	Misshapen-like kinase 1	22.38
ATP6V1G1	V-type proton ATPase subunit G 1	22.43
ROCK1	Rho-associated protein kinase 1	22.43
AIMP2	Aminoacyl tRNA synthase complex-interacting multifunctional protein 2	22.53
RSU1	Ras suppressor protein 1	22.64
NFKB1	Nuclear factor NF-kappa-B p105 subunit	22.70
BAG6	Large proline-rich protein BAG6	22.91
GNB1	Guanine nucleotide-binding protein G(I)/G(S)/G(T) subunit beta-1	22.92
INPP4A	Type I inositol 3,4-bisphosphate 4-phosphatase	22.98

EIF2B3	Translation initiation factor eIF-2B subunit gamma	23.18
MOB4	MOB-like protein phocein	23.27
CYP51A1	Lanosterol 14-alpha demethylase	23.28
MIF4GD	MIF4G domain-containing protein	23.29
NAA30	N-alpha-acetyltransferase 30	23.33
AP2A2	AP-2 complex subunit alpha-2	23.34
RAPH1	Ras-associated and pleckstrin homology domains-containing protein 1	23.35
MAPKAPK2	MAP kinase-activated protein kinase 2	23.47
RPS3A	40S ribosomal protein S3a	23.55
TCEB1	Transcription elongation factor B polypeptide 1	23.58
SYNPO	Synaptopodin	23.61
SAE1	SUMO-activating enzyme subunit 1	23.63
ALKBH5	Probable alpha-ketoglutarate-dependent dioxygenase ABH5	23.71
LDLRAP1	Low density lipoprotein receptor adapter protein 1	23.74
SYNC	Syncoilin	23.82
NAPA	Alpha-soluble NSF attachment protein	23.94
VPS29	Vacuolar protein sorting-associated protein 29	23.99
PAWR	PRKC apoptosis WT1 regulator protein	24.00
AP1M1	AP-1 complex subunit mu-1	24.02
AP1B1	AP-1 complex subunit beta-1	24.07
WDR61	WD repeat-containing protein 61	24.16
PSMG1	Proteasome assembly chaperone 1	24.16
LIN7C	Protein lin-7 homolog C	24.17
PDCD4	Programmed cell death protein 4	24.18
NCK1	Cytoplasmic protein NCK1	24.19
RAB23	Ras-related protein Rab-23	24.19
ACSS2	Acetyl-coenzyme A synthetase	24.23
EPS8L2	Epidermal growth factor receptor kinase substrate 8-like protein 2	24.27
PACS1	Phosphofurin acidic cluster sorting protein 1	24.34
FLNB	Filamin-B	24.50
DNAJB4	DnaJ homolog subfamily B member 4	24.52

PDLIM2	PDZ and LIM domain protein 2	24.53
YAP1	Yorkie homolog	24.57
ARFGAP1	ADP-ribosylation factor GTPase-activating protein 1	24.62
HSPB8	Heat shock protein beta-8	24.69
PACSIN3	Protein kinase C and casein kinase substrate in neurons protein 3	24.82
DFFA	DNA fragmentation factor subunit alpha	24.86
EIF4E	Eukaryotic translation initiation factor 4E	24.86
PLEKHO2	Pleckstrin homology domain-containing family O member 2	24.89
PFKL	6-phosphofructokinase, liver type	24.95
GNL1	Guanine nucleotide-binding protein-like 1	24.96
MYL9	Myosin regulatory light polypeptide 9	24.99
C6orf108	Deoxyribonucleoside 5-monophosphate N-glycosidase	25.04
CHMP2B	Charged multivesicular body protein 2b	25.06
RCAN1	Calcipressin-1	25.50
ATG4B	Cysteine protease ATG4B	25.51
PDLIM7	PDZ and LIM domain protein 7	25.53
NEXN	Nexilin	25.57
TGFB1I1	Transforming growth factor beta-1-induced transcript 1 protein	25.58
DSP	Desmoplakin	25.62
NDRG3	Protein NDRG3	25.68
LMOD1	Leiomodin-1	25.75
KCTD10	Adapter for CUL3-mediated RhoA degradation protein 3	25.86
TUBA4A	Tubulin alpha-4A chain	25.92
PPP1R14A	Protein phosphatase 1 regulatory subunit 14A	26.18
STAT1	Signal transducer and activator of transcription 1-alpha/beta	26.25
VCL	Vinculin	26.43
SORBS2	Sorbin And SH3 Domain Containing 2	26.68
PDLIM5	PDZ and LIM domain protein 5	26.96
RRAS2	Ras-related protein R-Ras2	27.28
TAGLN	Transgelin	28.52

Supplementary Table S2: Total proteins significantly up/ downregulated in schwannoma compared to Schwann cells

Gene symbol	Protein names	Log2 FC
ALDOC	Fructose-bisphosphate aldolase C	26.32
PSMB5	Proteasome subunit beta type-5	23.42
TAGLN	Transgelin	22.47
FLNC	Filamin-C	5.71
CALD1	Caldesmon	3.54
LASP1	LIM and SH3 domain protein 1	3.13
ALDOA	Fructose-bisphosphate aldolase A	1.98
CAPZB	F-actin-capping protein subunit beta	1.69
MYL6	Myosin light polypeptide 6	1.61
MAP1A	Microtubule-associated protein 1A;MAP1 light chain LC2	1.51
PSMA1	Proteasome subunit alpha type-1;Proteasome subunit alpha type	1.49
CLIC1	Chloride intracellular channel protein 1	1.25
ANXA5	Annexin A5;Annexin	1.20
PRDX1	Peroxiredoxin-1	1.13
GSTP1	Glutathione S-transferase P	1.06
ACTN4	Alpha-actinin-4	1.01
GSTK1	Glutathione S-transferase kappa 1	-1.03
CTNNA1	Catenin alpha-1	-1.12
ATP2A2	Sarcoplasmic/endoplasmic reticulum calcium ATPase 2	-1.15
HSP90B1	Endoplasmin	-1.16
ATP5B	ATP synthase subunit beta, mitochondrial;ATP synthase subunit beta	-1.29
YWHAZ	14-3-3 protein zeta/delta	-1.31
EIF3A	Eukaryotic translation initiation factor 3 subunit A	-1.33
ETFB	Electron transfer flavoprotein subunit beta	-1.40
RPSA	40S ribosomal protein SA	-1.44
RPL26	60S ribosomal protein L26	-1.50
CAP1	Adenylyl cyclase-associated protein 1	-1.57
PDIA3	Protein disulfide-isomerase A3	-1.83
RPL4	60S ribosomal protein L4	-1.91

ITGAV	Integrin alpha-V;Integrin alpha-V heavy chain;Integrin alpha-V light chain	-1.96
LGALS3	Galectin-3	-2.04
RPN1	Dolichyl-diphosphooligosaccharide--protein glycosyltransferase subunit 1	-2.42
SPAG9	C-Jun-amino-terminal kinase-interacting protein 4	-3.15
EIF4G1	Eukaryotic translation initiation factor 4 gamma 1	-3.18
HNRNPM	Heterogeneous nuclear ribonucleoprotein M	-3.89
NES	Nestin	-5.87
PACSIN2	Protein kinase C and casein kinase substrate in neurons protein 2	-21.40
SEC24B	Protein transport protein Sec24B	-21.56
BCLAF1	Bcl-2-associated transcription factor 1	-21.85
SMARCC2	SWI/SNF complex subunit SMARCC2	-21.99
HECTD1	E3 ubiquitin-protein ligase HECTD1	-22.22
DIP2B	Disco-interacting protein 2 homolog B	-22.45
SART3	Squamous cell carcinoma antigen recognized by T-cells 3	-22.65
NUP214	Nuclear pore complex protein Nup214	-22.66
RANBP2	E3 SUMO-protein ligase RanBP2;Putative peptidyl-prolyl cis-trans isomerase	-22.87
HNRNPA0	Heterogeneous nuclear ribonucleoprotein A0	-23.06
DHX15	Putative pre-mRNA-splicing factor ATP-dependent RNA helicase DHX15	-23.08
H1FX	Histone H1x	-23.11
SLC27A4	Long-chain fatty acid transport protein 4	-23.15
RPL10	60S ribosomal protein L10	-23.18
FXR1	Fragile X mental retardation syndrome-related protein 1	-23.26
SMC2	Structural maintenance of chromosomes protein 2	-23.37
SH3PXD2A	SH3 and PX domain-containing protein 2A	-23.39
S E P 1 0	Septin-10	-23.39
HLA-C	HLA class I histocompatibility antigen, Cw-12 alpha chain	-23.39
KLC1	Kinesin light chain 1	-23.44
SVIL	Supervillin	-23.47
KIF13B	Kinesin-like protein KIF13B	-23.48
NUMA1	Nuclear mitotic apparatus protein 1	-23.61
HSPH1	Heat shock protein 105 kDa	-23.65

RHOB	Rho-related GTP-binding protein RhoB	-23.68
OXCT1	Succinyl-CoA:3-ketoacid-coenzyme A transferase 1, mitochondrial	-23.70
IMPA1	Inositol monophosphatase 1	-23.87
LMNB2	Lamin-B2	-23.88
NDUFS3	NADH dehydrogenase [ubiquinone] iron-sulfur protein 3, mitochondrial	-23.91
COL7A1	Collagen alpha-1(VII) chain	-23.98
IMPDH2	Inosine-5-monophosphate dehydrogenase 2	-24.01
KHSRP	Far upstream element-binding protein 2	-24.14
NNT	NAD(P) transhydrogenase, mitochondrial	-24.18
RPS15	40S ribosomal protein S15	-24.21
GBE1	1,4-alpha-glucan-branching enzyme	-24.23
ODZ3	Teneurin-3	-24.30
HIGD1A	HIG1 domain family member 1A	-24.36
DDX3X	ATP-dependent RNA helicase DDX3X;ATP-dependent RNA helicase DDX3Y	-24.38
NOMO2	Nodal modulator 2;Nodal modulator 1;Nodal modulator 3	-24.40
ERH	Enhancer of rudimentary homolog	-24.42
COX5A	Cytochrome c oxidase subunit 5A, mitochondrial	-24.48
PLOD1	Procollagen-lysine,2-oxoglutarate 5-dioxygenase 1	-24.58
PSMD4	26S proteasome non-ATPase regulatory subunit 4	-24.63
PAK2	Serine/threonine-protein kinase PAK 2;PAK-2p27;PAK-2p34	-24.65
CD59	CD59 glycoprotein	-24.69
RPS9	40S ribosomal protein S9	-24.73
PCDH1	Protocadherin-1	-24.75
RBBP4	Histone-binding protein RBBP4	-24.76
PYGB	Glycogen phosphorylase, brain form	-24.83
SF3B2	Splicing factor 3B subunit 2	-24.90
HIST1H2BB	Histone H2B type 1-B	-24.95
NAMPT	Nicotinamide phosphoribosyltransferase	-25.05
RPL36	60S ribosomal protein L36	-25.05
GAS7	Growth arrest-specific protein 7	-25.06
CDH19	Cadherin-19	-25.10

SRI	Sorcin	-25.18
XRCC5	X-ray repair cross-complementing protein 5	-25.19
MMP14	Matrix metalloproteinase-14	-25.45
PPIF	Peptidyl-prolyl cis-trans isomerase F, mitochondrial;Peptidyl-prolyl cis-trans isomerase	-25.47
EIF3K	Eukaryotic translation initiation factor 3 subunit K	-25.48
HMGB3	High mobility group protein B3	-25.65
FKBP2	Peptidyl-prolyl cis-trans isomerase FKBP2	-25.67
CRLF1	Cytokine receptor-like factor 1	-25.76
FUBP1	Far upstream element-binding protein 1	-25.77
COX4I1	Cytochrome c oxidase subunit 4 isoform 1, mitochondrial	-25.86
RPL9	60S ribosomal protein L9	-25.95
RPL13	60S ribosomal protein L13	-26.03
HINT1	Histidine triad nucleotide-binding protein 1	-26.15
RPS17	40S ribosomal protein S17;40S ribosomal protein S17-like	-26.48
XRCC6	X-ray repair cross-complementing protein 6	-26.61
HLA-DRB1	HLA class II histocompatibility antigen, DRB1-4 beta chain	-26.66
ATP5I	ATP synthase subunit e, mitochondrial	-26.82
PLXNB3	Plexin-B3	-26.99

Supplementary Table S3: Phosphoproteins significantly downregulated in primary meningioma compared to HMC

Gene symbol	Protein name	Log2 FC
TALDO1	Transaldolase	-1.14
PSMA5	Proteasome subunit alpha ty-5	-1.15
HSP90AB1	Heat shock protein HSP 90-beta	-1.15
HNRNPU	Heterogeneous nuclear ribonucleoprotein U	-1.18
DDX3X	Isoform 2 of ATP-dependent RNA helicase DDX3X	-1.18
SNX1	Sorting nexin-1	-1.18
RPS3	40S ribosomal protein S3	-1.18
MAP2K2	Dual specificity mitogen-activated protein kinase kinase 2	-1.24
PSMA3	Isoform 2 of Proteasome subunit alpha ty-3	-1.27
PSMA1	Proteasome subunit alpha ty-1	-1.28
DCTN1	Isoform 3 of Dynactin subunit 1	-1.33
FAM129B	Niban-like protein 1	-1.34
HIST2H2BE	Histone H2B ty 2-E	-1.40
LRRC47	Leucine-rich repeat-containing protein 47	-1.42
AP2B1	AP-2 complex subunit beta	-1.46
PDLIM4	PDZ and LIM domain protein 4	-1.46
RPS6	40S ribosomal protein S6	-1.49
SORBS3	Vinexin	-1.51
ILK	Integrin-linked protein kinase	-1.56
CCDC25	Coiled-coil domain-containing protein 25	-1.59
NOP58	Nucleolar protein 58	-1.59
HSP90B1	Endoplasmin	-1.62
CLINT1	Clathrin interactor 1	-1.65
EHD2	EH domain-containing protein 2	-1.66
PSMB7	Proteasome subunit beta ty-7	-1.72
PSMB1	Proteasome subunit beta ty-1	-1.72
CNN3	Calponin-3	-1.78
FLNA	Isoform 2 of Filamin-A	-1.79
PSMB6	Proteasome subunit beta ty-6	-1.84

HNRNPC	Heterogeneous nuclear ribonucleoproteins C1/C2 (Fragment)	-1.97
PDHA1	Pyruvate dehydrogenase E1 component subunit alpha, somatic form, mitochondrial	-2.02
HNRNPUL1	Isoform 2 of Heterogeneous nuclear ribonucleoprotein U-like protein 1	-2.02
MAP2K1	Dual specificity mitogen-activated protein kinase kinase 1	-2.03
SPAG9	C-Jun-amino-terminal kinase-interacting protein 4	-2.05
PGRMC2	Membrane-associated progesterone receptor component 2	-2.12
USO1	General vesicular transport factor p115	-2.17
PTRF	Polymerase I and transcript release factor	-2.17
HDLBP	Vigilin	-2.35
PSMA2	Proteasome subunit alpha ty-2	-2.37
S E P 9	Isoform 5 of Septin-9	-2.52
MAP4	Microtubule-associated protein	-2.57
WDR44	Isoform 2 of WD repeat-containing protein 44	-2.63
DBN1	Isoform 3 of Drebrin	-2.98
AKAP12	Isoform 2 of A-kinase anchor protein 12	-2.99
S E P 1 1	Septin 11, isoform CRA	-3.46
EPB41L3	Isoform B of Band 4.1-like protein 3	-4.59
APBB1	Isoform 2 of Amyloid beta A4 precursor protein-binding family B member 1	-19.22
FMNL3	Formin-like protein 3	-19.53
NCSTN	Nicastrin (Fragment)	-19.69
CARS	Isoform 2 of Cysteine--tRNA ligase, cytoplasmic	-19.74
LP1	Proline-, glutamic acid- and leucine-rich protein 1	-19.79
XRCC1	DNA repair protein XRCC1	-19.89
IBTK	Isoform 2 of Inhibitor of Bruton tyrine kinase	-19.90
NEK1	Isoform 4 of Serine/threonine-protein kinase Nek1	-19.97
DIAPH1	Diaphanous homolog 1 (Drosophila), isoform CRA	-20.02
ECI2	Isoform 2 of Enoyl-CoA delta isomerase 2, mitochondrial	-20.02
QARS	Glutamine--tRNA ligase	-20.04
USP32	Ubiquitin carboxyl-terminal hydrolase 32	-20.07
KIAA0196	WASH complex subunit strumllin	-20.08
CUL4B	Isoform 2 of Cullin-4B	-20.11

TP53BP2	Isoform 2 of Apoptosis-stimulating of p53 protein 2	-20.13
NBAS	Isoform 2 of Neuroblastoma-amplified sequence	-20.17
YWHAH	14-3-3 protein eta	-20.19
XPO6	Exporting 6, isoform CRA	-20.19
STRN	Isoform 2 of Striating	-20.20
TFRC	Transferrin receptor protein 1	-20.21
BCAS3	Isoform 5 of Breast carcinoma-amplified sequence 3	-20.23
BCAR1	Isoform 4 of Breast cancer anti-estrogenic resistance protein 1	-20.25
MYO5A	Isoform 2 of Unconventional myin-Va	-20.27
ARAP3	Arf-GAP with Rho-GAP domain, ANK repeat and PH domain-containing protein 3	-20.28
SPIRE1	Isoform 2 of Protein spire homolog 1	-20.34
INPP4A	Ty I initol 3,4-bisphphate 4-phphatase	-20.35
NOC2L	Nucleolar complex protein 2 homolog	-20.35
IKBKAP	Elongator complex protein 1	-20.35
PIK3R4	Phosphoinositide 3-kinase regulatory subunit 4	-20.36
SMC1A	Structural maintenance of chromosomes protein 1A	-20.37
STK10	Serine/threonine-protein kinase 10	-20.40
ARFGEF1	Brefeldin A-inhibited guanine nucleotide-exchange protein 1	-20.45
ZZEF1	Zinc finger ZZ-ty and EF-hand domain-containing protein 1	-20.47
KPNB1	Importin subunit beta-1	-20.49
IGFBP3	Insulin-like growth factor-binding protein 3	-20.50
MPZL1	Isoform 4 of Myelin protein zero-like protein 1	-20.50
FARP1	FERM, RhoGEF and pleckstrin domain-containing protein 1	-20.51
CEP170	Isoform 3 of Centrosomal protein of 170 kDa	-20.55
THOC2	THO complex subunit 2	-20.56
UTP14A	Isoform 3 of U3 small nucleolar RNA-associated protein 14 homolog A	-20.57
RPP40	Isoform 2 of Ribonuclease P protein subunit p40	-20.58
CAMSAP1	Calmodulin-regulated secretin-associated protein 1	-20.59
CCDC9	Coiled-coil domain-containing protein 9	-20.59
COL1A1	Collagen alpha-1(I) chain	-20.61
TBC1D10B	TBC1 domain family member 10B	-20.63

NOC4L	Nucleolar complex protein 4 homolog	-20.66
VPS26A	Vacuolar protein sorting-associated protein 26A	-20.67
CCAR2	Isoform 2 of Cell cycle and apoptosis regulator protein 2	-20.68
WAPAL	Wings apart-like protein homolog	-20.70
ACTR2	Actin-related protein 2	-20.70
SUGP2	SURP and G-patch domain-containing protein 2	-20.71
DHX38	Pre-mRNA-splicing factor ATP-dependent RNA helicase PRP16	-20.71
TCEB3	Transcription elongation factor B polypeptide 3	-20.72
PAK1	Serine/threonine-protein kinase PAK 1	-20.74
ARIH2	E3 ubiquitin-protein ligase ARIH2	-20.74
SYNJ1	Synaptojanin-1	-20.74
ATP6V1A	V-ty proton ATPase catalytic subunit A	-20.75
ASMTL	Isoform 2 of N-acetylserotonin O-methyltransferase-like protein	-20.76
EXC10	Exome component 10	-20.77
RICTOR	Rapamycin-insensitive companion of mTOR	-20.77
PHLDB2	Isoform 2 of Pleckstrin homology-like domain family B member 2	-20.78
PRMT3	Protein arginine N-methyltransferase 3	-20.79
MYO6	Isoform 6 of Unconventional myosin-VI	-20.82
MTMR6	Myotubularin-related protein 6	-20.86
FKBP8	peptidyl-prolyl cis-trans isomerase FKBP8	-20.88
PSMA3	Proteasome subunit alpha ty-3	-20.89
SND1	Staphylococcal nuclease domain-containing protein 1	-20.89
ATP2B1	Isoform K of Plasma membrane calcium-transporting ATPase 1	-20.91
VPS41	Isoform Short of Vacuolar protein sorting-associated protein 41 homolog	-20.95
STRIP1	Striatin-interacting protein 1	-20.95
DBR1	Lariat debranching enzyme	-20.95
TANC1	Protein TANC1	-20.96
STK11IP	Serine/threonine-protein kinase 11-interacting protein	-20.98
ANKRD17	Isoform 6 of Ankyrin repeat domain-containing protein 17	-21.00
KIAA1468	Isoform 2 of Lis domain and HEAT repeat-containing protein KIAA1468	-21.00
RBM28	RNA-binding protein 28	-21.02

TOP2B	Isoform Beta-1 of DNA topoisomerase 2-beta	-21.04
DICER1	Endoribonuclease Dicer	-21.06
SGPL1	Sphingine-1-phphate lyase 1	-21.10
GAK	Cyclin-G-associated kinase	-21.10
FAM114A2	Protein FAM114A2	-21.10
RABGAP1	Rab GTPase-activating protein 1	-21.11
KIAA1217	Sickle tail protein homolog	-21.12
RPS3A	40S ribomal protein S3a (Fragment)	-21.14
WDR11	WD repeat-containing protein 11	-21.14
NIFK	MKI67 FHA domain-interacting nucleolar phosphoprotein	-21.15
IMP3	U3 small nucleolar ribonucleoprotein protein IMP3	-21.15
FAM21A	WASH complex subunit FAM21A	-21.16
INTS3	Isoform 3 of Integrator complex subunit 3	-21.16
CBL	E3 ubiquitin-protein ligase CBL	-21.17
ARHGEF12	Rho guanine nucleotide exchange factor 12	-21.17
CDC42BPB	Serine/threonine-protein kinase MRCK beta	-21.18
WDFY3	Isoform 2 of WD repeat and FYVE domain-containing protein 3	-21.19
PLCB1	1-phphatidylinitol 4,5-bisphphate phosphodiesterase beta-1	-21.19
TLN2	Talin-2	-21.20
PRKD1	Serine/threonine-protein kinase D1	-21.20
IPO4	Importin-4	-21.21
SBF1	Myotubularin-related protein 5	-21.21
FAF1	FAS-associated factor 1	-21.21
ABL1	Tyrine-protein kinase ABL1	-21.21
DOCK5	Dedicator of cytokinesis protein 5	-21.24
UGGT1	Isoform 2 of UDP-glucose:glycoprotein glucyltransferase 1	-21.25
TJP2	Isoform C1 of Tight junction protein ZO-2	-21.29
BIRC6	Baculoviral IAP repeat-containing protein 6	-21.30
FMNL2	Isoform 2 of Formin-like protein 2	-21.30
ASCC3	Activating signal cointegrator 1 complex subunit 3	-21.30
PPIL4	peptidyl-prolyl cis-trans isomerase-like 4	-21.31

MESDC2	LDLR chaperone MESD	-21.32
RAPGEF2	Rap guanine nucleotide exchange factor 2	-21.33
TXLNA	Alpha-taxin	-21.34
HMGCL	3-hydroxymethyl-3-methylglutaryl-Coenzyme A lyase (Hydroxymethylglutaricaciduria)	-21.34
SNX17	Isoform 2 of Sorting nexin-17	-21.35
EEF2K	Eukaryotic elongation factor 2 kinase	-21.35
ARMC9	Isoform 2 of LisH domain-containing protein ARMC9	-21.37
BPL2	Isoform 2 of Oxysterol-binding protein-related protein 2	-21.38
MLLT4	Isoform 1 of Afadin	-21.39
POLR1A	DNA-directed RNA polymerase	-21.39
DIP2B	Disco-interacting protein 2 homolog B	-21.41
ITCH	Isoform 2 of E3 ubiquitin-protein ligase Itchy homolog	-21.41
SERPINB12	Serpin B12	-21.43
REEP3	Receptor expression-enhancing protein 3	-21.44
DMXL1	DmX-like protein 1	-21.45
DHRS7	Isoform 2 of Dehydrogenase/reductase SDR family member 7	-21.45
RUVBL1	RuvB-like 1	-21.46
PIK3C2A	Phosphatidylinitol 4-phphate 3-kinase C2 domain-containing subunit alpha	-21.47
KIF13B	Kinesin-like protein KIF13B	-21.47
FAM91A1	Protein FAM91A1	-21.47
CMSS1	Protein CMSS1 (Fragment)	-21.48
STX4	Syntaxin-4	-21.49
ATIC	Isoform 2 of Bifunctional purine biosynthesis protein PURH	-21.50
SF3A1	Splicing factor 3A subunit 1	-21.50
S1	scadillo homolog	-21.50
HSPA4	Heat shock 70 kDa protein 4	-21.51
NEDD4	Isoform 4 of E3 ubiquitin-protein ligase NEDD4	-21.52
UPF2	Regulator of nonsense transcripts 2	-21.52
AZGP1	Zinc-alpha-2-glycoprotein	-21.52
PFKL	6-phphofructokinase, liver ty	-21.53
EMD	Emerin	-21.54

TNPO1	Isoform 2 of Transportin-1	-21.54
NONO	Non-POU domain-containing octamer-binding protein	-21.54
DOCK10	Dedicator of cytokinesis protein 10	-21.55
DOCK6	Dedicator of cytokinesis protein 6	-21.56
UBR4	Isoform 3 of E3 ubiquitin-protein ligase UBR4	-21.57
GIGYF2	Isoform 3 of RQ amino acid-rich with GYF domain-containing protein 2	-21.57
PRKRA	Interferon-inducible double-stranded RNA-dependent protein kinase activator A	-21.58
MYO1B	Isoform 2 of Unconventional myosin-Ib	-21.58
MACF1	Microtubule-actin crs-linking factor 1, isoforms 1/2/3/5	-21.59
IPO9	Importin-9	-21.60
PTEN	Phosphatidylinitol 3,4,5-trisphphate 3-phphatase and dual-specificity protein phosphatase	-21.61
UBE4B	Isoform 2 of Ubiquitin conjugation factor E4 B	-21.62
USP4	Isoform 2 of Ubiquitin carboxyl-terminal hydrolase 4	-21.63
GGH	Gamma-glutamyl hydrolase	-21.64
RQCD1	Cell differentiation protein RCD1 homolog	-21.64
BPL9	Oxysterol-binding protein	-21.64
DHX16	Putative pre-mRNA-splicing factor ATP-dependent RNA helicase DHX16	-21.66
EXC4	Exome complex component RRP41	-21.67
NIP7	60S ribosome subunit biogenesis protein NIP7 homolog	-21.68
GPN3	GPN-loop GTPase 3	-21.69
CDK5RAP3	CDK5 regulatory subunit-associated protein 3	-21.70
PWP2	periodic tryptophan protein 2 homolog	-21.70
PPP4R1	Isoform 2 of Serine/threonine-protein phosphatase 4 regulatory subunit 1	-21.71
S E P 8	Isoform 2 of Septin-8	-21.72
PFKM	6-phphofructokinase, muscle ty	-21.73
RPL10	60S ribosomal protein L10	-21.73
KIF2A	Isoform 2 of Kinesin-like protein KIF2A	-21.73
HDAC6	Histone deacetylase 6	-21.74
GRK5	G protein-coupled receptor kinase 5	-21.74
LDHB	L-lactate déshydrogénase B chain	-21.74
MYO1E	Unconventional myosin-Ie	-21.74

EIF2AK4	Isoform 2 of Eukaryotic translation initiation factor 2-alpha kinase 4	-21.74
HELZ	Probable helicase with zinc finger domain	-21.75
SMEK1	Isoform 2 of Serine/threonine-protein phosphatase 4 regulatory subunit 3A	-21.75
S1	Son of sevenless homolog 1	-21.75
USP11	Ubiquitin carboxyl-terminal hydrolase	-21.76
MDH1	Malate dehydrogenase, cytoplasmic	-21.77
FAM160B1	Protein FAM160B1	-21.77
GTPBP4	Nucleolar GTP-binding protein 1	-21.78
PLEKHA5	Pleckstrin homology domain-containing family A member 5	-21.79
SMARCA5	SWI/SNF-related matrix-associated actin-dependent regulator of chromatin	-21.79
ASCC2	Activating signal cointegrator 1 complex subunit 2	-21.79
CC2D1B	Coiled-coil and C2 domain-containing protein 1B (Fragment)	-21.80
ARAP1	Isoform 7 of Arf-GAP with Rho-GAP domain	-21.80
MGEA5	Bifunctional protein NCOAT	-21.81
LLGL1	Lethal(2) giant larvae protein homolog 1	-21.82
ABI2	Isoform 2 of Abl interactor 2	-21.84
TCEA1	Transcription elongation factor A protein 1	-21.84
CPD	Carboxypeptidase D	-21.86
FNDC3B	Fibronectin ty III domain-containing protein 3B	-21.86
SIPA1	Signal-induced proliferation-associated protein 1	-21.86
KIF1C	Kinesin-like protein KIF1C	-21.86
RPS2	40S ribomal protein S2 (Fragment)	-21.86
PUM1	Pumilio homolog 1 (Fragment)	-21.87
DDX23	Probable ATP-dependent RNA helicase DDX23	-21.87
ANK3	Isoform 3 of Ankyrin-3	-21.87
PSMD14	26S proteasome non-ATPase regulatory subunit 14	-21.87
EPS15	Epidermal growth factor receptor substrate 15	-21.88
DLGAP4	Isoform 3 of Disks large-associated protein 4	-21.89
PI4KB	Isoform 2 of Phosphatidylinitol 4-kinase beta	-21.89
PPM1F	Protein phosphatase 1F	-21.90
AP1B1	Isoform C of AP-1 complex subunit beta-1	-21.90

LMAN2	Vesicular integral-membrane protein VIP36	-21.91
ITGA4	Integrin alpha-4	-21.92
ABR	Isoform Short of Active breakpoint cluster region-related protein	-21.93
WDR13	WD repeat-containing protein 13	-21.96
AP1M1	AP-1 complex subunit mu-1	-21.97
ARHGAP5	Isoform 2 of Rho GTPase-activating protein 5	-21.97
ZNF622	Zinc finger protein 622	-21.97
HS1BP3	HCLS1-binding protein 3	-21.98
HTT	Huntingtin	-21.98
C16orf62	Oesophageal cancer associated protein, isoform CRA	-21.99
MSH6	DNA mismatch repair protein Msh6	-21.99
CRK	Adapter molecule crk	-21.99
IK	Protein Red	-22.00
DHX57	Putative ATP-dependent RNA helicase DHX57	-22.01
CLASP1	CLIP-associating protein 1	-22.01
DIS3L2	DIS3-like exonuclease 2	-22.01
NUP205	Nuclear pore complex protein Nup205	-22.03
FAM177A1	Protein FAM177A1	-22.03
HEATR5A	Isoform 2 of HEAT repeat-containing protein 5A	-22.04
CCT5	T-complex protein 1 subunit epsilon	-22.05
FN1	Ugl-Y3	-22.05
TEX264	Testis-expressed sequence 264 protein	-22.06
CENPV	Isoform 3 of Centromere protein V	-22.07
NUP107	Nuclear pore complex protein Nup107	-22.07
PLS3	Plastin-3	-22.10
CCNK	Cyclin-K	-22.10
TUBGCP2	Gamma-tubulin complex component 2	-22.12
TTC37	Tetratricoptide repeat protein 37	-22.12
TMX3	Protein disulfide-isomerase TMX3	-22.13
EDC3	Enhancer of mRNA-decapping protein 3	-22.15
ROCK2	Rho-associated protein kinase 2	-22.16

KIF1B	Isoform 2 of Kinesin-like protein KIF1B	-22.16
ARCN1	Coatomer subunit delta	-22.17
SART1	U4/U6.U5 tri-snRNP-associated protein 1	-22.20
SRC	Proto-oncogene tyrine-protein kinase Src	-22.20
HNRNPM	Isoform 2 of Heterogeneous nuclear ribonucleoprotein M	-22.22
PRKCDBP	Protein kinase C delta-binding protein	-22.22
CD248	Endialin	-22.24
LARP4	La-related protein 4	-22.24
SPCS2	Signal peptidase complex subunit 2	-22.25
USP8	Ubiquitin carboxyl-terminal hydrolase 8	-22.26
PRKAG2	Isoform B of 5-AMP-activated protein kinase subunit gamma-2	-22.29
HEXB	Beta-hexaminidase subunit beta	-22.29
BAIAP2	Isoform 3 of Brain-specific angiogenesis inhibitor 1-associated protein 2	-22.30
CD2AP	CD2-associated protein	-22.30
RER1	Protein RER1 (Fragment)	-22.32
ASAP1	Arf-GAP with SH3 domain, ANK repeat and PH domain-containing protein 1	-22.32
FAM120A	Constitutive coactivator of PPAR-gamma-like protein 1	-22.32
YTHDC2	Probable ATP-dependent RNA helicase YTHDC2	-22.33
TRIM16	Tripartite motif-containing protein 16	-22.33
MAPKAPK2	MAP kinase-activated protein kinase 2	-22.34
UBXN7	UBX domain-containing protein 7	-22.35
PIP	Prolactin-inducible protein	-22.35
DSG1	Desmoglein-1	-22.35
PKN2	Isoform 3 of Serine/threonine-protein kinase N2	-22.36
VCL	Isoform 1 of Vinculin	-22.37
NF2	Isoform 3 of Merlin	-22.37
PAPOLA	Poly(A) polymerase alpha	-22.38
ERP44	Endoplasmic reticulum resident protein 44	-22.38
PAK4	Serine/threonine-protein kinase PAK 4	-22.38
CDK17	Cyclin-dependent kinase 17	-22.39
CTBP1	Isoform 2 of C-terminal-binding protein 1	-22.39

PPP2R5D	Isoform Delta-3 of Serine/threonine-protein phosphatase 2A	-22.39
USP7	Ubiquitin carboxyl-terminal hydrolase	-22.39
DPM1	Dolichol-phosphate mannyltransferase subunit 1	-22.41
MICAL1	Protein-methionine sulfoxide oxidase MICAL1	-22.43
SKIV2L	Helicase SKI2W	-22.44
RILPL1	RILP-like protein 1	-22.44
1 SV	Uncharacterized protein FLJ45252	-22.45
C6orf203	Uncharacterized protein C6orf203	-22.45
AP2A2	AP-2 complex subunit alpha-2	-22.45
COBLL1	Isoform 4 of Cordon-bleu protein-like 1	-22.46
CTPS2	CTP synthase 2	-22.46
EXOC2	Exocyst complex component 2	-22.47
RAB12	Ras-related protein Rab-12	-22.47
EIF3A	Eukaryotic translation initiation factor 3 subunit A	-22.47
MON2	Protein MON2 homolog	-22.48
ADARB1	Double-stranded RNA-specific editase 1	-22.48
TPM1	Tropomyosin 1 (Alpha), isoform CRA	-22.48
PDS5B	Isoform 2 of Sister chromatid cohesion protein PDS5 homolog B	-22.52
PPIP5K2	Isoform 2 of Inositol hexakisphosphate and diphosphoinositol-ntakisphosphate kinase 2	-22.53
NSUN2	tRNA (cytosine(34)-C(5))-methyltransferase	-22.53
SAFB	Isoform 2 of Scaffold attachment factor B1	-22.53
ATP2A2	Isoform 5 of Sarcoplasmic/endoplasmic reticulum calcium ATPase 2	-22.53
SF3A3	Splicing factor 3A subunit 3	-22.53
PRPF31	U4/U6 small nuclear ribonucleoprotein Prp31	-22.55
ATXN2	Isoform 2 of Ataxin-2	-22.56
EFTUD2	Isoform 2 of 116 kDa U5 small nuclear ribonucleoprotein component	-22.57
SF1	Isoform 4 of Splicing factor 1	-22.57
FAM65A	Isoform 2 of Protein FAM65A	-22.58
RRP12	RRP12-like protein	-22.58
PPFIBP1	Isoform 4 of Liprin-beta-1	-22.58
NAGK	N-acetyl-D-glucamine kinase	-22.58

DDX27	Probable ATP-dependent RNA helicase DDX27	-22.60
GPX8	Probable glutathione peroxidase 8	-22.60
DDX54	ATP-dependent RNA helicase DDX54	-22.62
ARFGAP2	ADP-ribosylation factor GTPase-activating protein 2	-22.62
RAB2A	Ras-related protein Rab-2A	-22.63
ARAF	Serine/threonine-protein kinase A-Raf	-22.63
SF3B3	Splicing factor 3B subunit 3	-22.66
PRPF3	U4/U6 small nuclear ribonucleoprotein Prp3	-22.67
AP2M1	Isoform 2 of AP-2 complex subunit mu	-22.67
COMT	Isoform Soluble of Catechol O-methyltransferase	-22.67
EPB41L2	Band 4.1-like protein 2	-22.67
PRMT5	Protein arginine N-methyltransferase 5	-22.68
DUSP1	Dual specificity protein phosphatase 1	-22.69
GEP	Probable tRNA N6-adenine threonylcarbamoyltransferase	-22.70
FOCAD	Focadhesin	-22.71
MYO9B	Isoform Short of Unconventional myin-IXb	-22.72
ARFGAP3	ADP-ribosylation factor GTPase-activating protein 3	-22.72
DHX15	Putative pre-mRNA-splicing factor ATP-dependent RNA helicase DHX15	-22.73
GLRX3	Glutaredoxin-3	-22.74
EXOC1	Isoform 2 of Exocyst complex component 1	-22.74
ARHGEF40	Isoform 4 of Rho guanine nucleotide exchange factor 40	-22.75
CSNK1D	Isoform 2 of Casein kinase I isoform delta	-22.76
NAA15	N-alpha-acetyltransferase 15, NatA auxiliary subunit	-22.76
CNOT1	Isoform 2 of CCR4-NOT transcription complex subunit 1	-22.77
DKC1	H/ACA ribonucleoprotein complex subunit 4	-22.79
USP14	Ubiquitin carboxyl-terminal hydrolase	-22.79
MLEC	Malectin	-22.79
GIPC1	PDZ domain-containing protein GIPC1	-22.79
SEC11A	Signal peptidase complex catalytic subunit SEC11A	-22.80
PDGFRB	Platelet-derived growth factor receptor beta	-22.81
UBE2O	Ubiquitin-conjugating enzyme E2 O	-22.83

AKT3	Isoform 2 of RAC-gamma serine/threonine-protein kinase	-22.83
HDAC2	Histone deacetylase	-22.84
ANK2	Ankyrin-2	-22.85
PRPSAP1	Isoform 2 of Phosphoribyl pyrophosphate synthase-associated protein 1	-22.86
CNTNAP1	Contactin-associated protein 1	-22.88
IARS	Isoleucine--tRNA ligase, cytoplasmic	-22.91
PDLIM7	PDZ and LIM domain protein 7	-22.92
RPP30	Ribonuclease P protein subunit p30	-22.94
PLCG1	1-phphatidylinitol 4,5-bisphphate phosphodiesterase gamma-1	-22.94
PI4KA	Phosphatidylinitol 4-kinase alpha	-22.95
mTOR	Serine/threonine-protein kinase mTOR	-22.96
DNM2	Isoform 2 of Dynamin-2	-22.96
PIP4K2A	Phosphatidylinitol 5-phphate 4-kinase ty-2 alpha	-22.96
XRN2	5-3 exoribonuclease 2	-22.97
RRAS2	Ras-related protein R-Ras2	-22.98
NASP	Nuclear autoantigenic srm protein	-23.02
PPP2R5E	Serine/threonine-protein phosphatase 2A 56 kDa regulatory subunit epsilon isoform	-23.06
DCLK1	Isoform 1 of Serine/threonine-protein kinase DCLK1	-23.08
WDR77	Methylene protein 50	-23.09
TMED9	Transmembrane emp24 domain-containing protein 9	-23.11
EHBP1	EH domain-binding protein 1	-23.13
BAIAP2L1	Brain-specific angiogenesis inhibitor 1-associated protein 2-like protein 1	-23.14
NEXN	Nexilin	-23.14
STT3A	Dolichyl-diphosphooligaccharide--protein glycyltransferase subunit STT3A	-23.14
RPL5	60S ribosomal protein L5	-23.17
S E P 5	Septin-5	-23.17
SEC61A1	Protein transport protein Sec61 subunit alpha isoform 1	-23.18
RPL11	60S ribosomal protein L11	-23.20
PGK1	Phosphoglycerate kinase 1	-23.21
CDC42EP1	Isoform 2 of Cdc42 effector protein 1	-23.22
RASA3	Ras GTPase-activating protein 3	-23.25

SYNJ2	Synaptojanin-2	-23.28
INPPL1	Phosphatidylinitol 3,4,5-trisphphate 5-phphatase 2	-23.30
GEMIN5	Gem-associated protein 5	-23.31
GPN1	GPN-loop GTPase 1	-23.31
C20orf27	UPF0687 protein C20orf27	-23.37
PUS1	tRNA pseudouridine synthase (Fragment)	-23.38
TMEM43	Transmembrane protein 43	-23.41
CKAP5	Isoform 2 of Cytoskeleton-associated protein 5	-23.43
IFI16	Isoform 3 of Gamma-interferon-inducible protein 16	-23.49
RPS24	Isoform 2 of 40S ribosomal protein S24	-23.51
TRIO	Triple functional domain protein	-23.53
PKN1	Serine/threonine-protein kinase N1	-23.54
CDK16	Cyclin-dependent kinase 16	-23.56
PBDC1	Protein PBDC1	-23.58
SH3BP1	SH3 domain-binding protein 1	-23.62
SEC22B	Vesicle-trafficking protein SEC22b	-23.64
CLNS1A	Methylome subunit pICln	-23.65
PACS1	Phosphofurin acidic cluster sorting protein 1	-23.67
GNL3	Isoform 2 of Guanine nucleotide-binding protein-like 3	-23.70
SURF4	Isoform 2 of Surfeit locus protein 4	-23.70
ARFGAP1	ADP-ribosylation factor GTPase-activating protein 1	-23.70
CTNNA1	Catenin alpha-1	-23.78
RPL18	60S ribosomal protein L18 (Fragment)	-23.79
RRBP1	Ribose-binding protein 1	-23.85
AMPD2	AMP deaminase 2 (Fragment)	-23.88
TGFB1I1	Transforming growth factor beta-1-induced transcript 1 protein	-24.06
PPP1R18	Phosphotensin	-24.09
SNRPD1	Small nuclear ribonucleoprotein Sm D1	-24.11
RPS9	40S ribosomal protein S9	-24.13
NAV1	Isoform 2 of Neuron navigator 1	-24.15
CAD	CAD protein	-24.17

MRTO4	mRNA turnover protein 4 homolog	-24.18
MAP1S	MAP1S light chain	-24.19
IGF2BP3	Insulin-like growth factor 2 mRNA-binding protein 3	-24.30
SEC61B	Protein transport protein Sec61 subunit beta	-24.40
HP1BP3	Heterochromatin protein 1-binding protein 3	-24.45
USP47	Ubiquitin carboxyl-terminal hydrolase	-24.56
RAP1B	Isoform 3 of Ras-related protein Rap-1b	-24.69
PPIB	peptidyl-prolyl cis-trans isomerase B	-24.71
SSR1	Translocon-associated protein subunit alpha	-25.38
PITPNB	Phphatidylinitol transfer protein beta isoform	-25.40
KCTD12	BTB/POZ domain-containing protein KCTD12	-25.71

Supplementary Table S4: Total proteins significantly up/ downregulated in primary meningioma compared to HMC

Gene symbol	Protein name	Log2 FC
RBGP1	Rab GTPase-activating protein 1	26.52
KIF14	Kinesin-like protein KIF14	26.28
MAP1A	Microtubule-associated protein 1A	25.24
HSPB6	Heat shock protein beta-6	24.58
COBA1	Isoform C of Collagen alpha-1(XI) chain	24.50
FRIH	Ferritin heavy chain	24.19
ADIRF	Adipogenesis regulatory factor	23.73
IBP7	Isoform 2 of Insulin-like growth factor-binding protein 7	23.50
ALDR	Aldose reductase	23.46
RS30	40S ribosomal protein S30	23.20
ACBP	Acyl-CoA-binding protein	23.09
FRIL	Ferritin light chain	23.08
GDIR2	Rho GDP-dissociation inhibitor 2	22.82
TYB4	Thymosin beta-4	22.81
MGST1	Microsomal glutathione S-transferase 1	22.76
ICAM1	Intercellular adhesion molecule 1	22.42
TENX	Isoform 3 of Tenascin-X	22.34
F5GY99	Polypeptide N-acetylgalactosaminyltransferase 1 soluble form	22.33
CBPA4	Isoform 2 of Carboxypeptidase A4	22.23
GPX1	Glutathione peroxidase 1	22.21
PTN12	Tyrosine-protein phosphatase non-receptor type 12	22.07
AP2S1	AP-2 complex subunit sigma	22.01
GPX4	Isoform Cytoplasmic of Phospholipid hydroperoxide glutathione peroxidase	21.98
S10AD	Protein S100-A13	21.93
CPPED	Calcineurin-like phosphoesterase domain-containing protein 1	21.91
B4DUX5	Methionine aminopeptidase 2	21.90
ACACA	Isoform 4 of Acetyl-CoA carboxylase 1	21.86
THIC	Acetyl-CoA acetyltransferase, cytosolic	21.82
B4DZ70	Malic enzyme	21.79

SUMO2	Isoform 2 of Small ubiquitin-related modifier 2	21.78
ATOX1	Copper transport protein ATOX1	21.74
C9JWU9	Mesoderm-specific transcript homolog protein (Fragment)	21.74
GT251	Procollagen galactosyltransferase 1	21.57
TP53B	Tumor suppressor p53-binding protein 1	21.51
AMRP	Alpha-2-macroglobulin receptor-associated protein	21.50
FBN1	Fibrillin-1	21.49
HMCS1	Hydroxymethylglutaryl-CoA synthase, cytoplasmic	21.47
J3QRG6	Cyclin-dependent kinase inhibitor 2A, isoforms 1/2/3	21.45
ACSL4	Isoform Short of Long-chain-fatty-acid--CoA ligase 4	21.45
S4R371	Fatty acid-binding protein, heart (Fragment)	21.40
BDH2	3-hydroxybutyrate dehydrogenase type 2	21.38
WDR44	Isoform 4 of WD repeat-containing protein 44	21.37
SKIV2	Helicase SKI2W	21.25
YKT6	Synaptobrevin homolog YKT6	21.14
FADS2	Fatty acid desaturase 2	21.12
E41L1	Isoform 2 of Band 4.1-like protein 1	21.10
UBL5	Ubiquitin-like protein 5	21.06
EIF3H	Eukaryotic translation initiation factor 3 subunit H	21.04
MAOM	NAD-dependent malic enzyme, mitochondrial	21.03
CLCB	Isoform Non-brain of Clathrin light chain B	21.00
PRC2C	Isoform 6 of Protein PRRC2C	20.98
TRI25	E3 ubiquitin/ISG15 ligase TRIM25	20.98
PGM2	Phosphoglucomutase-2	20.97
RN213	E3 ubiquitin-protein ligase RNF213	20.88
J3KNL6	Protein transport protein Sec16A	20.81
UBQL2	Ubiquilin-2	20.80
PDCD5	Programmed cell death protein 5	20.79
MTND	1,2-dihydroxy-3-keto-5-methylthiopentene dioxygenase	20.77
DPM3	Dolichol-phosphate mannosyltransferase subunit 3	20.77
PRP19	Pre-mRNA-processing factor 19	20.70

NMT1	Glycylpeptide N-tetradecanoyltransferase 1	20.68
E41L3	Isoform B of Band 4.1-like protein 3	20.59
H0YBL1	Inositol monophosphatase 1 (Fragment)	20.34
LAMA5	Laminin subunit alpha-5	20.24
HMGA1	Isoform HMG-Y of High mobility group protein HMG-I/HMG-Y	20.23
CPIN1	Isoform 3 of Anamorsin	20.23
MVD1	Diphosphomevalonate decarboxylase	20.11
DBLOH	Isoform 2 of Diablo homolog, mitochondrial	20.11
CMBL	Carboxymethylenebutenolidase homolog	20.06
LACTB	Serine beta-lactamase-like protein LACTB, mitochondrial	19.95
MGP	Matrix Gla protein	19.92
B3KQ95	Squalene synthase	19.91
PLEC	Isoform 3 of Plectin	19.89
TLN2	Talin-2	19.86
SYUG	Gamma-synuclein	19.81
NEUA	N-acylneuraminate cytidylyltransferase	19.79
Q5H9A7	Metalloproteinase inhibitor 1	19.73
MCCB	Isoform 2 of Methylcrotonoyl-CoA carboxylase beta chain, mitochondrial	19.65
CHIP	E3 ubiquitin-protein ligase CHIP	19.61
HDGR2	Isoform 2 of Hepatoma-derived growth factor-related protein 2	19.60
A8MUB1	Tubulin alpha-4A chain	19.55
R4GN55	YTH domain-containing family protein 3	19.46
LYPA1	Isoform 2 of Acyl-protein thioesterase 1	19.43
E9PF19	Transducin beta-like protein 2	19.43
E9PEM5	Lipopolysaccharide-responsive and beige-like anchor protein	19.38
DHCR7	7-dehydrocholesterol reductase	19.37
CCDC6	Coiled-coil domain-containing protein 6	19.29
AAPK1	5-AMP-activated protein kinase catalytic subunit alpha-1	19.21
BIG1	Brefeldin A-inhibited guanine nucleotide-exchange protein 1	19.21
H0YDU8	Serine/threonine-protein phosphatase (Fragment)	19.19
ERG7	Isoform 2 of Lanosterol synthase	19.13

TCOF	Isoform 8 of Treacle protein	19.09
ELP1	Elongator complex protein 1	19.06
COMD9	Isoform 2 of COMM domain-containing protein 9	19.02
ACAD9	Acyl-CoA dehydrogenase family member 9, mitochondrial	19.00
SC24B	Isoform 2 of Protein transport protein Sec24B	19.00
K7EIJ0	WW domain-binding protein 2 (Fragment)	18.85
NXN	Nucleoredoxin	18.79
AKAP9	Isoform 3 of A-kinase anchor protein 9	18.74
NHLC2	NHL repeat-containing protein 2	18.74
HYPK	Huntingtin-interacting protein K	18.59
BID	BH3-interacting domain death agonist	18.58
J3KP84	Ethylmalonyl-CoA decarboxylase	18.58
PLCG1	1-phosphatidylinositol 4,5-bisphosphate phosphodiesterase gamma-1	18.55
EBP	3-beta-hydroxysteroid-Delta(8),Delta(7)-isomerase	18.52
LACB2	Beta-lactamase-like protein 2	18.43
DRG1	Developmentally-regulated GTP-binding protein 1	18.43
B4DME2	Protein phosphatase 1 regulatory subunit 12C	18.32
SVIL	Isoform 2 of Supervillin	18.19
WIBG	Isoform 2 of Partner of Y14 and mago	17.96
SGPL1	Sphingosine-1-phosphate lyase 1	17.90
IMA5	Importin subunit alpha-5	17.74
RPB1	DNA-directed RNA polymerase II subunit RPB1	17.64
TES	Isoform 2 of Testin	17.59
MP2K3	Isoform 1 of Dual specificity mitogen-activated protein kinase kinase 3	17.45
DNJC7	Isoform 2 of DnaJ homolog subfamily C member 7	17.31
YLPM1	Isoform 3 of YLP motif-containing protein 1	17.13
GCC2	GRIP and coiled-coil domain-containing protein 2	17.01
E9PC52	Histone-binding protein RBBP7	17.00
J3QSY4	H/ACA ribonucleoprotein complex subunit 2	16.96
UBXN4	UBX domain-containing protein 4	16.82
ZN428	Zinc finger protein 428	16.74

B3KR64	Calcium-binding mitochondrial carrier protein Aralar1	16.65
MYO5A	Isoform 2 of Unconventional myosin-Va	16.64
TGON2	Isoform 4 of Trans-Golgi network integral membrane protein 2	16.49
TB10B	TBC1 domain family member 10B	16.37
PUR8	Adenylosuccinate lyase	16.00
ZCCHL	Zinc finger CCCH-type antiviral protein 1-like	15.35
HTRA1	Serine protease HTRA1	15.07
FHL1	Isoform 1 of Four and a half LIM domains protein 1	5.11
E9PIR7	Thioredoxin reductase 1, cytoplasmic	4.37
ENAH	Isoform 3 of Protein enabled homolog	4.11
E5RHG8	Transcription elongation factor B polypeptide 1 (Fragment)	3.63
SRBS2	Isoform 9 of Sorbin and SH3 domain-containing protein 2	3.55
TGM2	Protein-glutamine gamma-glutamyltransferase 2	3.04
ACLY	ATP-citrate synthase	3.00
SH3L1	SH3 domain-binding glutamic acid-rich-like protein	2.98
C9J0K6	Sorcin	2.97
SIAS	Sialic acid synthase	2.92
FAS	Fatty acid synthase	2.89
NTF2	Nuclear transport factor 2	2.74
SAHH	Adenosylhomocysteinase	2.73
LASP1	LIM and SH3 domain protein 1	2.63
SYVC	Valine--tRNA ligase	2.56
PDLI5	PDZ and LIM domain protein 5	2.51
SUMF1	Isoform 2 of Sulfatase-modifying factor 1	2.49
FKB1A	Peptidyl-prolyl cis-trans isomerase FKBP1A	2.44
AKA12	A-kinase anchor protein 12	2.30
FKB10	Peptidyl-prolyl cis-trans isomerase FKBP10	2.27
COTL1	Coactosin-like protein	2.20
COPD	Coatomer subunit delta	2.15
UGPA	UTP--glucose-1-phosphate uridylyltransferase	2.10
TPD54	Tumor protein D54	2.10

OSBP1	Oxysterol-binding protein 1	2.09
THIO	Thioredoxin	2.08
VAT1	Synaptic vesicle membrane protein VAT-1 homolog	2.01
TCTP	Translationally-controlled tumor protein	2.00
IDI1	Isopentenyl-diphosphate Delta-isomerase 1	1.99
PEA15	Astrocytic phosphoprotein PEA-15	1.98
S10AG	Protein S100-A16	1.97
SODC	Superoxide dismutase [Cu-Zn]	1.91
TXNL1	Thioredoxin-like protein 1	1.88
FINC	Isoform 3 of Fibronectin	1.77
S10A6	Protein S100-A6	1.72
TKT	Transketolase	1.72
PCYOX	Prenylcysteine oxidase 1	1.67
RS3	40S ribosomal protein S3	1.65
ETHE1	Persulfide dioxygenase ETHE1, mitochondrial	1.64
KCC2D	Isoform Delta 6 of Calcium/calmodulin-dependent protein kinase type II subunit	1.63
H3BPE1	Microtubule-actin cross-linking factor 1, isoforms 1/2/3/5	1.61
G6PD	Glucose-6-phosphate 1-dehydrogenase	1.59
EF1B	Elongation factor 1-beta	1.56
TFG	Isoform 2 of Protein TFG	1.54
F8W031	Uncharacterized protein (Fragment)	1.48
STIP1	Stress-induced-phosphoprotein 1	1.44
HEBP1	Heme-binding protein 1	1.42
IPYR	Inorganic pyrophosphatase	1.37
ECHB	Trifunctional enzyme subunit beta, mitochondrial	1.36
EFTU	Elongation factor Tu, mitochondrial	1.36
ANXA3	Annexin A3	1.35
PRDX6	Peroxiredoxin-6	1.33
FLNC	Filamin-C	1.32
PYGB	Glycogen phosphorylase, brain form	1.31
6PGD	6-phosphogluconate dehydrogenase, decarboxylating	1.29

SYNC	Asparagine--tRNA ligase, cytoplasmic	1.28
B4DVE7	Annexin	1.26
AP3B1	AP-3 complex subunit beta-1	1.25
PPME1	Protein phosphatase methylesterase 1	1.24
TX1B3	Tax1-binding protein 3	1.22
MAP1B	Microtubule-associated protein 1B	1.21
UBP14	Isoform 2 of Ubiquitin carboxyl-terminal hydrolase 14	1.20
E9PKL9	GDP-L-fucose synthase (Fragment)	1.16
DREB	Drebrin	1.13
MANF	Mesencephalic astrocyte-derived neurotrophic factor	1.11
DHE3	Glutamate dehydrogenase 1, mitochondrial	1.10
ERP29	Endoplasmic reticulum resident protein 29	1.08
ECHA	Trifunctional enzyme subunit alpha, mitochondrial	1.03
PDIA1	Protein disulfide-isomerase	1.00
NEK7	Serine/threonine-protein kinase Nek7	-1.01
PTPA	Isoform 1 of Serine/threonine-protein phosphatase 2A activator	-1.06
RS13	40S ribosomal protein S13	-1.06
RAB5C	Ras-related protein Rab-5C	-1.09
NAA15	N-alpha-acetyltransferase 15, NatA auxiliary subunit	-1.09
I3L0H8	ATP-dependent RNA helicase DDX19A	-1.10
BIEA	Biliverdin reductase A	-1.12
AIMP2	Aminoacyl tRNA synthase complex-interacting multifunctional protein 2	-1.12
PP2AA	Serine/threonine-protein phosphatase 2A catalytic subunit alpha isoform	-1.14
RS26	40S ribosomal protein S26	-1.15
G6PI	Glucose-6-phosphate isomerase	-1.17
SCRN1	Secernin-1	-1.17
RS17L	40S ribosomal protein S17-like	-1.19
CPNS1	Calpain small subunit 1	-1.21
DDX6	Probable ATP-dependent RNA helicase DDX6	-1.22
PSA3	Isoform 2 of Proteasome subunit alpha type-3	-1.22
EXOC4	Exocyst complex component 4	-1.22

RS16	40S ribosomal protein S16	-1.22
PP1A	Serine/threonine-protein phosphatase PP1-alpha catalytic subunit	-1.22
DDX3X	Isoform 2 of ATP-dependent RNA helicase DDX3X	-1.22
TPPC3	Isoform 2 of Trafficking protein particle complex subunit 3	-1.23
ODO2	Dihydrolipoyllysine-residue succinyltransferase	-1.24
B4DJA5	Ras-related protein Rab-5A	-1.24
ENOA	Alpha-enolase	-1.24
UGDH	UDP-glucose 6-dehydrogenase	-1.25
RS18	40S ribosomal protein S18	-1.28
RS4X	40S ribosomal protein S4, X isoform	-1.35
TPIS	Isoform 2 of Triosephosphate isomerase	-1.35
SF3B1	Splicing factor 3B subunit 1	-1.39
HMOX2	Heme oxygenase 2	-1.39
ROA1	Isoform 2 of Heterogeneous nuclear ribonucleoprotein A1	-1.41
PURA	Transcriptional activator protein Pur-alpha	-1.41
JIP4	Isoform 4 of C-Jun-amino-terminal kinase-interacting protein 4	-1.42
ODO1	2-oxoglutarate dehydrogenase, mitochondrial	-1.43
SRP19	Signal recognition particle 19 kDa protein	-1.44
SURF4	Isoform 2 of Surfeit locus protein 4	-1.45
SRP14	Signal recognition particle 14 kDa protein	-1.47
UBA1	Ubiquitin-like modifier-activating enzyme 1	-1.48
RS19	40S ribosomal protein S19	-1.49
DPP9	Dipeptidyl peptidase 9	-1.50
TNPO1	Isoform 2 of Transportin-1	-1.50
DDX1	ATP-dependent RNA helicase DDX1	-1.50
VAPA	Vesicle-associated membrane protein-associated protein A	-1.51
LIPB1	Isoform 2 of Liprin-beta-1	-1.52
HS90A	Heat shock protein HSP 90-alpha	-1.55
ACOT9	Isoform 3 of Acyl-coenzyme A thioesterase 9, mitochondrial	-1.55
XPO2	Exportin-2	-1.56
TM109	Transmembrane protein 109	-1.60

SAR1A	GTP-binding protein SAR1a	-1.60
EDF1	Isoform 2 of Endothelial differentiation-related factor 1	-1.60
HS105	Isoform Beta of Heat shock protein 105 kDa	-1.61
EIF3E	Eukaryotic translation initiation factor 3 subunit E	-1.61
IMDH2	Inosine-5-monophosphate dehydrogenase 2	-1.61
PGAM1	Phosphoglycerate mutase 1	-1.61
RAB7A	Ras-related protein Rab-7a	-1.62
CYBP	Calcyclin-binding protein	-1.63
ETUD1	Isoform 2 of Elongation factor Tu GTP-binding domain-containing protein 1	-1.65
UTRO	Utrophin	-1.71
PTBP1	Polypyrimidine tract-binding protein 1	-1.72
TWF1	Twinfilin-1	-1.77
IPO5	Importin-5	-1.83
RS20	40S ribosomal protein S20	-1.88
GBB1	Guanine nucleotide-binding protein G(I)/G(S)/G(T) subunit beta-1	-1.88
RHOG	Rho-related GTP-binding protein RhoG	-1.89
HNRH1	Heterogeneous nuclear ribonucleoprotein H	-1.90
K6PL	6-phosphofructokinase, liver type	-1.93
LDHA	L-lactate dehydrogenase A chain	-1.93
RS25	40S ribosomal protein S25	-1.96
CATB	Cathepsin B	-1.97
HPRT	Hypoxanthine-guanine phosphoribosyltransferase	-2.00
AN32B	Isoform 2 of Acidic leucine-rich nuclear phosphoprotein 32 family member B	-2.00
SP16H	FACT complex subunit SPT16	-2.08
PRS6B	26S protease regulatory subunit 6B	-2.10
XPO1	Exportin-1	-2.15
RADI	Radixin	-2.20
STAT1	Signal transducer and activator of transcription 1-alpha/beta	-2.21
M0R0F0	40S ribosomal protein S5 (Fragment)	-2.22
RAGP1	Ran GTPase-activating protein 1	-2.23
A8MXP9	Matrin-3	-2.25

UN45A	Isoform 2 of Protein unc-45 homolog A	-2.26
THOP1	Thimet oligopeptidase	-2.31
AFAP1	Actin filament-associated protein 1	-2.32
IPO7	Importin-7	-2.35
VAMP3	Vesicle-associated membrane protein 3	-2.44
ROA0	Heterogeneous nuclear ribonucleoprotein A0	-2.47
SF3A1	Splicing factor 3A subunit 1	-2.48
EIF3F	Eukaryotic translation initiation factor 3 subunit F	-2.49
LARP1	La-related protein 1	-2.51
UBE4A	Ubiquitin conjugation factor E4 A	-2.52
MBB1A	Myb-binding protein 1A	-2.59
H2B1L	Histone H2B type 1-L	-2.60
DNM1L	Isoform 4 of Dynamin-1-like protein	-2.73
CTND1	Isoform 1A of Catenin delta-1	-2.73
CPSF5	Cleavage and polyadenylation specificity factor subunit 5	-2.74
EMD	Emerin	-2.77
CCAR2	Cell cycle and apoptosis regulator protein 2	-2.87
E2AK2	Interferon-induced, double-stranded RNA-activated protein kinase	-3.00
EZRI	Ezrin	-3.49
CTNA1	Catenin alpha-1	-3.50
TIF1B	Transcription intermediary factor 1-beta	-3.79
PALLD	Isoform 3 of Palladin	-3.93
CKAP5	Cytoskeleton-associated protein 5	-4.09
MGN	Protein mago nashi homolog	-4.46
EGFR	Epidermal growth factor receptor	-4.81
VDAC2	Voltage-dependent anion-selective channel protein 2	-4.92
K1C18	Keratin, type I cytoskeletal 18	-6.34
VIME	Vimentin	-6.96
VDAC1	Voltage-dependent anion-selective channel protein 1	-7.06
E5RGV5	Nucleolysin TIA-1 isoform p40	-16.48
ARFP2	Isoform 3 of Arfaptin-2	-16.61

D6RF48	Syntaxin-18	-17.00
EDC3	Enhancer of mRNA-decapping protein 3	-17.10
RU2A	U2 small nuclear ribonucleoprotein A	-17.21
MGLL	Monoglyceride lipase	-17.29
B4DPW1	Nuclear pore complex protein Nup85	-17.31
TIAR	Nucleolysin TIAR	-17.33
ENDD1	Endonuclease domain-containing 1 protein	-17.40
ASPP2	Isoform 2 of Apoptosis-stimulating of p53 protein 2	-17.43
H3BVG8	UPF0505 protein C16orf62 (Fragment)	-17.49
B4DNI9	Vacuolar protein sorting-associated protein 52 homolog	-17.55
OSGEP	Probable tRNA N6-adenosine threonylcarbamoyltransferase	-17.57
SYCM	Probable cysteine--tRNA ligase, mitochondrial	-17.59
J3KS22	L-xylulose reductase (Fragment)	-17.63
PEX5	Isoform 2 of Peroxisomal targeting signal 1 receptor	-17.64
E9PGE5	TBC1 domain family member 23	-17.65
DPOA2	DNA polymerase alpha subunit B	-17.68
G8JLC6	Melanoma inhibitory activity protein 3	-17.83
SSRG	Translocon-associated protein subunit gamma	-17.98
AHR	Aryl hydrocarbon receptor	-17.98
B7WP74	Pre-mRNA-splicing factor CWC22 homolog (Fragment)	-18.07
ENOG	Gamma-enolase	-18.15
D6RDI2	Luc7-like protein 3 (Fragment)	-18.15
B7ZLW7	MTR protein	-18.16
Q5VW33	BRO1 domain-containing protein BROX (Fragment)	-18.16
HXK2	Hexokinase-2	-18.18
NU160	Nuclear pore complex protein Nup160	-18.21
FA65A	Isoform 2 of Protein FAM65A	-18.29
CIP2A	Isoform 2 of Protein CIP2A	-18.31
V9GYH7	Proteasome assembly chaperone 2	-18.31
PTN14	Tyrosine-protein phosphatase non-receptor type 14	-18.31
CDK13	Isoform 2 of Cyclin-dependent kinase 13	-18.37

RNBP6	Ran-binding protein 6	-18.38
E9PJ81	UBX domain-containing protein 1 (Fragment)	-18.44
GLRX5	Glutaredoxin-related protein 5, mitochondrial	-18.45
ASCC3	Activating signal cointegrator 1 complex subunit 3	-18.49
TMED5	Transmembrane emp24 domain-containing protein 5	-18.50
SPTC2	Serine palmitoyltransferase 2	-18.52
PSME4	Proteasome activator complex subunit 4	-18.54
TGFI1	Transforming growth factor beta-1-induced transcript 1 protein	-18.56
B4E2J1	ATPase family AAA domain-containing protein 1	-18.57
F8W9D1	5-AMP-activated protein kinase subunit gamma-1	-18.57
PGP	Phosphoglycolate phosphatase	-18.65
INO1	Isoform 3 of Inositol-3-phosphate synthase 1	-18.67
RT28	28S ribosomal protein S28, mitochondrial	-18.70
ARHL2	Poly(ADP-ribose) glycohydrolase ARH3	-18.70
B7WPF4	Ubiquitin carboxyl-terminal hydrolase	-18.71
U3KQJ1	Polymerase delta-interacting protein 2	-18.71
F5H1E5	Conserved oligomeric Golgi complex subunit 2	-18.78
MTX2	Metaxin-2	-18.79
UBE3C	Ubiquitin-protein ligase E3C	-18.80
KIF3A	Kinesin-like protein KIF3A	-18.83
FADD	FAS-associated death domain protein	-18.84
NUP98	Isoform 6 of Nuclear pore complex protein Nup98-Nup96	-18.85
RT09	28S ribosomal protein S9, mitochondrial	-18.86
H7BYD0	NADH dehydrogenase [ubiquinone] 1 alpha subcomplex subunit 5 (Fragment)	-18.89
IF4A3	Eukaryotic initiation factor 4A-III	-18.89
ARG28	Isoform 4 of Rho guanine nucleotide exchange factor 28	-18.90
KANK2	Isoform 3 of KN motif and ankyrin repeat domain-containing protein 2	-18.92
CBS	Cystathionine beta-synthase	-18.93
ZN622	Zinc finger protein 622	-18.97
K0020	Pumilio domain-containing protein KIAA0020	-18.99
ARBK2	Beta-adrenergic receptor kinase 2	-19.00

VPS53	Isoform 4 of Vacuolar protein sorting-associated protein 53 homolog	-19.01
RAB9A	Ras-related protein Rab-9A	-19.04
E9PQX9	Dr1-associated corepressor	-19.05
SHLB1	Endophilin-B1	-19.10
C9JA93	TBC1 domain family member 15 (Fragment)	-19.12
B4DKA8	Ubiquitin carboxyl-terminal hydrolase	-19.13
LANC1	LanC-like protein 1	-19.14
RETST	Isoform 2 of All-trans-retinol 13,14-reductase	-19.15
SMAD3	Isoform 3 of Mothers against decapentaplegic homolog 3	-19.16
E9PHM2	Probable leucine--tRNA ligase, mitochondrial	-19.16
LSM3	U6 snRNA-associated Sm-like protein LSm3	-19.16
H0YJL5	Vesicle transport through interaction with t-SNAREs homolog 1B (Fragment)	-19.19
M0QZ24	Uncharacterized protein (Fragment)	-19.21
NR2CA	Nuclear receptor 2C2-associated protein	-19.21
F8VSC5	SCY1-like protein 2 (Fragment)	-19.21
NADAP	Kanadaptin	-19.22
GIT2	Isoform 11 of ARF GTPase-activating protein GIT2	-19.24
DNJC2	Isoform 2 of DnaJ homolog subfamily C member 2	-19.24
SRR	Serine racemase	-19.26
MK67I	MKI67 FHA domain-interacting nucleolar phosphoprotein	-19.27
BYST	Bystin	-19.27
NDUS7	NADH dehydrogenase [ubiquinone] iron-sulfur protein 7, mitochondrial	-19.27
OGFD1	2-oxoglutarate and iron-dependent oxygenase domain-containing protein 1	-19.27
GSDMD	Gasdermin-D	-19.29
C9JIK8	Cysteine protease ATG4B (Fragment)	-19.33
PCH2	Pachytene checkpoint protein 2 homolog	-19.34
RIFK	Riboflavin kinase	-19.35
H3BMM5	Uncharacterized protein	-19.37
UK114	Ribonuclease UK114	-19.38
VTI1A	Isoform 1 of Vesicle transport through interaction with t-SNAREs homolog 1A	-19.38
F8W1Z6	Protein MON2 homolog	-19.38

OGT1	UDP-N-acetylglucosamine--peptide N-acetylglucosaminyltransferase	-19.38
TCEA1	Isoform 2 of Transcription elongation factor A protein 1	-19.41
SMUF2	E3 ubiquitin-protein ligase SMURF2	-19.41
ASPG	N(4)-(beta-N-acetylglucosaminyl)-L-asparaginase	-19.42
SFR15	Isoform 3 of Splicing factor, arginine/serine-rich 15	-19.44
HIBCH	3-hydroxyisobutyryl-CoA hydrolase, mitochondrial	-19.44
EI2BB	Translation initiation factor eIF-2B subunit beta	-19.45
RBM28	Isoform 2 of RNA-binding protein 28	-19.45
HAP28	28 kDa heat- and acid-stable phosphoprotein	-19.45
ARP10	Actin-related protein 10	-19.46
PPID	Peptidyl-prolyl cis-trans isomerase D	-19.46
SAP18	Histone deacetylase complex subunit SAP18 (Fragment)	-19.47
VAC14	Protein VAC14 homolog	-19.47
ELOV1	Isoform 2 of Elongation of very long chain fatty acids protein 1	-19.48
RT29	Isoform 2 of 28S ribosomal protein S29, mitochondrial	-19.49
RFA2	Replication protein A 32 kDa subunit	-19.50
B4DFQ4	COMM domain-containing protein 1	-19.53
E7EQI7	WASH complex subunit strumpellin	-19.54
M0QXN5	Nuclear pore glycoprotein p62	-19.54
DCTP1	dCTP pyrophosphatase 1	-19.56
ILVBL	Acetolactate synthase-like protein	-19.57
G3V2T4	Legumain (Fragment)	-19.58
CLAP1	Isoform 2 of CLIP-associating protein 1	-19.58
F5H5C2	Nuclear pore complex protein Nup133	-19.58
G5E9W7	28S ribosomal protein S22, mitochondrial	-19.59
B4DTE8	Phospholipid scramblase 1	-19.60
F5H2H5	Ankyrin repeat and LEM domain-containing protein 2	-19.60
FKBP8	Peptidyl-prolyl cis-trans isomerase FKBP8	-19.61
E7ES96	Presenilin-1	-19.61
FNTA	Isoform 2 of Protein farnesyltransferase/geranylgeranyltransferase type-1 subunit alpha	-19.61
SREK1	Isoform 2 of Splicing regulatory glutamine/lysine-rich protein 1	-19.61

COMD4	COMM domain-containing protein 4	-19.62
H3BMU1	IST1 homolog (Fragment)	-19.62
HMOX1	Heme oxygenase 1	-19.64
E7EQZ7	Protein Red (Fragment)	-19.64
ABD12	Monoacylglycerol lipase ABHD12	-19.65
ASCC2	Activating signal cointegrator 1 complex subunit 2	-19.65
TAOK1	Isoform 3 of Serine/threonine-protein kinase TAO1	-19.67
DAG1	Dystroglycan	-19.68
ARMX3	Armadillo repeat-containing X-linked protein 3	-19.71
EVA1B	Protein eva-1 homolog B	-19.71
GOGA7	Isoform 2 of Golgin subfamily A member 7	-19.72
CSN7B	COP9 signalosome complex subunit 7b	-19.72
Q5TDF0	Cancer-related nucleoside-triphosphatase	-19.72
NUDC3	NudC domain-containing protein 3	-19.75
NU214	Isoform 2 of Nuclear pore complex protein Nup214	-19.75
F5H8F7	Set1/Ash2 histone methyltransferase complex subunit ASH2	-19.77
TEX10	Isoform 2 of Testis-expressed sequence 10 protein	-19.77
C9JKF1	Sterile alpha motif domain-containing protein 9 (Fragment)	-19.79
NCBP2	Nuclear cap-binding protein subunit 2	-19.79
EXOC5	Exocyst complex component 5	-19.80
INT1	Integrator complex subunit 1	-19.80
CPT2	Carnitine O-palmitoyltransferase 2, mitochondrial	-19.80
ADPPT	L-aminoadipate-semialdehyde dehydrogenase-phosphopantetheinyl transferase	-19.81
TBG2	Tubulin gamma-2 chain	-19.81
B4DDV1	Interferon-induced protein with tetratricopeptide repeats 5	-19.81
DYL2	Dynein light chain 2, cytoplasmic	-19.82
LAS1L	Isoform 2 of Ribosomal biogenesis protein LAS1L	-19.82
NOP58	Nucleolar protein 58	-19.82
RABL6	Rab-like protein 6	-19.83
MACD1	O-acetyl-ADP-ribose deacetylase MACROD1	-19.84
NUD16	U8 snoRNA-decapping enzyme	-19.84

IN35	Interferon-induced 35 kDa protein	-19.85
F5H019	GPI transamidase component PIG-S	-19.85
UBE4B	Isoform 2 of Ubiquitin conjugation factor E4 B	-19.86
NDUS2	Isoform 2 of NADH dehydrogenase [ubiquinone] iron-sulfur protein 2	-19.86
RM01	39S ribosomal protein L1, mitochondrial	-19.87
RIOK2	Isoform 2 of Serine/threonine-protein kinase RIO2	-19.89
UB2L6	Ubiquitin/ISG15-conjugating enzyme E2 L6	-19.90
TOP2A	DNA topoisomerase 2-alpha	-19.90
IKKB	Inhibitor of nuclear factor kappa-B kinase subunit beta	-19.92
A6NJ11	Ubiquitin fusion degradation protein 1 homolog	-19.94
B4DWW1	ADP-ribosylation factor-like protein 1	-19.94
QSOX2	Sulfhydryl oxidase 2	-19.94
SH24A	Isoform 2 of SH2 domain-containing protein 4A	-19.95
NU205	Nuclear pore complex protein Nup205	-19.95
CK5P3	CDK5 regulatory subunit-associated protein 3	-19.97
F6T1Q0	2,5-phosphodiesterase 12	-19.97
EXOC8	Exocyst complex component 8	-19.98
CTCF	Transcriptional repressor CTCF	-19.98
WAPL	Wings apart-like protein homolog	-20.00
G5E9Z2	Cisplatin resistance related protein CRR9p, isoform CRA	-20.02
NT5C	Isoform 2 of 5(3)-deoxyribonucleotidase, cytosolic type	-20.02
PNPT1	Polyribonucleotide nucleotidyltransferase 1, mitochondrial	-20.03
NEDD4	Isoform 4 of E3 ubiquitin-protein ligase NEDD4	-20.03
OSTF1	Osteoclast-stimulating factor 1	-20.07
CTL2	Isoform 3 of Choline transporter-like protein 2	-20.08
F5GZY7	Gamma-aminobutyric acid receptor-associated protein-like 1 (Fragment)	-20.10
B3KQZ9	Tumor necrosis factor receptor type 1-associated DEATH domain protein	-20.10
RAB31	Ras-related protein Rab-31	-20.11
VAMP4	Isoform 2 of Vesicle-associated membrane protein 4	-20.12
B7ZKK9	PPP2R5E protein	-20.13
TOR1B	Torsin-1B	-20.14

BPNT1	3(2),5-bisphosphate nucleotidase 1	-20.16
EXOC7	Isoform 2 of Exocyst complex component 7	-20.16
ADT3	ADP/ATP translocase 3	-20.16
F5H669	Cleavage and polyadenylation-specificity factor subunit 7 (Fragment)	-20.16
GAK	Cyclin-G-associated kinase	-20.17
SPAG5	Sperm-associated antigen 5	-20.17
B4DKR0	Syntaxin 5A, isoform CRA	-20.18
HBS1L	Isoform 3 of HBS1-like protein	-20.18
F5H604	CLIP-associating protein 2	-20.20
H0YMB3	GMP reductase 2	-20.20
SPAT5	Isoform 2 of Spermatogenesis-associated protein 5	-20.22
KPRA	Phosphoribosyl pyrophosphate synthase-associated protein 1	-20.23
B3KWW1	Probable ATP-dependent RNA helicase DDX58	-20.23
IPO11	Importin-11	-20.24
F8WAK8	Cohesin subunit SA-2	-20.25
TOR1A	Torsin-1A	-20.26
RAP2B	Ras-related protein Rap-2b	-20.30
CDK5	Cyclin-dependent kinase 5	-20.30
CN37	Isoform CNPI of 2,3-cyclic-nucleotide 3-phosphodiesterase	-20.31
RM14	39S ribosomal protein L14, mitochondrial	-20.31
PUS7	Pseudouridylate synthase 7 homolog	-20.33
PMVK	Phosphomevalonate kinase	-20.34
HEAT2	HEAT repeat-containing protein 2	-20.34
RAB23	Ras-related protein Rab-23	-20.37
PPIH	Peptidyl-prolyl cis-trans isomerase H	-20.37
E9PS97	Alpha-parvin (Fragment)	-20.39
BICD2	Protein bicaudal D homolog 2	-20.39
E7EUT8	Splicing factor 3A subunit 3	-20.40
CATC	Dipeptidyl peptidase 1	-20.40
ARF5	ADP-ribosylation factor 5	-20.40
NFKB2	Isoform 4 of Nuclear factor NF-kappa-B p100 subunit	-20.40

IGHG1	Ig gamma-1 chain C region	-20.41
DNJC5	DnaJ homolog subfamily C member 5	-20.41
B4DDS3	Cleft lip and palate associated transmembrane protein 1, isoform CRA	-20.42
BAZ1B	Tyrosine-protein kinase BAZ1B	-20.42
SAP	Prosaposin	-20.42
B4E329	Phosphoribosyl pyrophosphate synthase-associated protein 2	-20.44
IPO8	Importin-8	-20.45
B4E2V5	Erythrocyte band 7 integral membrane protein	-20.47
PLCD3	1-phosphatidylinositol 4,5-bisphosphate phosphodiesterase delta-3	-20.49
DDX50	ATP-dependent RNA helicase DDX50	-20.49
GNL1	Guanine nucleotide-binding protein-like 1	-20.50
KIF11	Kinesin-like protein KIF11	-20.52
DP13B	DCC-interacting protein 13-beta	-20.54
EXOC2	Exocyst complex component 2	-20.55
S4R3N1	Protein HSPE1-MOB4	-20.55
COX5A	Cytochrome c oxidase subunit 5A, mitochondrial	-20.55
C9JBB3	Tissue factor pathway inhibitor (Fragment)	-20.55
NC2B	Protein Dr1	-20.56
FAF2	FAS-associated factor 2	-20.56
J3QR44	Cyclin-dependent kinase 11B	-20.57
RB11A	Ras-related protein Rab-11A	-20.58
PRPS2	Ribose-phosphate pyrophosphokinase 2	-20.58
TIM14	Mitochondrial import inner membrane translocase subunit TIM14	-20.58
J3KSI4	Mannose-P-dolichol utilization defect 1 protein	-20.60
CX7A2	Cytochrome c oxidase subunit 7A2, mitochondrial	-20.62
CAB39	Calcium-binding protein 39	-20.63
A16A1	Aldehyde dehydrogenase family 16 member A1	-20.64
EXC6B	Exocyst complex component 6B	-20.65
TIM50	Mitochondrial import inner membrane translocase subunit TIM50	-20.66
TFIP8	Isoform 3 of Tumor necrosis factor alpha-induced protein 8	-20.66
RT34	28S ribosomal protein S34, mitochondrial	-20.67

NU107	Nuclear pore complex protein Nup107	-20.67
GNAS1	Isoform XLas-2 of Guanine nucleotide-binding protein G(s) subunit alpha	-20.69
PPGB	Lysosomal protective protein	-20.71
Q71TU5	Casein kinase 1, alpha 1, isoform CRA	-20.71
RU2B	U2 small nuclear ribonucleoprotein B	-20.72
E9PFH4	Transportin-3	-20.73
DOCK7	Isoform 4 of Dedicator of cytokinesis protein 7	-20.73
RM41	39S ribosomal protein L41, mitochondrial	-20.73
PCP	Lysosomal Pro-X carboxypeptidase	-20.74
TXTP	Tricarboxylate transport protein, mitochondrial	-20.75
RIR1	Ribonucleoside-diphosphate reductase large subunit	-20.75
IMA4	Importin subunit alpha-4	-20.76
NDUA4	NADH dehydrogenase [ubiquinone] 1 alpha subcomplex subunit 4	-20.77
S4A7	Isoform 11 of Sodium bicarbonate cotransporter 3	-20.78
HIG2A	HIG1 domain family member 2A, mitochondrial	-20.78
TBC9B	Isoform 2 of TBC1 domain family member 9B	-20.81
NDUA9	NADH dehydrogenase [ubiquinone] 1 alpha subcomplex subunit 9	-20.82
VLDLR	Isoform Short of Very low-density lipoprotein receptor	-20.82
LYPL1	Isoform 2 of Lysophospholipase-like protein 1	-20.85
RRP12	Isoform 2 of RRP12-like protein	-20.85
SMRC1	SWI/SNF complex subunit SMARCC1	-20.86
UCRI	Cytochrome b-c1 complex subunit Rieske, mitochondrial	-20.86
J3KQG4	Glucosylceramidase	-20.86
LAP2B	Lamina-associated polypeptide 2, isoforms beta/gamma	-20.86
NQO2	Ribosyldihydronicotinamide dehydrogenase [quinone]	-20.86
J3KQE0	SUN domain-containing protein 2	-20.88
TOM22	Mitochondrial import receptor subunit TOM22 homolog	-20.89
GYS1	Isoform 2 of Glycogen [starch] synthase, muscle	-20.89
CUL5	Cullin-5	-20.89
PSIP1	PC4 and SFRS1-interacting protein	-20.89
PAPS1	Bifunctional 3-phosphoadenosine 5-phosphosulfate synthase 1	-20.89

F134A	Protein FAM134A	-20.90
PLXB2	Plexin-B2	-20.91
IR3IP	Immediate early response 3-interacting protein 1	-20.91
CTBP1	Isoform 2 of C-terminal-binding protein 1	-20.93
EXOC1	Isoform 2 of Exocyst complex component 1	-20.94
OCAD2	OCIA domain-containing protein 2	-20.94
PP1R7	Protein phosphatase 1 regulatory subunit 7	-20.97
SRPR	Isoform 2 of Signal recognition particle receptor subunit alpha	-20.98
M0QX35	Paf1, RNA polymerase II associated factor, homolog (S. cerevisiae)	-20.99
ATP5H	Isoform 2 of ATP synthase subunit d, mitochondrial	-20.99
B1AJQ6	Syntaxin-12 (Fragment)	-20.99
NDUA8	NADH dehydrogenase [ubiquinone] 1 alpha subcomplex subunit 8	-21.00
LMNB2	Lamin-B2	-21.00
Q6IQ42	FUSIP1 protein	-21.03
ODP2	Dihydrolipoyllysine-residue acetyltransferase	-21.04
RBP56	Isoform Short of TATA-binding protein-associated factor 2N	-21.04
KCRS	Creatine kinase S-type, mitochondrial	-21.05
DNJA2	DnaJ homolog subfamily A member 2	-21.07
G8JLI6	Prolyl 3-hydroxylase 3	-21.09
PA1B3	Platelet-activating factor acetylhydrolase IB subunit gamma	-21.11
PABP2	Isoform 2 of Polyadenylate-binding protein 2	-21.12
ATD3A	Isoform 2 of ATPase family AAA domain-containing protein 3A	-21.13
KPCA	Protein kinase C alpha type	-21.15
ARHG7	Isoform 1 of Rho guanine nucleotide exchange factor 7	-21.15
RAB5B	Ras-related protein Rab-5B	-21.15
TOM34	Mitochondrial import receptor subunit TOM34	-21.18
1B42	HLA class I histocompatibility antigen, B-42 alpha chain	-21.18
PSB10	Proteasome subunit beta type-10	-21.20
DCUP	Uroporphyrinogen decarboxylase	-21.22
STK10	Serine/threonine-protein kinase 10	-21.23
TSR1	Pre-rRNA-processing protein TSR1 homolog	-21.24

SMC1A	Structural maintenance of chromosomes protein 1A	-21.25
TAP1	Antigen peptide transporter 1	-21.26
F2Z2V0	Copine-1 (Fragment)	-21.26
NDUB4	Isoform 2 of NADH dehydrogenase [ubiquinone] 1 beta subcomplex subunit 4	-21.26
XRN2	Isoform 2 of 5-3 exoribonuclease 2	-21.27
NDUAD	NADH dehydrogenase [ubiquinone] 1 alpha subcomplex subunit 13	-21.27
DHRS7	Isoform 2 of Dehydrogenase/reductase SDR family member 7	-21.27
SCPDL	Saccharopine dehydrogenase-like oxidoreductase	-21.28
E9PIE4	Mitochondrial carrier homolog 2 (Fragment)	-21.33
F8WJN3	Cleavage and polyadenylation-specificity factor subunit 6	-21.35
TM14C	Transmembrane protein 14C	-21.35
SNX24	Isoform 2 of Sorting nexin-24	-21.35
UBP15	Isoform 2 of Ubiquitin carboxyl-terminal hydrolase 15	-21.38
FGF1	Fibroblast growth factor 1	-21.40
GTR1	Solute carrier family 2, facilitated glucose transporter member 1	-21.41
SPB4	Serpin B4	-21.41
EXOC3	Isoform 2 of Exocyst complex component 3	-21.41
RHG18	Isoform 2 of Rho GTPase-activating protein 18	-21.42
GGH	Gamma-glutamyl hydrolase	-21.43
A2MG	Alpha-2-macroglobulin	-21.46
STML2	Stomatin-like protein 2, mitochondrial	-21.48
CIP4	Cdc42-interacting protein 4	-21.48
J3QQY2	Transmembrane and coiled-coil domain-containing protein 1	-21.48
PRP8	Pre-mRNA-processing-splicing factor 8	-21.49
CAV2	Isoform Beta of Caveolin-2	-21.50
SEC63	Translocation protein SEC63 homolog	-21.51
SYPL1	Isoform 2 of Synaptophysin-like protein 1	-21.52
RAVR1	Isoform 2 of Ribonucleoprotein PTB-binding 1	-21.53
CATZ	Cathepsin Z	-21.53
COX20	Cytochrome c oxidase protein 20 homolog	-21.54
NDUBA	NADH dehydrogenase [ubiquinone] 1 beta subcomplex subunit 10	-21.55

SPB12	Serpin B12	-21.55
SDCB1	Syntenin-1	-21.55
B1ANR0	Poly(A) binding protein, cytoplasmic 4 (Inducible form), isoform CRA	-21.57
HDHD1	Pseudouridine-5-monophosphatase	-21.63
SNP23	Synaptosomal-associated protein 23	-21.67
M0R0W6	Tyrosine-protein kinase receptor UFO	-21.68
A8MXQ1	Pituitary tumor-transforming gene 1 protein-interacting protein	-21.69
MSH2	DNA mismatch repair protein Msh2	-21.69
COPG2	Coatomer subunit gamma-2	-21.74
RAB3B	Ras-related protein Rab-3B	-21.75
Q5T760	Serine/arginine-rich-splicing factor 11 (Fragment)	-21.76
SAR1B	GTP-binding protein SAR1b	-21.76
VDAC3	Voltage-dependent anion-selective channel protein 3	-21.79
QCR2	Cytochrome b-c1 complex subunit 2, mitochondrial	-21.80
EPN1	Isoform 3 of Epsin-1	-21.85
2A5D	Isoform Delta-3 of Serine/threonine-protein phosphatase 2A	-21.86
GPDM	Isoform 2 of Glycerol-3-phosphate dehydrogenase, mitochondrial	-21.91
C9JAW5	HIG1 domain family member 1A, mitochondrial	-21.91
DYLT1	Dynein light chain Tctex-type 1	-21.91
D3DR31	Interferon-induced protein with tetratricopeptide repeats 1	-21.91
H7C1U8	Apolipoprotein O (Fragment)	-21.93
SCMC1	Calcium-binding mitochondrial carrier protein SCaMC-1	-21.94
NASP	Nuclear autoantigenic sperm protein	-21.94
M2OM	Mitochondrial 2-oxoglutarate/malate carrier protein	-21.94
MOT4	Monocarboxylate transporter 4	-21.98
U3KQ30	Secretory carrier-associated membrane protein 1	-21.99
STING	Stimulator of interferon genes protein	-22.02
PP4R1	Isoform 2 of Serine/threonine-protein phosphatase 4 regulatory subunit 1	-22.05
SYJ2B	Synaptojanin-2-binding protein	-22.08
I3L4X2	Multidrug resistance-associated protein 1 (Fragment)	-22.14
GNA11	Guanine nucleotide-binding protein subunit alpha-11	-22.21

SATT	Neutral amino acid transporter A	-22.22
UFL1	Isoform 2 of E3 UFM1-protein ligase 1	-22.28
HCDH	Hydroxyacyl-coenzyme A dehydrogenase, mitochondrial OS	-22.37
NCBP1	Nuclear cap-binding protein subunit 1	-22.37
LTOR1	Ragulator complex protein LAMTOR1	-22.39
SCRIB	Protein scribble homolog	-22.43
CTNB1	Catenin beta-1	-22.45
MCM7	DNA replication licensing factor MCM7	-22.47
SFXN1	Sideroflexin-1	-22.49
CND3	Condensin complex subunit 3	-22.49
MCM4	DNA replication licensing factor MCM4	-22.53
ISG15	Ubiquitin-like protein ISG15	-22.55
TOM70	Mitochondrial import receptor subunit TOM70	-22.56
WASF2	Wiskott-Aldrich syndrome protein family member 2	-22.57
MGST3	Microsomal glutathione S-transferase 3	-22.58
CTNA2	Isoform 3 of Catenin alpha-2	-22.61
J3QRU4	Vesicle-associated membrane protein 2	-22.62
ASNS	Isoform 2 of Asparagine synthetase [glutamine-hydrolyzing]	-22.62
MCM3	DNA replication licensing factor MCM3	-22.66
ATP5I	ATP synthase subunit e, mitochondrial	-22.71
TRIPC	Isoform 2 of E3 ubiquitin-protein ligase TRIP12	-22.71
ANK1	Isoform Er9 of Ankyrin-1	-22.71
PLAK	Junction plakoglobin	-22.72
K1468	Isoform 2 of LisH domain and HEAT repeat-containing protein KIAA1468	-22.73
NDUS3	NADH dehydrogenase [ubiquinone] iron-sulfur protein 3, mitochondrial	-22.82
SLN11	Schlafen family member 11	-22.87
SPSY	Spermine synthase	-22.95
CND1	Condensin complex subunit 1	-22.96
Q5URX0	Beta-hexosaminidase subunit beta	-23.06
CY1	Cytochrome c1, heme protein, mitochondrial	-23.07
C1TM	Monofunctional C1-tetrahydrofolate synthase, mitochondrial	-23.09

C9JYQ9	60S ribosomal protein L22-like 1	-23.18
ATPK	Isoform 3 of ATP synthase subunit f, mitochondrial	-23.21
LAP2	Isoform 7 of Protein LAP2	-23.31
SMC2	Structural maintenance of chromosomes protein 2	-23.38
MCM2	DNA replication licensing factor MCM2	-23.45
LMNB1	Lamin-B1	-23.48
A8MWK3	Cadherin-2	-23.48
PELP1	Proline-, glutamic acid- and leucine-rich protein 1	-23.52
SCRB2	Lysosome membrane protein 2	-23.70
ITA6	Isoform Alpha-6X2A of Integrin alpha-6	-23.73
AL1A3	Aldehyde dehydrogenase family 1 member A3	-23.75
LETM1	LETM1 and EF-hand domain-containing protein 1, mitochondrial	-23.76
E9PN17	ATP synthase subunit g, mitochondrial	-23.77
IMMT	Isoform 2 of Mitochondrial inner membrane protein	-23.84
COX41	Cytochrome c oxidase subunit 4 isoform 1, mitochondrial	-24.00
COX2	Cytochrome c oxidase subunit 2	-24.06
MX1	Interferon-induced GTP-binding protein Mx1	-24.11
F8W7Q4	Protein FAM162A	-24.18
AAAT	Neutral amino acid transporter B(0)	-24.20
CSPG4	Chondroitin sulfate proteoglycan 4	-24.21
ADT2	ADP/ATP translocase 2	-24.68
ATPO	ATP synthase subunit O, mitochondrial	-24.71
HBA	Hemoglobin subunit alpha	-24.71
J3KPX7	Prohibitin-2	-24.95
ECE1	Isoform D of Endothelin-converting enzyme 1	-25.19
ANXA8	Annexin A8	-25.27
PHB	Prohibitin	-26.02

Supplementary Table S5: Phosphoproteins significantly up/ downregulated in Ben-Men-1 cells compared to HMC

Gene symbol	Protein name	Log2 FC
ANXA8	Annexin A8;Annexin A8-like protein 1;Annexin A8-like protein 2;Annexin	22.50
FAM192A	Protein FAM192A	22.46
DDA1	DET1- and DDB1-associated protein 1	22.38
C10orf47	Uncharacterized protein C10orf47	21.89
HNRNPR	Heterogeneous nuclear ribonucleoprotein R	21.85
NPM3	Nucleoplasmin-3	21.81
SCP2	Non-specific lipid-transfer protein	21.61
TERT	Telomerase reverse transcriptase	21.46
C12orf43	Uncharacterized protein C12orf43	21.33
MAT2A	S-adenosylmethionine synthase isoform type-2;S-adenosylmethionine synthase	21.25
CNPY2	Protein canopy homolog 2	21.24
RAB11FIP1	Rab11 family-interacting protein 1	21.17
STAU2	Double-stranded RNA-binding protein Staufen homolog 2	21.10
GBE1	1,4-alpha-glucan-branching enzyme	21.08
ZFP36L1	Zinc finger protein 36, C3H1 type-like 1	21.08
RPS21	40S ribosomal protein S21	21.05
DEPTOR	DEP domain-containing mTOR-interacting protein	21.02
UHRF2	E3 ubiquitin-protein ligase UHRF2	20.93
CBR3	Carbonyl reductase [NADPH] 3	20.88
IWS1	Protein IWS1 homolog	20.85
CDCA5	Sororin	20.82
AMPH	Amphiphysin	20.79
KIAA1598	Shootin-1	20.76
CACYBP	Calcyclin-binding protein	20.70
ALPK2	Alpha-protein kinase 2	20.68
ARFGEF3	Brefeldin A-inhibited guanine nucleotide-exchange protein 3	20.62
ITPA	Inosine triphosphate pyrophosphatase	20.61
IVNS1ABP	Influenza virus NS1A-binding protein	20.53
JMY	Junction-mediating and -regulatory protein	20.39

TAGLN2	Transgelin-2	20.29
NSUN5	Putative methyltransferase NSUN5	20.27
TRAPPC1	Trafficking protein particle complex subunit 1	20.16
DTX3L	E3 ubiquitin-protein ligase DTX3L	20.08
SCAF11	Protein SCAF11	20.05
RPL32	60S ribosomal protein L32	19.99
S100A10	Protein S100-A10	19.88
APOBEC3C	Probable DNA dC->dU-editing enzyme APOBEC-3C	19.86
KLHDC4	Kelch domain-containing protein 4	19.85
MRPS14	28S ribosomal protein S14, mitochondrial	19.84
C16orf88	Protein C16orf88	19.84
MRPL1	39S ribosomal protein L1, mitochondrial	19.82
MBD2	Methyl-CpG-binding domain protein 2	19.79
NOM1	Nucleolar MIF4G domain-containing protein 1	19.79
CRNKL1	Crooked neck-like protein 1	19.64
SYNRG	Synergin gamma	19.57
CLPTM1L	Cleft lip and palate transmembrane protein 1-like protein	19.55
NPHP3	Nephrocystin-3	19.44
RGS10	Regulator of G-protein signaling 10	19.40
NCOR2	Nuclear receptor corepressor 2	19.34
RBM34	RNA-binding protein 34	19.29
ARID1A	AT-rich interactive domain-containing protein 1A	19.25
CWC27	Peptidyl-prolyl cis-trans isomerase CWC27 homolog	19.14
HIST1H1C	Histone H1.2	6.72
KRT18	Keratin, type I cytoskeletal 18	5.30
ANK1	Ankyrin-1	4.84
DDB2	DNA damage-binding protein 2	4.75
STAT1	Signal transducer and activator of transcription 1-alpha/beta	4.58
EZR	Ezrin	4.52
LIMCH1	LIM and calponin homology domains-containing protein 1	4.46
PSMB9	Proteasome subunit beta type-9;Proteasome subunit beta type	4.28

CRYAB	Alpha-crystallin B chain	4.23
PDLIM2	PDZ and LIM domain protein 2	3.95
CDK1	Cyclin-dependent kinase 1	3.87
SLC9A3R1	Na(+)/H(+) exchange regulatory cofactor NHE-RF1	3.76
ZNF185	Zinc finger protein 185	3.72
DNAJC6	Putative tyrosine-protein phosphatase auxilin	3.70
TCEAL5	Transcription elongation factor A protein-like 5;Transcription elongation factor A protein-like 3	3.56
SYAP1	Synapse-associated protein 1	3.52
FOXC2	Forkhead box protein C2	3.47
EPS8L2	Epidermal growth factor receptor kinase substrate 8-like protein 2	3.37
DPYSL3	Dihydropyrimidinase-related protein 3	3.22
PDE1C	Calcium/calmodulin-dependent 3,5-cyclic nucleotide phosphodiesterase 1C	3.16
MLTK	Mitogen-activated protein kinase kinase kinase MLT	3.14
LYSMD2	LysM and putative peptidoglycan-binding domain-containing protein 2	3.11
SAMHD1	SAM domain and HD domain-containing protein 1	3.04
ANXA3	Annexin A3;Annexin	3.03
ARSB	Arylsulfatase B	3.01
LMNA	Prelamin-A/C;Lamin-A/C	2.99
CDK2	Cyclin-dependent kinase 2	2.95
MOSPD2	Motile sperm domain-containing protein 2	2.92
DCK	Deoxycytidine kinase	2.90
DDX24	ATP-dependent RNA helicase DDX24	2.87
NCEH1	Neutral cholesterol ester hydrolase 1	2.80
TNS3	Tensin-3	2.80
TOP2A	DNA topoisomerase 2-alpha	2.75
DYNLL1	Dynein light chain 1, cytoplasmic	2.75
CSDE1	Cold shock domain-containing protein E1	2.74
MRE11A	Double-strand break repair protein MRE11A	2.71
FAM169A	Protein FAM169A	2.70
RPS27	40S ribosomal protein S27	2.65
CAP2	Adenylyl cyclase-associated protein 2;Adenylyl cyclase-associated protein	2.63

SUPT16H	FACT complex subunit SPT16	2.61
CORO1C	Coronin-1C	2.60
PPM1H	Protein phosphatase 1H	2.58
EHBP1L1	EH domain-binding protein 1-like protein 1	2.57
API5	Apoptosis inhibitor 5	2.49
IQGAP3	Ras GTPase-activating-like protein IQGAP3	2.46
HMGB2	High mobility group protein B2	2.45
FTSJD2	Cap-specific mRNA (nucleoside-2-O-)-methyltransferase 1	2.41
RECQL	ATP-dependent DNA helicase Q1	2.41
RPL24	60S ribosomal protein L24	2.33
PTPN14	Tyrosine-protein phosphatase non-receptor type 14	2.30
DOPEY2	Protein dopey-2	2.30
C3orf26	Uncharacterized protein C3orf26	2.27
HCA90	Targeting protein for Xklp2	2.23
FNBP1	Formin-binding protein 1	2.20
PSIP1	PC4 and SFRS1-interacting protein	2.17
PSME2	Proteasome activator complex subunit 2	2.16
CTSC	Dipeptidyl peptidase 1;Dipeptidyl peptidase 1 exclusion domain chain	2.15
DEK	Protein DEK	2.14
DHX29	ATP-dependent RNA helicase DHX29	2.13
SPIN1	Spindlin-1	2.12
RPL31	60S ribosomal protein L31	2.12
HIST1H2BJ	Histone H2B type 1-J;Histone H2B type 2-E	2.09
CPQ	Carboxypeptidase Q	2.08
DDX5	Probable ATP-dependent RNA helicase DDX5	2.05
MICAL2	Protein-methionine sulfoxide oxidase MICAL2	2.04
UCK2	Uridine-cytidine kinase 2	2.03
FMR1	Fragile X mental retardation protein 1	2.03
DRAP1	Dr1-associated corepressor	2.01
MYOF	Myoferlin	2.01
RPS14	40S ribosomal protein S14	2.00

CALM2	Calmodulin	1.98
EIF1AX	Eukaryotic translation initiation factor 1A, X-chromosomal	1.97
PSMB10	Proteasome subunit beta type-10	1.94
PUS7	Pseudouridylate synthase 7 homolog	1.90
DHX9	ATP-dependent RNA helicase A	1.90
FRMD6	FERM domain-containing protein 6	1.87
CTSD	Cathepsin D;Cathepsin D light chain;Cathepsin D heavy chain	1.85
HIST1H2BK	Histone H2B type 1-K	1.84
PSME3	Proteasome activator complex subunit 3	1.83
EPHA2	Ephrin type-A receptor 2	1.80
NONO	Non-POU domain-containing octamer-binding protein	1.79
DDX50	ATP-dependent RNA helicase DDX50	1.78
FNIP1	Rap guanine nucleotide exchange factor 6	1.77
DDB1	DNA damage-binding protein 1	1.76
AHNAK2	Protein AHNAK2	1.76
FKBP4	Peptidyl-prolyl cis-trans isomerase FKBP4;Peptidyl-prolyl cis-trans isomerase FKBP4	1.76
SSRP1	FACT complex subunit SSRP1	1.75
EGFR	Epidermal growth factor receptor	1.75
SMAD3	Mothers against decapentaplegic homolog 3	1.74
SRSF2	Serine/arginine-rich splicing factor 2	1.73
CSE1L	Exportin-2	1.71
P4HA2	Prolyl 4-hydroxylase subunit alpha-2	1.69
DNAJC17	DnaJ homolog subfamily C member 17	1.68
RNPEP	Aminopeptidase B	1.68
NOB1	RNA-binding protein NOB1	1.68
C17orf49	Chromatin complexes subunit BAP18	1.68
HNRNPM	Heterogeneous nuclear ribonucleoprotein M	1.67
SNRPD3	Small nuclear ribonucleoprotein Sm D3	1.66
ANAPC7	Anaphase-promoting complex subunit 7	1.65
UNC45A	Protein unc-45 homolog A	1.63
ERCC6	DNA excision repair protein ERCC-6	1.62

RFC5	Replication factor C subunit 5	1.61
AFAP1	Actin filament-associated protein 1	1.60
MECP2	Methyl-CpG-binding protein 2	1.60
PPA2	Inorganic pyrophosphatase 2, mitochondrial	1.60
CTSA	Lysosomal protective protein	1.59
CALU	Isoform 4 of Calumenin	1.58
PSME1	Proteasome activator complex subunit 1	1.57
SRSF7	Serine/arginine-rich splicing factor 7	1.56
BAZ1B	Tyrosine-protein kinase BAZ1B	1.56
RPL19	60S ribosomal protein L19	1.55
PFDN2	Prefoldin subunit 2	1.54
DIAPH1	Protein diaphanous homolog 1	1.54
TALDO1	Transaldolase	1.53
PRKDC	DNA-dependent protein kinase catalytic subunit	1.53
RPL28	60S ribosomal protein L28	1.52
TJP2	Tight junction protein ZO-2	1.50
PLCD1	1-phosphatidylinositol 4,5-bisphosphate phosphodiesterase delta-1	1.50
HSPB1	Heat shock protein beta-1	1.50
HIST1H2AG	Histone H2A type 1	1.49
SPTLC2	Serine palmitoyltransferase 2	1.48
NSFL1C	NSFL1 cofactor p47	1.48
CBX3	Chromobox protein homolog 3	1.48
DDX46	Probable ATP-dependent RNA helicase DDX46	1.47
DHX15	Putative pre-mRNA-splicing factor ATP-dependent RNA helicase DHX15	1.47
SLC9A3R2	Na(+)/H(+) exchange regulatory cofactor NHE-RF2	1.45
PCBP1	Poly(rC)-binding protein 1	1.44
CUTA	Protein CutA	1.44
NMNAT1	Nicotinamide mononucleotide adenylyltransferase 1	1.44
MYH3	myosin, heavy chain 3	1.41
PSMB8	Proteasome subunit beta type-8	1.40
RAD50	DNA repair protein RAD50	1.40

TMPO	Lamina-associated polypeptide 2, isoforms beta/gamma;Thymopoietin;Thymopentin	1.40
HSPA8	Heat shock cognate 71 kDa protein	1.40
DOCK5	Dedicator of cytokinesis protein 5	1.39
MAGOHB	Protein mago nashi homolog 2	1.39
C7orf50	Uncharacterized protein C7orf50	1.39
HIST1H4A	Histone H4	1.38
RFC4	Replication factor C subunit 4	1.38
RNH1	Ribonuclease inhibitor	1.35
ANKHD1	Ankyrin repeat and KH domain-containing protein 1	1.35
WDR70	WD repeat-containing protein 70	1.34
RPRD1B	Regulation of nuclear pre-mRNA domain-containing protein 1B	1.34
LNPEP	Leucyl-cystinyl aminopeptidase;Leucyl-cystinyl aminopeptidase, pregnancy serum form	1.32
PPP1R13L	RelA-associated inhibitor	1.31
LDHA	L-lactate dehydrogenase A chain	1.30
MSH6	DNA mismatch repair protein Msh6	1.30
MYL6	myosin, light chain 6	1.28
RBM39	RNA-binding protein 39	1.26
EIF2AK2	Interferon-induced, double-stranded RNA-activated protein kinase	1.26
HSPA4	Heat shock 70 kDa protein 4	1.25
C7orf55	Isoform 2 of UPF0562	1.23
HP1BP3	Heterochromatin protein 1-binding protein 3	1.23
SMC4	Structural maintenance of chromosomes protein 4;Structural maintenance of chromosomes protein	1.23
CTPS	CTP synthase 1	1.23
FLNB	Filamin-B	1.23
HSPA1A	Heat shock 70 kDa protein 1A/1B	1.21
ACTN4	Alpha-actinin-4	1.21
SKP1	S-phase kinase-associated protein 1	1.21
TBC1D9B	TBC1 domain family member 9B	1.20
LRRFIP2	Leucine-rich repeat flightless-interacting protein 2	1.20
DHX16	Putative pre-mRNA-splicing factor ATP-dependent RNA helicase DHX16	1.19
MYO1C	Unconventional myosin-Ic	1.18

MYLK	Myosin light chain kinase, smooth muscle;Myosin light chain kinase, smooth muscle, deglutamylated form	1.18
DNAJA1	DnaJ homolog subfamily A member 1	1.18
SUPT6H	Transcription elongation factor SPT6	1.17
BAIAP2	Brain-specific angiogenesis inhibitor 1-associated protein 2	1.17
THBS1	Thrombospondin-1	1.17
HEXA	Beta-hexosaminidase subunit alpha	1.14
NOL9	Polynucleotide 5-hydroxyl-kinase NOL9	1.14
PPM1G	Protein phosphatase 1G	1.10
SRP68	Signal recognition particle 68 kDa protein	1.10
RPS6KA4	Ribosomal protein S6 kinase alpha-4;Ribosomal protein S6 kinase	1.08
TMEM189	Ubiquitin-conjugating enzyme E2 variant 1;Ubiquitin-conjugating enzyme E2 variant 2	1.08
WAPAL	Wings apart-like protein homolog	1.08
STIP1	Stress-induced-phosphoprotein 1	1.07
PABPN1	Polyadenylate-binding protein 2	1.07
GEMIN5	Gem-associated protein 5	1.07
PABPC1	Polyadenylate-binding protein 1;Polyadenylate-binding protein 4;Polyadenylate-binding protein 3	1.07
DDX10	Probable ATP-dependent RNA helicase DDX10	1.07
TNPO1	Transportin-1	1.06
DNAJA2	DnaJ homolog subfamily A member 2	1.06
PUF60	Poly(U)-binding-splicing factor PUF60	1.02
TCEB2	Transcription elongation factor B polypeptide 2	1.02
ZNF326	DBIRD complex subunit ZNF326	1.01
ARHGAP35	Rho GTPase-activating protein 35	1.01
YWHAE	14-3-3 protein epsilon	1.01
DHX38	Pre-mRNA-splicing factor ATP-dependent RNA helicase PRP16	1.01
CBX1	Chromobox protein homolog 1	1.01
SNX2	Sorting nexin-2	1.01
SRP72	Signal recognition particle 72 kDa protein	1.00
TMOD3	Tropomodulin-3	1.00
CKAP5	Cytoskeleton-associated protein 5	0.99
ENO1	Alpha-enolase	0.98

ANP32A	Acidic leucine-rich nuclear phosphoprotein 32 family member A	0.98
DSP	Desmoplakin	0.97
CAPN2	Calpain-2 catalytic subunit	0.97
FAM160B1	Protein FAM160B1	0.96
NRD1	Nardilysin	0.94
DDX3X	ATP-dependent RNA helicase DDX3X	0.94
PPP2R1A	Serine/threonine-protein phosphatase 2A 65 kDa regulatory subunit A alpha isoform	0.93
ARHGAP18	Rho GTPase-activating protein 18	0.93
RP11-114F7.3	Dynamin-binding protein	0.92
GAPDH	Glyceraldehyde-3-phosphate dehydrogenase	0.92
RPS18	40S ribosomal protein S18	0.91
RBBP4	Histone-binding protein RBBP4	0.91
KDM5C	Lysine-specific demethylase 5C;Lysine-specific demethylase 5D	0.91
XRN1	5-3 exoribonuclease 1	0.91
RPS3A	40S ribosomal protein S3a	0.90
PTPN11	Tyrosine-protein phosphatase non-receptor type 11	0.89
ARAP1	Arf-GAP with Rho-GAP domain, ANK repeat and PH domain-containing protein 1	0.89
HSP90AA1	Heat shock protein HSP 90-alpha	0.88
IMPDH2	Inosine-5-monophosphate dehydrogenase 2	0.87
GTF2E1	General transcription factor IIE subunit 1	0.86
EXOSC10	Exosome component 10	0.86
GSPT1	Eukaryotic peptide chain release factor GTP-binding subunit ERF3A	0.86
YTHDC2	Probable ATP-dependent RNA helicase YTHDC2	0.85
USP9X	Probable ubiquitin carboxyl-terminal hydrolase FAF-X	0.85
FAM50A	Protein FAM50A	0.84
C9orf142	Uncharacterized protein C9orf142	0.84
ZC3H11A	Zinc finger CCCH domain-containing protein 11A	0.83
SPIRE1	Protein spire homolog 1	0.83
PFKP	6-phosphofructokinase type C	0.81
HECTD1	E3 ubiquitin-protein ligase HECTD1	0.81
TNPO3	Transportin-3	0.79

WHSC2	Negative elongation factor A	0.78
STRAP	Serine-threonine kinase receptor-associated protein	0.78
SRSF1	Serine/arginine-rich splicing factor 1	0.77
OXCT1	Succinyl-CoA:3-ketoacid-coenzyme A transferase 1, mitochondrial	0.77
FAM120A	Constitutive coactivator of PPAR-gamma-like protein 1	0.76
TXLNA	Alpha-taxilin	0.76
DDX41	Probable ATP-dependent RNA helicase DDX41	0.76
CROCC	Rootletin	0.72
HNRNPA1	Heterogeneous nuclear ribonucleoprotein A1;Heterogeneous nuclear ribonucleoprotein A1-like 2	0.72
CDK7	Cyclin-dependent kinase 7	0.70
ARFGAP2	ADP-ribosylation factor GTPase-activating protein 2	0.70
PSMD2	26S proteasome non-ATPase regulatory subunit 2	0.70
MLLT4	Afadin	0.69
TTLL5	Tubulin polyglutamylase TTLL5	0.67
RIC8A	Synembryn-A	0.67
CLINT1	Clathrin interactor 1	0.66
CAST	Calpastatin	0.66
LARP1	La-related protein 1	0.65
RNF213	E3 ubiquitin-protein ligase RNF213	0.64
IMP3	U3 small nucleolar ribonucleoprotein protein IMP3	0.64
YWHAZ	14-3-3 protein zeta/delta	0.61
UBL4A	Ubiquitin-like protein 4A	0.60
ALKBH5	Probable alpha-ketoglutarate-dependent dioxygenase ABH5	0.60
BAG6	Large proline-rich protein BAG6	0.57
SNRNP70	U1 small nuclear ribonucleoprotein 70 kDa	0.57
DDX23	Probable ATP-dependent RNA helicase DDX23	0.57
EIF4G2	Eukaryotic translation initiation factor 4 gamma 2	0.54
SPTLC1	Serine palmitoyltransferase 1	0.53
TBCD	Tubulin-specific chaperone D	0.53
SNTB2	Beta-2-syntrophin	0.51
HNRNPUL2	Heterogeneous nuclear ribonucleoprotein U-like protein 2	0.51

PKM2	Pyruvate kinase isozymes M1/M2;Pyruvate kinase	0.49
CTIF	CBP80/20-dependent translation initiation factor	0.44
CPSF7	Cleavage and polyadenylation specificity factor subunit 7	0.44
HUWE1	E3 ubiquitin-protein ligase HUWE1	0.43
PPIL4	Peptidyl-prolyl cis-trans isomerase-like 4	0.42
TECR	Trans-2,3-enoyl-CoA reductase	0.41
SP100	Nuclear autoantigen Sp-100	0.41
NAA15	N-alpha-acetyltransferase 15, NatA auxiliary subunit	0.34
UTP18	U3 small nucleolar RNA-associated protein 18 homolog	-0.22
FAM40A	Protein FAM40A	-0.39
KHNYN	Protein KHNYN	-0.42
VCL	Vinculin	-0.45
EXOC4	Exocyst complex component 4	-0.50
ACACA	Acetyl-CoA carboxylase 1;Biotin carboxylase	-0.51
TUBGCP2	Gamma-tubulin complex component 2	-0.52
PDIA4	Protein disulfide-isomerase A4	-0.52
PPP4R1	Serine/threonine-protein phosphatase 4 regulatory subunit 1	-0.58
HSP90B1	Endoplasmin	-0.58
PARVA	Alpha-parvin	-0.58
PUS1	tRNA pseudouridine synthase A, mitochondrial;Pseudouridine synthase	-0.61
CDC42EP1	Cdc42 effector protein 1	-0.64
SUGP2	SURP and G-patch domain-containing protein 2	-0.65
AP2A2	AP-2 complex subunit alpha-2	-0.66
PRRC1	Protein PRRC1	-0.66
DIP2B	Disco-interacting protein 2 homolog B	-0.67
PSMB1	Proteasome subunit beta type-1	-0.67
NOP56	Nucleolar protein 56	-0.68
VIM	Vimentin	-0.69
AP3S1	AP-3 complex subunit sigma-1	-0.69
SETD7	Histone-lysine N-methyltransferase SETD7	-0.72
PPFIBP1	Liprin-beta-1	-0.72

PPP1R12A	Protein phosphatase 1 regulatory subunit 12A	-0.75
STRN3	Striatin-3	-0.76
USP11	Ubiquitin carboxyl-terminal hydrolase 11;Ubiquitin carboxyl-terminal hydrolase	-0.79
SRPK2	SRSF protein kinase 2;SRSF protein kinase 2 N-terminal;SRSF protein kinase 2 C-terminal	-0.80
UBE2Z	Ubiquitin-conjugating enzyme E2 Z	-0.81
MAP4	Microtubule-associated protein	-0.83
DNAJC1	DnaJ homolog subfamily C member 1	-0.83
DDRGK1	DDRGK domain-containing protein 1	-0.85
SCYL1	N-terminal kinase-like protein	-0.86
PCYT1A	Choline-phosphate cytidylyltransferase A	-0.88
UBE3C	Ubiquitin-protein ligase E3C	-0.88
PKN1	Serine/threonine-protein kinase N1	-0.89
C16orf62	UPF0505 protein C16orf62	-0.90
ATG7	Ubiquitin-like modifier-activating enzyme ATG7	-0.92
NCK2	Cytoplasmic protein NCK2	-0.92
LIMS1	LIM and senescent cell antigen-like-containing domain protein 1	-0.94
PSMB5	Proteasome subunit beta type-5	-0.94
PIK3R4	Phosphoinositide 3-kinase regulatory subunit 4	-0.95
PI4KB	Phosphatidylinositol 4-kinase beta	-0.95
FAM129B	Niban-like protein 1	-0.95
ARHGAP10	Rho GTPase-activating protein 10	-0.95
OTUD7B	OTU domain-containing protein 7B	-0.95
ANXA11	Annexin A11;Annexin	-0.97
NUMBL	Numb-like protein	-0.97
Uncharacterised	Uncharacterized protein FLJ45252	-0.98
ITGB1	Integrin beta-1	-0.98
PSMA2	Proteasome subunit alpha type-2	-0.99
DCAF7	DDB1- and CUL4-associated factor 7	-1.00
RLTPR	Leucine-rich repeat-containing protein 16C	-1.01
USO1	General vesicular transport factor p115	-1.01
MAGED2	Melanoma-associated antigen D2	-1.02

NEDD4	E3 ubiquitin-protein ligase NEDD4;E3 ubiquitin-protein ligase	-1.02
MRPS9	28S ribosomal protein S9, mitochondrial	-1.03
ARHGEF40	Rho guanine nucleotide exchange factor 40	-1.03
PIP	Prolactin-inducible protein	-1.04
NAV1	Neuron navigator 1	-1.05
PRKACB	cAMP-dependent protein kinase catalytic subunit beta	-1.05
CSNK1D	Casein kinase I isoform delta	-1.05
PSMB2	Proteasome subunit beta type-2	-1.05
DRG1	Developmentally-regulated GTP-binding protein 1	-1.06
POLR1C	DNA-directed RNA polymerases I and III subunit RPAC1	-1.06
ARHGAP12	Rho GTPase-activating protein 12	-1.06
TOR1AIP1	Torsin-1A-interacting protein 1	-1.07
KIAA1432	Protein RIC1 homolog	-1.08
LUZP1	Leucine zipper protein 1	-1.10
UBE4B	Ubiquitin conjugation factor E4 B	-1.10
GPN1	GPN-loop GTPase 1	-1.11
PXN	Paxillin	-1.11
HELZ	Probable helicase with zinc finger domain	-1.12
CDK17	Cyclin-dependent kinase 17	-1.13
UFL1	E3 UFM1-protein ligase 1	-1.14
LIN7C	Protein lin-7 homolog C	-1.14
SRPRB	Signal recognition particle receptor subunit beta	-1.15
BZW2	Basic leucine zipper and W2 domain-containing protein 2	-1.16
TAB1	TGF-beta-activated kinase 1 and MAP3K7-binding protein 1	-1.16
SNX18	Sorting nexin-18	-1.16
PACS1	Phosphofurin acidic cluster sorting protein 1	-1.16
RRBP1	Ribosome-binding protein 1	-1.16
ASCC2	Activating signal cointegrator 1 complex subunit 2	-1.16
PSMB7	Proteasome subunit beta type-7	-1.18
DRG2	Developmentally-regulated GTP-binding protein 2	-1.18
RPN1	Dolichyl-diphosphooligosaccharide--protein glycosyltransferase subunit 1	-1.19

IKBIP	Inhibitor of nuclear factor kappa-B kinase-interacting protein	-1.19
ACTR10	Actin-related protein 10	-1.19
COL1A1	Collagen alpha-1(I) chain	-1.20
CENPV	Isoform 3 of Centromere protein V	-1.20
BSG	Basigin	-1.21
ABL1	Tyrosine-protein kinase ABL1	-1.21
TTC37	Tetratricopeptide repeat protein 37	-1.23
PDLIM5	PDZ and LIM domain protein 5	-1.24
LEPREL4	Synaptonemal complex protein SC65	-1.24
HS1BP3	HCLS1-binding protein 3	-1.25
HMGCL	Hydroxymethylglutaryl-CoA lyase, mitochondrial	-1.25
ASAP1	Arf-GAP with SH3 domain, ANK repeat and PH domain-containing protein 1	-1.26
PTPN12	Tyrosine-protein phosphatase non-receptor type 12	-1.26
SRPR	Signal recognition particle receptor subunit alpha	-1.27
OPTN	Optineurin	-1.27
COPS4	COP9 signalosome complex subunit 4	-1.27
CTNND1	Catenin delta-1	-1.27
RTN1	Reticulon-1	-1.28
ST13	Hsc70-interacting protein;Putative protein FAM10A5;Putative protein FAM10A4	-1.30
RTN4	Reticulon-4	-1.31
PPP2R5B	Serine/threonine-protein phosphatase 2A 56 kDa regulatory subunit beta isoform	-1.32
COMT	Catechol O-methyltransferase	-1.33
NXN	Nucleoredoxin	-1.34
PLCB1	1-phosphatidylinositol 4,5-bisphosphate phosphodiesterase beta-1	-1.34
ATG4B	Cysteine protease ATG4B	-1.35
SYNJ2	Synaptojanin-2	-1.35
NCOA7	Nuclear receptor coactivator 7	-1.37
S E P 9	Septin-9	-1.38
LEPRE1	Prolyl 3-hydroxylase 1	-1.39
SKIV2L	Helicase SKI2W	-1.40
DMD	Dystrophin	-1.42

RND3	Rho-related GTP-binding protein RhoE	-1.42
ASCC3	Activating signal cointegrator 1 complex subunit 3	-1.43
MYO5A	Unconventional myosin-Va	-1.44
RCAN1	Calcipressin-1	-1.46
NEXN	Nexilin	-1.47
STK39	STE20/SPS1-related proline-alanine-rich protein kinase	-1.47
SIRT2	NAD-dependent protein deacetylase sirtuin-2	-1.48
TRIM3	Tripartite motif-containing protein 3	-1.48
USP35	Ubiquitin carboxyl-terminal hydrolase 35	-1.50
GTPBP1	GTP-binding protein 1	-1.51
BCKDK	[3-methyl-2-oxobutanoate dehydrogenase [lipoamide]] kinase, mitochondrial	-1.52
EHBP1	EH domain-binding protein 1	-1.52
GIPC1	PDZ domain-containing protein GIPC1	-1.52
LEPREL2	Prolyl 3-hydroxylase 3	-1.52
VPS41	Vacuolar protein sorting-associated protein 41 homolog	-1.53
S E P 2	Septin-2	-1.56
ZZEF1	Zinc finger ZZ-type and EF-hand domain-containing protein 1	-1.57
CRELD1	Cysteine-rich with EGF-like domain protein 1	-1.59
PDLIM1	PDZ and LIM domain protein 1	-1.60
TANC1	Protein TANC1	-1.60
AAK1	AP2-associated protein kinase 1	-1.60
RPP40	Ribonuclease P protein subunit p40	-1.60
TGFB1I1	Transforming growth factor beta-1-induced transcript 1 protein	-1.61
PRDX6	Peroxiredoxin-6	-1.62
EPS15	Epidermal growth factor receptor substrate 15	-1.62
ASPH	Aspartyl/asparaginyl beta-hydroxylase	-1.62
MPZL1	Myelin protein zero-like protein 1	-1.64
AP1G1	AP-1 complex subunit gamma-1	-1.65
EPS8	Epidermal growth factor receptor kinase substrate 8	-1.66
RABGAP1L	Rab GTPase-activating protein 1-like	-1.67
AKAP2	A kinase (PRKA) anchor protein 2)	-1.67

BAIAP2L1	Brain-specific angiogenesis inhibitor 1-associated protein 2-like protein 1	-1.68
PLEKHA5	Pleckstrin homology domain-containing family A member 5	-1.68
RPN2	Dolichyl-diphosphooligosaccharide--protein glycosyltransferase subunit 2	-1.69
WDR13	WD repeat-containing protein 13	-1.71
LRPAP1	Alpha-2-macroglobulin receptor-associated protein	-1.72
CYB5R3	NADH-cytochrome b5 reductase 3	-1.75
DDOST	Dolichyl-diphosphooligosaccharide--protein glycosyltransferase 48 kDa subunit	-1.77
LCMT1	Leucine carboxyl methyltransferase 1	-1.79
PKP2	Plakophilin-2	-1.80
FHOD1	FH1/FH2 domain-containing protein 1	-1.82
MPST	3-mercaptopyruvate sulfurtransferase;Sulfurtransferase	-1.83
RAI14	Ankycorbin	-1.85
S E P 5	Septin-5	-1.85
WARS	Tryptophan--tRNA ligase, cytoplasmic;T1-TrpRS;T2-TrpRS	-1.87
HNRNPH2	Heterogeneous nuclear ribonucleoprotein H2	-1.88
VASP	Vasodilator-stimulated phosphoprotein	-1.90
CTNNB1	Catenin beta-1	-1.92
PGRMC1	Membrane-associated progesterone receptor component 1	-1.95
ARFGAP1	ADP-ribosylation factor GTPase-activating protein 1	-1.97
ITSN1	Intersectin-1	-2.01
VPS16	Vacuolar protein sorting-associated protein 16 homolog	-2.02
TOM1	Target of Myb protein 1	-2.02
AMPD2	AMP deaminase 2	-2.04
STK11IP	Serine/threonine-protein kinase 11-interacting protein	-2.08
FRMD8	FERM domain-containing protein 8	-2.08
ANK3	Ankyrin-3	-2.10
PACSIN2	Protein kinase C and casein kinase substrate in neurons protein 2	-2.12
TBC1D2B	TBC1 domain family member 2B	-2.15
DBN1	Isoform 3 of Drebrin	-2.19
FNDC3B	Fibronectin type III domain-containing protein 3B	-2.20
SKT	Sickle tail protein homolog	-2.21

PYGB	Glycogen phosphorylase, brain form	-2.22
ACTC1	Actin, alpha cardiac muscle 1	-2.24
PITPNB	Phosphatidylinositol transfer protein beta isoform	-2.24
OXSR1	Serine/threonine-protein kinase OSR1	-2.25
FMNL2	Formin-like protein 2	-2.30
MICAL1	Protein-methionine sulfoxide oxidase MICAL1	-2.32
SNTB1	Beta-1-syntrophin	-2.34
RAPGEF2	Rap guanine nucleotide exchange factor 2	-2.36
SERPINB12	Serpin B12	-2.39
CASK	Peripheral plasma membrane protein CASK	-2.43
SH3BP1	SH3 domain-binding protein 1	-2.44
PFKM	6-phosphofructokinase, muscle type	-2.49
RAP1B	Ras-related protein Rap-1b;Ras-related protein Rap-1b-like protein;Ras-related protein Rap-1A	-2.49
ACLY	ATP-citrate synthase	-2.50
PRKD1	Serine/threonine-protein kinase D1	-2.59
GRK5	G protein-coupled receptor kinase 5	-2.63
BCL2L13	Bcl-2-like protein 13	-2.70
TLN2	Talin-2	-2.72
TPI1	Triosephosphate isomerase	-2.75
KCTD12	BTB/POZ domain-containing protein KCTD12	-2.78
PITPNM1	Membrane-associated phosphatidylinositol transfer protein 1	-2.97
DCLK1	Serine/threonine-protein kinase DCLK1	-3.08
SUFU	Suppressor of fused homolog	-3.19
NF2	Merlin	-3.22
DOCK6	Dedicator of cytokinesis protein 6	-3.22
COBLL1	Cordon-bleu protein-like 1	-3.30
FN1	Fibronectin;Anastellin;Ugl-Y1;Ugl-Y2;Ugl-Y3	-3.32
SIPA1	Signal-induced proliferation-associated protein 1	-3.47
PLA2G4A	Cytosolic phospholipase A2;Phospholipase A2;Lysophospholipase	-3.63
AKAP12	A-kinase anchor protein 12	-3.63
ENDOD1	Endonuclease domain-containing 1 protein	-3.82

MVD	Diphosphomevalonate decarboxylase	-3.94
ARMC9	LisH domain-containing protein ARMC9	-4.25
TRIM16	Tripartite motif-containing protein 16	-4.56
IGF2BP3	Insulin-like growth factor 2 mRNA-binding protein 3	-4.70
EPB41L3	Isoform B of Band 4.1-like protein 3	-6.33
GFPT2	Glucosamine--fructose-6-phosphate aminotransferase [isomerizing] 2	-6.63
PPP1R12C	Protein phosphatase 1 regulatory subunit 12C	-19.38
PRKAR2B	cAMP-dependent protein kinase type II-beta regulatory subunit	-19.42
PPP1R9B	Neurabin-2	-19.60
MAP1A	Microtubule-associated protein 1A;MAP1 light chain LC2	-19.90
ATP5F1	ATP synthase subunit b, mitochondrial	-20.32
AMPD3	AMP deaminase 3	-20.36
SNX25	Sorting nexin-25	-20.39
PEX11B	Peroxisomal membrane protein 11B	-20.48
DNM1	Dynamin-1	-20.57
CEBPD	CCAAT/enhancer-binding protein delta	-20.60
JUP	Junction plakoglobin	-20.66
USP40	Ubiquitin carboxyl-terminal hydrolase 40	-20.68
NHSL1	NHS-like protein 1	-20.81
DENND2A	DENN domain-containing protein 2A	-21.08
RFTN1	Raftlin	-21.13
TES	Testin	-21.20
C12orf29	Uncharacterized protein C12orf29	-21.28
LRCH3	Leucine-rich repeat and calponin homology domain-containing protein 3	-21.30
BSDC1	BSD domain-containing protein 1	-21.52
FKBP5	Peptidyl-prolyl cis-trans isomerase FKBP5	-21.64
ROBO1	Roundabout homolog 1	-21.71
LMNA	Lamin A/C	-21.73
CPNE7	Copine-7	-21.75
PPP1R14A	Protein phosphatase 1 regulatory subunit 14A	-21.77
MGST1	Microsomal glutathione S-transferase 1	-22.19

PTGES	Prostaglandin E synthase	-22.62
RSU1	Ras suppressor protein 1	-22.73
PTK7	Inactive tyrosine-protein kinase 7	-23.01
CD248	Endosialin	-23.31
SCD	Acyl-CoA desaturase	-23.78
IGF2BP1	Insulin-like growth factor 2 mRNA-binding protein 1	-24.14

Supplementary Table S6: Total proteins significantly up/ downregulated in Ben-Men-1 cells compared to HMC

Gene symbol	Protein name	Log2 FC
ATP13A1	Probable cation-transporting ATPase 13A1	25.65
TNFRSF10D	Tumor necrosis factor receptor superfamily member 10D	25.05
TMEM109	Transmembrane protein 109	24.79
ITGB3	Integrin beta-3;Integrin beta	24.36
RBP1	Retinol-binding protein 1	24.16
LXN	Latexin	24.15
CTHRC1	Collagen triple helix repeat-containing protein 1	24.08
COL11A1	Collagen alpha-1(XI) chain	24.00
CD248	Endosialin	23.96
RPL21	60S ribosomal protein L21	23.94
PTGES	Prostaglandin E synthase	23.79
SLC7A5	Large neutral amino acids transporter small subunit 1	23.38
PTTG1IP	Pituitary tumor-transforming gene 1 protein-interacting protein	23.36
IGF2BP1	Insulin-like growth factor 2 mRNA-binding protein 1	23.31
IGFBP7	Insulin-like growth factor-binding protein 7	23.25
MTHFD2	Bifunctional methylenetetrahydrofolate dehydrogenase/cyclohydrolase, mitochondrial	23.21
ITGA8	Integrin alpha-8;Integrin alpha-8 heavy chain;Integrin alpha-8 light chain	23.20
VCAN	Versican core protein	23.16
ITGA4	Integrin alpha-4	23.02
DSG2	Desmoglein-2	22.82
SCARB1	Scavenger receptor class B member 1	22.81
PLAT	Tissue-type plasminogen activator;Tissue-type plasminogen activator chain A	22.79
TES	Testin	22.76
LDLR	Low-density lipoprotein receptor	22.75
POLR2C	DNA-directed RNA polymerase II subunit RPB3	22.71
DHRS3	Short-chain dehydrogenase/reductase 3	22.65
FTL	Ferritin light chain	22.48
ARHGDIB	Rho GDP-dissociation inhibitor 2	22.40
NUDT4	Diphosphoinositol polyphosphate phosphohydrolase 2	22.38

GPX1	Glutathione peroxidase 1	22.37
ISLR	Immunoglobulin superfamily containing leucine-rich repeat protein	22.36
PVRL2	Poliovirus receptor-related protein 2	22.35
TTLL12	Tubulin--tyrosine ligase-like protein 12	22.33
MGST1	Microsomal glutathione S-transferase 1	22.29
TNFRSF10B	Tumor necrosis factor receptor superfamily member 10B	22.27
SPG20	Spartin	22.12
NID2	Nidogen-2	22.07
CCDC88A	Girdin	22.07
HLA-A	HLA class I histocompatibility antigen, A-69 alpha chain	22.03
EMILIN2	EMILIN-2	22.00
MRPL15	39S ribosomal protein L15, mitochondrial	21.98
GLIPR2	Golgi-associated plant pathogenesis-related protein 1	21.97
RAB13	Ras-related protein Rab-13	21.89
CDC42EP4	Cdc42 effector protein 4	21.89
CIAPIN1	Anamorsin	21.88
PDCD4	Programmed cell death protein 4	21.84
DFFA	DNA fragmentation factor subunit alpha	21.82
SUCLG1	Succinyl-CoA ligase [ADP/GDP-forming] subunit alpha, mitochondrial	21.80
HSPA2	Heat shock-related 70 kDa protein 2	21.72
NUMB	Protein numb homolog	21.65
TGOLN2	Trans-Golgi network integral membrane protein 2	21.63
EXOSC4	Exosome complex component RRP41	21.59
CDK6	Cyclin-dependent kinase 6	21.53
SLC16A1	Monocarboxylate transporter 1	21.51
PRPF31	U4/U6 small nuclear ribonucleoprotein Prp31	21.45
PRPF4	U4/U6 small nuclear ribonucleoprotein Prp4	21.43
EHBP1	EH domain-binding protein 1	21.38
SEC16A	Protein transport protein Sec16A	21.35
LRRC17	Leucine-rich repeat-containing protein 17	21.35
NCOR2	Nuclear receptor corepressor 2	21.31

MORF4L2	Mortality factor 4-like protein 2	21.30
PCOLCE	Procollagen C-endopeptidase enhancer 1	21.27
MAPRE2	Microtubule-associated protein RP/EB family member 2	21.21
ITGA1	Integrin alpha-1	21.19
OXR1	Oxidation resistance protein 1	21.15
COBRA1	Negative elongation factor B	21.13
EXOSC2	Exosome complex component RRP4	21.12
PSMG2	Proteasome assembly chaperone 2	21.10
TGFB2	Transforming growth factor beta-2	21.08
SPAG7	Sperm-associated antigen 7	21.03
USE1	Vesicle transport protein USE1	21.01
PPAT	Amidophosphoribosyltransferase	20.98
MAP7D3	MAP7 domain-containing protein 3	20.95
ATP6AP2	Renin receptor	20.93
TRMT5	tRNA (guanine(37)-N1)-methyltransferase	20.89
LPCAT1	Lysophosphatidylcholine acyltransferase 1	20.87
ESF1	ESF1 homolog	20.87
TEX264	Testis-expressed sequence 264 protein	20.81
DCTN4	Dynactin subunit 4	20.66
CDH6	Cadherin-6	20.65
MARCKSL1	MARCKS-related protein	20.59
ASMTL	N-acetylserotonin O-methyltransferase-like protein	20.53
PCYT2	Ethanolamine-phosphate cytidylyltransferase	20.52
SPATS2	Spermatogenesis-associated serine-rich protein 2	20.51
FAM175B	BRISC complex subunit Abro1	20.49
PNKP	Bifunctional polynucleotide phosphatase/kinase	20.48
ARID1A	AT-rich interactive domain-containing protein 1A	20.34
TFPI2	Tissue factor pathway inhibitor 2	20.27
YY1	Transcriptional repressor protein YY1	20.20
ZC3H11A	Zinc finger CCCH domain-containing protein 11A	20.18
TTYH3	Protein tweety homolog 3	20.05

EXD2	Exonuclease 3-5 domain-containing protein 2	19.99
ZC3H14	Zinc finger CCCH domain-containing protein 14	19.87
ANAPC7	Anaphase-promoting complex subunit 7	19.64
C2orf29	UPF0760 protein C2orf29	19.14
CLDN11	Claudin-11	18.79
HERPUD1	Homocysteine-responsive endoplasmic reticulum-resident ubiquitin-like domain member 1 protein	16.63
NES	Nestin	4.84
PDLIM1	PDZ and LIM domain protein 1	4.81
COL1A1	Collagen alpha-1(I) chain	4.77
SPARC	SPARC	3.96
TGM2	Protein-glutamine gamma-glutamyltransferase 2	3.94
ANPEP	Aminopeptidase N	3.86
UCHL1	Ubiquitin carboxyl-terminal hydrolase isozyme L1	3.73
HNRNPM	Heterogeneous nuclear ribonucleoprotein M	3.71
LMNB2	Lamin-B2	3.67
GGT5	Gamma-glutamyltransferase 5	3.60
HNRNPC	Heterogeneous Nuclear Ribonucleoprotein C	3.58
COL1A2	Collagen alpha-2(I) chain	3.49
AKAP12	A-kinase anchor protein 12	3.36
TGFBI	Transforming growth factor-beta-induced protein ig-h3	3.34
NASP	Nuclear autoantigenic sperm protein	3.30
IGF2BP3	Insulin-like growth factor 2 mRNA-binding protein 3	3.18
COL18A1	Collagen alpha-1(XVIII) chain;Endostatin	3.15
DBN1	Drebrin	3.13
PRMT1	Protein arginine N-methyltransferase 1	3.05
RRBP1	Ribosome-binding protein 1	3.00
COL5A2	Collagen alpha-2(V) chain	2.97
SRSF9	Serine/arginine-rich splicing factor 9	2.92
STIP1	Stress-induced-phosphoprotein 1	2.88
CNN3	Calponin-3	2.77
HIST1H1B	Histone H1.5	2.74

FUBP1	Far upstream element-binding protein 1	2.66
SF3B2	Splicing factor 3B subunit 2	2.61
S E P 9	Septin-9	2.54
FN1	Fibronectin 1	2.53
LMNB1	Lamin-B1	2.53
COL5A1	Collagen alpha-1(V) chain	2.45
ITGA2	Integrin alpha-2	2.43
KHSRP	Far upstream element-binding protein 2	2.43
TOM1	Target of Myb protein 1	2.39
TIAL1	Nucleolysin TIAR	2.38
CNN2	Calponin-2	2.32
SERPINE1	Plasminogen activator inhibitor 1	2.29
ACO2	Aconitate hydratase, mitochondrial	2.27
ITGA5	Integrin alpha-5;Integrin alpha-5 heavy chain;Integrin alpha-5 light chain	2.23
NRP1	Neuropilin-1	2.22
FDPS	Farnesyl pyrophosphate synthase	2.15
SHMT2	Serine hydroxymethyltransferase, mitochondrial;Serine hydroxymethyltransferase	2.15
TPM3	Tropomyosin 3	2.14
NACA	Nascent polypeptide-associated complex subunit alpha	2.13
SLC25A6	ADP/ATP translocase 3	2.10
ST13;ST13P5	Hsc70-interacting protein;Putative protein FAM10A5	2.05
ATP1A1	Sodium/potassium-transporting ATPase subunit alpha-1	2.04
SMARCC1	SWI/SNF complex subunit SMARCC1	1.98
CKAP4	Cytoskeleton-associated protein 4	1.95
COL4A1	Collagen alpha-1(IV) chain;Arresten	1.95
COL6A2	Collagen alpha-2(VI) chain	1.93
RPL12	60S ribosomal protein L12	1.90
EPS8	Epidermal growth factor receptor kinase substrate 8	1.80
TFRC	Transferrin receptor protein 1;Transferrin receptor protein 1, serum form	1.70
HDLBP	Vigilin	1.68
FSCN1	Fascin	1.67

PDGFRB	Platelet-derived growth factor receptor beta	1.63
CTSD	Cathepsin D	1.61
YARS	Tyrosine--tRNA ligase, cytoplasmic	1.45
MYH9	Myosin-9	1.42
CCT8	T-complex protein 1 subunit theta	1.40
SND1	Staphylococcal nuclease domain-containing protein 1	1.32
KARS	Lysine--tRNA ligase	1.31
PRKAR2A	cAMP-dependent protein kinase type II-alpha regulatory subunit	1.30
UQCRFS1	Cytochrome b-c1 complex subunit Rieske, mitochondrial	1.30
PDIA4	Protein disulfide-isomerase A4	1.27
ANXA11	Annexin A11;Annexin	1.26
FKBP1A	Peptidyl-prolyl cis-trans isomerase FKBP1A	1.24
HNRNPH3	Heterogeneous nuclear ribonucleoprotein H3	1.22
PGM3	Phosphoacetylglucosamine mutase	1.22
FKBP4	Peptidyl-prolyl cis-trans isomerase FKBP4	1.19
SRSF1	Serine/arginine-rich splicing factor 1	1.13
HNRNPA3	Heterogeneous nuclear ribonucleoprotein A3	1.12
PLOD3	Procollagen-lysine,2-oxoglutarate 5-dioxygenase 3	1.10
UGP2	UTP--glucose-1-phosphate uridylyltransferase	1.08
RAC1;RAC3	Ras-related C3 botulinum toxin substrate 1;Ras-related C3 botulinum toxin substrate 3	1.06
FBL	rRNA 2-O-methyltransferase fibrillarin	1.06
M6PR	Cation-dependent mannose-6-phosphate receptor	1.05
ETFA	Electron transfer flavoprotein subunit alpha, mitochondrial	1.04
IDE	Insulin-degrading enzyme	-1.00
AK1	Adenylate kinase isoenzyme 1	-1.03
ANXA6	Annexin A6;Annexin	-1.03
DAB2	Disabled homolog 2	-1.05
XPOT	Exportin-T	-1.06
PSMA6	Proteasome subunit alpha type-6;Proteasome subunit alpha type	-1.12
EHD2	EH domain-containing protein 2	-1.14
RAB6A	RAB6A, Member RAS Oncogene Family	-1.17

AP3D1	AP-3 complex subunit delta-1	-1.17
RHOG	Rho-related GTP-binding protein RhoG	-1.17
OLA1	Obg-like ATPase 1	-1.18
AK4	Adenylate kinase isoenzyme 4, mitochondrial	-1.19
TOM1L2	TOM1-like protein 2	-1.19
GLS	Glutaminase kidney isoform, mitochondrial	-1.20
GDI1	Rab GDP dissociation inhibitor alpha	-1.20
RARS	Arginine--tRNA ligase, cytoplasmic	-1.23
TMED10	Transmembrane emp24 domain-containing protein 10	-1.24
STK24	Serine/threonine-protein kinase 24	-1.24
DNPEP	Aspartyl aminopeptidase	-1.25
PKM2	Pyruvate kinase isozymes M1/M2;Pyruvate kinase	-1.25
UBA1	Ubiquitin-like modifier-activating enzyme 1	-1.28
STOM	Erythrocyte band 7 integral membrane protein	-1.28
DDB1	DNA damage-binding protein 1	-1.28
RPS26	40S ribosomal protein S26;Putative 40S ribosomal protein S26-like 1	-1.34
LARS	Leucine--tRNA ligase, cytoplasmic	-1.39
NCAPG	Condensin complex subunit 3	-1.39
LTA4H	Leukotriene A-4 hydrolase	-1.42
SARS	Serine--tRNA ligase, cytoplasmic	-1.46
CNP	2,3-cyclic-nucleotide 3-phosphodiesterase	-1.46
RPL10	60S ribosomal protein L10	-1.46
ANXA4	Annexin A4;Annexin	-1.49
BLVRA	Biliverdin reductase A	-1.50
ESYT1	Extended synaptotagmin-1	-1.51
KPNA6	Importin subunit alpha-7;Importin subunit alpha	-1.53
MYO1E	Unconventional myosin-Ie	-1.54
OAT	Ornithine aminotransferase, mitochondrial	-1.54
C19orf10	UPF0556 protein C19orf10	-1.55
TMPO	Lamina-associated polypeptide 2, isoforms beta/gamma;Thymopoietin;Thymopentin	-1.56
H2AFZ	Histone H2A.Z;Histone H2A.V;Histone H2A	-1.57

UBE4A	Ubiquitin conjugation factor E4 A	-1.57
EZR	Ezrin	-1.57
CSNK1A1	Casein kinase I isoform alpha;Casein kinase I isoform alpha-like	-1.57
CYCS	Cytochrome c	-1.58
NPLOC4	Nuclear protein localization protein 4 homolog	-1.61
CTSD	Cathepsin D;Cathepsin D light chain;Cathepsin D heavy chain	-1.62
NT5C	5(3)-deoxyribonucleotidase, cytosolic type	-1.62
DPYSL3	Dihydropyrimidinase-related protein 3	-1.64
PRKCDBP	Protein kinase C delta-binding protein	-1.67
NME3	Nucleoside diphosphate kinase 3	-1.67
PLEC	Plectin	-1.69
LDHA	L-lactate dehydrogenase A chain	-1.69
NFKB2	Nuclear factor NF-kappa-B p100 subunit;Nuclear factor NF-kappa-B p52 subunit	-1.70
HK2	Hexokinase-2	-1.70
PIP4K2C	Phosphatidylinositol 5-phosphate 4-kinase type-2 gamma	-1.70
PAIP1	Polyadenylate-binding protein-interacting protein 1	-1.71
CTSC	Dipeptidyl peptidase 1	-1.71
PSMA7	Proteasome subunit alpha type-7	-1.72
GNPNAT1	Glucosamine 6-phosphate N-acetyltransferase	-1.73
ADK	Adenosine kinase	-1.74
GPD2	Glycerol-3-phosphate dehydrogenase, mitochondrial	-1.74
DSTN	Destrin	-1.75
LEPREL1	Prolyl 3-hydroxylase 2	-1.76
MYOF	Myoferlin	-1.80
ANXA3	Annexin A3;Annexin	-1.82
LOX	Protein-lysine 6-oxidase	-1.82
GRPEL1	GrpE protein homolog 1, mitochondrial	-1.85
UBLCP1	Ubiquitin-like domain-containing CTD phosphatase 1	-1.85
RNH1	Ribonuclease inhibitor	-1.87
ARHGAP18	Rho GTPase-activating protein 18	-1.88
PRPS1	Ribose-phosphate pyrophosphokinase 1;Ribose-phosphate pyrophosphokinase	-1.94

HLA-A	HLA class I histocompatibility antigen, A-3 alpha chain	-1.95
PGM1	Phosphoglucomutase-1	-1.97
SCCPDH	Saccharopine dehydrogenase-like oxidoreductase	-1.97
SF3B14	Pre-mRNA branch site protein p14	-1.98
PC	Pyruvate carboxylase, mitochondrial	-1.99
MTHFD1L	Monofunctional C1-tetrahydrofolate synthase, mitochondrial	-2.00
G6PD	Glucose-6-phosphate 1-dehydrogenase	-2.01
STK10	Serine/threonine-protein kinase 10	-2.01
PGAM1	Phosphoglycerate mutase 1	-2.02
GSTM2	Glutathione S-transferase Mu 2	-2.05
SPAG9	C-Jun-amino-terminal kinase-interacting protein 4	-2.09
CYR61	Protein CYR61	-2.11
GNA11	Guanine nucleotide-binding protein subunit alpha-11	-2.12
PSME1	Proteasome activator complex subunit 1	-2.12
CAPN2	Calpain-2 catalytic subunit	-2.13
MYO1B	Unconventional myosin-Ib	-2.15
PSMB3	Proteasome subunit beta type-3	-2.16
UAP1	UDP-N-acetylhexosamine pyrophosphorylase	-2.18
TNPO1	Transportin-1	-2.19
NEK7	Serine/threonine-protein kinase Nek7	-2.20
CAST	Calpastatin	-2.26
MARS	Methionine--tRNA ligase, cytoplasmic	-2.26
FGD4	FYVE, RhoGEF and PH domain-containing protein 4	-2.28
EIF2AK2	Interferon-induced, double-stranded RNA-activated protein kinase	-2.34
ATP6V0C	V-type proton ATPase 16 kDa proteolipid subunit	-2.34
IPO5	Importin-5	-2.35
EPHA2	Ephrin type-A receptor 2	-2.38
PGLS	6-phosphogluconolactonase	-2.39
PRDX5	Peroxiredoxin-5, mitochondrial	-2.41
ECE1	Endothelin-converting enzyme 1	-2.43
HSPB1	Heat shock protein beta-1	-2.54

PPIC	Peptidyl-prolyl cis-trans isomerase C	-2.54
MYO1C	Unconventional myosin-Ic	-2.55
STAT1	Signal transducer and activator of transcription 1-alpha/beta	-2.57
LGALS3	Galectin-3	-2.57
EGFR	Epidermal growth factor receptor	-2.61
ATL3	Atlastin GTPase 3	-2.65
HDHD1	Pseudouridine-5-monophosphatase	-2.67
PDLIM2	PDZ and LIM domain protein 2	-2.68
PNP	Purine nucleoside phosphorylase	-2.70
PDXK	Pyridoxal kinase	-2.70
UGDH	UDP-glucose 6-dehydrogenase	-2.73
RNPEP	Aminopeptidase B	-2.73
EIF4A2	Eukaryotic initiation factor 4A-II	-2.79
EHD1	EH domain-containing protein 1	-2.79
CCDC80	Coiled-coil domain-containing protein 80	-2.82
GALNT2	Polypeptide N-acetylgalactosaminyltransferase 2	-2.84
AXL	Tyrosine-protein kinase receptor UFO	-3.04
GBE1	1,4-alpha-glucan-branching enzyme	-3.17
AHNAK2	Protein AHNAK2	-3.17
PYGL	Glycogen phosphorylase, liver form;Phosphorylase	-3.23
ABHD14B	Abhydrolase domain-containing protein 14B	-3.24
ALDH1A3	Aldehyde dehydrogenase family 1 member A3	-3.29
DST	Dystonin	-3.32
ALCAM	CD166 antigen	-3.37
AFAP1	Actin filament-associated protein 1	-3.51
ACOT9	Acyl-coenzyme A thioesterase 9, mitochondrial	-3.55
MGLL	Monoglyceride lipase	-4.29
KRT18	Keratin, type I cytoskeletal 18	-4.48
EPS8L2	Epidermal growth factor receptor kinase substrate 8-like protein 2	-4.49
SPR	Sepiapterin reductase	-4.61
NQO1	NAD(P)H dehydrogenase [quinone] 1	-5.94

AAAS	Aladin	-19.79
MRI1	Methylthioribose-1-phosphate isomerase	-19.88
NOP10	H/ACA ribonucleoprotein complex subunit 3	-20.09
POLR1A	DNA-directed RNA polymerase I subunit RPA1;DNA-directed RNA polymerase	-20.11
IQGAP2	Ras GTPase-activating-like protein IQGAP2	-20.19
IQGAP3	Ras GTPase-activating-like protein IQGAP3	-20.30
DGKA	Diacylglycerol kinase alpha	-20.30
GCC1	GRIP and coiled-coil domain-containing protein 1	-20.45
CCDC132	Coiled-coil domain-containing protein 132	-20.53
ADRBK1	Beta-adrenergic receptor kinase 1;Beta-adrenergic receptor kinase 2	-20.54
WHSC2	Negative elongation factor A	-20.58
KIF13A	Kinesin-like protein KIF13A	-20.63
ZNF622	Zinc finger protein 622	-20.65
CCPG1	Cell cycle progression protein 1	-20.68
USP4	Ubiquitin carboxyl-terminal hydrolase 4;Ubiquitin carboxyl-terminal hydrolase	-20.71
ARHGEF40	Rho guanine nucleotide exchange factor 40	-20.80
TIMMDC1	Translocase of inner mitochondrial membrane domain-containing protein 1	-20.84
ZNF185	Zinc finger protein 185	-20.88
ARHGAP21	Rho GTPase-activating protein 21;Rho GTPase-activating protein 23	-20.95
HRSP12	Ribonuclease UK114	-20.99
MRPL12	39S ribosomal protein L12, mitochondrial	-20.99
C16orf13	UPF0585 protein C16orf13	-21.06
CUL1	Cullin-1	-21.14
MRPL38	39S ribosomal protein L38, mitochondrial	-21.14
MGAT1	Alpha-1,3-mannosyl-glycoprotein 2-beta-N-acetylglucosaminyltransferase	-21.19
KIF3A	Kinesin-like protein KIF3A	-21.30
COASY	Bifunctional coenzyme A synthase	-21.35
SNAPIN	SNARE-associated protein Snapin	-21.38
SEC24B	Protein transport protein Sec24B	-21.41
HTRA1	Serine protease HTRA1	-21.46
SCAF4	Splicing factor, arginine/serine-rich 15	-21.48

VAMP4	Vesicle-associated membrane protein 4	-21.50
MAN2B1	Lysosomal alpha-mannosidase	-21.51
BUD31	Protein BUD31 homolog	-21.51
PTP4A2	Protein tyrosine phosphatase type IVA 2	-21.55
PLXNA1	Plexin-A1	-21.55
PPIP5K2	Inositol hexakisphosphate and diphosphoinositol-pentakisphosphate kinase 2	-21.57
XPC	DNA repair protein complementing XP-C cells	-21.61
MAP4K4	Mitogen-activated protein kinase kinase kinase kinase 4	-21.61
HPCAL1	Hippocalcin-like protein 1	-21.67
PPP4C	Serine/threonine-protein phosphatase 4 catalytic subunit;Serine/threonine-protein phosphatase	-21.76
MMGT1	Membrane magnesium transporter 1	-21.79
JAG1	Protein jagged-1	-21.80
HINT2	Histidine triad nucleotide-binding protein 2, mitochondrial	-21.81
CLPTM1	Cleft lip and palate transmembrane protein 1	-21.87
AKR1C1	Aldo-keto reductase family 1 member C1;Aldo-keto reductase family 1 member C2	-21.88
POLD1	DNA polymerase delta catalytic subunit	-21.96
DOCK5	Dedicator of cytokinesis protein 5	-21.98
TRADD	Tumor necrosis factor receptor type 1-associated DEATH domain protein	-21.99
GNL2	Nucleolar GTP-binding protein 2	-22.05
MYH14	Myosin-14	-22.08
RBM12B	RNA-binding protein 12B	-22.08
GFM1	Elongation factor G, mitochondrial	-22.10
SCAMP1	Secretory carrier-associated membrane protein 1	-22.14
LYRM7	LYR motif-containing protein 7	-22.14
FYCO1	FYVE and coiled-coil domain-containing protein 1	-22.15
USP8	Ubiquitin carboxyl-terminal hydrolase 8;Ubiquitin carboxyl-terminal hydrolase	-22.17
COX7A2	Cytochrome c oxidase subunit 7A2, mitochondrial	-22.18
PARP14	Poly [ADP-ribose] polymerase 14	-22.21
TP53RK	TP53-regulating kinase	-22.21
SACM1L	Phosphatidylinositide phosphatase SAC1	-22.22
TFPI	Tissue factor pathway inhibitor	-22.24

DFNA5	Non-syndromic hearing impairment protein 5	-22.31
MRPS14	28S ribosomal protein S14, mitochondrial	-22.39
DNAJC5	DnaJ homolog subfamily C member 5	-22.41
MTPN	Myotrophin	-22.41
PPT1	Palmitoyl-protein thioesterase 1	-22.41
ELN	Elastin	-22.48
ALAD	Delta-aminolevulinic acid dehydratase	-22.50
VPS29	Vacuolar protein sorting-associated protein 29	-22.51
FGF1	Fibroblast growth factor 1	-22.51
LRRC32	Leucine-rich repeat-containing protein 32	-22.53
H2AFY	Core histone macro-H2A.1;Histone H2A;Core histone macro-H2A.2	-22.53
OPLAH	5-oxoprolinase	-22.54
COG7	Conserved oligomeric Golgi complex subunit 7	-22.56
PRSS23	Serine protease 23	-22.59
TAP1	Antigen peptide transporter 1	-22.61
TRIM25	E3 ubiquitin/ISG15 ligase TRIM25	-22.68
SLIT3	Slit homolog 3 protein	-22.69
COX5B	Cytochrome c oxidase subunit 5B, mitochondrial	-22.81
PROSC	Proline synthase co-transcribed bacterial homolog protein	-22.84
IER3IP1	Immediate early response 3-interacting protein 1	-22.94
SAMD9	Sterile alpha motif domain-containing protein 9	-22.96
BPGM	Bisphosphoglycerate mutase	-22.96
HIGD2A	HIG1 domain family member 2A	-23.00
SULT1A1	Sulfotransferase 1A1	-23.00
CTSZ	Cathepsin Z	-23.04
AKR1B1	Aldose reductase	-23.04
DCTD	Deoxycytidylate deaminase	-23.12
SLC44A2	Choline transporter-like protein 2	-23.13
KIAA1524	Protein CIP2A	-23.17
SYNE1	Nesprin-1	-23.21
GNG12	Guanine nucleotide-binding protein G(I)/G(S)/G(O) subunit gamma-12	-23.26

PARP10	Poly [ADP-ribose] polymerase 10	-23.49
SH2D4A	SH2 domain-containing protein 4A	-23.50
UQCRQ	Cytochrome b-c1 complex subunit 8	-23.55
ABI3BP	Target of Nesh-SH3	-23.77
HSPA4L	Heat shock 70 kDa protein 4L	-24.23
PHPT1	14 kDa phosphohistidine phosphatase	-24.50
C6orf108	Deoxyribonucleoside 5-monophosphate N-glycosidase	-24.76
THY1	Thy-1 membrane glycoprotein	-24.89

Supplementary Table S7: Phosphopeptides identified by TiO_2 phosphopeptide emrichment in Ben-Men-1 cells

Gene names	Protein names	Localization score	Peptide score	Modified sequence
ABCB10	ATP-binding cassette sub-family B member 10, mitochondrial	0.997604	94.688	_IRTS(ph)IFS(ph)SIIR_
ADGB	Androglobin	0.993943	90.827	_(ac)N(de)IEQY(ph)AVSIIR_
AGK	Acylglycerol kinase, mitochondrial	1	84.365	_(ac)MT(ph)VFFKT(ph)IR_
AGK	Acylglycerol kinase, mitochondrial	1	84.365	_(ac)MT(ph)VFFKT(ph)IR_
AHNAK	Neuroblast differentiation-associated protein AHNAK	1	98.766	_AS(ph)IGS(ph)IEGEAEAEASSPK_
AHNAK	Neuroblast differentiation-associated protein AHNAK	1	183.56	_AS(ph)IGS(ph)IEGEAEAEASSPK_
AHNAK	Neuroblast differentiation-associated protein AHNAK	0.997751	221.85	_ASIGSIEGEAEAEASS(ph)PK_
AHNAK	Neuroblast differentiation-associated protein AHNAK	1	124.2	_FKAEAPIPS(ph)PK_
AHNAK	Neuroblast differentiation-associated protein AHNAK	0.999755	198.1	_GKGGVTGS(ph)PEASISGSK_
AHNAK	Neuroblast differentiation-associated protein AHNAK	0.997794	178.56	_IPS(ph)GSGAASPTGSAVDIR_
AHNAK	Neuroblast differentiation-associated protein AHNAK	0.89232	238.89	_IPSGS(ph)GAAS(ph)PTGSAVDIR_
AHNAK	Neuroblast differentiation-associated protein AHNAK	0.997895	260.24	_IPSGSGAAS(ph)PTGSAVDIR_
AHNAK	Neuroblast differentiation-associated protein AHNAK	1	138.97	_IS(ph)APNVDFNIEGPK_
ARHGAP21	Rho GTPase-activating protein 21	1	96.745	_DIN(de)VIS(ph)S(ph)IIKS(ph)FFR_
ARHGAP21	Rho GTPase-activating protein 21	1	96.745	_DIN(de)VIS(ph)S(ph)IIKS(ph)FFR_
ARHGAP21	Rho GTPase-activating protein 21	1	96.745	_DIN(de)VIS(ph)S(ph)IIKS(ph)FFR_
ARNT2	Aryl hydrocarbon receptor nuclear translocator 2	0.949639	72.399	_EQICT(ph)SEN(de)SM(ox)T(ph)GRIIDIK_
BAIAP2	Brain-specific angiogenesis inhibitor 1-associated protein 2	1	62.203	_(ac)MEQFNPS(ph)IRN(de)FIAMGK_
BCLAF1	Bcl-2-associated transcription factor 1	1	257.37	_AEGEWEDQEAIDYFS(ph)DK_
BCLAF1	Bcl-2-associated transcription factor 1	1	145.81	_DIFDYS(ph)PPIHK_
BTBD7	BTB/POZ domain-containing protein 7	0.999985	88.239	_IADREPN(de)IIS(ph)GTAHS(ph)VN(de)KR_
C14orf135	Pecanex-like protein C14orf135	0.99998	58.274	_(ac)M(ox)S(ph)PDVPIINDYK_
C17orf85	Uncharacterized protein C17orf85	0.998917	136.14	_AEAPAGPAIGIPS(ph)PEAESGVDR_
C2orf73	Uncharacterized protein C2orf73	1	78.244	_EIKPGS(ph)RPT(ph)VPK_
C2orf73	Uncharacterized protein C2orf73	1	78.244	_EIKPGS(ph)RPT(ph)VPK_
CANX	Calnexin	1	122.33	_AEEDEIIN(de)RS(ph)PR_
CCDC102A	Coiled-coil domain-containing protein 102A	1	114.97	_AAQMEKT(ph)MRR_
CCDC120	Coiled-coil domain-containing protein 120	0.997046	52.391	_RSN(de)S(ph)S(ph)EAIIVDR_
CCDC120	Coiled-coil domain-containing protein 120	0.990636	52.391	_RSN(de)S(ph)S(ph)EAIIVDR_
CCDC86	Coiled-coil domain-containing protein 86	0.999758	155.86	_IGGIRPES(ph)PESITSVSR_

CCIN	Calicin	0.999901	54.281	_M(ox)S(ph)IPMDGT(ph)AVITK_
CCIN	Calicin	0.984891	54.281	_M(ox)S(ph)IPMDGT(ph)AVITK_
CEP170	Centrosomal protein of 170 kDa	0.999207	151.42	_ARIGEAS(ph)DSEIADADK_
CFL1	Cofilin-1	1	154.72	_(ac)AS(ph)GVAVSDGVIK_
CFL2	Cofilin-2	0.999232	130.21	_AS(ph)GVTVNDEVIK_
CHL1	Neural cell adhesion molecule L1-like protein	0.929466	52.576	_VMTPAVY(ph)APY(ph)DVK_
CHL1	Neural cell adhesion molecule L1-like protein	0.999938	52.576	_VMTPAVY(ph)APY(ph)DVK_
CHMP2B	Charged multivesicular body protein 2b	0.999361	98.337	_ATIS(ph)DEEIER_
CHMP6	Charged multivesicular body protein 6	1	76.679	_RY(ph)QEQIIDR_
COG8	Conserved oligomeric Golgi complex subunit 8	0.925939	50.149	_RM(ox)N(de)S(ph)ITIN(de)R_
CTH	Cystathionine gamma-lyase	0.999867	89.911	_AVAAIDGAKYCT(ph)N(de)R_
CTNNA1	Catenin alpha-1	0.999984	197.68	_TPEEIDDS(ph)DFETEDFDVR_
DDX4	Probable ATP-dependent RNA helicase DDX4	0.842258	68.845	_RDNT(ph)S(ph)TM(ox)GGFGVGK_
DDX4	Probable ATP-dependent RNA helicase DDX4	0.805702	68.845	_RDNT(ph)S(ph)TM(ox)GGFGVGK_
DPF1	DPF1 protein	1	55.452	_(ac)M(ox)AT(ph)AIQNPIK_
DST	Dystonin	0.91406	120.57	_S(ph)FSEDVISHK_
DYNC1LI1	Cytoplasmic dynein 1 light intermediate chain 1	0.9896	162.43	_KPVTVS(ph)PTTPTSPTEGEAS_
EEF1D	Elongation factor 1-delta	1	163.4	_KPATPAEDDEDDDIDIFGS(ph)DNEEEDK_
EGFR	Epidermal growth factor receptor	0.965891	137.64	_EIVEPIT(ph)PSGEAPNQAIIR_
EIF4EBP1	Eukaryotic translation initiation factor 4E-binding protein 1	0.762844	75.718	_VVIGDGVQIPPGDYSTT(ph)PGGTIFSTT(ph)PGGTR_
ELL	RNA polymerase II elongation factor ELL	0.999159	99.283	_QDSVS(ph)IRPS(ph)IR_
ELL	RNA polymerase II elongation factor ELL	0.999994	99.283	_QDSVS(ph)IRPS(ph)IR_
EXOSC9	Exosome complex component RRP45	0.951017	179.5	_APIDTS(ph)DVEEK_
EXPH5	Exophilin-5	0.999999	60.489	_S(ph)NGFGFN(de)AS(ph)T(ph)IIS(ph)S(ph)KKSPR_
EXPH5	Exophilin-5	0.999999	60.489	_S(ph)NGFGFN(de)AS(ph)T(ph)IIS(ph)S(ph)KKSPR_
EXPH5	Exophilin-5	0.892262	60.489	_S(ph)NGFGFN(de)AS(ph)T(ph)IIS(ph)S(ph)KKSPR_
EXPH5	Exophilin-5	0.999999	60.489	_S(ph)NGFGFN(de)AS(ph)T(ph)IIS(ph)S(ph)KKSPR_
FAM129B	Niban-like protein 1	0.999976	109.68	_AAPEAS(ph)SPPAS(ph)PIQHIIPGK_
FAM129B	Niban-like protein 1	1	88.708	_GIIAQGIRPES(ph)PPPAGPIIN(de)GAPAGESPQPK_
FAM3C	Protein FAM3C	1	78.428	_GINVAIANGKT(ph)GEVIDT(ph)K_
FAM3C	Protein FAM3C	1	78.428	_GINVAIANGKT(ph)GEVIDT(ph)K_
FAM83H	Protein FAM83H	0.999992	128.76	_KGS(ph)PTPGFSTR_

FHDC1	FH2 domain-containing protein 1	0.999192	78.505	_KDS(ph)SRTT(ph)IGR_
FHDC1	FH2 domain-containing protein 1	0.887568	78.505	_KDS(ph)SRTT(ph)IGR_
FKBP15	FK506-binding protein 15	0.969712	131.72	_SSIS(ph)GDEEDEIFK_
FLNB	Filamin-B	0.999993	150.26	_IVS(ph)PGSANETSSIIVESVTR_
FNDC3B	Fibronectin type III domain-containing protein 3B	0.999992	115.12	_INS(ph)PPSSIYK_
FOXK2	Forkhead box protein K2	1	169.67	_EGS(ph)PAPIEPEPGAAQPK_
FRYL	Protein Furry Homolog-Like	1	58.487	_N(de)IIMS(ph)N(de)IT(ph)IDPDVK_
FRYL	Protein Furry Homolog-Like	1	58.487	_N(de)IIMS(ph)N(de)IT(ph)IDPDVK_
G3BP1	Ras GTPase-activating protein-binding protein 1	0.842968	172.83	_S(ph)SSPAPADIAQTVQEDIR_
GBE1	1,4-alpha-glucan-branching enzyme	1	98.392	_(ac)MN(de)IAKVRY(ph)K_
GGH	Gamma-glutamyl hydrolase	1	72.315	_KFFN(de)VIT(ph)T(ph)N(de)T(ph)DGK_
GGH	Gamma-glutamyl hydrolase	1	72.315	_KFFN(de)VIT(ph)T(ph)N(de)T(ph)DGK_
GGH	Gamma-glutamyl hydrolase	1	72.315	_KFFN(de)VIT(ph)T(ph)N(de)T(ph)DGK_
GRHL1	Grainyhead-like protein 1 homolog	0.777196	55.885	_GIPIN(de)IQVDTYS(ph)Y(ph)N(de)NR_
GRHL1	Grainyhead-like protein 1 homolog	0.928346	55.885	_GIPIN(de)IQVDTYS(ph)Y(ph)N(de)NR_
HIST1H1B	Histone H1.5	0.983235	264.38	_S(ph)ETAPAETATPAPVEK_
HIST1H1B	Histone H1.5	0.843748	107.03	_(ac)SET(ph)APAETATPAPVEK_
HIST1H1D	Histone H1.3	0.896168	176.81	_(ac)SETAPIAPTIPAPAEKT(ph)PVK_
HLTF	Helicase-like transcription factor	1	86.539	_T(ph)IQRPVT(ph)MGDEGGIRR_
HLTF	Helicase-like transcription factor	1	86.539	_T(ph)IQRPVT(ph)MGDEGGIRR_
HN1	Hematological and neurological expressed 1 protein	0.996105	177.12	_RNS(ph)SEASSGDFIDIK_
HSD17B6	17-beta-hydroxysteroid dehydrogenase type 6	0.999792	56.424	_ET(ph)Y(ph)GQQYFDAIYNIM(ox)K_
HSD17B6	17-beta-hydroxysteroid dehydrogenase type 6	0.821576	56.424	_ET(ph)Y(ph)GQQYFDAIYNIM(ox)K_
IGF2BP2	Insulin-like growth factor 2 mRNA-binding protein 2	0.812876	137.69	_ISYIPDEEVS(ph)SPSPPQR_
IGF2R	Cation-independent mannose-6-phosphate receptor	1	134.25	_IVSFHDDS(ph)DEDIIHI_
IL17RA	Interleukin-17 receptor A	0.991167	71.527	_QEM(ox)VES(ph)NSKIIVICS(ph)R_
IL17RA	Interleukin-17 receptor A	0.999497	71.527	_QEM(ox)VES(ph)NSKIIVICS(ph)R_
INPP4B	Type II inositol 3,4-bisphosphate 4-phosphatase	1	72.531	_Y(ph)AFN(de)M(ox)IQIMAFPK_
KIAA1432	Protein RIC1 homolog	0.999674	54.103	_SDGPNTTAGIQVIQEVS(ph)M(ox)S(ph)R_
KIAA1432	Protein RIC1 homolog	0.999916	54.103	_SDGPNTTAGIQVIQEVS(ph)M(ox)S(ph)R_
KIRREL	Kin of IRRE-like protein 1	0.996509	53.453	_(ac)M(ox)IS(ph)IIVWIITISDTFS(ph)QGTQT(ph)R_
KIRREL	Kin of IRRE-like protein 1	0.9037	53.453	_(ac)M(ox)IS(ph)IIVWIITISDTFS(ph)QGTQT(ph)R_

KIRREL	Kin of IRRE-like protein 1	0.944559	53.453	_(ac)M(ox)IS(ph)IIVWIITISDTFS(ph)QGTQT(ph)R_
KLC1	Kinesin light chain 1	0.999414	132.31	_ASS(ph)INVINVGGK_
KLC4	Kinesin light chain 4	1	149.07	_AAS(ph)INYIN(de)QPSAAPIQVSR_
KPNA3	Importin subunit alpha-3	0.942758	107.88	_NVPQEESIEDS(ph)DVDADFK_
KRT18	Keratin, type I cytoskeletal 18	0.888985	192.1	_PVSSAASVYAGAGGS(ph)GSR_
LAMA5	Laminin subunit alpha-5	1	65.423	_GVHNAS(ph)IAIS(ph)AS(ph)IGR_
LAMA5	Laminin subunit alpha-5	1	65.423	_GVHNAS(ph)IAIS(ph)AS(ph)IGR_
LAMA5	Laminin subunit alpha-5	1	65.423	_GVHNAS(ph)IAIS(ph)AS(ph)IGR_
LMO7	LIM domain only protein 7	0.999053	184.83	_IPS(ph)PTSPFSSISQDQAATSK_
LMO7	LIM domain only protein 7	1	101.53	_RGES(ph)IDNIDSPR_
LMO7	LIM domain only protein 7	1	101.53	_RGES(ph)IDNIDS(ph)PR_
LMO7	LIM domain only protein 7	0.997294	177.87	_GGREGFES(ph)DTDSEFTFK_
LPIN2	Phosphatidate phosphatase LPIN2	0.953262	163.79	_IPAYIAT(ph)SPIPTEDQFFK_
LRCH4	Leucine-rich repeat and calponin homology domain-containing protein 4	0.999638	113.73	_(ac)AAAVAAPIAAGGEEAAATTSVPGS(ph)PGIPGRR_
LRRFIP1	Leucine-rich repeat flightless-interacting protein 1	0.936353	183.25	_RGS(ph)GDTSISIDTEASIR_
LRRFIP2	Leucine-rich repeat flightless-interacting protein 2	0.871779	191.2	_RGSGDTS(ph)SIIDPDTSISEIR_
LTN1	E3 ubiquitin-protein ligase listerin	0.894774	76.015	_IIYHIFRIM(ox)PENPT(ph)Y(ph)AET(ph)AVEVPN(de)K_
LTN1	E3 ubiquitin-protein ligase listerin	0.976466	76.015	_IIYHIFRIM(ox)PENPT(ph)Y(ph)AET(ph)AVEVPN(de)K_
LTN1	E3 ubiquitin-protein ligase listerin	0.974281	76.015	_IIY(ph)HIFRIM(ox)PEN(de)PT(ph)YAET(ph)AVEVPN(de)K_
LTN1	E3 ubiquitin-protein ligase listerin	0.879649	73.405	_IIYHIFRIM(ox)PENPT(ph)Y(ph)AET(ph)AVEVPN(de)K_
LUZP1	Leucine zipper protein 1	1	124.84	_EKPDS(ph)DDDIDIASIVTAK_
MAEL	Protein maelstrom homolog	1	130.01	_HM(ox)AKAS(ph)EIR_
MAN2C1	Alpha-mannosidase 2C1	1	82.55	_RIS(ph)N(de)T(ph)DGIPR_
MAN2C1	Alpha-mannosidase 2C1	1	82.55	_RIS(ph)N(de)T(ph)DGIPR_
MAP1B	Microtubule-associated protein 1B;MAP1 light chain LC1	0.996306	149.44	_ESS(ph)PIYS(ph)PTFSDSTSAVK_
MAP1B	Microtubule-associated protein 1B;MAP1 light chain LC1	1	226.75	_S(ph)PPIIGSESAYESFISADDK_
MAP1B	Microtubule-associated protein 1B;MAP1 light chain LC1	1	133.78	_VQS(ph)IEGEKIS(ph)PK_
MAP1B	Microtubule-associated protein 1B;MAP1 light chain LC1	1	133.78	_VQSIEGEKIS(ph)PK_
MAP1B	Microtubule-associated protein 1B;MAP1 light chain LC1	0.997993	101.6	_VSAEAEVAPVSPEVT(ph)QEVVEEHCAS(ph)PEDK_
MAP3K7	Mitogen-activated protein kinase kinase kinase 7	0.999917	156.36	_S(ph)IQDITVTGTEPGQVSSR_
MAP4	Microtubule-associated protein;Microtubule-associated protein 4	1	191.96	_DVT(ph)PPPETEVVIIK_
MCM2	DNA replication licensing factor MCM2	1	157.47	_GIIYDS(ph)DEEDEERPAR_

MEI1	Meiosis inhibitor protein 1	1	74.392	_(ac)M(ox)CINIIS(ph)APEK_
MPHOSPH8	M-phase phosphoprotein 8	1	128.98	_GAEAFGDS(ph)EEDGEDVFEVEK_
MTA3	Metastasis-associated protein MTA3	0.993189	78.964	_IKQVY(ph)IPT(ph)YK_
MTA3	Metastasis-associated protein MTA3	0.99512	78.964	_IKQVY(ph)IPT(ph)YK_
NDRG1	Protein NDRG1	0.970147	115.87	_TAS(ph)GSSVTSIDGTR_
NDUFV3	NADH dehydrogenase [ubiquinone] flavoprotein 3, mitochondrial	0.997076	114.4	_VAS(ph)PSPSGSVIFTDEGVPK_
NIPBL	Nipped-B-like protein	0.996521	87.083	_AMGIMDKISTDKT(ph)VK_
NUCKS1	Nipped-B-like protein	0.85053	84.762	_VVDYSQFQES(ph)DDADEDYGRDSGPPTK_
OR2G3	Olfactory receptor 2G3	0.847765	57.432	_(ac)M(ox)GIGN(de)ES(ph)SIMDFIIIGFSDHPR_
PA2G4	Proliferation-associated protein 2G4	1	220.66	_S(ph)GEDEQQEQTIAEDIVVTK_
PAK2	Serine/threonine-protein kinase PAK 2;PAK-2p27;PAK-2p34	0.996758	122.69	_YIS(ph)FTPPEK_
PAK6	Serine/threonine-protein kinase PAK 6	1	76.943	_(ac)MPGPGT(ph)MFR_
PARP12	Poly [ADP-ribose] polymerase 12	0.999673	106.67	_RIS(ph)T(ph)ASSVTK_
PATL1	Protein PAT1 homolog 1	0.873804	92.993	_RSTS(ph)PIIGS(ph)PPVR_
PATL1	Protein PAT1 homolog 1	0.999875	92.993	_RSTS(ph)PIIGS(ph)PPVR_
PDLIM2	PDZ and LIM domain protein 2	1	141.6	_AGDSAVIVIPPS(ph)PGPR_
PDLIM2	PDZ and LIM domain protein 2	1	225.2	_AGS(ph)PFS(ph)PPPSSSSITGEAAISR_
PDLIM2	PDZ and LIM domain protein 2	0.99988	208.97	_AGS(ph)PFS(ph)PPPSSSSITGEAAISR_
PDLIM2	PDZ and LIM domain protein 2	0.988311	202.97	_GGTPAFIPSSIS(ph)PQSSIPASR_
PDPK1	3-phosphoinositide-dependent protein kinase 1	0.999999	147.87	_ANS(ph)FVGTAQYVSPEIITEK_
PGK1	Phosphoglycerate kinase 1;Phosphoglycerate kinase	1	119.32	_AIES(ph)PERPFIAIIGGAK_
PGRMC2	Membrane-associated progesterone receptor component 2	0.981148	119.38	_IIKPGEEPSEYT(ph)DEEDTK_
PKM2	Pyruvate kinase isozymes M1/M2;Pyruvate kinase;Pyruvate kinase	0.999992	151.07	_IDIDS(ph)PPITAR_
PLEC	Plectin	0.998864	137.89	_EIEEVS(ph)PETPVVPATTQR_
PLXND1	Plexin-D1	0.975323	78.326	_IN(de)IN(de)ES(ph)M(ox)QVVSRR_
PPP1CA	Serine/threonine-protein phosphatase PP1-alpha catalytic subunit	0.906835	87.388	_(ac)MSDS(ph)EKIN(de)IDS(ph)IIGR_
PPP1CA	Serine/threonine-protein phosphatase PP1-alpha catalytic subunit	0.999832	87.388	_(ac)MSDS(ph)EKIN(de)IDS(ph)IIGR_
PPP1R12A	Protein phosphatase 1 regulatory subunit 12A	0.764795	111.01	_TGS(ph)YGAIAEITASK_
PRDM6	Putative histone-lysine N-methyltransferase PRDM6	1	105.03	_AEPPPDS(ph)IRPR_
PTCD1	Pentatricopeptide repeat-containing protein 1	0.984478	60.307	_SQVT(ph)PNT(ph)HIY(ph)SAIINAAIR_
PTCD1	Pentatricopeptide repeat-containing protein 1	0.808628	60.307	_SQVT(ph)PNT(ph)HIY(ph)SAIINAAIR_
RAB12	Ras-related protein Rab-12	0.999908	131.04	_AGGGGGIGAGS(ph)PAISGGQGR_

RAVER1	Ribonucleoprotein PTB-binding 1	1	153.36	_(ac)AADVSVTHRPPIS(ph)PK_
RBM5	RNA-binding protein 5	0.999864	187.72	_GIVAAYSGDS(ph)DNEEEIVER_
RIMBP3C	RIMS-binding protein 3C;RIMS-binding protein 3B	1	55.469	_VFVAIS(ph)DY(ph)NPIVM(ox)S(ph)AN(de)IK_
RIMBP3C	RIMS-binding protein 3C;RIMS-binding protein 3B	1	55.469	_VFVAIS(ph)DY(ph)NPIVM(ox)S(ph)AN(de)IK_
RIMBP3C	RIMS-binding protein 3C;RIMS-binding protein 3B	1	55.469	_VFVAIS(ph)DY(ph)NPIVM(ox)S(ph)AN(de)IK_
RIMS2	Regulating synaptic membrane exocytosis protein 2	0.999689	86.539	_S(ph)M(ox)PSIM(ox)TGRSAPPSPAISR_
RPS20	40S ribosomal protein S20	0.999988	78.964	_(ac)M(ox)PT(ph)KTIRITTR_
RYR2	Ryanodine receptor 2	0.903271	51.888	_Y(ph)N(de)EVM(ox)QAINM(ox)S(ph)AAITARK_
RYR2	Ryanodine receptor 2	0.998608	51.888	_Y(ph)N(de)EVM(ox)QAINM(ox)S(ph)AAITARK_
S E P 2	Septin-2	1	146.78	_IYHIPDAES(ph)DEDEDFK_
SIPA1L1	Signal-induced proliferation-associated 1-like protein 1	0.990593	146.2	_IIDIES(ph)PTPESQK_
SKIV2L	Helicase SKI2W	0.996422	123.95	_ASS(ph)IEDIVIK_
SLC12A4	Solute carrier family 12 member 4	0.999188	141.1	_IESIYS(ph)DEEDESAVGADK_
SLC25A32	Mitochondrial folate transporter/carrier	0.995834	55.975	_(ac)TICIT(ph)NPIWVT(ph)K_
SLC25A32	Mitochondrial folate transporter/carrier	0.999995	55.975	_(ac)TICIT(ph)NPIWVT(ph)K_
SLIT3	Slit homolog 3 protein	0.991623	125.03	_DS(ph)Y(ph)VEIASAKVR_
SLIT3	Slit homolog 3 protein	0.975311	125.03	_DS(ph)Y(ph)VEIASAKVR_
SMC4	Structural maintenance of chromosomes protein 4	0.807338	245.61	_TES(ph)PATAAETASEEIDN(de)R_
SNTB2	Beta-2-syntrophin	1	144.73	_GPAGEAGAS(ph)PPVR_
SP100	Nuclear autoantigen Sp-100	1	235.25	_SEPVINN(de)DNPIES(ph)NDEK_
SRRM1	Serine/arginine repetitive matrix protein 1	0.999926	139.66	_RIS(ph)PSAS(ph)PPR_
SRRM1	Serine/arginine repetitive matrix protein 1	0.944856	139.66	_RIS(ph)PSAS(ph)PPR_
SULT1B1	Sulfotransferase family cytosolic 1B member 1	1	104.82	_(ac)MIS(ph)PKDIIR_
SUMO1	Small ubiquitin-related modifier 1	0.999985	97.095	_(ac)S(ph)DQEAKPSTEDIGDKK_
SYNE2	Nesprin-2	0.999949	60.246	_T(ph)IS(ph)HHAS(ph)TVQM(ox)AIEDS(ph)EQK_
SYNE2	Nesprin-2	0.829057	60.246	_T(ph)IS(ph)HHAS(ph)TVQM(ox)AIEDS(ph)EQK_
SYNE2	Nesprin-2	0.998905	60.246	_T(ph)IS(ph)HHAS(ph)TVQM(ox)AIEDS(ph)EQK_
SYNE2	Nesprin-2	0.999996	60.246	_T(ph)IS(ph)HHAS(ph)TVQM(ox)AIEDS(ph)EQK_
SYNPO	Synaptopodin	0.99999	85.932	_AAS(ph)PAKPSSIDIVPNIPK_
TCOF1	Treacle protein	1	227.08	_KIGAGEGGEASVS(ph)PEK_
TCTN1	Tectonic-1	0.999993	64.069	_FPSSITS(ph)SICTDNNPAAFIVN(de)QAVKCT(ph)R_
TJP2	Tight junction protein ZO-2	0.89833	71.927	_AAS(ph)S(ph)DQIRDNSPPPAFKPEPPK_

TJP2	Tight junction protein ZO-2	1	127.61	_DNS(ph)PPPAFKPEPPK_
TK2	Thymidine kinase 2, mitochondrial	0.993357	51.771	_WGIT(ph)IQT(ph)YVQIT(ph)M(ox)IDR_
TK2	Thymidine kinase 2, mitochondrial	0.994665	51.771	_WGIT(ph)IQT(ph)YVQIT(ph)M(ox)IDR_
TMPO	Lamina-associated polypeptide 2, isoform alpha	0.832309	142.88	_S(ph)STPIPTISSSAENTR_
TNKS1BP1	182 kDa tankyrase-1-binding protein	0.999944	116.2	_YESQEPIAGQES(ph)PIPIATR_
TOP2B	DNA topoisomerase 2-beta	1	185.34	_FDS(ph)NEEDSASVFSPSFGIK_
TP53BP1	Tumor suppressor p53-binding protein 1	1	217.73	_S(ph)PEPEVISTQEDIFDQSN(de)K_
TRAFD1	TRAF-type zinc finger domain-containing protein 1	0.797962	125.52	_IDSQPQETS(ph)PEIPR_
TRIM28	Transcription intermediary factor 1-beta	0.983773	140.31	_(ac)AASAAAASAAAASAASGS(ph)PGPGEGSAGGEK_
TRIO	Triple functional domain protein	0.999308	95.834	_AGAAS(ph)PINS(ph)PISSAVPSIGK_
TRIO	Triple functional domain protein	0.833841	95.834	_AGAAS(ph)PINS(ph)PISSAVPSIGK_
TSPAN16	Tetraspanin-16	1	109	_(ac)RDVS(ph)PN(de)VIHQK_
UBE2NL	Putative ubiquitin-conjugating enzyme E2 N-like	1	114.31	_TNEAQAIET(ph)AR_
UBE2W	Ubiquitin-conjugating enzyme E2 W	0.999369	76.073	_RS(ph)WGDGSIM(ox)ASM(ox)QK_
UBR1	E3 ubiquitin-protein ligase UBR1	1	54.974	_T(ph)GPFCVN(de)HEPGRAGT(ph)IKEN(de)S(ph)R_
UBR1	E3 ubiquitin-protein ligase UBR1	1	54.974	_T(ph)GPFCVN(de)HEPGRAGT(ph)IKEN(de)S(ph)R_
UBR1	E3 ubiquitin-protein ligase UBR1	1	54.974	_T(ph)GPFCVN(de)HEPGRAGT(ph)IKEN(de)S(ph)R_
Uncharacterised	Uncharacterised	0.999999	82.645	_(ac)M(ox)T(ph)KEIDESR_
URGCP	Upregulator of cell proliferation	0.999969	103.88	_(ac)AS(ph)PGHSDIGEVAPEIK_
USP24	Ubiquitin carboxyl-terminal hydrolase 24	1	127.79	_VSDQNS(ph)PVIPK_
USP31	Ubiquitin carboxyl-terminal hydrolase 31	0.994276	77.744	_SVGS(ph)FM(ox)S(ph)RVIK_
USP31	Ubiquitin carboxyl-terminal hydrolase 31	0.998569	77.744	_SVGS(ph)FM(ox)S(ph)RVIK_
USP53	Inactive ubiquitin carboxyl-terminal hydrolase 53	0.942239	96.391	_QRENQKFPTDN(de)ISS(ph)S(ph)N(de)R_
USP53	Inactive ubiquitin carboxyl-terminal hydrolase 53	0.999999	96.391	_QRENQKFPTDN(de)ISS(ph)S(ph)N(de)R_
WDR44	WD repeat-containing protein 44	1	125.73	_VGN(de)ES(ph)PVQEIK_
ZNF687	Zinc finger protein 687	0.997795	163.68	_ATDIPASAS(ph)PPPVAGVPFFK_

Supplementary Table S8: Phosphoproteins significantly up/ downregulated in both primary meningioma and Ben-Men-1 cells compared to HMC

Gene symbol	Protein name	Log2 FC Meningioma	Log2 FC Ben-Men-1
MAP4	Microtubule-associated protein	-2.57	-0.83
IGF2BP3	Insulin-like growth factor 2 mRNA-binding protein 3	-24.30	-4.70
DDX3X	ATP-dependent RNA helicase DDX3X	-1.18	0.94
GIPC1	PDZ domain-containing protein GIPC1	-22.79	-1.52
SYNJ2	Synaptojanin-2	-23.28	-1.35
DCLK1	Serine/threonine-protein kinase DCLK1	-23.08	-3.08
DHX15	Putative pre-mRNA-splicing factor ATP-dependent RNA helicase DHX15	-22.73	1.47
ZZEF1	Zinc finger ZZ-type and EF-hand domain-containing protein 1	-20.47	-1.57
TGFB1I1	Transforming growth factor beta-1-induced transcript 1 protein	-24.06	-1.61
CALU	Isoform 4 of Calumenin	1.75	1.58
DHX16	Putative pre-mRNA-splicing factor ATP-dependent RNA helicase DHX16	-21.66	1.19
USO1	General vesicular transport factor p115	-2.17	-1.01
RPP40	Ribonuclease P protein subunit p40	-20.58	-1.60
AP2A2	AP-2 complex subunit alpha-2	-22.45	-0.66
UBE4B	Ubiquitin conjugation factor E4 B	-21.62	-1.10
MPZL1	Myelin protein zero-like protein 1	-20.50	-1.64
TRIM16	Tripartite motif-containing protein 16	-22.33	-4.56
ABL1	Tyrosine-protein kinase ABL1	-21.21	-1.21
COL1A1	Collagen alpha-1(I) chain	-20.61	-1.20
CTSD	Cathepsin D;Cathepsin D light chain;Cathepsin D heavy chain	24.61	1.85
PFKM	6-phosphofructokinase, muscle type	-21.73	-2.49
PIP	Prolactin-inducible protein	-22.35	-1.04
HSP90B1	Endoplasmin	-1.62	-0.58
VCL	Vinculin	-22.37	-0.45
PSMB1	Proteasome subunit beta type-1	-1.72	-0.67
COMT	Catechol O-methyltransferase	-22.67	-1.33
PSMA2	Proteasome subunit alpha type-2	-2.37	-0.99
DNAJA1	DnaJ homolog subfamily A member 1	21.16	1.18
HSPA4	Heat shock 70 kDa protein 4	-21.51	1.25

NF2	Merlin	-22.37	-3.22
TALDO1	Transaldolase	-1.14	1.53
TXLNA	Alpha-taxilin	-21.34	0.76
EPS15	Epidermal growth factor receptor substrate 15	-21.88	-1.62
NEDD4	E3 ubiquitin-protein ligase NEDD4;E3 ubiquitin-protein ligase	-21.52	-1.02
CSNK1D	Casein kinase I isoform delta	-22.76	-1.05
PSMB2	Proteasome subunit beta type-2	2.06	-1.05
VPS41	Vacuolar protein sorting-associated protein 41 homolog	-20.95	-1.53
ST13	Hsc70-interacting protein;Putative protein FAM10A5;Putative protein FAM10A4	-0.95	-1.30
HNRNPM	Heterogeneous nuclear ribonucleoprotein M	-22.22	1.67
MSH6	DNA mismatch repair protein Msh6	-21.99	1.30
MLLT4	Afadin	-21.39	0.69
RAP1B	Ras-related protein Rap-1b	-24.69	-2.49
CDC42EP1	Cdc42 effector protein 1	-23.22	-0.64
EXOSC10	Exosome component 10	-20.77	0.86
AKAP12	A-kinase anchor protein 12	-2.99	-3.63
PSME1	Proteasome activator complex subunit 1	1.63	1.57
SPIRE1	Protein spire homolog 1	-20.34	0.83
NEXN	Nexilin	-23.14	-1.47
ANK3	Ankyrin-3	-21.87	-2.10
CKAP5	Cytoskeleton-associated protein 5	-23.43	0.99
CLINT1	Clathrin interactor 1	-1.65	0.66
NONO	Non-POU domain-containing octamer-binding protein	-21.54	1.79
SKIV2L	Helicase SKI2W	-22.44	-1.40
PKN1	Serine/threonine-protein kinase N1	-23.54	-0.89
DBN1	Isoform 3 of Drebrin	-2.98	-2.19
FNDC3B	Fibronectin type III domain-containing protein 3B	-21.86	-2.20
HS1BP3	HCLS1-binding protein 3	-21.98	-1.25
HP1BP3	Heterochromatin protein 1-binding protein 3	-24.45	1.23
SKT	Sickle tail protein homolog	-21.12	-2.21
FAM40A	Protein FAM40A	-20.95	-0.39

FAM160B1	Protein FAM160B1	-21.77	0.96
TTC37	Tetratricopeptide repeat protein 37	-22.12	-1.23
PACS1	Phosphofurin acidic cluster sorting protein 1	-23.67	-1.16
Uncharacterised	Uncharacterized protein FLJ45252	-22.45	-0.98
ARMC9	LisH domain-containing protein ARMC9	-21.37	-4.25
WAPAL	Wings apart-like protein homolog	-20.70	1.08
CENPV	Isoform 3 of Centromere protein V	-22.07	-1.20
PPFIBP1	Liprin-beta-1	-22.58	-0.72
ASCC3	Activating signal cointegrator 1 complex subunit 3	-21.30	-1.43
ARFGAP1	ADP-ribosylation factor GTPase-activating protein 1	-23.70	-1.97
EHBP1	EH domain-binding protein 1	-23.13	-1.52
NAV1	Neuron navigator 1	-24.15	-1.05
MICAL1	Protein-methionine sulfoxide oxidase MICAL1	-22.43	-2.32
GEMIN5	Gem-associated protein 5	-23.31	1.07
ARHGEF40	Rho guanine nucleotide exchange factor 40	-22.75	-1.03
PPP4R1	Serine/threonine-protein phosphatase 4 regulatory subunit 1	-21.71	-0.58
PPIL4	Peptidyl-prolyl cis-trans isomerase-like 4	-21.31	0.42
DHX38	Pre-mRNA-splicing factor ATP-dependent RNA helicase PRP16	-20.71	1.01
TNPO1	Transportin-1	-21.54	1.06
USP9X	Probable ubiquitin carboxyl-terminal hydrolase FAF-X	0.70	0.85
MAGOHB	Protein mago nashi homolog 2	1.71	1.39
KCTD12	BTB/POZ domain-containing protein KCTD12	-25.71	-2.78
SIPA1	Signal-induced proliferation-associated protein 1	-21.86	-3.47
DOCK6	Dedicator of cytokinesis protein 6	-21.56	-3.22
ARAP1	Arf-GAP with Rho-GAP domain, ANK repeat and PH domain-containing protein 1	-21.80	0.89
FMNL2	Formin-like protein 2	-21.30	-2.30
FAM129B	Niban-like protein 1	-1.34	-0.95
PSMB7	Proteasome subunit beta type-7	-1.72	-1.18
PIK3R4	Phosphoinositide 3-kinase regulatory subunit 4	-20.36	-0.95
TUBGCP2	Gamma-tubulin complex component 2	-22.12	-0.52
DDX23	Probable ATP-dependent RNA helicase DDX23	-21.87	0.57

NAA15	N-alpha-acetyltransferase 15, NatA auxiliary subunit	-22.76	0.34
TANC1	Protein TANC1	-20.96	-1.60
ASCC2	Activating signal cointegrator 1 complex subunit 2	-21.79	-1.16
WDR13	WD repeat-containing protein 13	-21.96	-1.71
YTHDC2	Probable ATP-dependent RNA helicase YTHDC2	-22.33	0.85
DOCK5	Dedicator of cytokinesis protein 5	-21.24	1.39
UBE2Z	Ubiquitin-conjugating enzyme E2 Z	-0.66	-0.81
PLEKHA5	Pleckstrin homology domain-containing family A member 5	-21.79	-1.68
CD248	Endosialin	-22.24	-23.31
PLCB1	1-phosphatidylinositol 4,5-bisphosphate phosphodiesterase beta-1	-21.19	-1.34
IMP3	U3 small nucleolar ribonucleoprotein protein IMP3	-21.15	0.64
FAM120A	Constitutive coactivator of PPAR-gamma-like protein 1	-22.32	0.76
DIP2B	Disco-interacting protein 2 homolog B	-21.41	-0.67
RRBP1	Ribosome-binding protein 1	-23.85	-1.16
PI4KB	Phosphatidylinositol 4-kinase beta	-21.89	-0.95
TJP2	Tight junction protein ZO-2	-21.29	1.50
S E P 9	Septin-9	-2.52	-1.38
BAIAP2L1	Brain-specific angiogenesis inhibitor 1-associated protein 2-like protein 1	-23.14	-1.68
ASAP1	Arf-GAP with SH3 domain, ANK repeat and PH domain-containing protein 1	-22.32	-1.26
EPB41L3	Isoform B of Band 4.1-like protein 3	-4.59	-6.33
SH3BP1	SH3 domain-binding protein 1	-23.62	-2.44
TLN2	Talin-2	-21.20	-2.72
RAPGEF2	Rap guanine nucleotide exchange factor 2	-21.33	-2.36

Supplementary Table S9: Proteins identified in a PDLIM2 co-immuinoprecipitation experiment

Gene symbol	Protein name
RPSAP58	40S ribosomal protein SA
ALDOC	Fructose-bisphosphate aldolase C;Fructose-bisphosphate aldolase
CAPZB	F-actin-capping protein subunit beta
CANX	Calnexin
ATP5C1	ATP synthase subunit gamma, mitochondrial;ATP synthase gamma chain
SCML2	Sex comb on midleg-like protein 2
MAP4	Microtubule-associated protein;Microtubule-associated protein 4
EEF1G	Elongation factor 1-gamma
XRN2	5-3 exoribonuclease 2
TKT	Transketolase
HADHB	Trifunctional enzyme subunit beta, mitochondrial;3-ketoacyl-CoA thiolase
PDIA6	Protein disulfide-isomerase A6
RAN	GTP-binding nuclear protein Ran
RPL31	60S ribosomal protein L31
MYL6	Myosin light polypeptide 6
PGK1	Phosphoglycerate kinase 1;Phosphoglycerate kinase
PCMT1	Protein-L-isoaspartate O-methyltransferase;Protein-L-isoaspartate(D-aspartate) O-methyltransferase
RPL37A	60S ribosomal protein L37a
CALD1	Caldesmon
LASP1	LIM and SH3 domain protein 1
MBNL1	Muscleblind-like protein 1;Muscleblind-like protein 3
RPL9	60S ribosomal protein L9
RPS3A	40S ribosomal protein S3a
S E P 1 1	Septin-11
FLNB	Filamin-B
TCP1	T-complex protein 1 subunit alpha
DDOST	Dolichyl-diphosphooligosaccharide--protein glycosyltransferase 48 kDa subunit
RAVER1	Ribonucleoprotein, PTB-Binding 1
MDH2	Malate dehydrogenase, mitochondrial;Malate dehydrogenase

CACNA1C	Voltage-dependent L-type calcium channel subunit alpha-1C
PUF60	Poly(U)-binding-splicing factor PUF60
CRYAB	Alpha-crystallin B chain
ALCAM	CD166 antigen
PHB2	Prohibitin-2
MTHFD1	C-1-tetrahydrofolate synthase, cytoplasmic
TUBA1C	Tubulin alpha-1C chain
MYO1C	Unconventional myosin-Ic
P4HB	Protein disulfide-isomerase
RBMS2	RNA-binding motif, single-stranded-interacting protein 2
FN1	Fibronectin;Anastellin;Ugl-Y1;Ugl-Y2;Ugl-Y3
RTN4	Reticulon-4
PDIA3	Protein disulfide-isomerase A3
ZYX	Zyxin
ATP5B	ATP synthase subunit beta, mitochondrial;ATP synthase subunit beta
RPS17	40S ribosomal protein S17;40S ribosomal protein S17-like
SRP14	Signal recognition particle 14 kDa protein
NCL	Nucleolin
NONO	Non-POU domain-containing octamer-binding protein
MAP3K3	Mitogen-activated protein kinase kinase kinase 3
EIF4A1	Eukaryotic initiation factor 4A-I;Eukaryotic initiation factor 4A-II
RPL13	60S ribosomal protein L13
GPI	Glucose-6-phosphate isomerase
RPS5	40S ribosomal protein S5;40S ribosomal protein S5, N-terminally processed
GIPC1	PDZ domain-containing protein GIPC1
P4HA2	Prolyl 4-hydroxylase subunit alpha-2
ACSL4	Long-chain-fatty-acid--CoA ligase 4
UGDH	UDP-glucose 6-dehydrogenase
CRTAP	Cartilage-associated protein
LMNA	Prelamin-A/C;Lamin-A/C
SLC25A5	ADP/ATP translocase 2

RPLP0	60S acidic ribosomal protein P0;60S acidic ribosomal protein P0-like
ITGB1	Integrin beta-1;Integrin beta
NPM1	Nucleophosmin
CTSD	Cathepsin D;Cathepsin D light chain;Cathepsin D heavy chain
HSPA1A	Heat shock 70 kDa protein 1A/1B;Heat shock 70 kDa protein 6;Heat shock 70 kDa protein 1-like
HSP90AB1	Heat shock protein HSP 90-beta
CNP	2,3-cyclic-nucleotide 3-phosphodiesterase
HSPD1	60 kDa heat shock protein, mitochondrial
PABPC1	Polyadenylate-binding protein 1
SLC25A6	ADP/ATP translocase 3;ADP/ATP translocase 1
RNH1	Ribonuclease inhibitor
EEF2	Elongation factor 2
P4HA1	Prolyl 4-hydroxylase subunit alpha-1
HSP90B1	Endoplasmin
VCL	Vinculin
PGAM1	Phosphoglycerate mutase 1;Phosphoglycerate mutase 2
MX1	Interferon-induced GTP-binding protein Mx1
PAICS	Multifunctional protein ADE2
SPRR2G	Small proline-rich protein 2G
UQCRC2	Cytochrome b-c1 complex subunit 2, mitochondrial
PPIB	Peptidyl-prolyl cis-trans isomerase B
RPS3	40S ribosomal protein S3
ATP5A1	ATP synthase subunit alpha, mitochondrial
DDX6	Probable ATP-dependent RNA helicase DDX6
LOX	Protein-lysine 6-oxidase
MARCKS	Myristoylated alanine-rich C-kinase substrate
RPL12	60S ribosomal protein L12
HSPA4	Heat shock 70 kDa protein 4
STAT1	Signal transducer and activator of transcription 1-alpha/beta
RPS27	40S ribosomal protein S27;40S ribosomal protein S27-like
RPL5	60S ribosomal protein L5

RPS10	40S ribosomal protein S10;Putative 40S ribosomal protein S10-like
IQGAP1	Ras GTPase-activating-like protein IQGAP1
ATP5O	ATP synthase subunit O, mitochondrial
TUFM	Elongation factor Tu, mitochondrial
SERPINH1	Serpin H1
HNRNPM	Heterogeneous nuclear ribonucleoprotein M
CAPZA1	F-actin-capping protein subunit alpha-1
VCP	Transitional endoplasmic reticulum ATPase
RPS20	40S ribosomal protein S20
YWHAG	14-3-3 protein gamma;14-3-3 protein gamma, N-terminally processed
PPP1CA	Serine/threonine-protein phosphatase PP1-alpha catalytic subunit
RPS16	40S ribosomal protein S16
YWHAE	14-3-3 protein epsilon
RPS18	40S ribosomal protein S18
RPS11	40S ribosomal protein S11
PSMC6	26S protease regulatory subunit 10B
RPS4X	40S ribosomal protein S4, X isoform
RPL23	60S ribosomal protein L23
RPS25	40S ribosomal protein S25
RPL10A	60S ribosomal protein L10a
PPIA	Peptidyl-prolyl cis-trans isomerase A;Peptidyl-prolyl cis-trans isomerase
AP2B1	AP-2 complex subunit beta
YBX1	Nuclease-sensitive element-binding protein 1;DNA-binding protein A
ACTC1	Actin, alpha cardiac muscle 1
TUBB4B	Tubulin beta-4B chain
HNRNPU	Heterogeneous nuclear ribonucleoprotein U
PFKP	6-phosphofructokinase type C
LGALS3BP	Galectin-3-binding protein
LOXL1	Lysyl oxidase homolog 1
AHNAK	Neuroblast differentiation-associated protein AHNAK
TUBB3	Tubulin beta-3 chain

TUBB2A	Tubulin beta-2A chain;Tubulin beta-2B chain
MVP	Major vault protein
PLEC	Plectin
PCBP1	Poly(rC)-binding protein 1
PTPN14	Tyrosine-protein phosphatase non-receptor type 14
DPYSL2	Dihydropyrimidinase-related protein 2
HLA-C	HLA class I histocompatibility antigen, Cw-6 alpha chainchain
LEPRE1	Prolyl 3-hydroxylase 1
DECR2	Peroxisomal 2,4-dienoyl-CoA reductase
TLN1	Talin-1
C1orf57	Cancer-related nucleoside-triphosphatase
PTRF	Polymerase I and transcript release factor
MRPL14	39S ribosomal protein L14, mitochondrial
GPR155	Integral membrane protein GPR155
LEPREL1	Prolyl 3-hydroxylase 2
KIAA1967	DBIRD complex subunit KIAA1967
SCCPDH	Saccharopine dehydrogenase-like oxidoreductase
PPP1R13L	RelA-associated inhibitor
PALLD	Palladin
LARP4B	La-related protein 4B
LRRC59	Leucine-rich repeat-containing protein 59
ZC3HAV1L	Zinc finger CCCH-type antiviral protein 1-like
PDLIM2	PDZ and LIM domain protein 2
RBM14	RNA-binding protein 14
VAT1	Synaptic vesicle membrane protein VAT-1 homolog
TUBB6	Tubulin beta-6 chain
EHD1	EH domain-containing protein 1
SLC25A22	Mitochondrial glutamate carrier 1
QPCTL	Glutaminyl-peptide cyclotransferase-like protein
FAM120A	Constitutive coactivator of PPAR-gamma-like protein 1
DNAJB11	DnaJ homolog subfamily B member 11

ACOT9	Acyl-coenzyme A thioesterase 9, mitochondrial
SAMHD1	SAM domain and HD domain-containing protein 1
SQRDL	Sulfide:quinone oxidoreductase, mitochondrial
SAMHD1	SAM domain and HD domain-containing protein 1
SQRDL	Sulfide Quinone Reductase-Like

Supplementary Table S10: Proteins identified in a pSTAT1_Y701 co-immunoprecipitation experiment

Gene symbol	Protein name
RS29	40S ribosomal protein S29
RPSA	40S ribosomal protein SA (Fragment)
RPL23A	60S ribosomal protein L23a
SLC25A6	ADP/ATP translocase 3 (Fragment)
ACTN4	Alpha-actinin-4
AMY1B	Alpha-amylase 1 (Fragment)
ATPA	ATP synthase subunit alpha, mitochondrial
ATPO	ATP synthase subunit O, mitochondrial
BASP1	Brain acid soluble protein 1
CLIP1	CAP-Gly domain-containing linker protein 1
CRTAP	Cartilage-associated protein
CSTA	Cystatin-A
CKAP4	Cytoskeleton-associated protein 4
DSG1	Desmoglein-1
DST	Dystonin
TRIM21	E3 ubiquitin-protein ligase TRIM21
ENPL	Endoplasmin
IF2B	Eukaryotic translation initiation factor 2 subunit 2
IF2G	Eukaryotic translation initiation factor 2 subunit 3
CAZA1	F-actin-capping protein subunit alpha-1
HS90A	Heat shock protein HSP 90-alpha
HBB	Hemoglobin subunit beta
IGLL5	Immunoglobulin lambda-like polypeptide 5
FINC	Isoform 10 of Fibronectin
GOLM1	Isoform 2 of Golgi membrane protein 1
P3H2	Isoform 2 of Prolyl 3-hydroxylase 2
STOX2	Isoform 2 of Storkhead-box protein 2
DUS3L	Isoform 2 of tRNA-dihydrouridine(47) synthase [NAD(P)(+)]-like
CUX1	Isoform 3 of Homeobox protein cut-like 1

MRCKA	Isoform 3 of Serine/threonine-protein kinase MRCK alpha
AKAP9	Isoform 5 of A-kinase anchor protein 9
CALD1	Isoform 5 of Caldesmon
MK14	Isoform CSBP1 of Mitogen-activated protein kinase 14
PLAK	Junction plakoglobin
KRT19	Keratin, type I cytoskeletal 19 (Fragment)
PUR6	Multifunctional protein ADE2
HSD17B4	Peroxisomal multifunctional enzyme type 2
PDIA3	Protein disulfide isomerase family A, member 3, isoform CRA
S10A9	Protein S100-A9
RABGAP1	Rab GTPase-activating protein 1
RALGAPA2	Ral GTPase-activating protein subunit alpha-2
LATS1	Serine/threonine-protein kinase LATS1
SERPH	Serpin H1 OS
STAT1	Signal transducer and activator of transcription 1-alpha/beta
SBSN	Suprabasin
TAGL	Transgelin
TUBB	Tubulin beta chain
Uncharacterised	Uncharacterized protein

References

Aarhus, M., O. Bruland, H. A. Saetran, S. J. Mork, M. Lund-Johansen and P. M. Knappskog (2010). "Global gene expression profiling and tissue microarray reveal novel candidate genes and down-regulation of the tumor suppressor gene CAV1 in sporadic vestibular schwannomas." Neurosurgery **67**(4): 998-1019; discussion 1019.

Aavikko, M., S. P. Li, S. Saarinen, P. Alhopuro, E. Kaasinen, E. Morgunova, Y. Li, K. Vesanen, M. J. Smith, D. G. Evans, M. Poyhonen, A. Kiuru, A. Auvinen, L. A. Aaltonen, J. Taipale and P. Vahteristo (2012). "Loss of SUFU function in familial multiple meningioma." Am J Hum Genet **91**(3): 520-526.

Agarwal, R., S. Liebe, M. L. Turski, S. J. Vidwans, F. Janku, I. Garrido-Laguna, J. Munoz, R. Schwab, J. Rodon, R. Kurzrock, V. Subbiah and G. Pan-Cancer Working (2014). "Targeted therapy for hereditary cancer syndromes: neurofibromatosis type 1, neurofibromatosis type 2, and Gorlin syndrome." Discov Med **18**(101): 323-330.

Agnihotri, S., I. Gugel, M. Remke, A. Bornemann, G. Pantazis, S. C. Mack, D. Shih, S. K. Singh, N. Sabha, M. D. Taylor, M. Tatagiba, G. Zadeh and B. Krischek (2014). "Gene-expression profiling elucidates molecular signaling networks that can be therapeutically targeted in vestibular schwannoma." J Neurosurg **121**(6): 1434-1445.

Ahmad, Z., C. M. Brown, A. K. Patel, A. F. Ryan, R. Ongkeko and J. K. Doherty (2010). "Merlin knockdown in human Schwann cells: clues to vestibular schwannoma tumorigenesis." Otol Neurotol **31**(3): 460-466.

Aktary, Z. and M. Pasdar (2012). "Plakoglobin: role in tumorigenesis and metastasis." Int J Cell Biol **2012**: 189521.

Alanin, M. C., C. Klausen, P. Caye-Thomasen, C. Thomsen, K. Fugleholm, L. Poulsgaard, U. Lassen, M. Mau-Sorensen and K. F. Hofland (2014). "The effect of bevacizumab on vestibular schwannoma tumour size and hearing in patients with neurofibromatosis type 2." Eur Arch Otorhinolaryngol.

Ammoun, S., C. H. Cunliffe, J. C. Allen, L. Chiriboga, F. G. Giancotti, D. Zagzag, C. O. Hanemann and M. A. Karajannis (2010). "ErbB/HER receptor activation and preclinical efficacy of lapatinib in vestibular schwannoma." Neuro Oncol **12**(8): 834-843.

Ammoun, S., C. Flaiz, N. Ristic, J. Schuldt and C. O. Hanemann (2008). "Dissecting and targeting the growth factor-dependent and growth factor-independent extracellular signal-regulated kinase pathway in human schwannoma." Cancer Res **68**(13): 5236-5245.

Ammoun, S. and C. O. Hanemann (2011). "Emerging therapeutic targets in schwannomas and other Merlin-deficient tumors." Nat Rev Neurol **7**(7): 392-399.

Ammoun, S., L. Provenzano, L. Zhou, M. Barczyk, K. Evans, D. A. Hilton, S. Hafizi and C. O. Hanemann (2014). "Axl/Gas6/NFkappaB signalling in schwannoma pathological proliferation, adhesion and survival." Oncogene **33**(3): 336-346.

Ammoun, S., N. Ristic, C. Matthies, D. A. Hilton and C. O. Hanemann (2010). "Targeting ERK1/2 activation and proliferation in human primary schwannoma cells with MEK1/2 inhibitor AZD6244." Neurobiol Dis **37**(1): 141-146.

Ammoun, S., M. C. Schmid, J. Triner, P. Manley and C. O. Hanemann (2011). "Nilotinib alone or in combination with selumetinib is a drug candidate for neurofibromatosis type 2." Neuro Oncol **13**(7): 759-766.

Ammoun, S., M. C. Schmid, L. Zhou, N. Ristic, E. Ercolano, D. A. Hilton, C. M. Perks and C. O. Hanemann (2012). "Insulin-like growth factor-binding protein-1 (IGFBP-1) regulates human schwannoma proliferation, adhesion and survival." Oncogene **31**(13): 1710-1722.

Amsterdam, A., K. C. Sadler, K. Lai, S. Farrington, R. T. Bronson, J. A. Lees and N. Hopkins (2004). "Many ribosomal protein genes are cancer genes in zebrafish." PLoS Biol **2**(5): E139.

Arzt, L., H. Kothmaier, I. Halbwedl, F. Quehenberger and H. H. Popper (2014). "Signal transducer and activator of transcription 1 (STAT1) acts like an oncogene in malignant pleural mesothelioma." Virchows Arch **465**(1): 79-88.

Asghar, U., A. K. Witkiewicz, N. C. Turner and E. S. Knudsen (2015). "The history and future of targeting cyclin-dependent kinases in cancer therapy." Nat Rev Drug Discov **14**(2): 130-146.

Assiddiq, B. F., K. Y. Tan, W. Toy, S. P. Chan, P. K. Chong and Y. P. Lim (2012). "EGFR S1166 phosphorylation induced by a combination of EGF and gefitinib has a potentially negative impact on lung cancer cell growth." J Proteome Res **11**(8): 4110-4119.

Baughn, L. B., M. Di Liberto, R. Niesvizky, H. J. Cho, D. Jayabalan, J. Lane, F. Liu and S. Chen-Kiang (2009). "CDK2 phosphorylation of Smad2 disrupts TGF-beta transcriptional regulation in resistant primary bone marrow myeloma cells." J Immunol **182**(4): 1810-1817.

Baumgarten, P., B. Brokinkel, J. Zinke, C. Zachskorn, H. Ebel, F. K. Albert, W. Stummer, K. H. Plate, P. N. Harter, M. Hasselblatt and M. Mittelbronn (2013). "Expression of vascular endothelial growth factor (VEGF) and its receptors VEGFR1 and VEGFR2 in primary and recurrent WHO grade III meningiomas." Histol Histopathol **28**(9): 1157-1166.

Baxter, D. S., A. Orrego, J. V. Rosenfeld and T. Mathiesen (2014). "An audit of immunohistochemical marker patterns in meningioma." J Clin Neurosci **21**(3): 421-426.

Bello, L., J. Zhang, D. C. Nikas, J. F. Strasser, R. M. Villani, D. A. Cheresh, R. S. Carroll and P. M. Black (2000). "Alpha(v)beta3 and alpha(v)beta5 integrin expression in meningiomas." Neurosurgery **47**(5): 1185-1195.

Bianchi, A. B., S. I. Mitsunaga, J. Q. Cheng, W. M. Klein, S. C. Jhanwar, B. Seizinger, N. Kley, A. J. Klein-Szanto and J. R. Testa (1995). "High frequency of inactivating mutations in the neurofibromatosis type 2 gene (NF2) in primary malignant mesotheliomas." Proc Natl Acad Sci U S A **92**(24): 10854-10858.

Bie, L., G. Zhao, Y. Ju and B. Zhang (2011). "Integrative genomic analysis identifies CCNB1 and CDC2 as candidate genes associated with meningioma recurrence." Cancer Genet **204**(10): 536-540.

Bijlsma, E. K., R. Brouwer-Mladin, D. A. Bosch, A. Westerveld and T. J. Hulsebos (1992). "Molecular characterization of chromosome 22 deletions in schwannomas." Genes Chromosomes Cancer **5**(3): 201-205.

Blume-Jensen, P. and T. Hunter (2001). "Oncogenic kinase signalling." Nature **411**(6835): 355-365.

Bocchini, C. E., M. M. Kasembeli, S. H. Roh and D. J. Tweardy (2014). "Contribution of chaperones to STAT pathway signaling." JAKSTAT **3**(3): e970459.

Boin, A., A. Couvelard, C. Couderc, I. Brito, D. Filipescu, M. Kalamarides, P. Bedossa, L. De Koning, C. Danelsky, T. Dubois, P. Hupe, D. Louvard and D. Lallemand (2014). "Proteomic screening identifies a YAP-driven signaling network linked to tumor cell proliferation in human schwannomas." Neuro Oncol **16**(9): 1196-1209.

Bonnal, S., L. Vigevani and J. Valcarcel (2012). "The spliceosome as a target of novel antitumour drugs." Nat Rev Drug Discov **11**(11): 847-859.

Bowe, R. A., O. T. Cox, V. Ayllon, E. Tresse, N. C. Healy, S. J. Edmunds, M. Huigsloot and R. O'Connor (2014). "PDLIM2 regulates transcription factor activity in epithelial-to-mesenchymal transition via the COP9 signalosome." Mol Biol Cell **25**(1): 184-195.

Brastianos, P. K., P. M. Horowitz, S. Santagata, R. T. Jones, A. McKenna, G. Getz, K. L. Ligon, E. Palescandolo, P. Van Hummelen, M. D. Ducar, A. Raza, A. Sunkavalli, L. E. Macconaill, A. O. Stemmer-Rachamimov, D. N. Louis, W. C. Hahn, I. F. Dunn and R. Beroukhim (2013). "Genomic sequencing of meningiomas identifies oncogenic SMO and AKT1 mutations." Nat Genet **45**(3): 285-289.

Bretscher, A., D. Chambers, R. Nguyen and D. Reczek (2000). "ERM-Merlin and EBP50 protein families in plasma membrane organization and function." Annu Rev Cell Dev Biol **16**: 113-143.

Buckley, P. G., K. K. Mantripragada, T. Diaz de Stahl, A. Piotrowski, C. M. Hansson, H. Kiss, D. Vetrie, I. T. Ernberg, M. Nordenskjold, L. Bolund, M. Sainio, G. A. Rouleau, M. Niimura, A. J. Wallace, D. G. Evans, G. Grigelionis, U. Menzel and J. P. Dumanski (2005). "Identification of genetic aberrations on chromosome 22 outside the NF2 locus in schwannomatosis and neurofibromatosis type 2." Hum Mutat **26**(6): 540-549.

Burke, P., K. Schooler and H. S. Wiley (2001). "Regulation of epidermal growth factor receptor signaling by endocytosis and intracellular trafficking." Mol Biol Cell **12**(6): 1897-1910.

Burns, S. S., E. M. Akhmametyeva, J. L. Oblinger, M. L. Bush, J. Huang, V. Senner, C. S. Chen, A. Jacob, D. B. Welling and L. S. Chang (2013). "Histone deacetylase inhibitor AR-42 differentially affects cell-cycle transit in meningeal and meningioma cells, potently inhibiting NF2-deficient meningioma growth." Cancer Res **73**(2): 792-803.

Cacev, T., G. Aralica, B. Loncar and S. Kapitanovic (2014). "Loss of NF2/Merlin expression in advanced sporadic colorectal cancer." Cell Oncol (Dordr) **37**(1): 69-77.

Carvalho, L. H., I. Smirnov, G. S. Baia, Z. Modrusan, J. S. Smith, P. Jun, J. F. Costello, M. W. McDermott, S. R. Vandenberg and A. Lal (2007). "Molecular signatures define two main classes of meningiomas." Mol Cancer **6**: 64.

Caspi, M., G. Perry, N. Skalka, S. Meisel, A. Firsow, M. Amit and R. Rosin-Arbesfeld (2014). "Aldolase positively regulates of the canonical Wnt signaling pathway." Mol Cancer **13**: 164.

Caye-Thomasen, P., R. Borup, S. E. Stangerup, J. Thomsen and F. C. Nielsen (2010). "Deregulated genes in sporadic vestibular schwannomas." Otol Neurotol **31**(2): 256-266.

Caye-Thomasen, P., K. Werther, A. Nalla, T. C. Bog-Hansen, H. J. Nielsen, S. E. Stangerup and J. Thomsen (2005). "VEGF and VEGF receptor-1 concentration in vestibular schwannoma homogenates correlates to tumor growth rate." Otol Neurotol **26**(1): 98-101.

Chamberlain, M. C. (2011). "Bevacizumab for the treatment of recurrent glioblastoma." Clin Med Insights Oncol **5**: 117-129.

Chambliss, A. B. and D.W. Chan (2016). "Precision medicine: from pharmacogenomics to pharmacoproteomics." Clin Proteomics **13**:25.

Chang, X., L. Shi, F. Gao, J. Russin, L. Zeng, S. He, T. C. Chen, S. L. Giannotta, D. J. Weisenberger, G. Zada, K. Wang and W. J. Mack (2013). "Genomic and transcriptome analysis revealing an oncogenic functional module in meningiomas." Neurosurg Focus **35**(6): E3.

Chen, Y., Q. Xu, D. Ji, Y. Wei, H. Chen, T. Li, B. Wan, L. Yuan, R. Huang and G. Chen (2015). "Inhibition of pentose phosphate pathway suppresses acute myelogenous leukemia." Tumour Biol.

Chishti, A. H., A. C. Kim, S. M. Marfatia, M. Lutchman, M. Hanspal, H. Jindal, S. C. Liu, P. S. Low, G. A. Rouleau, N. Mohandas, J. A. Chasis, J. G. Conboy, P. Gascard, Y. Takakuwa, S. C. Huang, E. J. Benz, Jr., A. Bretscher, R. G. Fehon, J. F. Gusella, V. Ramesh, F. Solomon, V. T. Marchesi, S. Tsukita, S. Tsukita, K. B. Hoover and *et al.* (1998). "The FERM domain: a unique module involved in the linkage of cytoplasmic proteins to the membrane." Trends Biochem Sci **23**(8): 281-282.

Christiaans, I., S. B. Kenter, H. C. Brink, T. A. van Os, F. Baas, P. van den Munckhof, A. M. Kidd and T. J. Hulsebos (2011). "Germline SMARCB1 mutation and somatic NF2 mutations in familial multiple meningiomas." J Med Genet **48**(2): 93-97.

Clark, J. J., M. Provenzano, H. R. Diggelmann, N. Xu, S. S. Hansen and M. R. Hansen (2008). "The ErbB inhibitors trastuzumab and erlotinib inhibit growth of vestibular schwannoma xenografts in nude mice: a preliminary study." Otol Neurotol **29**(6): 846-853.

Clark, V. E., E. Z. Erson-Omay, A. Serin, J. Yin, J. Cotney, K. Ozduman, T. Avsar, J. Li, P. B. Murray, O. Henegariu, S. Yilmaz, J. M. Gunel, G. Carrion-Grant, B. Yilmaz, C. Grady, B. Tanrikulu, M. Bakircioglu, H. Kaymakcalan, A. O. Caglayan, L. Sencar, E. Ceyhun, A. F. Atik, Y. Bayri, H. Bai, L. E. Kolb, R. M. Hebert, S. B. Omay, K. Mishra-Gorur, M. Choi, J. D. Overton, E. C. Holland, S. Mane, M. W. State, K. Bilguvar, J. M. Baehring, P. H. Gutin, J. M. Piepmeier, A. Vortmeyer, C. W. Brennan, M. N. Pamir, T. Kilic, R. P. Lifton, J. P. Noonan, K. Yasuno and M. Gunel (2013). "Genomic analysis of non-NF2 meningiomas reveals mutations in TRAF7, KLF4, AKT1, and SMO." Science **339**(6123): 1077-1080.

Cohen, P. (2000). "The regulation of protein function by multisite phosphorylation--a 25 year update." Trends Biochem Sci **25**(12): 596-601.

Commins, D. L., R. D. Atkinson and M. E. Burnett (2007). "Review of meningioma histopathology." Neurosurg Focus **23**(4): E3.

Cooper, J. and F. G. Giancotti (2014). "Molecular insights into NF2/Merlin tumor suppressor function." FEBS Lett **588**(16): 2743-2752.

Cox, J., M. Y. Hein, C. A. Luber, I. Paron, N. Nagaraj and M. Mann (2014). "Accurate proteome-wide label-free quantification by delayed normalization and maximal peptide ratio extraction, termed MaxLFQ." Mol Cell Proteomics **13**(9): 2513-2526.

Cox, J. and M. Mann (2008). "MaxQuant enables high peptide identification rates, individualized p.p.b.-range mass accuracies and proteome-wide protein quantification." Nat Biotechnol **26**(12): 1367-1372.

Cox, J., N. Neuhauser, A. Michalski, R. A. Scheltema, J. V. Olsen and M. Mann (2011). "Andromeda: a peptide search engine integrated into the MaxQuant environment." J Proteome Res **10**(4): 1794-1805.

Curto, M., B. K. Cole, D. Lallemand, C. H. Liu and A. I. McClatchey (2007). "Contact-dependent inhibition of EGFR signaling by Nf2/Merlin." J Cell Biol **177**(5): 893-903.

Daniels, T. R., E. Bernabeu, J. A. Rodriguez, S. Patel, M. Kozman, D. A. Chiappetta, E. Holler, J. Y. Ljubimova, G. Helguera and M. L. Penichet (2012). "The transferrin receptor and the targeted delivery of therapeutic agents against cancer." Biochim Biophys Acta **1820**(3): 291-317.

Deevi, R. K., O. T. Cox and R. O'Connor (2014). "Essential function for PDLIM2 in cell polarization in three-dimensional cultures by feedback regulation of the beta1-integrin-RhoA signaling axis." Neoplasia **16**(5): 422-431.

Desgrosellier, J. S. and D. A. Cheresh (2010). "Integrins in cancer: biological implications and therapeutic opportunities." Nat Rev Cancer **10**(1): 9-22.

Diaz-Ramos, A., A. Roig-Borrellas, A. Garcia-Melero and R. Lopez-Alemany (2012). "alpha-Enolase, a multifunctional protein: its role on pathophysiological situations." J Biomed Biotechnol **2012**: 156795.

Dvorakova, M., R. Nenutil and P. Bouchal (2014). "Transgelins, cytoskeletal proteins implicated in different aspects of cancer development." Expert Rev Proteomics **11**(2): 149-165.

Elias, J. E. and S. P. Gygi (2010). "Target-decoy search strategy for mass spectrometry-based proteomics." Methods Mol Biol **604**: 55-71.

Escudier, B. and M. Gore (2011). "Axitinib for the management of metastatic renal cell carcinoma." Drugs R D **11**(2): 113-126.

Evans, D. G. (2009). "Neurofibromatosis type 2 (NF2): a clinical and molecular review." Orphanet J Rare Dis **4**: 16.

Evans, D. G., J. M. Birch, R. T. Ramsden, S. Sharif and M. E. Baser (2006). "Malignant transformation and new primary tumours after therapeutic radiation for benign disease: substantial risks in certain tumour prone syndromes." J Med Genet **43**(4): 289-294.

Evans, D. G., S. M. Huson, D. Donnai, W. Neary, V. Blair, V. Newton and R. Harris (1992). "A clinical study of type 2 neurofibromatosis." Q J Med **84**(304): 603-618.

Evans, D. G., A. Moran, A. King, S. Saeed, N. Gurusinghe and R. Ramsden (2005). "Incidence of vestibular schwannoma and neurofibromatosis type 2 in the North West of England over a 10-year period: higher incidence than previously thought." Otol Neurotol **26**(1): 93-97.

Fang, M., J. Yuan, C. Peng and Y. Li (2014). "Collagen as a double-edged sword in tumor progression." Tumour Biol **35**(4): 2871-2882.

Feist, P. and A. B. Hummon (2015). "Proteomic challenges: sample preparation techniques for microgram-quantity protein analysis from biological samples." Int J Mol Sci **16**(2): 3537-3563.

Felley-Bosco, E. and R. Stahel (2014). "Hippo/YAP pathway for targeted therapy." Transl Lung Cancer Res **3**(2): 75-83.

Fevre-Montange, M., J. Champier, A. Durand, A. Wierinckx, J. Honnorat, J. Guyotat and A. Jouvet (2009). "Microarray gene expression profiling in meningiomas: differential expression according to grade or histopathological subtype." Int J Oncol **35**(6): 1395-1407.

Finehout, E. J., J. R. Cantor and K. H. Lee (2005). "Kinetic characterization of sequencing grade modified trypsin." Proteomics **5**(9): 2319-2321.

Flaiz, C., J. Chernoff, S. Ammoun, J. R. Peterson and C. O. Hanemann (2009). "PAK kinase regulates Rac GTPase and is a potential target in human schwannomas." Exp Neurol **218**(1): 137-144.

Flaiz, C., T. Utermark, D. B. Parkinson, A. Poetsch and C. O. Hanemann (2008). "Impaired intercellular adhesion and immature adherens junctions in Merlin-deficient human primary schwannoma cells." Glia **56**(5): 506-515.

Fraenzer, J. T., H. Pan, L. Minimo, Jr., G. M. Smith, D. Knauer and G. Hung (2003). "Overexpression of the NF2 gene inhibits schwannoma cell proliferation through promoting PDGFR degradation." Int J Oncol **23**(6): 1493-1500.

Franceschini, A., D. Szklarczyk, S. Frankild, M. Kuhn, M. Simonovic, A. Roth, J. Lin, P. Minguez, P. Bork, C. von Mering and L. J. Jensen (2013). "STRING v9.1: protein-protein interaction networks, with increased coverage and integration." Nucleic Acids Res **41**(Database issue): D808-815.

Fukuda, I., Y. Hirabayashi-Ishioka, I. Sakikawa, T. Ota, M. Yokoyama, T. Uchiumi and A. Morita (2013). "Optimization of enrichment conditions on TiO_2 chromatography using glycerol as an additive reagent for effective phosphoproteomic analysis." J Proteome Res **12**(12): 5587-5597.

Funaba, M., C. M. Zimmerman and L. S. Mathews (2002). "Modulation of Smad2-mediated signaling by extracellular signal-regulated kinase." J Biol Chem **277**(44): 41361-41368.

Garcia-Rendueles, M. E., J. C. Ricarte-Filho, B. R. Untch, I. Landa, J. A. Knauf, F. Voza, V. E. Smith, I. Ganly, B. S. Taylor, Y. Persaud, G. Oler, Y. Fang, S. C. Jhanwar, A. Viale, A. Heguy, K. H. Huberman, F. Giancotti, R. Ghossein and J. A. Fagin (2015). "NF2 Loss Promotes Oncogenic RAS-Induced Thyroid Cancers via YAP-Dependent Transactivation of RAS Proteins and Sensitizes Them to MEK Inhibition." Cancer Discov **5**(11): 1178-1193.

Gary, R. and A. Bretscher (1995). "Ezrin self-association involves binding of an N-terminal domain to a normally masked C-terminal domain that includes the F-actin binding site." Mol Biol Cell **6**(8): 1061-1075.

Geiger, T. and R. Zaidel-Bar (2012). "Opening the floodgates: proteomics and the integrin adhesome." Curr Opin Cell Biol **24**(5): 562-568.

Ghigna, C., C. Valacca and G. Biamonti (2008). "Alternative splicing and tumor progression." Curr Genomics **9**(8): 556-570.

Goutagny, S., E. Raymond, M. Esposito-Farese, S. Trunet, C. Mawrin, D. Bernardeschi, B. Larroque, O. Sterkers, M. Giovannini and M. Kalamarides (2015). "Phase II study of mTORC1 inhibition by everolimus in neurofibromatosis type 2 patients with growing vestibular schwannomas." J Neurooncol **122**(2): 313-320.

Guo, H., Z. Mi, D. E. Bowles, S. D. Bhattacharya and P. C. Kuo (2010). "Osteopontin and protein kinase C regulate PDLIM2 activation and STAT1 ubiquitination in LPS-treated murine macrophages." J Biol Chem **285**(48): 37787-37796.

Gyorffy, B., Gyorffy, A and Z. Tulassay (2005). "The problem of multiple testing and solutions for genome-wide studies." Orv Hetil **146**(12): 559-63.

Haase, D., S. Schmidl, C. Ewald, R. Kalff, C. Huebner, R. Firsching, G. Keilhoff, M. Evert, W. Paulus, D. H. Gutmann, A. Lal and C. Mawrin (2010). "Fatty acid synthase as a novel target for meningioma therapy." Neuro Oncol **12**(8): 844-854.

Hanahan, D. and R. A. Weinberg (2011). "Hallmarks of cancer: the next generation." Cell **144**(5): 646-674.

Hanemann, C. O. (2008). "Magic but treameningiomas? Tumours due to loss of Merlin." Brain **131**(Pt 3): 606-615.

Hanemann, C. O., B. Bartelt-Kirbach, R. Diebold, K. Kampchen, S. Langmesser and T. Utermark (2006). "Differential gene expression between human schwannoma and control Schwann cells." Neuropathol Appl Neurobiol **32**(6): 605-614.

Hartsock, A. and W. J. Nelson (2008). "Adherens and tight junctions: structure, function and connections to the actin cytoskeleton." Biochim Biophys Acta **1778**(3): 660-669.

Healy, N. C. and R. O'Connor (2009). "Sequestration of PDLIM2 in the cytoplasm of monocytic/macrophage cells is associated with adhesion and increased nuclear activity of NF-kappaB." J Leukoc Biol **85**(3): 481-490.

Hennigan, R. F., C. A. Moon, L. M. Parysek, K. R. Monk, G. Morfini, S. Berth, S. Brady and N. Ratner (2013). "The NF2 tumor suppressor regulates microtubule-based vesicle trafficking via a novel Rac, MLK and p38(SAPK) pathway." Oncogene **32**(9): 1135-1143.

Hideshima, T., D. Chauhan, P. Richardson and K. C. Anderson (2005). "Identification and validation of novel therapeutic targets for multiple myeloma." J Clin Oncol **23**(26): 6345-6350.

Hilton, D. A. and C. O. Hanemann (2014). "Schwannomas and their pathogenesis." Brain Pathol **24**(3): 205-220.

Hilton, D. A., N. Ristic and C. O. Hanemann (2009). "Activation of ERK, AKT and JNK signalling pathways in human schwannomas in situ." Histopathology **55**(6): 744-749.

Hilton, D. A., A. Shivane, L. Kirk, K. Bassiri, D. G. Enki and C. O. Hanemann (2015). "Activation of multiple growth factor signalling pathways is frequent in meningiomas." Neuropathology.

Hirokawa, Y., A. Tikoo, J. Huynh, T. Utermark, C. O. Hanemann, M. Giovannini, G. H. Xiao, J. R. Testa, J. Wood and H. Maruta (2004). "A clue to the therapy of neurofibromatosis type 2: NF2/Merlin is a PAK1 inhibitor." Cancer J **10**(1): 20-26.

Houshmandi, S. S., R. J. Emnett, M. Giovannini and D. H. Gutmann (2009). "The neurofibromatosis type 2 protein, Merlin, regulates glial cell growth in an ErbB2- and Src-dependent manner." Mol Cell Biol **29**(6): 1472-1486.

Huang da, W., B. T. Sherman and R. A. Lempicki (2009). "Systematic and integrative analysis of large gene lists using DAVID bioinformatics resources." Nat Protoc **4**(1): 44-57.

Huang, Y. C., K. C. Wei, C. N. Chang, P. Y. Chen, P. W. Hsu, C. P. Chen, C. S. Lu, H. L. Wang, D. H. Gutmann and T. H. Yeh (2014). "Transglutaminase 2 expression is increased as a function of malignancy grade and negatively regulates cell growth in meningioma." PLoS One **9**(9): e108228.

Hulsebos, T. J., A. S. Plomp, R. A. Wolterman, E. C. Robanus-Maandag, F. Baas and P. Wesseling (2007). "Germline mutation of INI1/SMARCB1 in familial schwannomatosis." Am J Hum Genet **80**(4): 805-810.

Jacob, A., T. X. Lee, B. A. Neff, S. Miller, B. Welling and L. S. Chang (2008). "Phosphatidylinositol 3-kinase/AKT pathway activation in human vestibular schwannoma." Otol Neurotol **29**(1): 58-68.

Jacob, A., J. Oblinger, M. L. Bush, V. Brendel, G. Santarelli, A. R. Chaudhury, S. Kulp, K. M. La Perle, C. S. Chen, L. S. Chang and D. B. Welling (2012). "Preclinical validation of AR42, a novel histone deacetylase inhibitor, as treatment for vestibular schwannomas." Laryngoscope **122**(1): 174-189.

Jacoby, L. B., D. Jones, K. Davis, D. Kronn, M. P. Short, J. Gusella and M. MacCollin (1997). "Molecular analysis of the NF2 tumor-suppressor gene in schwannomatosis." Am J Hum Genet **61**(6): 1293-1302.

Jaffer, Z. M. and J. Chernoff (2002). "p21-activated kinases: three more join the Pak." Int J Biochem Cell Biol **34**(7): 713-717.

James, M. F., S. Han, C. Polizzano, S. R. Plotkin, B. D. Manning, A. O. Stemmer-Rachamimov, J. F. Gusella and V. Ramesh (2009). "NF2/Merlin is a novel negative regulator of mTOR complex 1, and activation of mTORC1 is associated with meningioma and schwannoma growth." Mol Cell Biol **29**(15): 4250-4261.

James, M. F., J. M. Lelke, M. Maccollin, S. R. Plotkin, A. O. Stemmer-Rachamimov, V. Ramesh and J. F. Gusella (2008). "Modeling NF2 with human arachnoidal and meningioma cell culture systems: NF2 silencing reflects the benign character of tumor growth." Neurobiol Dis **29**(2): 278-292.

Janknecht, R. (2010). "Multi-talented DEAD-box proteins and potential tumor promoters: p68 RNA helicase (DDX5) and its paralog, p72 RNA helicase (DDX17)." Am J Transl Res **2**(3): 223-234.

Jones, G. N., C. Tep, W. H. Towns, 2nd, G. Mihai, I. D. Tonks, G. F. Kay, P. M. Schmalbrock, A. O. Stemmer-Rachamimov, S. O. Yoon and L. S. Kirschner (2008). "Tissue-specific ablation of Prkar1a causes schwannomas by suppressing neurofibromatosis protein production." Neoplasia **10**(11): 1213-1221.

Jura, N., N. F. Endres, K. Engel, S. Deindl, R. Das, M. H. Lamers, D. E. Wemmer, X. Zhang and J. Kuriyan (2009). "Mechanism for activation of the EGF receptor catalytic domain by the juxtamembrane segment." Cell **137**(7): 1293-1307.

Kaempchen, K., K. Mielke, T. Utermark, S. Langmesser and C. O. Hanemann (2003). "Upregulation of the Rac1/JNK signaling pathway in primary human schwannoma cells." Hum Mol Genet **12**(11): 1211-1221.

Kang, M., K. H. Lee, H. S. Lee, Y. H. Park, C. W. Jeong, J. H. Ku, H. H. Kim and C. Kwak (2016). "PDLIM2 suppression efficiently reduces tumor growth and invasiveness of human castration-resistant prostate cancer-like cells." Prostate **76**(3): 273-285.

Karajannis, M. A., G. Legault, M. Hagiwara, M. S. Ballas, K. Brown, A. O. Nusbaum, T. Hochman, J. D. Goldberg, K. M. Koch, J. G. Golfinos, J. T. Roland and J. C. Allen (2012). "Phase II trial of lapatinib in adult and pediatric patients with neurofibromatosis type 2 and progressive vestibular schwannomas." Neuro Oncol **14**(9): 1163-1170.

Karpievitch, Y. V., A. R. Dabney and R. D. Smith (2012). "Normalization and missing value imputation for label-free LC-MS analysis." BMC Bioinformatics **13 Suppl 16**: S5.

Kharma, B., T. Baba, N. Matsumura, H. S. Kang, J. Hamanishi, R. Murakami, M. M. McConechy, S. Leung, K. Yamaguchi, Y. Hosoe, Y. Yoshioka, S. K. Murphy, M. Mandai, D. G. Hunstman and I. Konishi (2014). "STAT1 drives tumor progression in serous papillary endometrial cancer." Cancer Res **74**(22): 6519-6530.

Kiosses, W. B., S. J. Shattil, N. Pampori and M. A. Schwartz (2001). "Rac recruits high-affinity integrin alphavbeta3 to lamellipodia in endothelial cell migration." Nat Cell Biol **3**(3): 316-320.

Kissil, J. L., E. W. Wilker, K. C. Johnson, M. S. Eckman, M. B. Yaffe and T. Jacks (2003). "Merlin, the product of the Nf2 tumor suppressor gene, is an inhibitor of the p21-activated kinase, Pak1." Mol Cell **12**(4): 841-849.

Kluba, M., Y. Engelborghs, J. Hofkens and H. Mizuno (2015). "Inhibition of Receptor Dimerization as a Novel Negative Feedback Mechanism of EGFR Signaling." PLoS One **10**(10): e0139971.

Knowlton, A. A., M. Grenier, S. R. Kirchhoff and M. Salfity (2000). "Phosphorylation at tyrosine-524 influences nuclear accumulation of HSP72 with heat stress." Am J Physiol Heart Circ Physiol **278**(6): H2143-2149.

Knudson, A (2001). "Two genetic hits (more or less) to cancer." Nat Rev Cancer **1(**2): 157-162.

Koschny, R., C. Boehm, M. R. Sprick, T. L. Haas, H. Holland, L. X. Xu, W. Krupp, W. C. Mueller, M. Bauer, T. Koschny, M. Keller, P. Sinn, J. Meixensberger, H. Walczak and T. M. Ganten (2014). "Bortezomib sensitizes primary meningioma cells to TRAIL-induced apoptosis by enhancing formation of the death-inducing signaling complex." J Neuropathol Exp Neurol **73**(11): 1034-1046.

Krcmery, J., T. Camarata, A. Kulisz and HG Simon (2010). "Nucleocytoplasmic functions of the PDZ-LIM protein family: new insights into organ development." Bioessays **32**(2):100-8.

Kuroda, I., Y. Shintani, M. Motokawa, S. Abe and M. Furuno (2004). "Phosphopeptide-selective column-switching RP-HPLC with a titania precolumn." Anal Sci **20**(9): 1313-1319.

Lallemand, D., M. Curto, I. Saotome, M. Giovannini and A. I. McClatchey (2003). "NF2 deficiency promotes tumorigenesis and metastasis by destabilizing adherens junctions." Genes Dev **17**(9): 1090-1100.

Lallemand, D., J. Manent, A. Couvelard, A. Watilliaux, M. Siena, F. Chareyre, A. Lampin, M. Niwa-Kawakita, M. Kalamarides and M. Giovannini (2009). "Merlin regulates transmembrane receptor accumulation and signaling at the plasma membrane in primary mouse Schwann cells and in human schwannomas." Oncogene **28**(6): 854-865.

Lallemand, D., A. L. Saint-Amaux and M. Giovannini (2009). "Tumor-suppression functions of Merlin are independent of its role as an organizer of the actin cytoskeleton in Schwann cells." J Cell Sci **122**(Pt 22): 4141-4149.

Larsen, M. R., T. E. Thingholm, O. N. Jensen, P. Roepstorff and T. J. Jorgensen (2005). "Highly selective enrichment of phosphorylated peptides from peptide mixtures using titanium dioxide microcolumns." Mol Cell Proteomics **4**(7): 873-886.

Laurendeau, I., M. Ferrer, D. Garrido, N. D'Haene, P. Ciavarelli, A. Basso, M. Vidaud, I. Bieche, I. Salmon and I. Szijan (2010). "Gene expression profiling of the hedgehog signaling pathway in human meningiomas." Mol Med **16**(7-8): 262-270.

Lemeer, S. and A. J. Heck (2009). "The phosphoproteomics data explosion." Curr Opin Chem Biol **13**(4): 414-420.

Leu, J. I., J. Pimkina, A. Frank, M. E. Murphy and D. L. George (2009). "A small molecule inhibitor of inducible heat shock protein 70." Mol Cell **36**(1): 15-27.

Li, Q., M. R. Nance, R. Kulikauskas, K. Nyberg, R. Fehon, P. A. Karplus, A. Bretscher and J. J. Tesmer (2007). "Self-masking in an intact ERM-Merlin protein: an active role for the central alpha-helical domain." J Mol Biol **365**(5): 1446-1459.

Li, T., J. Zhang, F. Zhu, W. Wen, T. Zykova, X. Li, K. Liu, C. Peng, W. Ma, G. Shi, Z. Dong, A. M. Bode and Z. Dong (2011). "P21-activated protein kinase (PAK2)-mediated c-Jun phosphorylation at 5 threonine sites promotes cell transformation." Carcinogenesis **32**(5): 659-666.

Li, W., J. Cooper, L. Zhou, C. Yang, H. Erdjument-Bromage, D. Zagzag, M. Snuderl, M. Ladanyi, C. O. Hanemann, P. Zhou, M. A. Karajannis and F. G. Giancotti (2014). "Merlin/NF2 loss-driven tumorigenesis linked to CRL4(DCAF1)-mediated inhibition of the hippo pathway kinases Lats1 and 2 in the nucleus." Cancer Cell **26**(1): 48-60.

Li, X., Y. Huang, J. Jiang and S. J. Frank (2008). "ERK-dependent threonine phosphorylation of EGF receptor modulates receptor downregulation and signaling." Cell Signal **20**(11): 2145-2155.

Li, Y., H. Zhou, F. Li, S. W. Chan, Z. Lin, Z. Wei, Z. Yang, F. Guo, C. J. Lim, W. Xing, Y. Shen, W. Hong, J. Long and M. Zhang (2015). "Angiomotin binding-induced activation of Merlin/NF2 in the Hippo pathway." Cell Res **25**(7): 801-817.

Lottrich, M., C. Mawrin, K. Chamaon, E. Kirches, K. Dietzmann and B. Freigang (2007). "Expression of transforming growth factor-beta receptor type 1 and type 2 in human sporadic vestibular Schwannoma." Pathol Res Pract **203**(4): 245-249.

Loughran, G., N. C. Healy, P. A. Kiely, M. Huigsloot, N. L. Kedersha and R. O'Connor (2005). "Mystique is a new insulin-like growth factor-I-regulated PDZ-LIM domain protein that

promotes cell attachment and migration and suppresses Anchorage-independent growth." Mol Biol Cell **16**(4): 1811-1822.

Lusis, E. A., M. R. Chicoine and A. Perry (2005). "High throughput screening of meningioma biomarkers using a tissue microarray." J Neurooncol **73**(3): 219-223.

MacCollin, M., W. Woodfin, D. Kronn and M. P. Short (1996). "Schwannomatosis: a clinical and pathologic study." Neurology **46**(4): 1072-1079.

Magrassi, L., C. De-Fraja, L. Conti, G. Butti, L. Infuso, S. Govoni and E. Cattaneo (1999). "Expression of the JAK and STAT superfamilies in human meningiomas." J Neurosurg **91**(3): 440-446.

Maillo, A., A. Orfao, A. B. Espinosa, J. M. Sayagues, M. Merino, P. Sousa, M. Lara and M. D. Tabernero (2007). "Early recurrences in histologically benign/grade I meningiomas are associated with large tumors and coexistence of monosomy 14 and del(1p36) in the ancestral tumor cell clone." Neuro Oncol **9**(4): 438-446.

Mainiero, F., C. Murgia, K. K. Wary, A. M. Curatola, A. Pepe, M. Blumemberg, J. K. Westwick, C. J. Der and F. G. Giancotti (1997). "The coupling of alpha6beta4 integrin to Ras-MAP kinase pathways mediated by Shc controls keratinocyte proliferation." EMBO J **16**(9): 2365-2375.

Maitra, S., R. M. Kulikauskas, H. Gavilan and R. G. Fehon (2006). "The tumor suppressors Merlin and Expanded function cooperatively to modulate receptor endocytosis and signaling." Curr Biol **16**(7): 702-709.

Makino, K., H. Nakamura, T. Hide, S. Yano, J. Kuroda, K. Iyama and J. Kuratsu (2012). "Fatty acid synthase is a predictive marker for aggressiveness in meningiomas." J Neurooncol **109**(2): 399-404.

Makrantoni, V., R. Antrobus, C. H. Botting and P. J. Coote (2005). "Rapid enrichment and analysis of yeast phosphoproteins using affinity chromatography, 2D-PAGE and peptide mass fingerprinting." Yeast **22**(5): 401-414.

Marte, B. (2013). "Tumour heterogeneity." Nature **501**(7647): 327.

Massague, J. (2008). "A very private TGF-beta receptor embrace." Mol Cell **29**(2): 149-150.

Mawrin, C. and A. Perry (2010). "Pathological classification and molecular genetics of meningiomas." J Neurooncol **99**(3): 379-391.

Meimoun, P., F. Ambard-Bretteville, C. Colas-des Francs-Small, B. Valot and J. Vidal (2007). "Analysis of plant phosphoproteins." Anal Biochem **371**(2): 238-246.

Metodiev, M. V., A. Timanova and D. E. Stone (2004). "Differential phosphoproteome profiling by affinity capture and tandem matrix-assisted laser desorption/ionization mass spectrometry." Proteomics **4**(5): 1433-1438.

Morrison, H., T. Sperka, J. Manent, M. Giovannini, H. Ponta and P. Herrlich (2007). "Merlin/neurofibromatosis type 2 suppresses growth by inhibiting the activation of Ras and Rac." Cancer Res **67**(2): 520-527.

Morrow, K. A., S. Das, B. J. Metge, K. Ye, M. S. Mulekar, J. A. Tucker, R. S. Samant and L. A. Shevde (2011). "Loss of tumor suppressor Merlin in advanced breast cancer is due to post-translational regulation." J Biol Chem **286**(46): 40376-40385.

Mowen, K. and M. David (2000). "Regulation of STAT1 nuclear export by Jak1." Mol Cell Biol **20**(19): 7273-7281.

Mukherjee, J., D. Kamnasaran, A. Balasubramaniam, I. Radovanovic, G. Zadeh, T. R. Kiehl and A. Guha (2009). "Human schwannomas express activated platelet-derived growth factor receptors and c-kit and are growth inhibited by Gleevec (Imatinib Mesylate)." Cancer Res **69**(12): 5099-5107.

Mullen, G. E. and L. Yet (2015). "Progress in the development of fatty acid synthase inhibitors as anticancer targets." Bioorg Med Chem Lett **25**(20): 4363-4369.

Muranen, T., M. Gronholm, A. Lampin, D. Lallemand, F. Zhao, M. Giovannini and O. Carpen (2007). "The tumor suppressor Merlin interacts with microtubules and modulates Schwann cell microtubule cytoskeleton." Hum Mol Genet **16**(14): 1742-1751.

Murray, L. B., Y. K. Lau and Q. Yu (2012). "Merlin is a negative regulator of human melanoma growth." PLoS One **7**(8): e43295.

Nordqvist, A. C., M. Peyrard, H. Pettersson, T. Mathiesen, V. P. Collins, J. P. Dumanski and M. Schalling (1997). "A high ratio of insulin-like growth factor II/insulin-like growth factor

binding protein 2 messenger RNA as a marker for anaplasia in meningiomas." Cancer Res **57**(13): 2611-2614.

Nunes, F. P., V. L. Merker, D. Jennings, P. A. Caruso, E. di Tomaso, A. Muzikansky, F. G. Barker, 2nd, A. Stemmer-Rachamimov and S. R. Plotkin (2013). "Bevacizumab treatment for meningiomas in NF2: a retrospective analysis of 15 patients." PLoS One **8**(3): e59941.

Okamoto, H., J. Li, A. O. Vortmeyer, H. Jaffe, Y. S. Lee, S. Glasker, T. S. Sohn, W. Zeng, B. Ikejiri, M. A. Proescholdt, C. Mayer, R. J. Weil, E. H. Oldfield and Z. Zhuang (2006). "Comparative proteomic profiles of meningioma subtypes." Cancer Res **66**(20): 10199-10204.

Olsen, J. V., B. Blagoev, F. Gnad, B. Macek, C. Kumar, P. Mortensen and M. Mann (2006). "Global, in vivo, and site-specific phosphorylation dynamics in signaling networks." Cell **127**(3): 635-648.

Pachow, D., N. Andrae, N. Kliese, F. Angenstein, O. Stork, A. Wilisch-Neumann, E. Kirches and C. Mawrin (2013). "mTORC1 inhibitors suppress meningioma growth in mouse models." Clin Cancer Res **19**(5): 1180-1189.

Park, G. H., S. J. Lee, H. Yim, J. H. Han, H. J. Kim, Y. B. Sohn, J. M. Ko and S. Y. Jeong (2014). "TAGLN expression is upregulated in NF1-associated malignant peripheral nerve sheath tumors by hypomethylation in its promoter and subpromoter regions." Oncol Rep **32**(4): 1347-1354.

Paul, N. R., J. L. Allen, A. Chapman, M. Morlan-Mairal, E. Zindy, G. Jacquemet, L. Fernandez del Ama, N. Ferizovic, D. M. Green, J. D. Howe, E. Ehler, A. Hurlstone and P. T. Caswell (2015). "alpha5beta1 integrin recycling promotes Arp2/3-independent cancer cell invasion via the formin FHOD3." J Cell Biol **210**(6): 1013-1031.

Petrilli, A., A. Copik, M. Posadas, L. S. Chang, D. B. Welling, M. Giovannini and C. Fernandez-Valle (2014). "LIM domain kinases as potential therapeutic targets for neurofibromatosis type 2." Oncogene **33**(27): 3571-3582.

Petrilli, A. M., M. A. Fuse, M. S. Donnan, M. Bott, N. A. Sparrow, D. Tondera, J. Huffziger, C. Frenzel, C. S. Malany, C. J. Echeverri, L. Smith and C. Fernandez-Valle (2014). "A

chemical biology approach identified PI3K as a potential therapeutic target for neurofibromatosis type 2." Am J Transl Res **6**(5): 471-493.

Peyre, M., C. Salaud, E. Clermont-Taranchon, M. Niwa-Kawakita, S. Goutagny, C. Mawrin, M. Giovannini and M. Kalamarides (2015). "PDGF activation in PGDS-positive arachnoid cells induces meningioma formation in mice promoting tumor progression in combination with Nf2 and Cdkn2ab loss." Oncotarget **6**(32): 32713-32722.

Pfister, C., H. Pfrommer, M. S. Tatagiba and F. Roser (2012). "Vascular endothelial growth factor signals through platelet-derived growth factor receptor beta in meningiomas in vitro." Br J Cancer **107**(10): 1702-1713.

Pinkse, M. W., P. M. Uitto, M. J. Hilhorst, B. Ooms and A. J. Heck (2004). "Selective isolation at the femtomole level of phosphopeptides from proteolytic digests using 2D-NanoLC-ESI-MS/MS and titanium oxide precolumns." Anal Chem **76**(14): 3935-3943.

Piotrowski, A., J. Xie, Y. F. Liu, A. B. Poplawski, A. R. Gomes, P. Madanecki, C. Fu, M. R. Crowley, D. K. Crossman, L. Armstrong, D. Babovic-Vuksanovic, A. Bergner, J. O. Blakeley, A. L. Blumenthal, M. S. Daniels, H. Feit, K. Gardner, S. Hurst, C. Kobelka, C. Lee, R. Nagy, K. A. Rauen, J. M. Slopis, P. Suwannarat, J. A. Westman, A. Zanko, B. R. Korf and L. M. Messiaen (2014). "Germline loss-of-function mutations in LZTR1 predispose to an inherited disorder of multiple schwannomas." Nat Genet **46**(2): 182-187.

Plotkin, S. R., V. L. Merker, C. Halpin, D. Jennings, M. J. McKenna, G. J. Harris and F. G. Barker, 2nd (2012). "Bevacizumab for progressive vestibular schwannoma in neurofibromatosis type 2: a retrospective review of 31 patients." Otol Neurotol **33**(6): 1046-1052.

Pranjol, M. Z., N. Gutowski, M. Hannemann and J. Whatmore (2015). "The Potential Role of the Proteases Cathepsin D and Cathepsin L in the Progression and Metastasis of Epithelial Ovarian Cancer." Biomolecules **5**(4): 3260-3279.

Puttmann, S., V. Senner, S. Braune, B. Hillmann, R. Exeler, C. H. Rickert and W. Paulus (2005). "Establishment of a benign meningioma cell line by hTERT-mediated immortalization." Lab Invest **85**(9): 1163-1171.

Quan, M., J. Cui, T. Xia, Z. Jia, D. Xie, D. Wei, S. Huang, Q. Huang, S. Zheng and K. Xie (2015). "Merlin/NF2 Suppresses Pancreatic Tumor Growth and Metastasis by Attenuating the FOXM1-Mediated Wnt/beta-catenin Signaling." Cancer Res.

Rak, R., R. Haklai, G. Elad-Tzfadia, H. J. Wolfson, S. Carmeli and Y. Kloog (2014). "Novel LIMK2 Inhibitor Blocks Panc-1 Tumor Growth in a mouse xenograft model." Oncoscience **1**(1): 39-48.

Rappsilber, J., Y. Ishihama and M. Mann (2003). "Stop and go extraction tips for matrix-assisted laser desorption/ionization, nanoelectrospray, and LC/MS sample pretreatment in proteomics." Anal Chem **75**(3): 663-670.

Reimand, J. and G. D. Bader (2013). "Systematic analysis of somatic mutations in phosphorylation signaling predicts novel cancer drivers." Mol Syst Biol **9**: 637.

Ritterson Lew, C. and D. R. Tolan (2012). "Targeting of several glycolytic enzymes using RNA interference reveals aldolase affects cancer cell proliferation through a non-glycolytic mechanism." J Biol Chem **287**(51): 42554-42563.

Robinson, M. S. (2015). "Forty Years of Clathrin-coated Vesicles." Traffic **16**(12): 1210-1238.

Rodriguez, F. J., C. A. Stratakis and D. G. Evans (2012). "Genetic predisposition to peripheral nerve neoplasia: diagnostic criteria and pathogenesis of neurofibromatoses, Carney complex, and related syndromes." Acta Neuropathol **123**(3): 349-367.

Rong, R., E. I. Surace, C. A. Haipek, D. H. Gutmann and K. Ye (2004). "Serine 518 phosphorylation modulates Merlin intramolecular association and binding to critical effectors important for NF2 growth suppression." Oncogene **23**(52): 8447-8454.

Rong, R., X. Tang, D. H. Gutmann and K. Ye (2004). "Neurofibromatosis type 2 (NF2) tumor suppressor Merlin inhibits phosphatidylinositol 3-kinase through binding to PIKE-L." Proc Natl Acad Sci U S A **101**(52): 18200-18205.

Rouleau, G. A., P. Merel, M. Lutchman, M. Sanson, J. Zucman, C. Marineau, K. Hoang-Xuan, S. Demczuk, C. Desmaze, B. Plougastel and *et al.* (1993). "Alteration in a new gene encoding a putative membrane-organizing protein causes neuro-fibromatosis type 2." Nature **363**(6429): 515-521.

Rubashkin, M. G., L. Cassereau, R. Bainer, C. C. DuFort, Y. Yui, G. Ou, M. J. Paszek, M. W. Davidson, Y. Y. Chen and V. M. Weaver (2014). "Force engages vinculin and promotes tumor progression by enhancing PI3K activation of phosphatidylinositol (3,4,5)-triphosphate." Cancer Res **74**(17): 4597-4611.

Rugo, H. S., A. J. Chien, S. X. Franco, A. T. Stopeck, A. Glencer, S. Lahiri, M. C. Arbushites, J. Scott, J. W. Park, C. Hudis, B. Nulsen and M. N. Dickler (2012). "A phase II study of lapatinib and bevacizumab as treatment for HER2-overexpressing metastatic breast cancer." Breast Cancer Res Treat **134**(1): 13-20.

Ruprecht, B., H. Koch, G. Medard, M. Mundt, B. Kuster and S. Lemeer (2015). "Comprehensive and reproducible phosphopeptide enrichment using iron immobilized metal ion affinity chromatography (Fe-IMAC) columns." Mol Cell Proteomics **14**(1): 205-215.

Ruttledge, M. H., A. A. Andermann, C. M. Phelan, J. O. Claudio, F. Y. Han, N. Chretien, S. Rangaratnam, M. MacCollin, P. Short, D. Parry, V. Michels, V. M. Riccardi, R. Weksberg, K. Kitamura, J. M. Bradburn, B. D. Hall, P. Propping and G. A. Rouleau (1996). "Type of mutation in the neurofibromatosis type 2 gene (NF2) frequently determines severity of disease." Am J Hum Genet **59**(2): 331-342.

Sabha, N., K. Au, S. Agnihotri, S. Singh, R. Mangat, A. Guha and G. Zadeh (2012). "Investigation of the in vitro therapeutic efficacy of nilotinib in immortalized human NF2-null vestibular schwannoma cells." PLoS One **7**(6): e39412.

Santamaria, E., V. Sanchez-Quiles, J. Fernandez-Irigoyen and F. J. Corrales (2012). "A combination of affinity chromatography, 2D DIGE, and mass spectrometry to analyze the phosphoproteome of liver progenitor cells." Methods Mol Biol **909**: 165-180.

Sanzey, M., S. A. Abdul Rahim, A. Oudin, A. Dirkse, T. Kaoma, L. Vallar, C. Herold-Mende, R. Bjerkvig, A. Golebiewska and S. P. Niclou (2015). "Comprehensive analysis of glycolytic enzymes as therapeutic targets in the treatment of glioblastoma." PLoS One **10**(5): e0123544.

Saydam, O., O. Senol, T. B. Schaaij-Visser, T. V. Pham, S. R. Piersma, A. O. Stemmer-Rachamimov, T. Wurdinger, S. M. Peerdeman and C. R. Jimenez (2010).

"Comparative protein profiling reveals minichromosome maintenance (MCM) proteins as novel potential tumor markers for meningiomas." J Proteome Res **9**(1): 485-494.

Schmitt, E., M. Gehrmann, M. Brunet, G. Multhoff and C. Garrido (2007). "Intracellular and extracellular functions of heat shock proteins: repercussions in cancer therapy." J Leukoc Biol **81**(1): 15-27.

Schroeder, R. D., L. S. Angelo and R. Kurzrock (2014). "NF2/Merlin in hereditary neurofibromatosis type 2 versus cancer: biologic mechanisms and clinical associations." Oncotarget **5**(1): 67-77.

Scieglinska, D., A. Gogler-Piglowska, D. Butkiewicz, M. Chekan, E. Malusecka, J. Harasim, A. Habryka and Z. Krawczyk (2014). "HSPA2 is expressed in human tumors and correlates with clinical features in non-small cell lung carcinoma patients." Anticancer Res **34**(6): 2833-2840.

Scoles, D. R., D. P. Huynh, M. S. Chen, S. P. Burke, D. H. Gutmann and S. M. Pulst (2000). "The neurofibromatosis type 2 tumor suppressor protein interacts with hepatocyte growth factor-regulated tyrosine kinase substrate." Hum Mol Genet **9**(11): 1567-1574.

Seo, J. H., K. H. Park, E. J. Jeon, K. H. Chang, H. Lee, W. Lee and Y. S. Park (2015). "Proteomic analysis of vestibular schwannoma: conflicting role of apoptosis on the pathophysiology of sporadic vestibular schwannoma." Otol Neurotol **36**(4): 714-719.

Shapiro, I. M., V. N. Kolev, C. M. Vidal, Y. Kadariya, J. E. Ring, Q. Wright, D. T. Weaver, C. Menges, M. Padval, A. I. McClatchey, Q. Xu, J. R. Testa and J. A. Pachter (2014). "Merlin deficiency predicts FAK inhibitor sensitivity: a synthetic lethal relationship." Sci Transl Med **6**(237): 237ra268.

Sharma, K., R. C. D'Souza, S. Tyanova, C. Schaab, J. R. Wisniewski, J. Cox and M. Mann (2014). "Ultradeep human phosphoproteome reveals a distinct regulatory nature of Tyr and Ser/Thr-based signaling." Cell Rep **8**(5): 1583-1594.

Sharma, S., S. Ray, A. Moiyadi, E. Sridhar and S. Srivastava (2014). "Quantitative proteomic analysis of meningiomas for the identification of surrogate protein markers." Sci Rep **4**: 7140.

Sharma, S., S. Ray, S. Mukherjee, A. Moiyadi, E. Sridhar and S. Srivastava (2015). "Multipronged quantitative proteomic analyses indicate modulation of various signal transduction pathways in human meningiomas." Proteomics **15**(2-3): 394-407.

Sher, I., C. O. Hanemann, P. A. Karplus and A. Bretscher (2012). "The tumor suppressor Merlin controls growth in its open state, and phosphorylation converts it to a less-active more-closed state." Dev Cell **22**(4): 703-705.

Shevchenko, A., M. Wilm, O. Vorm and M. Mann (1996). "Mass spectrometric sequencing of proteins silver-stained polyacrylamide gels." Anal Chem **68**(5): 850-858.

Shishiba, T., M. Niimura, F. Ohtsuka and N. Tsuru (1984). "Multiple cutaneous neurilemmomas as a skin manifestation of neurilemmomatosis." J Am Acad Dermatol **10**(5 Pt 1): 744-754.

Shuai, K., A. Ziemiecki, A. F. Wilks, A. G. Harpur, H. B. Sadowski, M. Z. Gilman and J. E. Darnell (1993). "Polypeptide signalling to the nucleus through tyrosine phosphorylation of Jak and Stat proteins." Nature **366**(6455): 580-583.

Siegel, M. and C. Khosla (2007). "Transglutaminase 2 inhibitors and their therapeutic role in disease states." Pharmacol Ther **115**(2): 232-245.

Slusarz, K. M., V. L. Merker, A. Muzikansky, S. A. Francis and S. R. Plotkin (2014). "Long-term toxicity of bevacizumab therapy in neurofibromatosis type 2 patients." Cancer Chemother Pharmacol **73**(6): 1197-1204.

Smith, M. J. (2015). "Germline and somatic mutations in meningiomas." Cancer Genet **208**(4): 107-114.

Smole, Z., C. R. Thoma, K. T. Applegate, M. Duda, K. L. Gutbrodt, G. Danuser and W. Krek (2014). "Tumor suppressor NF2/Merlin is a microtubule stabilizer." Cancer Res **74**(1): 353-362.

Stewart, II, T. Thomson and D. Figeys (2001). "18O labeling: a tool for proteomics." Rapid Commun Mass Spectrom **15**(24): 2456-2465.

Takishima, K., I. Griswold-Prenner, T. Ingebritsen and M. R. Rosner (1991). "Epidermal growth factor (EGF) receptor T669 peptide kinase from 3T3-L1 cells is an EGF-stimulated "MAP" kinase." Proc Natl Acad Sci U S A **88**(6): 2520-2524.

Tanaka, T., M. J. Grusby and T. Kaisho (2007). "PDLIM2-mediated termination of transcription factor NF-kappaB activation by intranuclear sequestration and degradation of the p65 subunit." Nat Immunol **8**(6): 584-591.

Tanaka, T., A. Shibazaki, R. Ono and T. Kaisho (2014). "HSP70 mediates degradation of the p65 subunit of nuclear factor kappaB to inhibit inflammatory signaling." Sci Signal **7**(356): ra119.

Tanaka, T., M. A. Soriano and M. J. Grusby (2005). "SLIM is a nuclear ubiquitin E3 ligase that negatively regulates STAT signaling." Immunity **22**(6): 729-736.

Teis, D., W. Wunderlich and L. A. Huber (2002). "Localization of the MP1-MAPK scaffold complex to endosomes is mediated by p14 and required for signal transduction." Dev Cell **3**(6): 803-814.

Thang, N. D., I. Yajima, M. Y. Kumasaka, M. Iida, T. Suzuki and M. Kato (2015). "Deltex-3-like (DTX3L) stimulates metastasis of melanoma through FAK/PI3K/AKT but not MEK/ERK pathway." Oncotarget **6**(16): 14290-14299.

Topolska-Wos, A. M., W. J. Chazin and A. Filipek (2016). "CacyBP/SIP - Structure and variety of functions." Biochim Biophys Acta **1860**(1 Pt A): 79-85.

Torrado, M., V. V. Senatorov, R. Trivedi, R. N. Fariss and S. I. Tomarev (2004). "Pdlim2, a novel PDZ-LIM domain protein, interacts with alpha-actinins and filamin A." Invest Ophthalmol Vis Sci **45**(11): 3955-3963.

Torres-Martin, M., L. Lassaletta, A. Isla, J. M. De Campos, G. R. Pinto, R. R. Burbano, J. S. Castresana, B. Melendez and J. A. Rey (2014). "Global expression profile in low grade meningiomas and schwannomas shows upregulation of PDGFD, CDH1 and SLIT2 compared to their healthy tissue." Oncol Rep **32**(6): 2327-2334.

Torres-Martin, M., L. Lassaletta, J. San-Roman-Montero, J. M. De Campos, A. Isla, J. Gavilan, B. Melendez, G. R. Pinto, R. R. Burbano, J. S. Castresana and J. A. Rey (2013). "Microarray analysis of gene expression in vestibular schwannomas reveals SPP1/MET signaling pathway and androgen receptor deregulation." Int J Oncol **42**(3): 848-862.

Uesaka, T., T. Shono, S. O. Suzuki, A. Nakamizo, H. Niiro, M. Mizoguchi, T. Iwaki and T. Sasaki (2007). "Expression of VEGF and its receptor genes in intracranial schwannomas." J Neurooncol **83**(3): 259-266.

Utermark, T., K. Kaempchen and C. O. Hanemann (2003). "Pathological adhesion of primary human schwannoma cells is dependent on altered expression of integrins." Brain Pathol **13**(3): 352-363.

van der Flier, A. and A. Sonnenberg (2001). "Structural and functional aspects of filamins." Biochim Biophys Acta **1538**(2-3): 99-117.

van Sluis, M. and B. McStay (2014). "Ribosome biogenesis: Achilles heel of cancer?" Genes Cancer **5**(5-6): 152-153.

Wang, X., Y. Gong, D. Wang, Q. Xie, M. Zheng, Y. Zhou, Q. Li, Z. Yang, H. Tang, Y. Li, R. Hu, X. Chen and Y. Mao (2012). "Analysis of gene expression profiling in meningioma: deregulated signaling pathways associated with meningioma and EGFL6 overexpression in benign meningioma tissue and serum." PLoS One **7**(12): e52707.

Watson, M. A., D. H. Gutmann, K. Peterson, M. R. Chicoine, B. K. Kleinschmidt-DeMasters, H. G. Brown and A. Perry (2002). "Molecular characterization of human meningiomas by gene expression profiling using high-density oligonucleotide microarrays." Am J Pathol **161**(2): 665-672.

Wen, Z., Z. Zhong and J. E. Darnell, Jr. (1995). "Maximal activation of transcription by Stat1 and Stat3 requires both tyrosine and serine phosphorylation." Cell **82**(2): 241-250.

Wernicke, A. G., A. P. Dicker, M. Whiton, J. Ivanidze, T. Hyslop, E. H. Hammond, A. Perry, D. W. Andrews and L. Kenyon (2010). "Assessment of Epidermal Growth Factor Receptor (EGFR) expression in human meningioma." Radiat Oncol **5**: 46.

Wiemels, J., M. Wrensch and E. B. Claus (2010). "Epidemiology and etiology of meningioma." J Neurooncol **99**(3): 307-314.

Wilisch-Neumann, A., N. Kliese, D. Pachow, T. Schneider, J. P. Warnke, W. E. Braunsdorf, F. D. Bohmer, P. Hass, D. Pasemann, C. Helbing, E. Kirches and C. Mawrin (2013). "The integrin inhibitor cilengitide affects meningioma cell motility and invasion." Clin Cancer Res **19**(19): 5402-5412.

Wisniewski, J. R., N. Nagaraj, A. Zougman, F. Gnad and M. Mann (2010). "Brain phosphoproteome obtained by a FASP-based method reveals plasma membrane protein topology." J Proteome Res **9**(6): 3280-3289.

Wong, H. K., J. Lahdenranta, W. S. Kamoun, A. W. Chan, A. I. McClatchey, S. R. Plotkin, R. K. Jain and E. di Tomaso (2010). "Anti-vascular endothelial growth factor therapies as a novel therapeutic approach to treating neurofibromatosis-related tumors." Cancer Res **70**(9): 3483-3493.

Wrobel, G., P. Roerig, F. Kokocinski, K. Neben, M. Hahn, G. Reifenberger and P. Lichter (2005). "Microarray-based gene expression profiling of benign, atypical and anaplastic meningiomas identifies novel genes associated with meningioma progression." Int J Cancer **114**(2): 249-256.

Wu, F. H., Y. Yuan, D. Li, S. J. Liao, B. Yan, J. J. Wei, Y. H. Zhou, J. H. Zhu, G. M. Zhang and Z. H. Feng (2012). "Extracellular HSPA1A promotes the growth of hepatocarcinoma by augmenting tumor cell proliferation and apoptosis-resistance." Cancer Lett **317**(2): 157-164.

Xiao, G. H., R. Gallagher, J. Shetler, K. Skele, D. A. Altomare, R. G. Pestell, S. Jhanwar and J. R. Testa (2005). "The NF2 tumor suppressor gene product, Merlin, inhibits cell proliferation and cell cycle progression by repressing cyclin D1 expression." Mol Cell Biol **25**(6): 2384-2394.

Xie, B., J. Zhao, M. Kitagawa, J. Durbin, J. A. Madri, J. L. Guan and X. Y. Fu (2001). "Focal adhesion kinase activates Stat1 in integrin-mediated cell migration and adhesion." J Biol Chem **276**(22): 19512-19523.

Xie, R., S. Nguyen, K. McKeehan, F. Wang, W. L. McKeehan and L. Liu (2011). "Microtubule-associated protein 1S (MAP1S) bridges autophagic components with microtubules and mitochondria to affect autophagosomal biogenesis and degradation." J Biol Chem **286**(12): 10367-10377.

Yang, S. Y. and G. M. Xu (2001). "Expression of PDGF and its receptor as well as their relationship to proliferating activity and apoptosis of meningiomas in human meningiomas." J Clin Neurosci **8 Suppl 1**: 49-53.

Yi, C., S. Troutman, D. Fera, A. Stemmer-Rachamimov, J. L. Avila, N. Christian, N. L. Persson, A. Shimono, D. W. Speicher, R. Marmorstein, L. Holmgren and J. L. Kissil (2011). "A tight junction-associated Merlin-angiomotin complex mediates Merlin's regulation of mitogenic signaling and tumor suppressive functions." Cancer Cell **19**(4): 527-540.

Yoshizaki, A., T. Nakayama, S. Naito, C. Y. Wen and I. Sekine (2006). "Expressions of sonic hedgehog, patched, smoothened and Gli-1 in human intestinal stromal tumors and their correlation with prognosis." World J Gastroenterol **12**(35): 5687-5691.

Zhang, N., H. Bai, K. K. David, J. Dong, Y. Zheng, J. Cai, M. Giovannini, P. Liu, R. A. Anders and D. Pan (2010). "The Merlin/NF2 tumor suppressor functions through the YAP oncoprotein to regulate tissue homeostasis in mammals." Dev Cell **19**(1): 27-38.

Zhang, Y., Y. Y. Cho, B. L. Petersen, F. Zhu and Z. Dong (2004). "Evidence of STAT1 phosphorylation modulated by MAPKs, MEK1 and MSK1." Carcinogenesis **25**(7): 1165-1175.

Zhao, B., L. Li, Q. Lei and K. L. Guan (2010). "The Hippo-YAP pathway in organ size control and tumorigenesis: an updated version." Genes Dev **24**(9): 862-874.

Zhou, H., S. Di Palma, C. Preisinger, M. Peng, A. N. Polat, A. J. Heck and S. Mohammed (2013). "Toward a comprehensive characterization of a human cancer cell phosphoproteome." J Proteome Res **12**(1): 260-271.

Zhou, L., E. Ercolano, S. Ammoun, M. C. Schmid, M. A. Barczyk and C. O. Hanemann (2011). "Merlin-deficient human tumors show loss of contact inhibition and activation of Wnt/beta-catenin signaling linked to the PDGFR/Src and Rac/PAK pathways." Neoplasia **13**(12): 1101-1112.